

INTERFERENCE EFFECTS OF HYDRIDE FORMING ELEMENTS ON
BISMUTH DETERMINATION USING TUNGSTEN COIL SYSTEM AS
ELECTROTHERMAL VAPORIZER AND ELECTROTHERMAL ATOMIZER IN
ATOMIC SPECTROMETRY

A THESIS SUBMITTED TO
THE GRADUATE SCHOOL OF NATURAL AND APPLIED SCIENCES
OF
MIDDLE EAST TECHNICAL UNIVERSITY

BY

PINAR MERCAN

IN PARTIAL FULFILLMENT OF THE REQUIREMENTS
FOR
THE DEGREE OF DOCTOR OF PHILOSOPHY
IN
CHEMISTRY

FEBRUARY 2017

Approval of the Thesis;

**INTERFERENCE EFFECTS OF HYDRIDE FORMING ELEMENTS ON
BISMUTH DETERMINATION USING TUNGSTEN COIL SYSTEM AS
ELECTROTHERMAL VAPORIZER AND ELECTROTHERMAL
ATOMIZER IN ATOMIC SPECTROMETRY**

submitted by **PINAR MERCAN** in a partial fulfillment of the requirements for the degree of **Doctor of Philosophy in Chemistry Department, Middle East Technical University** by,

Prof. Dr. Gülbin Dural Ünver
Dean, Graduate School of **Natural and Applied Sciences** _____

Prof. Dr. Cihangir Tanyeli
Head of Department, **Chemistry** _____

Prof Dr. O. Yavuz Ataman
Supervisor, **Chemistry Department, METU** _____

Examining Committee Members:

Prof. Dr. G. İnci Gökmen
Chemistry Department, METU _____

Prof. Dr. O. Yavuz Ataman
Chemistry Department, METU _____

Prof. Dr. Nusret Ertuş
Faculty of Pharmacy, Gazi University _____

Prof. Dr. E. Hale Göktürk
Chemistry Department, METU _____

Prof. Dr. Orhan Acar
Chemistry Dept., Gazi University _____

Date: 23.02.2017

I hereby declare that all information in this document has been obtained and presented in accordance with academic rules and ethical conduct. I also declare that, as required by these rules and conduct, I have fully cited and referenced all material and results that are not original to this work.

Name, Last name: Pınar MERCAN

Signature:

ABSTRACT

INTERFERENCE EFFECTS OF HYDRIDE FORMING ELEMENTS ON BISMUTH DETERMINATION USING TUNGSTEN COIL SYSTEM AS ELECTROTHERMAL VAPORIZER AND ELECTROTHERMAL ATOMIZER IN ATOMIC SPECTROMETRY

Mercan, Pınar

Ph. D., Department of Chemistry

Supervisor: Prof. Dr. O. Yavuz Ataman

February 2017, 197pages

Tungsten coil (W-coil) has become an alternative tool for graphite tubes in atomic spectrometry for its high melting point, good electrical conductivity and low cost. Tungsten coil systems have been used in atomic spectrometry as both atomizers and vaporizers. Both approaches include advantages and disadvantages. In this work the behaviors of both approaches were investigated. Bismuth (Bi), one of the hydride forming elements, was selected as the analyte. The properties and performances of both techniques, namely electrothermal atomizer (ETA) and electrothermal vaporizer (ETV), were studied regarding analytical efficiency, interferences and practicability.

In this study, W-coil was used as an atom trap for preconcentration and atomization/revolatilization of volatile species of Bi, using hydride generation technique. In W-coil Atom Trap ETA system, the collected analyte species were atomized directly, since the W-coil was functioning as atomizer. In the system where W-coil was used as a vaporizer (W-coil Atom Trap ETV) the collected analyte

species were revolatilized rapidly and sent to quartz T-tube atomizer for measurement.

The experimental parameters were optimized for Bi with rhodium coated W-coil Atom Trap ETA and syringe attached rhodium coated W-coil atom trap ETA where the limits of detection obtained for this system were 0.046 and 0.018 ng/mL for 120 s trapping, respectively. Moreover, conditions for rhodium coated Atom Trap ETV and syringe attached rhodium coated W-coil Atom Trap ETV systems were optimized; the limits of detection for these systems were 0.047 and 0.026 ng/mL for 120 s trapping, respectively.

In literature, interferences of ETA and ETV systems have been investigated separately; however, any study regarding the comparison of interferences for both approaches has not been performed. In this study the interferences were studied by comparing the trends exhibited by both of the approaches. In order to understand the nature of the interference, a twin-channel hydride generation system containing two gas liquid separators was used. For Rh coated W-coil atom trap ETA system, among the selected interference elements, Te and Sb suppressed significantly the signals. On the other hand, Rh coated W-coil atom trap ETV system for Bi had a completely different behavior pattern compared to Rh coated W-coil atom trap ETA system. By using the twin-channel system, a detailed interference study with Rh coated W-coil atom trap ETV system was carried out. It was found that As, Se and Sb enhanced the analytical signal of Bi significantly and the interferences most probably took place in the revolatilization stage.

Keywords: W-coil, electrothermal atomization, electrothermal vaporization, atom trap, AAS, bismuth, interference.

ÖZ

ATOMİK SPEKTROMETRİDE TUNGSTEN SARMAL SİSTEMİNİN ELEKTROTERMAL ATOMLAŞTIRICI VE ELEKTROTERMAL BUHARLAŞTIRICI OLARAK UYGULANMASIYLA HİDRÜR OLUŞTURAN ELEMENTLERİN BİZMUT TAYİNİNE GİRİŞİM ETKİLERİ

Mercan, Pınar

Doktora, Kimya Bölümü

Tez Yöneticisi: Prof. Dr. O. Yavuz Ataman

Şubat 2017, 197 sayfa

Tungsten sarmalı atomik spectrometride yüksek erime noktası, iyi elektrik iletkenliği ve maliyetinin düşük olması sebeplerinden dolayı grafit tüplere seçenек olmuştur. Atomik spectrometride tungsten sarmal sistemleri hem atomlaştırıcı hem buharlaştırıcı olarak kullanılmaktadır. Bu iki uygulamanın avantaj ve dezavantajları vardır. Bu çalışmada, her iki yaklaşım da incelenmiştir. Uçucu bileşik oluşturan elementlerden Bizmut (Bi) analit olarak seçilmiştir. Atomlaştırıcı ve buharlaştırıcı sistemlerinin özellikleri bu element kullanılarak saptanmıştır. Elektrotermal atomlaştırıcı (ETA) ve Elektrotermal buharlaştırıcı (ETV) sistemleri özellik ve performansları; analitik verimlilikleri, girişim davranışları ve kullanım kolaylıkları açısından değerlendirilmiştir.

Bu çalışmada, hidrür oluşturma tekniğiyle W-sarmal, uçucu bileşiklerin özenleştirilmesi ve atomlaştırılması/buharlaştırılması için atom tuzağı olarak kullanılmıştır. W-sarmal atom tuzağı ETA sisteminde, W-sarmal atomlaştırıcı olarak kullanıldığından sarmal üzerinde toplanan analit türleri doğrudan buharlaşarak atomlaştırılmıştır. W-sarmalının buharlaştırıcı olarak kullanıldığı sistemde ise (W-

sarmal atom tuzağı ETV), sarmal üzerinde biriktirilen analit türleri buharlaştırılmış ve ölçüm için kuvars T-tüp atomlaştırıcıya gönderilmiştir.

Deneysel değişkenler rodyum kaplı W-sarmal Atom Tuzağı ETA ve şırıngalı rodyum kaplı W-sarmal Atom Tuzağı ETA için optimize edilmiştir; bu iki sistemde gözlenebilirlik sınırları 120 s tuzaklama süresi için 0.046 ve 0.018 ng/mL olarak bulunmuştur. Deneysel değişkenler rodyum kaplı W-sarmal Atom Tuzağı ETV ve şırıngalı rodyum kaplı W-sarmal Atom Tuzağı ETV çalışılmıştır, Bu sistemler için gözlenebilirlik sınırı 120 s tuzaklama süresi için 0.047 ve 0.026 olarak belirlenmiştir.

Literatürde ETA ve ETV sistemleri için girişim çalışmaları ayrı ayrı incelenmiştir; bununla birlikte her ikisinin girişim davranışlarının kıyaslanarak incelenmesine ise yer verilmemiştir. Bu çalışmada, girişim etkileri her iki sistem için de çalışılmıştır ve girişim elementlerinin etkileri karşılaştırılmıştır. Girişim elementlerinin etkilerini daha iyi gözlemleyebilmek için çift kanallı hidrür oluşturma sistemi kullanılmıştır. Bu sistemde iki tane gaz sıvı ayırıcı içeren çift kanallı hidrür oluşturma aygıtı kullanılmıştır. Rodyum kaplı W-sarmal Atom Tuzaklayıcı ETA sisteminde girişim elementlerinden Te ve Sb, bizmutun analitik sinyalini önemli ölçüde azaltmıştır. Rodyum kaplı W-sarmal Atom Tuzaklayıcı ETV sisteminde ise farklı bir tablo ortaya çıkmıştır. ETV için çift kanallı hidrür oluşturma aygıtıyla ayrıntılı bir çalışma yapılmıştır. Bizmutun analitik sinyali As, Sb ve Se varlığında önemli ölçüde artmıştır. Bu artış, büyük ihtimalle tungsten yüzeyinde toplanan bizmut türlerinin tungsten yüzeyinden buharlaştırma aşamasında meydana gelmektedir.

Anahtar kelimeler: W-sarmalı, elektrotermal atomlaştırıcı, elektrotermal buharlaştırıcı, atom tuzaklayıcı, AAS, bizmut, girişimler.

*to my dear son, husband and precious
family..*

ACKNOWLEDGEMENTS

The preparation of this important document would not have been possible without the support, hard work and endless efforts of a large number of individuals.

I would like to express my deep and sincere gratitude to my advisor Prof. Dr. O. Yavuz Ataman. His wide knowledge and logical way of thinking have been of great value for me. His understanding, encouraging and personal guidance have provided a good basis not for the present thesis but also for my life.

I wish to thank Prof. Dr. E. Hale Göktürk and Prof. Dr. Nusret Ertaş for their guidance.

I am deeply grateful to Assoc. Prof Dr. Gülay Ertaş for her important support throughout this work.

I truly thank Dr. Emrah Yıldırım and Dr. Selin Bora for their endless support and friendship. They were always ready to give a hand whenever I needed.

I owe many thanks to my dear friends Dr. Tuğba Lekesiz and Derya Çelik Özhava who were with me in this sometimes challenging process to share their valuable opinions and comments.

I would like to thank Başak Düğencili, Erhan Özdemir, Sezin Atıcı, Canan Höçük and Bilgi Er for their help whenever I need and for their friendship.

I also would like to thank C-50 lab members, Yeliz Akpınar, Nehir Utku, Dilek Ünal and Zuhul Vanlı for enjoyable time and friendship.

My special thanks also goes to Eda Durkan for her endless friendship and supportI would like to thank Halil Memiş for his help on Argon and Hydrogen gas tanks and

regarding the preparation of glass tubes that were designed for this study, I should also thank to Hamit aęlar and Aziz aęlar.

I am forever grateful to my husband Grkem Mercan for his patience, support and belief in me. It makes me feel an extraordinarily lucky person to know that he was, is and will be there for me whenever I call for help.

My deepest gratitude goes to my beloved parents Yksel and İsmail Akay and brother, Eren Emin Akay who always supported me and believed in me. Without their, especially my parents' encouragement and immeasurable sacrifice, I could never finish this journey.

Lastly, my son Kaan Ege Mercan involved in this journey. His presence was so precious that he makes everything wonderful in my life. He is my miracle.

TABLE OF CONTENTS

TABLE OF CONTENTS

ABSTRACT	v
ÖZ.....	vii
ACKNOWLEDGEMENTS	x
TABLE OF CONTENTS	xii
LIST OF TABLES	xvii
LIST OF FIGURES.....	xx
CHAPTERS	
1. INTRODUCTION.....	1
1.1. Electrothermal Atomization (ETA).....	1
1.1.1. Graphite Atomizer ETAAS	3
1.1.2. Metal Atomizer ETAAS.....	5
1.1.3. Interferences	7
1.2. Electrothermal Vaporization (ETV).....	9
1.2.1. Graphite Furnace ETV	10
1.2.2. Metal Vaporizer ETV	11
1.2.3. Interferences	13
1.3. Vapor Generation	13
1.3.1. Hydride Generation AAS	15
1.3.1.1. Atomization in HGAAS	18
1.4. <i>In situ</i> Atom Trapping Techniques.....	20

1.4.1.	Graphite Furnace Trap	21
1.4.2.	Quartz Atom Trap	23
1.4.3.	Metal Atom Traps	23
1.5.	Interferences	25
1.5.1.	Liquid phase interferences	26
1.5.2.	Gas-phase interferences	27
1.6.	Bismuth	28
1.6.1.	Occurrences	28
1.6.2.	Application	29
1.6.3.	Human Exposure and Toxicity	30
1.6.4.	Determination of Bi.....	30
1.7.	Purpose of the Study	32
2.	EXPERIMENTAL	33
2.1.	Instrumentation	33
2.2.	Chemicals and reagents.....	34
2.3.	Hydride Generation System	35
2.4.	Atomization Units and Atom Cell.....	37
2.4.1.	Continuous Flow Hydride Generation System	37
2.4.2.	W-coil Atom Trap ETA	39
2.4.3.	W-coil Atom Trap ETV	42
2.5.	W-coil as a Vaporization Unit.....	42
2.6.	Trap System	44
2.7.	Interference study	44
2.7.1.	Instrumentation	45
2.7.2.	Interference study with W-coil Atom Trap ETA and W-coil Atom Trap ETV	46
2.8.	Procedures	48
2.8.1.	Continuous Flow Hydride Generation System	48

2.8.2.	W-coil Atom Trap ETA	48
2.8.3.	W-coil Atom Trap ETV	50
2.8.4.	Interference Study	51
2.8.4.1.	Continuous Flow Hydride Generation System.....	51
2.8.4.2.	W-coil Atom Trap ETA	52
2.8.4.3.	W-coil Atom Trap ETV	54
2.8.5.	Coating of W-coil Surface.....	56
2.8.6.	Temperature Measurement of W-coil	56
2.9.	Accuracy Check	57
3.	RESULTS AND DISCUSSION	59
3.1.	Continuous Flow Hydride Generation System.....	60
3.1.1.	Optimization of HCl and NaBH ₄ Concentrations	60
3.1.2.	Optimization of Sample and Reductant Flow Rate	62
3.1.3.	Optimization of Stripping Argon Flow Rate.....	63
3.1.4.	Calibration Plot and Linear Range for CF-HGAAS system	65
3.2.	Rh coated W-coil Atom Trap Electrothermal Atomization System	67
3.2.1.	Optimization of Argon Flow Rate at Trapping and Atomization Stages	68
3.2.2.	Optimization of Hydrogen Flow Rate at Trapping and Atomization Stages	70
3.2.3.	Optimization of Trapping and Atomization Temperatures	72
3.2.4.	Optimization of Collection Period	74
3.2.5.	Calibration Plot and Linear Range for Rh coated W-coil Atom Trap ETA System	76
3.2.6.	Analytical Figures of Merit	78
3.3.	Syringe Attached Rh Coated W-coil Atom Trap Electrothermal Atomization System	78
3.3.1.	Optimization of Argon Flow Rate at Trapping and Atomization Stages	79

3.3.2.	Optimization of Hydrogen Flow Rate at Trapping and Atomization Stages	81
3.3.3.	Optimization of Trapping and Atomization Temperatures	83
3.3.4.	Optimization of Collection Period	84
3.3.5.	Calibration Plot and Linear Range for Syringe Attached Rh coated W-coil Atom Trap ETA System.....	86
3.3.6.	Analytical Figures of Merit.....	88
3.3.7.	Accuracy of the Method.....	89
3.4.	Rh coated W-coil Atom Trap Electrothermal Vaporization System	90
3.4.1.	Optimization of Stripping Argon Flow Rate at Trapping and Revolatilization Stages.....	90
3.4.2.	Optimization of Stripping Hydrogen Flow Rate at Trapping and Revolatilization Stages.....	92
3.4.3.	Optimization of Trapping and Revolatilization Temperatures	94
3.4.4.	Calibration Plot and Linear Range for Rh coated W-coil Atom Trap ETV System	95
3.4.5.	Analytical Figures of Merit.....	97
3.5.	Syringe Attached Rh Coated W-coil Atom Trap Electrothermal Vaporization System	97
3.5.1.	Optimization of Stripping Argon Flow Rate at Trapping and Revolatilization stages	98
3.5.2.	Optimization of Carrier Argon Flow Rate at Trapping and Revolatilization Stages.....	100
3.5.3.	Optimization of Hydrogen Flow Rate at Trapping and Revolatilization Stages	102
3.5.4.	Optimization of Trapping and Revolatilization Temperatures	103
3.5.5.	Calibration Plot and Linear Range for Syringe Attached Rh coated W-coil Atom Trap ETV System.....	106
3.5.6.	Analytical Figures of Merit.....	109
3.5.7.	Accuracy of the Method.....	110
3.6.	The Comparison of the Developed Methods	111

3.7.	Interference Study	113
3.7.1.	Interference Study with Rh coated W-coil Atom Trap ETA System.....	113
3.7.2.	Interference Study with Rh coated W-coil Atom Trap ETV System.....	116
3.7.3.	Interference Study with Twin-channel Hydride Generation System	121
3.7.3.1.	Interference Study with CF-HGAAS System	122
3.7.3.2.	Interference Study with Rh-coated W-coil Atom Trap ETA System	124
3.7.3.2.1	Trapping and Atomization Temperature Ranges for Interference Elements.....	126
3.7.3.3.	The Interference Study with Rh-coated W-coil Atom Trap ETV System	132
3.7.3.3.1	Trapping and Revolatilization Temperature Ranges for Interference Elements.....	134
3.7.3.3.2	Effect of Interferent during Continuous Flow Hydride Generation, Trapping and Revolatilization Stages in ETV	139
3.7.3.3.3	Effect of Increasing Temperature on the Behavior of Interferents at Revolatilization Stage	152
3.7.3.3.4	Bismuth as an Interference Element.....	157
3.8.	The Comparison of ETA and ETV Systems	159
4.	CONCLUSIONS.....	165
	REFERENCES.....	171
	CURRICULUM VITAE	195

LIST OF TABLES

TABLES

Table 2.1 Operating conditions of Varian AA140	33
Table 2.2 Operating conditions of Varian AA140 for interference elements.	45
Table 2.3 Hydride generation, trapping and release (atomization) conditions for As, Sb, Se, Te and Sn with Rh coated W-coil Atom Trap ETA.	53
Table 2.4 Hydride generation, trapping and release (revolatilization) conditions for As, Sb, Se, Te and Sn with W-coil atom trap ETV.....	55
Table 2.5 Temperature program used for W-coil surface with Rh.	56
Table 2.6 Certified values for Trace Elements in SRM 1643e.	57
Table 3.1 Optimized parameters for CF-HGAAS system.	65
Table 3.2 Analytical figures of merit for CF-HGAAS system.	67
Table 3.3 Optimum conditions used for Rh coated W-coil atom trap ETA system. .	75
Table 3.4 Analytical figures of merit for Rh coated W-coil Atom Trap ETA. Volatile Bi species were trapped for 120 s at a flow rate of 3.0 mL/min.	78
Table 3.5 Optimum conditions used for syringe attached Rh coated W-coil atom trap ETA system.....	85
Table 3.6 Analytical figures of merit for syringe attached Rh coated W-coil atom trap ETA system. Volatile Bi species were for 120 s at a flow rate of 3.0 mL/min.	88
Table 3.7 Analytical figures of merit for syringe attached Rh coated W-coil atom trap ETA, Rh coated W-coil atom trap ETA and CF-HGAAS systems.	89
Table 3.8 Result of the analysis of CRM and the certified values for Bi using syringe attached Rh coated W-coil Atom Trap ETA system (n=3).....	89

Table 3.9 Optimum conditions used for Rh coated W-coil atom trap ETV system. .	95
Table 3.10 The analytical figures of merit for Rh coated W-coil Atom Trap ETV system. The volatile Bi species was trapped for 120 s at a flow rate of 3.0 mL/min.	97
Table 3.11 The optimum conditions used for syringe attached Rh coated W-coil atom trap ETV system.....	105
Table 3.12 Analytical figures of merit for Bi obtained for 60 s and 120 s collection period.....	109
Table 3.13 Analytical figures of merit for syringe attached Rh coated W-coil atom trap ETV, Rh coated W-coil atom trap ETV and CF-HGAAS systems.	110
Table 3.14 Result of the analysis of CRM and the certified values (n=3).	111
Table 3.15 Comparison of the limit of detection and the sample volume of the method with those of others in literature.....	112
Table 3.16 Interference studies performed with Rh coated W-coil Atom Trap ETA and Rh coated W-coil Atom Trap ETV. Bi concentration was 0.3 ng/mL.	119
Table 3.17 The results of interference study regarding the effects of interferent on the signal of Bi in the stages namely; CF-HG (1), untrapped CF-HG (2) and revolatilization (3) with twin-channel CF-HG system in which Bi and interferent in same solution (a) and separate solutions (b).	150
Table 3.18 Effect of revolatilization temperature on the behavior of As, Se and Sb in Rh coated W-coil atom Trap ETV experiments. The analyte concentration was 10.0 ng/mL and was trapped for 20 s. The concentration of As, Se and Sb was 500 fold interferent/Bi ratio. Analyte and interferent were in the same solution and pumped from same channel. Blank was transferred from the second channel. The trapping temperature was kept at 300 °C. Temperature of EHQTA was 950 °C.	154
Table 3.19 Effect of revolatilization temperature on the behavior of As, Se and Sb. The analyte concentration was 10.0 ng/mL. The concentration of As, Se and Sb was 500 fold interferent/Bi ratio. Analyte and interferent were in the separate solution and pumped from different channel. The trapping period was 20 seconds and the trapping temperature was kept at 300 °C.....	155

Table 3.20 The interference effect of Bi on Sb using Rh coated W-coil Atom Trap ETV system and optimized conditions for Sb(III). The concentration of Sb was 10.0 ng/mL in 0.1 mol/L HCl.	158
Table 3.21 The interference effect of Bi on Sb using Rh coated W-coil Atom Trap ETV system and optimized conditions for Bi. The concentration of Sb was 10.0 ng/mL in 1.0 mol/L HCl.	159
Table 3.22 Comparison of the analytical performance of the W-coil atom trap ETA and ETV systems.	161
Table 3.23 Effects of interference on the analytical signal of Bi with CF-HGAAS, Rh coated W-coil Atom Trap ETA and Rh coated W-coil Atom Trap ETV. The mass ratio (w/w) of interferent to analyte was 500 fold. Analyte concentration for CF-HGAAS was 10.0 ng/mL and 2.0 ng/mL for ETA and ETV systems.	162

LIST OF FIGURES

FIGURES

Figure 1.1 The schematic representation of GF atom trapping system [100].	21
Figure 1.2 W-coil atom trap placed inlet arm of the quartz T-tube [56].	24
Figure 2.1 The experimental set up for continuous flow hydride generation system for Bi.	36
Figure 2.2 Schematic representation of cylindrical type GLS.	36
Figure 2.3 The schematic representation of the EHQTA.	37
Figure 2.4 Lab-made ceramic electrical heater used to heat QTA to atomization temperature [160]	38
Figure 2.5 The atomization unit for W-coil Atom Trap ETA system.	39
Figure 2.6 The side view of W-coil Atom Trap ETA atomization unit.	40
Figure 2.7 The atomization unit used for syringe attached W-coil Atom Trap ETA system.	41
Figure 2.8 The side view of the syringe attached W-coil Atom Trap ETA atomization unit.	41
Figure 2.9 Vaporization unit for W-coil Atom Trap ETV system.	43
Figure 2.10 The syringe attached vaporization unit for W-coil Atom Trap ETV system.	43
Figure 2.11 Dimensions of W-coil extracted from a projector bulb.	44
Figure 2.12 Experimental set-up for twin-channel hydride generation system in which analyte and interference elements were transferred together using the same GLS.	46

Figure 2.13 Experimental set-up for twin-channel hydride generation system in which analyte and interference element were transferred separately.....	47
Figure 3.1 Variation of CF HGAAS signal with NaBH ₄ and HCl concentration for 20 ng/mL Bi sample solution. Sample and reductant flow rates were adjusted to 3.0 mL/min.....	61
Figure 3.2 Effect of sample flow rate on the analytical signal of 20 ng/mL Bi solution. Sample solution was prepared in 1.0 mol/L HCl and 0.5 % (w/v) NaBH ₄ was used.	62
Figure 3.3 Effect of reductant flow rate on 20 ng/mL Bi signal. The sample flow rate was 3.0 mL/min and prepared in 1.0 mol/L HCl. The concentration of NaBH ₄ was 0.5% (w/v).....	63
Figure 3.4 Effect of stripping Ar flow rate on analytical signal of 20 ng/mL Bi. Sample solution was prepared in 1.0 mol/L HCl solution and pumped at 3.0 mL/min flow rate. 0.5% (w/v) NaBH ₄ was used at a flow rate of 3.0 mL/min.	64
Figure 3.5 Calibration plot for CF-HGAAS system for Bi solutions. Sample solution was prepared in 1.0 mol/L HCl solution and pumped at 3.0 mL/min flow rate. 0.5 % (w/v) NaBH ₄ was used at a flow rate of 3.0 mL/min.....	66
Figure 3.6 Linear portion calibration plot of the calibration plot obtained for CF-HGAAS system.....	67
Figure 3.7 Effect of Ar flow rate at trapping stage on signal of 5.0 ng/mL Bi solution trapped over 60 s time period with Rh coated W-coil Atom Trap ETA system. Sample solution was pumped at 3.0 mL/min. Trapping temperature and atomization temperatures were adjusted to 1064 °C and 1960 °C, respectively.....	69
Figure 3.8 Effect of Ar flow rate at atomization stage on signal of 5.0 ng/mL Bi solution trapped over 60 s time period with Rh coated W-coil Atom Trap ETA system. Sample solution was pumped at 3.0 mL/min. Trapping temperature and atomization temperatures were adjusted to 1064 °C and 1960 °C, respectively.....	70
Figure 3.9 Effect of H ₂ flow rate at trapping stage on signal of 5.0 ng/mL Bi solution trapped over 60 s time period with Rh coated W-coil Atom Trap ETA system.	

Sample solution was pumped at 3.0 mL/min. Trapping temperature and atomization temperatures were adjusted to 1064 °C and 1960 °C, respectively. 71

Figure 3.10 Effect of H₂ flow rate at atomization stage on signal of 5.0 ng/mL Bi solution trapped over 60 s time period with Rh coated W-coil Atom Trap ETA system. Sample solution was pumped at 3.0 mL/min. Trapping temperature and atomization temperatures were adjusted to 1064 °C and 1960 °C, respectively. 72

Figure 3.11 The effect of temperature at trapping and atomization stages on 5.0 ng/mL Bi trapped over 60 s. 73

Figure 3.12 Effect of trapping period on 5.0 ng/mL Bi signal. Sample was pumped at 3.0 mL/min. Trapping and atomization temperature were adjusted to 462 °C and 2177 °C, respectively. 74

Figure 3.13 Calibration plot obtained for Bi collected over 120 s. The sample flow rate was 3.0 mL/min; trapping and atomization temperatures were 462 °C and 2177 °C, respectively. 76

Figure 3.14 Linear portion of the calibration plot obtained for Bi trapped over 120 s. Sample flow rate was 3.0 mL/min; trapping and atomization temperatures were 462 °C and 2177 °C, respectively. 77

Figure 3.15 The analytical signal obtained by Rh coated W-coil atom trap ETA method for Bi; 6.0 mL of sample solution of 0.5 ng/mL Bi were collected for 120 s. 77

Figure 3.16 Effect of Ar flow rate on the signal for 2.0 ng/mL Bi at trapping stage. The sample flow rate was 3.0 mL/min and Bi was collected for 60 s. Trapping and atomization temperatures were 462 °C and 2177 °C, respectively. 80

Figure 3.17 Effect of Ar flow rate on the signal for 2.0 ng/mL Bi at atomization stage. The sample flow rate was 3.0 mL/min and collected for 60 s. Trapping and atomization temperatures were 462 °C and 2177 °C, respectively. 80

Figure 3.18 Effect of H₂ flow rate on the signal for 2.0 ng/mL Bi at trapping stage. The sample flow rate was 3.0 mL/min and collected for 60 s. Trapping and atomization temperatures were 462 °C and 2177 °C, respectively. 82

Figure 3.19 Effect of H ₂ flow rate on the signal for 2.0 ng/mL Bi at atomization stage. The sample flow rate was 3.0 mL/min and collected for 60 seconds. Trapping and atomization temperatures were 462 °C and 2177 °C, respectively.....	82
Figure 3.20 The effect of temperature at trapping and atomization stages on 2.0 ng/mL Bi trapped over 60 s. During the variations of trapping and atomization temperatures, a constant release temperature of 2177 °C and a constant trapping temperature of 462 °C, respectively, were employed.	83
Figure 3.21 Effect of collection period on analytical signal of 2.0 ng/mL Bi pumped at 3.0 mL/min.	84
Figure 3.22 Calibration plot obtained for Bi collected over 120 s. The sample flow rate was 3.0 mL/min, trapping and atomization temperatures were 462 °C and 2177°C, respectively.	86
Figure 3.23 Linear range of the calibration plot obtained for Bi collected over 120 s. The sample flow rate was 3.0 mL/min, trapping and atomization temperatures were 462 °C and 2177°C, respectively.	87
Figure 3.24 The analytical signal obtained by syringe attached Rh coated W-coil atom trap ETA method for Bi; 6.0 mL of sample solution of 0.4 ng/mL Bi were collected in 120 s.....	87
Figure 3.25 The effect of stripping argon flow rate at trapping stage on the signal of 2.0 ng/mL Bi that was collected for 60 s. The flow rate for H ₂ was 150 mL/min. Trapping and revolatilization temperatures were 262 °C and 1960 °C, respectively. Temperature of EHQTA was 950 °C.....	91
Figure 3.26 The effect of stripping argon flow rate at revolatilization stage on the signal of 2.0 ng/mL Bi that was collected for 60 s. The flow rate for H ₂ was 150 mL/min. Trapping and revolatilization temperatures were 262 °C and 1960 °C, respectively. Temperature of EHQTA was 950 °C.....	92
Figure 3.27 The effect of H ₂ flow rate at trapping stage on the signal of 2.0 ng/mL Bi that was collected for 60 s. Trapping and revolatilization temperatures were 262 °C and 1960 °C, respectively. Temperature of EHQTA was 950 °C.....	93

Figure 3.28 The effect of H₂ flow rate at trapping stage on the signal of 2.0 ng/mL Bi that was collected for 60 s. Trapping and revolatilization temperatures were 262 °C and 1960 °C, respectively. Temperature of EHQTA was 950 °C. 93

Figure 3.29 The effect of trapping and revolatilization temperatures on analytical signal for Bi trapped for 60 s. During the variations of collection and release temperatures, a constant release temperature of 1960 °C and a constant collection temperature of 180 °C, respectively, were employed. The signals were obtained by collecting 2.0 ng/mL Bi in 1.0 mol/L HCl. 94

Figure 3.30 Calibration plot obtained for Bi collected over 120 s. The sample flow rate was 3.0 mL/min; trapping and revolatilization temperatures were 180 °C and 1960°C, respectively. Temperature of EHQTA was 950 °C. 96

Figure 3.31 Linear range of the calibration plot obtained for Bi collected over 120 s. The sample flow rate was 3.0 mL/min; trapping and revolatilization temperatures were 180 °C and 1960 °C, respectively. Temperature of EHQTA was 950 °C. 96

Figure 3.32 Effect of stripping Ar flow rate on the analytical signal at the trapping period; H₂ flow rate was 100 mL/min, release Ar flow rate was 120 mL/min; 1.0 ng/mL Bi was used and pumped at 3.0 mL/min. 99

Figure 3.33 Effect of stripping Ar flow rate on the analytical signal at the revolatilization stage; H₂ flow rate was 100 mL/min, trapping Ar flow rate was 120 mL/min; 1.0 ng/mL Bi was used and pumped at 3.0 mL/min. 99

Figure 3.34 Effect of carrier Ar flow rate on the analytical signal at the trapping period; H₂ flow rate was 100 mL/min, stripping Ar flow rate was 120 mL/min; 1.0 ng/mL Bi was used and pumped at 3.0 mL/min. 101

Figure 3.35 Effect of carrier Ar flow rate on the analytical signal at the revolatilization period; H₂ flow rate was 100 mL/min, stripping Ar flow rate was 120 mL/min; 1.0 ng/mL Bi was used and pumped at 3.0 mL/min. 101

Figure 3.36 Effect of H₂ flow rate on the analytical signal at the trapping period; Ar flow rate was 120 mL/min; 1.0 ng/mL Bi was used and pumped at 3.0 mL/min. ... 102

Figure 3.37 Effect of H ₂ flow rate on the analytical signal at the revolatilization period; Ar flow rate was 120 mL/min; 1.0 ng/mL Bi was used and pumped at 3.0 mL/min.....	103
Figure 3.38 The effect of trapping and revolatilization temperatures on analytical signal for Bi. During the variations of collection and release temperatures, a constant release temperature of 1960 °C and a constant collection temperature of 300 °C, respectively, were employed. The signals were obtained by collecting 1.0 ng/mL Bi for 60 s trapping. The temperature of EHQTA was 950 °C.....	104
Figure 3.39 The calibration plot with syringe attached Rh coated W-coil Atom Trap ETV system for Bi collected for 120 s. The collection period was 120 s and sample flow rate was 3.0 mL/min.	106
Figure 3.40 Linear portion of the calibration plot for Bi collected for 120 s and best line equation.	107
Figure 3.41 The analytical signal obtained with syringe attached Rh coated W-coil Atom Trap ETV system for 0.2 ng/mL. The collection period was 120 s and sample flow rate was 3.0 mL/min.	107
Figure 3.42 The calibration plot for Bi with syringe attached Rh coated W-coil Atom Trap ETV system. The collection period was 60 s and sample flow rate was 3.0 mL/min.....	108
Figure 3.43 Linear portion of the calibration plot and best line equation for 60 s collection.	108
Figure 3.44 Interference effects of hydride forming elements on analytical signal of 0.3 ng/mL Bi collected for 60 s using Rh coated W-coil Atom Trap ETA. The trapping and atomization temperatures were 462 °C and 2177 °C, respectively.	114
Figure 3.45 Interference effects of transition metals on analytical signal of 0.3 ng/mL Bi collected for 60 s using Rh coated W-coil Atom Trap ETA. The trapping and atomization temperatures were 462 °C and 2177 °C, respectively.	115

Figure 3.46 Interference effects of earth-based elements on analytical signal of 0.3 ng/mL Bi collected for 60 s using Rh coated W-coil Atom Trap ETA. The trapping and atomization temperatures were 462 °C and 2177 °C, respectively..... 115

Figure 3.47 Interference effects of hydride forming elements on analytical signal of 0.3 ng/mL Bi collected for 60 s using Rh coated W-coil Atom Trap ETV. The trapping and revolatilization temperature were 300 °C and 1562 °C, respectively. The temperature of EHQTA was 950 °C..... 117

Figure 3.48 Interference effects of transition metals on analytical signal of 0.3 ng/mL Bi collected for 60 s using Rh coated W-coil Atom Trap ETV system. The trapping and revolatilization temperature were 300 °C and 1562 °C, respectively. The temperature of EHQTA was 950 °C..... 117

Figure 3.49 Interference effects of earth based element on analytical signal of 0.3 ng/mL Bi collected for 60 s Rh coated W-coil Atom Trap ETV system. The trapping and revolatilization temperature were 300 °C and 1542 °C, respectively. The temperature of EHQTA was 950 °C..... 118

Figure 3.50 Interference effects of hydride forming elements on analytical signal of 20 ng/mL Bi using twin-channel CF-HGAAS system. Analyte and interferent were placed in the same solution and pumped from one channel, from the second channel blank solution was transferred. The temperature of EHQTA was 950 °C. 123

Figure 3.51 Interference effects of hydride forming elements on analytical signal of 20 ng/mL Bi using twin-channel CF-HGAAS system. The analyte and interferent were transported from the separate channels of twin-channel hydride generators. Temperature of EHQTA was 950 °C. 124

Figure 3.52 Interference effects of hydride forming elements on analytical signal of 2.0 ng/mL Bi collected for 60 s using twin-channel CF-HG system of Rh coated W-coil Atom Trap ETA system. Analyte and interferent were placed in the same solution and pumped from one channel, from the second channel blank solution was transferred. The trapping and atomization temperatures were 462 °C and 2177 °C, respectively..... 125

Figure 3.53 Interference effects of hydride forming elements on analytical signal of 2.0 ng/mL Bi collected for 60 s using twin-channel CF-HG system of Rh coated W-coil Atom Trap ETA system. The analyte and interference were transported from the separate channels of twin-channel hydride generators. The trapping and atomization temperatures were 462 °C and 2177 °C, respectively. 126

Figure 3.54 The trapping and atomization behavior for 5.0 ng/mL As in 1.0 mol/L HCl using Rh coated W-coil Atom Trap ETA. The hydrides of As was collected for 60 s at a flow rate of 3.0 mL/min. During the investigation of trapping range the atomization temperature was 1742 °C and for atomization range, trapping temperature was kept at 1018 °C. 127

Figure 3.55 The trapping and atomization behavior for 5.0 ng/mL Sb in 1.0 mol/L HCl using Rh coated W-coil Atom Trap ETA. The hydrides of Sb were collected for 60 s at a flow rate of 3.0 mL/min. During the investigation of trapping range the atomization temperature was 2177 °C and for atomization range, trapping temperature was kept at 544 °C. 128

Figure 3.56 The trapping and atomization behavior for 10.0 ng/mL Se in 1.0 mol/L HCl using Rh coated W-coil Atom Trap ETA. The hydrides of Se were collected for 60 s at a flow rate of 3.0 mL/min. During the investigation of trapping range the atomization temperature was 2177 °C and for atomization range, trapping temperature was kept at 227 °C. 129

Figure 3.57 The trapping and atomization behavior for 5.0 ng/mL Te in 1.0 mol/L HCl using Rh coated W-coil Atom Trap ETA. The hydrides of Te were collected for 60 seconds at a flow rate of 3.0 mL/min. During the investigation of trapping range the atomization temperature was 2177 °C and for atomization range, trapping temperature was kept at 620 °C. 130

Figure 3.58 The trapping and atomization behavior for 100 ng/mL Sn in 1.0 mol/L HCl using Rh coated W-coil Atom Trap ETA. The hydrides of Sn were collected for 60 s at a flow rate of 3.0 mL/min. During the investigation of trapping range the atomization temperature was 2177 °C and for atomization range, trapping temperature was kept at 620 °C. 131

Figure 3.59 Interference effects of hydride forming elements on analytical signal of 2.0 ng/mL Bi collected for 60 s with twin-channel CF-HG system of Rh coated W-coil Atom Trap ETV. Analyte and interferent were placed in the same solution and pumped from one channel, from the second channel blank solution was transferred. The trapping and revolatilization temperatures were 300 °C and 1542 °C, respectively. Temperature of EHQTA was 950 °C..... 133

Figure 3.60 Interference effects of hydride forming elements on analytical signal of 2.0 ng/mL Bi collected for 60 s using twin-channel CF-HG system of Rh coated W-coil Atom Trap ETV. The analyte and interferent were transported from the separate channels of twin-channel hydride generators. The trapping and revolatilization temperatures were 300 °C and 1542 °C, respectively. Temperature in EHQTA was 950 °C..... 134

Figure 3.61 The trapping and revolatilization temperature behavior for 10.0 ng/mL As in 1.0 mol/L HCl using Rh coated W-coil Atom Trap ETV. The hydrides of As were collected for 60 s at a flow rate of 3.0 mL/min. During the investigation of trapping range, the revolatilization temperature was 1696 °C and for revolatilization range, trapping temperature was kept at 620 °C. Temperature of EHQTA was 950 °C. 135

Figure 3.62 The trapping and revolatilization temperature behavior for 10.0 ng/mL Sb in 1.0 mol/L HCl using Rh coated W-coil Atom Trap ETV. The hydrides of Sb were collected for 60 seconds at a flow rate of 3.0 mL/min. During the investigation of trapping range, the revolatilization temperature was 1696 °C and for revolatilization range, trapping temperature was kept at 262 °C. Temperature of EHQTA was 950 °C. 136

Figure 3.63 The trapping and revolatilization temperature behavior for 10.0 ng/mL Se 1.0 mol/L HCl using Rh coated W-oil Atom Trap ETV. The hydrides of Se were collected for 60 s at a flow rate of 3.0 mL/min. During the investigation of trapping range, the revolatilization temperature was 1696 °C and for revolatilization range, trapping temperature was kept at 277 °C. Temperature of EHQTA was 950 °C..... 137

Figure 3.64 The trapping and revolatilization temperature behavior for 10.0 ng/mL Te in 1.0 mol/L HCl using Rh coated W-coil Atom Trap ETV. The hydrides of Te were collected for 60 s at a flow rate of 3.0 mL/min. During the investigation of trapping range, the revolatilization temperature was 1696 °C and for revolatilization range, trapping temperature was kept at 262 °C. Temperature of EHQTA was 950 °C..... 138

Figure 3.65 The trapping and revolatilization temperature behavior for 1.0 mg/L Sn in 1.0 mol/L HCl using Rh coated W-coil Atom Trap ETV. The hydrides of Sn were collected for 60 s at a flow rate of 3.0 mL/min. During the investigation of trapping range, the revolatilization temperature was 1696 °C and for revolatilization range, trapping temperature was kept at 462 °C. Temperature of EHQTA was 950 °C..... 139

Figure 3.66 The schematic representation of the signal obtained from CF-HG, untrapped CF-HG and revolatilization..... 140

Figure 3.67 The effect of As on Bi signal regarding CF-HG, CF-HG of untrapped species and revolatilization stages. The Bi concentration was 10.0 ng/mL in 1.0 mol/L HCl and Bi was trapped for 20 s. As and Bi were in the same solution and pumped together from the same channel, the blank solution was transferred from the second channel. The trapping and revolatilization temperatures were 300 °C and 1542 °C, respectively. Temperature in EHQTA was 950 °C..... 141

Figure 3.68 The signals that were obtained for 10.0 ng/mL Bi, 500 ng/mL As + 10.0 ng/mL Bi and 5000 ng/mL As + 10.0 ng/mL Bi. The signals were taken during the revolatilization stage. As and Bi were in the same solution and transferred together from the same channel. 142

Figure 3.69 The effect of As on Bi signal regarding CF-HG, CF-HG of untrapped species and revolatilization stages. The Bi concentration was 10.0 ng/mL in 1.0 mol/L HCl and Bi was trapped for 20 s. As and Bi solutions were transferred separately. The trapping and revolatilization temperatures were 300 °C and 1542 °C, respectively. Temperature of EHQTA was 950 °C..... 143

Figure 3.70 The signals that were obtained for 10.0 ng/mL Bi, 500 ng/mL As + 10.0 ng/mL Bi and 5000 ng/mL As + 10.0 ng/mL Bi. The signals were taken during the

revolatilization stage. As and Bi were in separate solutions and transferred from different channels.	143
Figure 3.71 The effect of Sb on Bi signal regarding CF-HG, CF-HG of untrapped species and revolatilization stages. The Bi concentration was 10.0 ng/mL in 1.0 mol/L HCl and Bi was trapped for 20 s. Sb and Bi were in the same solution and pumped together from the same channel; the blank solution was transferred from the second channel. The trapping and revolatilization temperatures were 300 °C and 1542 °C, respectively. Temperature of EHQTA was 950 °C.	144
Figure 3.72 The signals that were obtained for 10.0 ng/mL Bi and 100 ng/mL Sb + 10.0 ng/mL Bi, 500 ng/mL Sb + 10.0 ng/mL Bi and 5000 ng/mL Sb+ 10.0 ng/mL Bi. The signals were taken during the revolatilization stage. Sb and Bi were in the same solution and transferred together from the same channel.	145
Figure 3.73 The effect of Sb on Bi signal regarding CF-HG, CF-HG of untrapped species and revolatilization stages. The Bi concentration was 10.0 ng/mL in 1.0 mol/L HCl and Bi was trapped for 20 s. Sb and Bi solutions were transferred separately. The trapping and revolatilization temperatures were 300 °C and 1542 °C, respectively. Temperature in EHQTA was 950 °C.	146
Figure 3.74 The signals that were obtained for 10.0 ng/mL Bi, 100 ng/mL Sb + 10.0 ng/mL Bi, 500 ng/mL Sb + 10.0 ng/mL Bi and 5000 ng/mL Sb + 10.0 ng/mL Bi solutions. The signals were taken during the revolatilization stage. Sb and Bi were in separate solutions and transferred from different channels.	146
Figure 3.75 The effect of Se on Bi signal regarding CF-HG, CF-HG of untrapped species and revolatilization stages. The Bi concentration was 10.0 ng/mL in 1.0 mol/L HCl and Bi was trapped for 20 s. Se and Bi were in the same solution and pumped together from the same channel, the blank solution was transferred from the second channel. The trapping and revolatilization temperatures were 300 °C and 1542 °C, respectively. Temperature of EHQTA was 950 °C.	147
Figure 3.76 The signals that were obtained for 10.0 ng/mL Bi and 5000 ng/L Se + 10.0 ng/mL Bi solutions. The signals were taken during the revolatilization stage. Se and Bi were in the same solution and transferred together from the same channel.	148

Figure 3.77 The effect of Se on Bi signal regarding CF-HG, CF-HG of untrapped species and revolatilization stages. The Bi concentration was 10.0 ng/mL in 1.0 mol/L HCl and Bi was trapped for 20s. Se and Bi solutions were transferred separately. The trapping and revolatilization temperatures were 300 °C and 1542 °C, respectively. Temperature of EHQTA was 950 °C..... 149

Figure 3.78 The signals that were obtained for 10.0 ng/mL Bi, 5.0 mg/L Se + 10.0 ng/mL Bi. The signals were taken during the revolatilization stage. Se and Bi were in separate solutions and transferred from different channels..... 149

Figure 3.79 The absorbance values of the signals obtained for 10.0 ng/mL Bi, 10.0 ng/mL+ 5.0 mg/L As, 10.0 ng/mL+ 5.0 mg/L Sb, and 10.0 ng/mL+ 5.0 mg/L Se. The signals were measured at 1542 °C, 1678 °C and 1780 °C. The trapping temperature was kept at 300 °C. Temperature in EHQTA was 950 °C. The analyte and interferent were in the same solution and transferred from the same channel. 156

Figure 3.80 The absorbance values of the signals obtained for 10.0 ng/mL Bi, 10.0 ng/mL+ 5.0 mg/L As, 10.0 ng/mL+ 5.0 mg/L Sb, and 10.0 ng/mL+ 5.0 mg/L Se. The signals were measured at 1542 °C, 1678 °C and 1780 °C. The trapping temperature was kept at 300 °C. Temperature in EHQTA was 950 °C. The analyte and interferent were transported separately from different channels. 156

Figure 3.81 The signals of 10.0 ng/mL Bi obtained at 1542 °C, 1678 °C and 1780 °C. Bi was trapped for 20 seconds at 300 °C. Temperature of EHQTA was 950 °C. (Red colored line indicates the background signal.)..... 157

Figure 3.82 Comparison of Bi signal obtained in the presence As with ETA and ETV systems. Analyte concentration was 2.0 ng/mL and trapping period was 60 s for both of the systems..... 163

Figure 3.83 Comparison of Bi signal obtained in the presence Sb with ETA and ETV systems. Analyte concentration was 2.0 ng/mL and trapping period was 60 s for both of the systems..... 164

Figure 3.84 Comparison of Bi signal obtained in the presence Se with ETA and ETV systems. Analyte concentration was 2.0 ng/mL and trapping period was 60 s for both of the systems..... 164

LIST OF ABBREVIATIONS

AAS	Atomic Absorption Spectrometry
AES	Atomic Emission Spectrometry
AFS	Atomic Fluorescence Spectrometry
CF-HG	Continuos Flow Hydride Generation
CVAAS	Cold Vapor Atomic Absorption Spectrometry
CVG	Chemical Vapor Generation
EcHG	Electrochemical Hydride Generation
EHQTA	Externally Heated Quartz T-tube Atomizer
ETA	Electrothemat Atomization
ETAAS	Electrothermal Atomic Absorption Spectrometry
ETAES	Electrothermal Atomic Emission Spectrometry
ETA-LEAFS	Electrothermal Atomization Laser Excited Atomic Fluorescence Spectrometry
ETV	Electrothermal Vaporization
ETV ICP-MS	Electrothermal Vaporization Inductively Coupled Plasma Mass Spectrometry
FAAS	Flame Atomic Absorption Spectrometry

FIGS	Flame-in-Gas-Shield
GF	Graphite Furnace
GFAAS	Graphite Furnace Atomic Absorption Spectrometry
GLS	Gas Liquid Separator
HGAAS	Hydride generation Atomic Absorption Spectrometry
ICP-MS	Inductively Coupled Plasma Mass Spectrometry
ICP-OES	Inductively Coupled Plasma Optical Emission Spectrometry
LOD	Limit of Detection
MDF	Miniature Diffusion Flame
MMQTA	Multiple Microflame Quartz T-Tube Atomizers
NOAEL	No Observed Adverse Effect
QTA	Quartz Tube Atomizer
RSD	Relative Standard Deviation
THB	Tetrahydroborate
VG	Vapor Generation

CHAPTER 1

INTRODUCTION

Trace element determination gains importance for the last decades since some of the elements are essential for human beings while some others have toxic effects at trace levels. Sensitivity of the analytical technique has become crucial for determination of elements at ultra trace levels. The most critical step in the analysis of a sample is the sample introduction. In atomic spectrometry, electrothermal atomization (ETA) and electrothermal vaporization (ETV) are commonly used systems for this purpose. Most widely used ETA and ETV units are graphite furnaces. Tungsten coil is an alternative tool for ETA and ETV systems having some advantages over graphite furnaces. In this chapter, information about ETA and ETV system and the use of tungsten coil as an ETA and ETV unit will be presented. Moreover, bismuth is selected as analyte and properties of this element will be listed in this chapter.

1.1. Electrothermal Atomization (ETA)

In the past, determination of trace elements in an unknown sample with ETA had some problems during the sample preparation including physical and/or chemical reactions that could cause the loss of analyte. Moreover, the sample matrix could affect the absorption signal in the analytical line and this could limit to reach adequate detection limits. These kind of constraints were limited the use of ETA; however the improvements done for ETA has solved the limitations and increased the capacity of ETA that is known as Electrothermal Atomic Absorption Spectrometry (ETAAS) [1]. This technique provides high sensitivity and selectivity

at a reasonable cost and is easily calibrated with the use of aqueous standards. It was initially used for analysis of solutions, but its application has become widened to direct solid sampling analysis [2]. Over the last decades, ETAAS has been widely used for trace element determinations in soil and sediments.

Flame Atomic Absorption Spectrometry (FAAS) offers rapid and easy analysis for variety of metals, however; its application is limited by its detection limits. ETAAS became an alternative to FAAS and allows the determination of metallic elements at $\mu\text{g/L}$ levels. They are commonly operated with graphite tubes having 3 to 6 mm inner diameter and 20 to 40 mm length. They are resistively heated by a high current and low voltage AC power supply [3]. Since the nebulization is eliminated, the residence time of the atoms during atomization is longer than FAAS, and this allows the higher sensitivity than obtained by FAAS.

L'vov was the first person who introduced the electrically heated furnace as an atomizer in 1957 [4]. He put a pinch of NaCl into the graphite furnace and heated the furnace slowly and watched how the radiation of a sodium lamp passing through the furnace and disappeared upon heating the furnace [5]. Graphite tube designed by L'vov was heated by a direct current arc before sample introduction into the carbon electrode. Sample was placed into the carbon electrode that is inserted in atomizer; and atomization took place in the preheated graphite furnace.

The design of commercial graphite tube atomizers was not based on the design of L'vov in which atomization took place in a preheated tube. The contribution for further development of graphite furnace AAS came from Massmann in 1965 [4]. Using a different design than that of L'vov, Massmann changed the system drastically and rather than introducing the sample into a preheated tube, the contents were atomized from the wall of tube by rapid heating. Massmann's graphite furnace was 5 cm long graphite tube and was heated by passing high current (500 A) and low voltage (10 V) along the tube.

Despite having some weak points regarding Massmann's design, all commercial electrothermal atomizers used in 1970s and 1980s were based on Massmann's

principle. The first commercial graphite furnace was developed by Perkin Elmer in 1970. The sensitivity obtained by this furnace was two to three orders of magnitude higher compared to flame techniques. Moreover it was used for the application of trace analysis of biological samples, natural waters and direct solid analysis [4]. ETAAS has been used widespread for many analyses and this has brought the requirement of several instrumental developments and analytical protocols. Modern furnace technology includes employing integrated absorbance and fast electronics to obtain accurate measurement of absorbance signal; pyrolytically coated graphite tubes to minimize analyte and graphite interactions; transversely heated graphite furnace to provide isothermal heating; an autosampler to improve precision; platform to eliminate interference and chemical modifiers to minimize interferences.

Metal atomizers have become alternatives to graphite tube atomizers since they are also electrically heated easily to high temperatures. Metals such as W, Mo, Ta are the metals that are used as atomizers for many years, but they have not been used commercially yet. The most popular ones are tungsten coil based atomizer. They are easily obtained from a bulb and suitable for the development of portable ETAAS.

1.1.1. Graphite Atomizer ETAAS

In electrothermal atomization AAS, the most commonly used atomizer is graphite furnaces. The models were originally proposed by L'vov and by Massmann as described in previous section. The graphite furnace designed by Massmann is most widely used. In this design, optical beam is passed through the graphite tube that is closed at both ends with quartz windows mounted in the cooled tube holders. Sample aliquots are introduced with micropipettes or computer controlled dispenser through the sample hole in the middle of the tube. The principal of operation is introducing a small amount of sample (5-100 μL) through a small opening to the inner surface of a graphite tube then, evaporating and ashing in the graphite tube. As the temperature is increased rapidly the sample is completely atomized.

Normal graphite furnaces have a varying temperature profile and there are

temperature differences along the tube that leads to changes of volatilization behavior of analyte from one sample to another. Use of transversally-heated furnace prevents this effect and keeps temperature constant over the whole tube. During atomization in graphite furnace a specific problem may originate from recombination of the atomized analyte and oxygen and other non-metals and this can lead to decrease in free atom concentration that is being measured. This situation occurs when the volatilized analyte enters to the cool medium that is the case in graphite tube. This can be prevented by introducing sample into a low-mass graphite platform located in the furnace. This allows very rapid heating and volatilization of the analyte into a furnace of having same temperature as the sample carrier, which reduces the risk of recombination during atomization [6].

The graphite tube is filled with an inert gas such as argon to prevent the entering of ambient air to the tube. Various stages of heating are required to dry sample, remove sample matrix and finally atomize the analyte. At the drying stage, the graphite tube is heated to the boiling point of solvent to remove any residual solvent from the sample. Ashing process is followed after drying stage to destruct the sample matrix by heating the tube between 350 and 1200 °C. Finally, the temperature of the graphite tube is raised to between 2000 and 3000 °C for 2-3 s, allowing the atomization of analyte atoms. At this stage internal gas flow is stopped to increase the residence time of analyte atoms in atomization unit. Additional heating cycle can be applied for the removal of any residual material. The majority of samples are introduced into graphite tubes in liquid form, including varying concentrations of dissolved solids [7]. The determination of trace metals in solid samples requires sample pretreatment including acid digestion [8,9]. This digestion step has some limitations regarding analyte loss or sample contamination and it ends up with high blank values. Therefore, direct solid analysis is much more convenient since the contamination risk is less, sample pretreatment is simpler, analyte loss is minimized, using dangerous and corrosive reagents used for sample pretreatment is avoided and it can be applied both organic and inorganic samples [10].

Direct analysis of solids by ETAAS includes two methods namely slurry and solid sampling. Slurry sampling combines the advantages of solid sampling and liquid

sampling. Atomizers and injection system used for the analysis of liquid samples are used for the slurry samples as well, but special devices are necessary for solid sampling. Dilution of high concentrated samples is easier with slurry sampling than that of solid sampling since it requires addition of graphite powder to dilute the solid sample [10]. Lopez-Garcia et al. [11] discussed the slurry-based procedures for rapid determination of As and Sb in soil and sediment samples by GFAAS. Slurry sampling for the determination of Hg in sewage sludge samples with ETAAS was performed by Baralkiewicz et al. and samples were analyzed by applying both direct method and method with digestion, resulting in no difference within the methods [12]. Slurry sampling ETAAS was applied for the determination of Pb in several fish samples. Palladium and ammonium nitrate were used as the modifier to obtain better signal. Because of having different sensitivity for lead in various fish slurries and aqueous solutions, the standard additions method was used for the determination of lead in these fish samples. The limit of detection of lead obtained from standard additions curve was about 0.053–0.058 µg/g in different samples [13].

Direct solid sample analysis with graphite furnace atomic absorption spectrometry was applied for the determination of total As in fish and other seafood. A mixture of 0.1% Pd + 0.06% Mg + 0.06% Triton X-100 was used as the chemical modifier, added in solution over the solid samples. The results obtained for several certified reference materials were not different from the certified values [14]. An analytical method was developed by Jesus et al. [15] for the determination of Sb PET container samples using direct analysis by graphite furnace atomic absorption spectrometry.

1.1.2. Metal Atomizer ETAAS

Graphite is the most widely used atomizer material in ETA as it has high purity, high melting point, inertness at high temperature. However, some limitations regarding graphite have led to development of metal atomizers and tungsten has been used predominantly. Tungsten has high melting point (3422 °C) [16]. Tungsten is also a

good electrical conductor; it is ductile and can be formed into different shapes. Tungsten is relatively inert, stable in both air and water and resistant to high concentration of many common acids such as hydrochloric, nitric and sulphuric acid. Moreover, tungsten is relatively inexpensive. All these properties of tungsten make it valuable material for the production of lamp filaments.

Tungsten finds place in analytical atomic spectrometry in the form of tubes, cups, boats, ribbons, strips, boards and wires. Among these forms, tungsten tubes (W-tubes) and tungsten coils (W-coil) have been reported more commonly [17]. Tungsten atomizers are usually purged with a mixture of hydrogen and argon to prevent the tungsten from oxidation at high temperature and provide a reducing environment for the atomization of analyte. When tungsten atomizers are compared with graphite atomizers, tungsten atomizers requires relatively simple power supply. There is no need for extra cooling system as in graphite atomizers, purge gas is sufficient for coolant. In graphite atomization, the determination of carbide forming elements is a limitation. On the other hand, tungsten atomizers are not prone to carbide formation and allow the determination of carbide forming elements. Heating rate of tungsten atomizer (30 K/ms) is approximately 10 times faster than that of graphite atomizer (2 K/ms) [18].

The introduction of tungsten atomizer dates back to 1972 and Williams and Piepmeier used tungsten filament as an atomizer for the first time in the literature [19]. Later, in 1986, Berndt and Schaldach proposed an open system operating with tungsten. In their study, they showed that sensitivity obtained by W-coil atomizer was similar to the graphite atomizer [20]. Since then usage of tungsten devices has been extended to other areas of atomic spectrometry such as ETAES [21] and ETA-LEAFS [22] as an atomizer and ICP-OES [23] and ICP-MS [24] as a vaporizer.

W-coil used as an ETA has been used for the analysis of broad range of samples including environmental waters, soft drinks, wines, milk, biological samples, clinical samples, food, high purity metals and compounds, rocks, soil, minerals, sediments, and even animal feces. Determination of Cd, Cr, Ni, and Pb in synthetic urine reference materials was performed with W-coil AAS system, where the W-coil

served as an atomizer. Their results were in good agreement with the certified values [20]. Silva et al. investigated the use of W-coil as electrothermal atomizer for the direct determination of barium at low concentrations in water samples [25]. Bruhn et al. used different chemical modifiers for the determination of As in biological samples [26]. Ir and Pd were found satisfactory as modifiers and provided better sensitivity compared to without modifier. Ionic liquid based-single drop microextraction preconcentration was coupled to W-coil ETAAS by Wen et al. [27] for the determination of ultra-trace cadmium and detection limit of 0.015 µg/L with 10 µL sample on W-coil was achieved. Pb level in blood was determined with W-coil ETAAS [28] by chelating blood Pb with ammonium pyrrolidine dithiocarbamate and extracting into methyl iso-butyl ketone. 20 µL of the organic phase were injected on the W-coil.

As W-coil atomizer in ETAAS, tungsten tubes find an important place in this area and are applied in analysis of various samples. Tungsten tube atomizers are well-known under the name of tungsten electrothermal atomization (WETA). Tungsten tubes are closed atomizers that have been characterized by nearly ideal isothermal behavior [29]. Aluminum in biological materials [30], beryllium in waste water [31] and manganese in river and sea-water reference materials [32] with a tungsten tube atomizer were investigated.

1.1.3. Interferences

Mainly two types of interference may occur in ETAAS studies. These are physical and chemical interferences. Physical interferences may be originated from differences in viscosity and surface tension, resulting in different degrees of wetting of the graphite tube surfaces with the sample solution. Moreover, changes in the diffusion of the sample solution into the graphite lead to physical interference. The first can be overcome with using a surfactant in the sample solution. The second effect can be suppressed by using pyrolytically coated graphite tubes.

The chemical interferences may stem from analyte loss during ashing stage. This kind of interference occurs specially with volatile elements such as As, Sb, Bi and Cd and elements forming volatile compounds. The analyte loss can be result from the formation of thermally stable compounds such as carbides and oxides that cannot be dissociated further and prevent analyte to atomize, lowering the signal. Pyrolytically coated graphite tubes can minimize this effect [6]. The non-spectral interferences in ETAAS have been assigned to gas-phase combination reactions between analyte and matrix decomposition products in the atomization step, blockage of analyte atoms in microparticles of matrix in the condensed phase that are gone out of the tube without decomposing in the atomization stage, formation of volatile compound between analyte and matrix before atomization and its loss by vaporization during atomization or pyrolysis stage depending on temperature. All these lead to suppression of the analyte sensitivity [33].

The usage of matrix modifiers in ETAAS provide analyte to separate from matrix, therefore physical and chemical interferences can be removed. The matrix modifiers are applied to decrease the volatility of analyte in order to prevent loss of analyte during pyrolysis, to transform all chemical forms of analyte species into a single form to atomize them at once and to volatilize matrix elements to prevent interference at atomization stage [34]. Many different modifiers have been used in ETAAS, however Pd+Mg nitrates have been most widely used modifiers that can be used for most of the analyte [35].

Oliviera et al. [36] investigated the influence of Na, K, Ca and Mg on lead with W-coil atomizer. The effect of Ca^{2+} and Mg^{2+} on atomization of Pb was less than that of Na^+ and K^+ . The interference effects of these elements on the atomization of Al, Ba, Cd, Co, Cr, Pb and Yb were discussed regarding the effect of protective gas composition in the atomization process. Ca was found to be the most serious interferent due to its high thermal stability (up to 1600°C) and to the possibility of double oxides formation [37]. Chemical modifiers in W-coil atomizer have been employed firstly for determination of Ba in water samples in 1994. The interference caused by larger amounts of Ca was minimized by the addition of ethylenediaminetetraacetic acid (EDTA) [25]. Permanent chemical modifier was

used for W-coil atomizer by Hou et al. The coil was treated with Ir with thermal decomposition and this coated surface was used for the determination of Se[38] .

1.2. Electrothermal Vaporization (ETV)

In all atomic spectrometric methods, one of the most important steps is sample introduction technique. The analytical performance of a method is highly dependent on the employed sample introduction technique. An ‘ideal’ sample introduction technique has to have high sample introduction efficiency, require low sample mass and be capable of analyzing different kind of samples having complex matrices [39]. However, it is difficult to meet these requirements even with the nebulization that is the most popular sample introduction technique in atomic spectrometry.

The most common sample introduction technique is pneumatic nebulization. However, it has some weak points including low transport efficiency (1-10 %) [40], large sample mass requirement, risk of blockage in nebulizer especially with solutions with high dissolved solid content and slurry samples [39]. In addition to nebulizers, hydride generation and liquid chromatography have served as sample introduction technique in atomic spectrometry. Laser ablation is also used for the introduction of solid materials to high temperature ionization source [41].

The electrothermal vaporization (ETV) technique that is developed from the atomizer source of graphite furnace atomic absorption spectrometry (GFAAS) has become an important device for the sample introduction to independent detection systems such as ICP-OES and ICP-MS. It has prominent properties compared with pneumatic nebulization. Firstly, sample introduction efficiencies are increased, resulted in lower detection limits. Secondly, the sample volume is minimized with ETV. The effects of matrix interferences are also decreased with applying appropriate sample pretreatment procedure. Finally, it can be employed for the direct analysis solid samples [39]. All these properties make ETV an attractive tool for sample introduction technique in atomic spectrometry. The most widely used device for ETV is the graphite tubes. Metal types of atomizers are also used as vaporizers.

1.2.1. Graphite Furnace ETV

Graphite furnace that is used as an atomizer in GFAAS has been used predominantly in ETV devices. The first graphite furnace ETV inductively coupled plasma emission system was introduced by Kirkbright et al. in 1978. Graphite rod vaporizer was used for the introduction of sample through 20 m distance to ICP-OES [42].

Graphite furnace employed as a vaporizer suffers from memory effect at high temperature due to analyte transfer into the inner surface of graphite tube and formation of refractory carbides. Pyrolytically coated graphite tubes or metallic carbide coated tubes can improve the performance of graphite furnace ETV [43].

The role of graphite furnace in ETAAS and ETV-ICP-OES/MS is completely different. For ETAAS, graphite furnace is not only a vaporizer but also an atomizer. The sample is dried, ashed and finally atomized. However, for ETV-ICP-OES/MS systems, the graphite furnace serves as a vaporizer only, in which sample is dried, ashed and vaporized. In this case, vaporized species from graphite furnace are transported into ICP, where excitation/ionization of the analyte takes place, thus graphite furnace is adjusted as a sample introduction device.

Analyte loss during transport of analyte species from the ETV unit to the excitation/ionization source is one of the potential disadvantages of ETV sample introduction technique. Non-linear calibration curves is the indication of analyte loss during transportation, but they become linear after addition of salt and Pd [44]. The first theoretical study regarding the analyte transport between ETV and the ICP source was carried out by Kantor [41]. The transport of analyte vapor from the ETV surface is dependent on the formation of stable nuclei of size exceeding a critical diameter. By increasing the analyte masses vaporized in ETV, the critical diameter decreased and this resulted in enhancement of the transport efficiency.

Inductively coupled plasma mass spectrometry (ICP-MS) coupled with slurry sampling electrothermal vaporization has been applied to determination of As, Cd, Hg and Pb in 0.5% (m/v) slurries of several herb samples. 1.0 % (m/v) 8-Hydroxyquinoline was used as the modifier to enhance the ion signals. The detection

limits obtained from standard addition curves were about 0.3, 0.1, 0.1 and 0.2 ng/g for As, Cd, Hg and Pb, respectively, in original herb samples [45]. The determination of Cu, As, Hg and Pb in vegetable oils was carried out with by ETV-ICP-MS. The oils were injected in the form of emulsions containing 5.0 % (w/v) vegetable oil, 1.5 % (v/v) Triton X-100 and 50 µg/mL ascorbic acid. Palladium nanoparticles (Pd-NPs) were used as modifier. The detection limits obtained from standard addition curves were 0.4, 0.5, 1.1 and 0.4 ng/g for Cu, As, Hg and Pb, respectively, in the original oil samples [46]. Determination of Cu, Cd, Pb, Bi and Se(IV) in sea-water with on-line separation using a flow injection system [47] and Co, Cu, Fe, Mn, Ni and V determination in diesel and biodiesel samples [48] were performed by graphite furnace ETV ICP-MS.

1.2.2. Metal Vaporizer ETV

Although graphite furnace is predominantly used as ETV devices in atomic spectrometry, metal vaporizers have also been used. Among the metals tungsten is more attractive because of its mass production, ease of use and small requirement for power supply. Tungsten coil ETV (W-coil ETV) has been used as an electrothermal vaporization sample introduction system in atomic absorption, emission and fluorescence spectrometry [49]. It has been used for the analysis of liquid, solid and slurry samples.

Tungsten coil ETV (W-coil ETV) has been used as electrothermal vaporizers for ICP. Since the vaporization of the sample takes place in the vaporizer, the plasma energy itself is not required to desolvate the sample; therefore more energy is available for atomization, ionization and excitation [50]. Simultaneous determination of 10 elements was achieved with W-coil ETV system coupled to ICP-OES by Levine et al. [51]. Picogram-level LODs were achieved and linear dynamic ranges were 3–5 orders of magnitude. W-coil was used for the thermal separation of Pb from elements, which may cause spectral interference, such as aluminum, manganese and iron, by use of a temperature ramp [52]. Davis et al. [53] used ETV ICP-AES to

determine Cd in urine samples. W-coil vaporizer was treated with Pd modifier and a detection limit of 0.2 µg/L was obtained. Moreover, total carbon in soft drink was determined using W-coil vaporizer with ICP-AES [54].

As with ICP-OES, ETV is an attractive sample introduction device for also ICP-MS due to high transport efficiency, potential for separation of matrix interference, being applicable for microamounts of liquid, solid and slurry samples. Graphite tubes are the most commonly used atomizers for ETV approaches. However, the disadvantage of graphite vaporizers include the occurrence of isobaric interferences by carbon species (i.e. ^{52}Cr and $^{40}\text{Ar}^{12}\text{C}$), the formation of refractory analyte carbides, and the limitation to vaporization temperatures below 2600 °C [17]. A tungsten coil is used to decompose the organic matrix and vaporize biodiesel samples for determination of P and Si electrothermal vaporization inductively coupled plasma mass spectrometry (ETV-ICP-MS) [55]. 10.0 µL sample aliquots are introduced manually on the coil with a micropipette. Limits of detection obtained for P and Si were 0.4 and 0.1 mg/kg, respectively.

The use of W-coil as an ETV device for the sample introduction to AAS is rather rare in comparison with ICP-MS. In AAS, using W-coil as an ETV device takes the advantage of formation of hydrides. The gaseous sample is trapped W-coil, with the release from W-coil, the analyte is liberated from matrix and transferred to atomizer. Cankur et al. developed a method for the determination of Bi in both water and geological matrices and W-coil serves as an ETV device in this study [56]. On-line trapping of Bi hydrides was carried out with W-coil that is placed within the inlet arm of externally heated quartz T-tube atomizer (EHQTA). The precision of the analytical system was found to be 5.8% RSD for 0.010 ng/mL. A detection limit of 0.0027 ng/mL (3s) was obtained with 18 ml of sample volume.

W-coil can be employed as sample introduction device also for Atomic Fluorescence Spectrometry (AFS). W-coil ETV was coupled to an Ar/H₂ flame atomic fluorescence spectrometer for the determination of eight traditional hydride-forming elements (i.e., As, Bi, Ge, Pb, Sb, Se, Sn, and Te) as well as Cd without chemical vapor generation [50]. 20 µL sample was manually pipetted onto the W-coil and

followed by a heating program to dry, ash and vaporize the sample. Analyte was vaporized off the coil surface and transported into the quartz tube atomizer of AFS for excitation of atomic fluorescence. The atomization took place in Ar/H₂ flame.

1.2.3. Interferences

The determination of elements at trace level in samples having complicated matrix is often problematic because of presence of interference. The outcome of matrix effect is the deterioration of the precision and accuracy of the results. Matrix components can cause nonspectroscopic interferences that can either suppress or enhance the signal. ETV devices offer the ability to separate sample matrix components from the analyte, thus reducing matrix interferences. The first step of analysis done with ETV is the drying. The next step is thermal decomposition that leads to pyrolysis of the sample matrix to minimize interferences. In this step modifiers are used generally, in gaseous, liquid and solid form, to enhance the efficiency of ashing and transport processes. The last step is evaporation process and transfer of products of evaporation into the atomizer. Separation of volatilization of the sample matrix and that of the analyte with the reduction in occurrence of spectral and non-spectral interferences is achieved by ETV-ICP-MS system [43]. Moreover, it is indicated that the tolerance towards the interference with ETV-ICP-MS is 10-25 times more than that is obtained by pneumatic nebulization [39].

1.3. Vapor Generation

Atomic spectroscopy methods are categorized into three groups regarding the interaction of radiation with free analyte atoms. These are atomic emission spectroscopy (AES), atomic fluorescence spectroscopy (AFS) and atomic absorption spectroscopy (AAS). In AES, the analyte is thermally atomized and free analyte atoms are excited usually by ICP. The return of excited atoms to lower energy levels produces emitted radiation and emission spectrum obtained by this way is used for

qualitative and quantitative analysis. In case of AFS, the analyte is atomized thermally and atomized analyte is irradiated by monochromatic radiation. Excited free analyte atoms return to lower energy states and emission occurs. The detection of emission gives information about concentration of the analyte in a sample. In AAS, atomization take place thermally; however in some case non-thermal atomization is also possible. The monochromatic radiation from a line source passes through the atomized species and the light is absorbed by the free atoms of analyte. Finally absorption detected by the system is used for the determination of analyte in the sample quantitatively.

Elements in the samples are determined sensitively by all atomic spectroscopy methods. AAS is the most popular method used in the atomic spectroscopy, since it is moderately economical regarding its investment and running costs. Moreover, it is robust and a well-established technique. AFS, is another method for its relatively low cost and ease of use. Its sensitivity is higher than that of AAS. ICP-AES is a multielement method and it requires a rather complicated apparatus compared to AAS and AFS.

The sensitivity of flame AAS is relatively low as compared to other atomic spectroscopy methods. The sensitivity problem originates from low efficiency of sample introduction and short residence time of the free analyte atoms in the measurement zone. The first problem is arising from nebulization in which the efficiency is around 1-10%. Therefore, most of the sample is not transferred to the atomizer. In addition, there is a dilution of sample by flame gases and resulting analyte concentration in the measurement zone is relatively low. The second deficiency was the short residence time of the free analyte atoms in the measurement zone that is few milliseconds. These deficiencies limit the sensitivity of AAS and improvement is required. ETAAS, cold vapor AAS (CVAAS) and hydride generation AAS (HGAAS) are introduced as sample introduction techniques and they provide 100-1000 fold sensitivity improvement compared to flame AAS [40].

In atomic spectroscopy, sample is introduced to the system in liquid, solid and gaseous phase. Gaseous phase sample introduction is achieved by vapor generation

(VG) where the analyte from the liquid sample is converted to gaseous phase by a chemical reaction. The set up of the VG system is relatively simple and the apparatus used for the set up has low cost. The matrix effects are eliminated by the separation of analyte from the matrix by VG and resulting in reduced interference. The limit of detection (LOD) is improved by efficient transportation of gaseous analyte to the atomizer. Another advantage of VG is its applicability to preconcentration of analyte [57,58] and elemental speciation analysis [59–61].

Numerous approaches are available for VG such as hydride generation (HG), alkylation, halide formation, and metal carbonyl generation [62]. HG is the most popular because of its easy implementation, fast reaction, and high yield. Moreover, alternative strategies are developed for VG in non-tetrahydroborate media by use ultraviolet radiation [63]. The use of photochemical vapor generation (photo-CVG), borane complexes for CVG, alkylation based on Grignard reactions, derivatization with tetraethylborate, cold vapor generation with stannous chloride, halide generation, electrochemical hydride generation, oxide generation, and formation of volatile chelates were reviewed [64]. Photo-CVG has brought an alternative approach of generation of volatile species for sample introduction in atomic spectroscopy methods.

1.3.1. Hydride Generation AAS

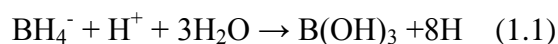
Hydride generation (HG) is a widely used sample introduction technique in which the analyte in an acidified sample is converted into volatile compound by a chemical or electrochemical reaction [65–67]. The first application of hydride generation as a sample introduction technique in AAS was introduced by Holak in 1969 for the determination of As [68]. The hydride species from As was produced from addition of Zn into solution containing hydrochloric acid and formed arsine was collected in a trap cooled with liquid nitrogen. When the reaction was ended, the trap was heated and arsine in nitrogen stream was transported to an argon-hydrogen diffusion flame

to obtain the absorbance measurement. Since then, the advantages of HG have been applied to all elements capable of forming volatile hydrides.

The earliest method utilized for HG was addition of Zn metal into sulphuric or hydrochloric acid solution. However, currently it is not used because of the more convenient reaction with tetrahydroborate (THB).

The most widely used technique for the generation of hydrides from mercury and cadmium cold vapors are the reaction of THB with in acidic medium due to the reduction of metal/acid. THB reaction is applicable for its high reduction yield, short reaction time, low blank contamination and ease of applicability for hydride forming elements. The most popular hydride forming elements are As, Se, Sb, Bi, Te, Ge, Pb and Sn [69]. Recently, transition and noble metals have been involved in HG following the reaction with THB [70], therefore making HG even more attractive as a sample introduction method for atomic spectroscopy.

The reaction mechanism between analyte and THB in acidic medium was firstly proposed by Robbins and Caruso in 1979 regarding the nascent hydrogen mechanism [71]. This theory is based on the hydrogen production after decomposition of THB in acidic medium:



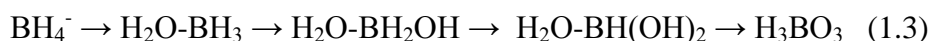
The produced nascent hydrogen reduces analyte to hydride:



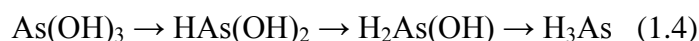
where m and n respectively are the valency of the analyte A in the sample solution and in hydride. Experimental proof for this mechanism has not been provided.

Although the nascent hydrogen mechanism has not been proven, it was generally accepted until D'Ulivo and coworkers closed out the nascent hydrogen mechanism persuasively and developed an alternative "hydrogen-transfer" theory [72]. The hydrogen-transfer theory includes two chain reactions. The stepwise hydrolysis of THB occurs in the first chain reaction and then the reaction keeps on with three

hydrolytic intermediates to boric acid; the loss of single B-H bond takes place in each step:



All hydroboron species can be present at least once in a reaction mixture depending on the pH of the medium. Each of four hydroboron species can react with the analyte in the second chain reaction in which hydrogen transfer from hydroboron species to the analyte occurs. In the following equation (1.4), arsenous acid is converted to arsine via the chain reaction. It contains three steps and in each step one OH group is substituted by a H atom:



As a sample introduction technique, HG has been applied for the analysis of various samples and can be coupled to any atomic detection systems. HG coupled to AAS has been of great importance since it eliminates the low sample transport efficiency with nebulization systems. Inorganic As species in ground water and synthetic experimental matrices were determined by Sigrist and Beldomenico [73] with hydride generation coupled to AAS using a flame-heated quartz atomizer. Elçi et al. [74] developed a method for the direct determination of Pb in wine and rum samples by using flow injection HG system coupled to AAS with flame-heated quartz atomizer. HG coupled to AFS has been used because of its wide linear dynamic range, low noise level, high sensitivity, speed of analysis, ease of operation, and low cost [75–77]. This system has been employed for the determination of As, Sb, Se, Te and Bi in milk sample [78], Se in vegetables [79], As, Bi, Te and Se in tea leaves [76]. In the last decade, interest has been arised in determining multiple hydride-forming elements, using ICP-OES [80–82] and ICP-MS [83,84].

As it is written above, the scope of HG has been expanded to several noble and transition metals [70]. Ag, Au, Cu, Zn, Cd, and As were determined by VG at room temperature by the addition of sodium tetrahydroborate(III) to an acidified solution of the analytes. LOD was ranging from 1.8 (Zn) to 420 ng (Au). The efficiency of the generation process is estimated to be $92 \pm 4\%$ for Au [85]. A vapor generation

process for the production of volatile species of Ag was developed by using AAS and ICP-OES detection. A characteristic mass of 0.12 ng was obtained using a miniature diffusion flame atomizer-AAS system, whereas a 38-fold higher sensitivity compared with conventional liquid nebulization was obtained with ICP-OES [86].

Electrochemical HG (EcHG) involves an electrochemical reaction yielding production of volatile species in an acidic medium. It employs electric current instead of a reducing chemical agent. This technique has been applied for the generation of hydrides from As, Bi, Cd, Ge, Sb, Se, Sn, and Tl and elemental Hg vapor in an electrolytic cell for analytical purposes in recent years [69]. The basic cell for EcHG consists of two compartments that are the anodic and cathodic spaces. HG takes place with sequential events. The analyte is diffused from solution to the cathode surface where it is reduced to its elemental state and deposits on the cathode surface. Hydride formation takes place and hydride species diffuse to the solution. The marked advantage of EcHG is the elimination of THB which is a potential source of contamination. Thus, the limit of detection can be improved. Arbab-Zavar et al. [87] developed a method for the determination of Cd in water samples by using electrochemical hydride generator. The limit of detection obtained by this system was 0.61 ng/mL.

1.3.1.1. Atomization in HGAAS

The final step for the determination of elements employing hydride generation is atomization and detection. Hydride atomization is the conversion of analyte hydrides into free analyte atoms with maximum efficiency and has to be optimized to obtain sufficient accuracy and signal-to-noise ratio.

The most frequently employed atomizers are conventional quartz tube atomizers (QTA), miniature diffusion flame (MDF), flame-in-gas-shield (FIGS), multiple microflame quartz T-tube atomizers (MMQTA), graphite furnaces, metal atomizers and metal furnaces.

Quartz tube atomizers are generally T-tube and horizontal arm is placed in the optical path of AA spectrometer. Generated hydride species are carried by gas stream flowing from the hydride generator and are brought to the atomizer from the inlet arm of the T-tube of the atomizer. QTA can be heated by either electrical resistance or air-acetylene flame to a temperature between 700 °C to 1100 °C. Thompson and Thomerson were the first at heating the atomizer with air-acetylene flame [88]. The first usage of electrically heated atomizer was introduced by Chu et al. [89].

Miniature diffusion flame (MDF) has simple design consisting of vertical quartz tube from which argon/hydrogen mixture is introduced with the hydrides of analyte to the atomizer. The temperature of MDF is ranging from 150 °C to 1300 °C. There is inhomogeneity of temperature between the outer and inner zone of the flame. The minimum temperature is observed in the lower part of the MDF, whereas the highest temperature profile is obtained in the outer zone of the flame where the reaction between hydrogen and ambient oxygen takes place. Hydrogen radicals are generated in the outer zone of the flame by the reaction between hydrogen and oxygen. Produced H radicals can diffuse into cooler inner parts of the flame, thus whole flame contains high concentration of H radicals that promote efficient atomization of analyte hydrides. The disadvantage of MDF is the short residence time of free atoms in the optical path and high atomizer noise [90–92].

Flame-in-gas-shield (FIGS) atomizers can be used in AAS and AFS. The design of FIGS is similar to MDF except the quartz capillary is inserted inside the quartz support tube. Very low flow of oxygen is introduced to burn the excess hydrogen at the end of the capillary to generate H radicals. Argon gas was used for shielding to protect the flame from ambient atmosphere [92].

Despite having some advantages, QTA has also drawbacks such as poor linearity, low resistance to atomization interference, insufficient H radicals concentration for hydride atomization. These drawbacks are mainly overcome by the introduction of new generation quartz tube atomizer that is MMQTA. The MMQTA consists of two concentric tubes. The inner tube contains small orifices along the tube. Gas containing oxygen is introduced through the outer tube and it enters from the orifices

of inner tube to react with the hydrogen present in the inner tube. Thus, microflames are generated at each orifices resulting the high H radical concentration along the tube [92,93].

Electrothermal atomizers have been used for on-line atomization of hydrides since the beginning of HG application. On-line hydride atomization in graphite furnaces takes place directly in furnace preheated to atomization temperature. On-line hydride atomization in GF has not been widely used since the coupling HG system to the GF atomizer is not convenient. In addition, *in situ* trapping of hydrides in the GF has been exclusively used for hydride atomization [94]. In-situ trapping in GF will be discussed in the following section.

Tungsten coil has been used as a substitution for GF in atomization of liquid samples and detailed information regarding W-coil as ETA was given in section 1.1.2. It has found place in literature for hydride atomization since it has advantages over GF. Ribeiro et al. used W-coil placed in quartz T-tube for atomization of arsine [95] and bismuthine [96].

Flame heated metal furnace made of Ni, Cr and Fe was used as a hydride atomizer [97,98]. Flame heated metal furnace was used for the Sb determination in environmental and pharmaceutical samples [98]. The detection limit obtained for Sb was 0.23 ng/mL. It is reported that metal has low cost and long lifetime compared to QTA.

1.4. *In situ* Atom Trapping Techniques

In situ trapping of hydrides is a valuable tool for preconcentration of analyte that makes possible to perform trace and ultrace analysis. *In situ* trapping is basically collection of analyte atoms on an appropriate surface/medium followed by transport of analyte to the detecting system as fast as possible. The trapping medium should fulfil the requirements including efficient trapping and easy releasing for the trapped

analyte atoms with minimum loss. Graphite, quartz and tungsten have served as trapping materials.

1.4.1. Graphite Furnace Trap

Trapping hydride species on the graphite tube surface is an easy and efficient way applied in the literature. Drasch et al. described the method of trapping hydrides in atomizer and subsequent atomization [99]. In this method, arsine was carried by a carrier to the GF heated to certain trapping temperature. Analyte adsorbed on the graphite surface was released and atomized at about 2000 °C.

Hydride introduction to the graphite tube is a critical step in terms of trapping efficiency; analyte should be introduced with minimum loss. There has to be an interface between hydride generator and GF. The most exclusively employed interface between hydride generator and GF is quartz capillary. It is inserted via sample port into the graphite tube [94]. The schematic representation of graphite furnace atom trapping system is given in Figure 1.1.

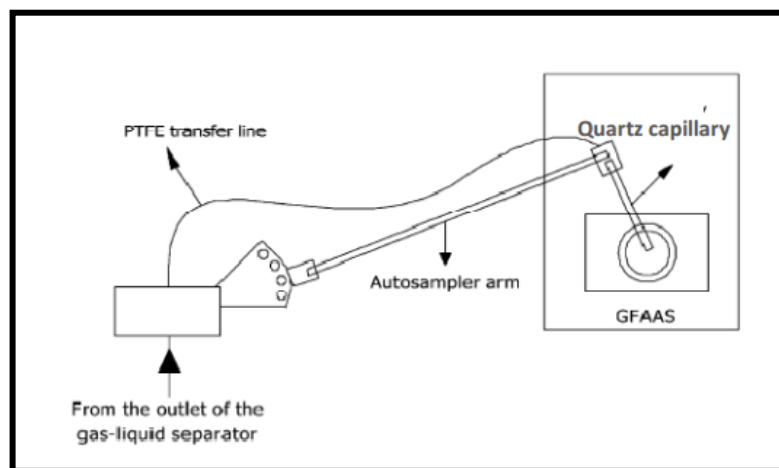


Figure 1.1 The schematic representation of GF atom trapping system [100].

It is recommended that quartz capillary should be positioned on the graphite inner surface as close as possible [92]. The first step of the *in situ* atom trapping in a GF is the introduction of generated hydrides from a gas-liquid separator via the quartz capillary interface into the inner surface of GF that is heated to trapping temperature (200-600 °C). During trapping period, the quartz capillary is kept inside the trapping medium. Secondly, when trapping period is over, quartz capillary is removed from the GF and trapped atoms are volatilized and atomized at a temperature greater than 2000 °C. A cleaning step is recommended to purify the graphite tube from water vapor and hydrogen. There are several studies in the literature regarding *in situ* atom trapping in GF. *In situ* trapping of H₂Te in a preheated GF whose surface was modified with Pd and Ru was performed [101]. 173-fold enhancement with respect to ETAAS was obtained for Ru coated graphite tube. LOD values 0.0064 and 0.0022 ng/mL for Pd and Ru treated ETAAS systems, respectively, for 180 s collection of 9.6 mL sample solution. Cd determination was performed with its *in situ* trapping in a Ir treated graphite furnace atomizer [102]. Volatile Cd species were generated by electrochemical hydride generation technique and LOD of the system was 1.0 ng/mL. Masrournia and Shadmehri [103] performed determination of Sn(II) by electrochemical hydride generation coupled to *in situ* trapping in graphite tube atomizer with a detection limit of 0.8 µg/L.

Sensitivity of the system can be improved by surface modification using high boiling point metals [104] and carbide-forming elements [105–107]. Application of temporary and permanent modifiers makes the lifetime of graphite tube longer and lowers the trapping and atomization temperatures. Sturgeon et al. investigated the applicability of Pd, Pt, Rh and Ru for surface treatment for the efficient trapping of volatile As, Sb, Se, Bi and Sn [108]. A method has been proposed for the determination of As by GFAAS with HG and *in situ* trapping using Pd–Zr chemical modifier [109]. The highest pyrolysis temperature and adsorption efficiency of arsine were achieved when Pd–Zr mixture was used as chemical modifier. The characteristic mass of the method was 18 pg and the absolute detection limit obtained for the developed method was 15pg.

1.4.2. Quartz Atom Trap

Another promising approach for atom trapping is the collection of hydrides on a quartz surface. The trapping medium can be either inlet arm of the quartz T-tube or crushed quartz pieces inserted in the inlet arm of the quartz T-tube and the atomization takes place in QTA [110–112]. The trapping medium is heated externally to trapping temperature. After the trapping period is finished, temperature is raised to revolatilization temperature. At this temperature, revolatilized species can be either atoms or molecules. As a result, the atomization of molecular species takes place. At revolatilization stage, H₂ gas is introduced to the system to obtain a reducing environment to make revolatilization of the trapped species easy [113].

Further improvement is performed with the replacement of QTA with MMQTA. One of the drawbacks of using quartz trap coupled to QTA is the consumption of trace amount of oxygen required for atomization of analytes such as As, Se, Sb etc. during trapping. This drawback is avoided by using MMQTA and the advantage of using MMQTA for atomization of analyte volatilized in the quartz tube trap is that it uses a separate oxygen supply to the atomization zone. As a result, the production of H radicals in the optical tube of the multiatomizer is not controlled by the oxygen contamination of gases introduced into the atomizer but by the supply of oxygen in the outer gas [114,115].

1.4.3. Metal Atom Traps

Metal surfaces have been used as in the literature. They are preferred because of the unnecessary requirement of external heating, heating resistively and high heating rate that make the control of changing temperature to the desired value easily.

An alternative to quartz and GF, W-coil has been employed most widely among the other metal traps for *in situ* trapping applications. W-coil can be resistively heated by passing electricity directly through the W-coil, whereas quartz trap requires an external heating system. Thus, higher heating rates can be obtained for W-coil than

the quartz trap. W-coil is obtained from a commercially available projector lamp, and thus it is obtained economically and readily. W-coil has first been used at about the same time as a trap for the determination of Bi and Se by two independent groups. The first group used W-coil in combination with a T-tube atomizer [56], whereas W-coil was used as both trapping medium and atomizer by the second group [116].

One of the application of W-coil proposed by Cankur et al. [56], W-coil is utilized in a way similar to quartz trap. It was placed in the inlet arm of the quartz T-tube of the QTA and connected to the power supply (Figure 1.2). The process of this system includes the trapping of generated hydrides on the surface of resistively heated W-coil, revolatilization of trapped species by increasing coil temperature when trapping period is over, lastly atomization of revolatilized species transported to atomizer (QTA) with purge gases. This system was used for the determination of Bi [56] and Cd with CVAAS [117]. The similar method was used for the determination of Sb [118] and Se [119]. The W-coil was used as an electrothermal vaporizer in addition to its usage as a trap in these studies. A separate ETV unit with W-coil coupled to AFS detection was employed as a sample introduction system for the determination of Bi [120] and inorganic speciation of As [121]. The use of W-coil was combined for hydride trapping and ETV sample introduction.

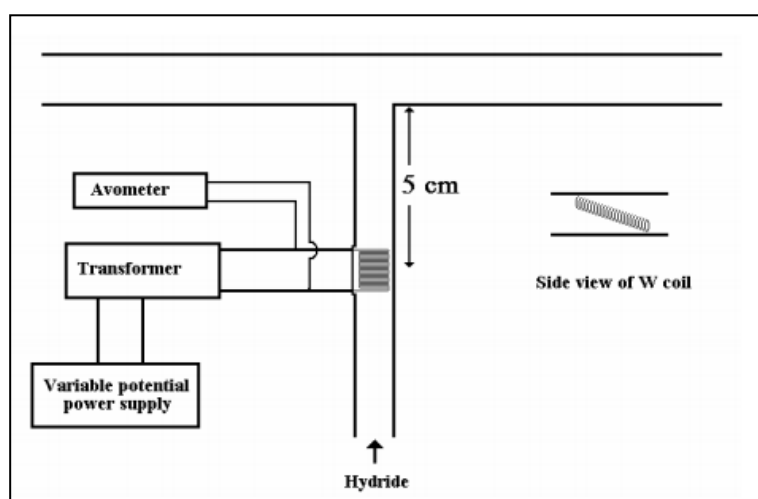


Figure 1.2 W-coil atom trap placed inlet arm of the quartz T-tube [56].

The other application is the usage of W-coil as both *in situ* trap and electrothermal atomizer. Souza et al. determined As and Se in biological and water samples by *in situ* hydride trapping in a W-coil atomizer [122]. Moreover, the determination of Sb [123] and Sn [124] were reported using Ir coated W-coil which served as both the trap and the atomizer.

W-coil surface can be coated with elements having high boiling and melting points. Trapping efficiency and interaction between trapped species and tungsten surface can be improved by surface modification of W-coil. W-coil was treated with Ir for trapping Sb hydrides [123]. It was stated that uncoated W-coil yielded poor sensitivity, broad and irreproducible signals. When W-coil was coated with Ir, significant increase in antimony signal was observed. Moreover, Barbosa et al. used an Rh coated W-coil for trapping selenium hydride and reported that coating was stable up to 300 measurements. Approximately, 2000 firings were possible with same W-coil [116].

For *in situ* trapping and HG systems, alternative metal traps have been suggested. A molybdenum foil strip for the determination of Sb and Bi [125], resistively heated platinum for Cd [126], an externally heated Au wire for Se [127] are studied dealing with alternative metal atom traps.

1.5. Interferences

HG provides the analyte separation from the matrix and this brings the advantage of reduced or eliminated interference. Moreover, sensitivity enhancement is achieved and preconcentration of the analyte is performed with the help of HG. However, some serious non-spectral interference may occur during hydride formation, transfer of analyte from solution and atomization. This is the main drawback of the system [128].

Mainly, source of interference may be categorized into two groups, namely; liquid-phase interferences and gas-phase interferences. Liquid-phase interferences take

place during hydride formation and hydride transfer from the solution to gas/aerosol phase. Volatile form interferent or interferent as a liquid spray causes gas-phase interferences.

In interference studies, detailed effects of gas phase interferences have been investigated by using twin-channel continuous flow hydride generator. In this set up analyte and interferent hydrides are generated separately in different channels. Analyte and interferent hydride come together upstream of gas liquid separators and are sent to the atomizer. D'ulivo and Dedina used twin-channel hydride generator to investigate interferences of As in Se atomization [129]. Twin-channel generator was used to eliminate liquid phase interference. A twin-channel hydride generation system was used for independent separate generation and introduction of analyte and interferent hydrides, i.e. in a simultaneous and/or sequential analyte–interferent and interferent–analyte mode of operation [130].

1.5.1. Liquid phase interferences

Liquid-phase interferences are observed in two groups; i) compound and ii) matrix interferences [94]. Both compound and matrix interferences are in the class of non-spectral interferences.

Compound interferences may result from the different forms of analyte present in the sample solution that causes the release of hydride to be different in time and amount for the sample and standard solutions. This situation is generally observed when organic bonds of the analyte cannot be decomposed completely during sample pretreatment and when the different valencies of analyte forms hydrides at lower efficiencies. The most serious inorganic compound that causes matrix interferences are ions of transition and noble metals e.g. Ni, Cu, Co, Fe, Ag, Au, Pd, Pt, and Rh [69].

As it is reported above, the most widely used reductant for HG is THB. The liquid-phase interferences can be originated from the competition between analyte and

interferent to react with THB at a given time, since there is always time limitation for analyte to react with THB. Suppression of analyte signal can be observed when interferent reacts more rapidly with THB than analyte. For instance, Se reacts more quickly than As with THB, thus the interference effect of Se on As is more effective than that of As on Se [131].

Analyte/analyte hydride and interferent may form insoluble precipitates that causes interferences in liquid-phase. The interference effect of Se and Te on Sb, As on Se, Te on As, Bi, Se and Sn were explained by formation of precipitates of the type Bi_2Se_3 , Sb_3Se_3 and GeSe_2 [132]. Generally this effect is observed in case of batch HG procedures. The usage of dilute hydrochloric acid could remove the precipitates by preventing the formation of insoluble compounds.

1.5.2. Gas-phase interferences

Gas-phase interferences can be divided into two groups according to the location they appear; transport and atomization interferences. Transport interferences may occur through the hydride generator and atomizer and cause delay and/or loss of analyte hydride. Atomization interferences depend on the hydride atomization mechanism and on the transfer of analyte to the atomizer [92].

Two mechanisms regarding interferences could be expected for atomization. First mechanism is related with the radical population in which interferent changes the hydrogen-free radical population in the atomizer. Interferent competes with analyte for hydrogen-free radical required for atomization and speeds up the recombination of analyte atoms resulting in polyatomic species, or particles. Second one is the analyte decay that takes place when the interferent accelerates the decay of free analyte atoms through the reaction between analyte and interferent in the gas phase [92,133]. The analyte decay type of interference takes place dominantly with the reaction of free analyte atoms in the free space. It occurs at high analyte concentration that causes formation of polyatomic species or particles by the

interferent atom recombination. The polyatomic species or particles speeds up the decay of the free atoms.

1.6. Bismuth

Bismuth is the member of Group VA of the Periodic Table of the elements. It has a typically metallic character and similar properties with lead, arsenic and antimony. The metal has an atomic weight 208.98, atomic number 83, density 9.79 g/cm³, melting point 271.3 °C, boiling point 1560 °C. Bismuth is the most diamagnetic of all metals, and its thermal conductivity is lower than that of any metal except mercury. It is known since ancient times but it was usually confused with lead, tin and antimony. It is naturally occurring as a stable heavy metal. It is less toxic than lead, that is why the alloys of Bi are replaced for products made from lead [134].

Bismuth is one of the rarest of elements. It was discovered by miners of Saxonia in the 15th century. Bismuth was first described in 1527 by the physician and alchemist Paracelsius (1493–1541). The atomic symbol of Bi was proposed by J. J. Berzelius in 1814. Bismuth occurs less rarely than mercury and also shows a more frequency of appearance as silver. It is found in its native form, and also in minerals such as bismuthite (bismuth subcarbonate, Bi₂O₂(CO₃)) and bismite (bismuth(III) oxide, Bi₂O₃) [135].

1.6.1. Occurrences

Bismuth has low abundance in the Earth's crust that is about 0.00002%. The concentration of Bi in argillous sediments is about 0.5 µg/g. The accumulation of Bi on coals and graphite shales has been reported as 5.0 µg/g [136]. Bismuth is not detectable in drinking water, soil solutions, or river water, however; it is detectable in sea water at low concentrations. Bismuth concentrations vary from 10 to 30 ng/L in seawater and from a few ng to a few µg/L in freshwater [137].

Bismuth occurs in the environment in the form of minerals bismuth ochre (Bi_2S_3), bismuth oxide (Bi_2O_3) and as native bismuth [$\text{Bi}(0)$]. The major species of bismuth in seawater is $[\text{BiCl}_4]^-$. Bismuth is found in the form of Bi^{3+} , BiOH^{2+} and BiO^+ in fresh waters according to the pH and E_h of the medium. In addition to natural occurrence of bismuth, compounds of Bi are introduced to the environment from chemical industry. It is used as a catalyst in the production of acrylonitrile as bismuth molybdophosphate. Bismuth is predominantly used in cosmetic products as pigments in eye shadows and lipsticks and as bismuth citrate in hair dye. Bismuth is consumed as bismuth subgallate in the pharmaceutical market for the treatment of infectious diseases, bismuth germanium oxide as a contrast substance and bismuth subcitrate for ulcer therapy. All these substances finally collected in waste water and enhance bismuth concentration in sewage sludge. Bismuth is found in the range of 5 mg/kg dry weight of sewage sludge, which is even higher than the amounts of antimony and arsenic [138].

1.6.2. Application

The main producers of bismuth are Peru, Japan, Mexico, Bolivia and Canada. The most of the bismuth production is made in USA as a by product while refining lead, copper, tin, silver and gold ores. About 64.5% of the produced bismuth is consumed in United States in low-melting alloys and metallurgical additives, including electronic, photo- and thermoelectronic applications [139,140] in producing malleable irons, as a thermocouple material, as an oxide catalyst [141] as a catalyst for making acrylic fibers, as ceramics [142], glasses, and enamels. Bismuth is also used in pigments in cosmetics and paints include bismuth.

Bismuth is widely used medicinal industry. Bismuth has been used (as tripotassium dicitratobismuthate) for the treatment of stomach upsets, and is used in combination with antibiotics to treat some stomach ulcers. Bismuth is also used (as bismuth oxide) in hemorrhoid creams. Soluble salts such as bismuth subsalicylate, sodium triglycollamate and trioglycolate have been used parenterally to treat infectious

diseases. The most current medical application is in the eradication of *H. Pylori* during the treatment or prevention of gastric and duodenal ulcers [143]. Three bismuth derivatives, bismuth subsalicylate, colloidal bismuth subcitrate and ranitidine bismuth citrate, has been commonly used in combination with antibiotics for this purpose. Bismuth subsalicylate is an inexpensive and effective compound for the treatment of traveler's diarrhea [144].

1.6.3. Human Exposure and Toxicity

Bismuth is not considered to be an essential element for plants and animals. Bismuth concentrations found in food are low, ranging from 0.1 to 1 $\mu\text{g}/\text{kg}$. Dietary intake of bismuth in the UK has been found as 0.4–0.7 $\mu\text{g}/\text{d}$. Higher exposures are reported in other countries like Japan (average 3.3 $\mu\text{g}/\text{d}$) [145]. Bismuth exposure from food and water is in minimal values and the use of medicinal products is the only occasional cases of intoxication of bismuth.

Bismuth is not toxic if administered orally. The LD-50 is 42000 mg/kg and the no-observed-adverse-effect level (NOAEL) is 1000 mg/kg [146]. Toxic effects of bismuth appears in the kidney, liver, skin with large bismuth doses, or with smaller doses repeated over a long period of time. Toxic effects of prolonged exposure of bismuth cause anorexia, nausea, vomiting, colicky abdominal pain and diarrhea [134]. Low amounts of bismuth are taken by healthy gastrointestinal tract, therefore toxic effects are rarely observed with normal intakes of bismuth. When bismuth in blood is below 50 $\mu\text{g}/\text{mL}$, toxicity in human is unlikely to take place [147].

1.6.4. Determination of Bi

Determination of Bi in different matrices has been performed with the application of several analytical techniques. Among the analytical techniques, the most widely employed techniques are ICP-MS, ICP-OES and ETAAS. Multi-element determination including Bi in urine samples were performed with ICP-MS and 5.0

ng/L limit of detection was achieved for Bi in this study [148]. Velitchkova et al. studied the determination of Bi in environmental samples by using ICP-AES with a detection limit of 4.0 ng/mL [149]. Barbosa et al. [150] and Magalhães et al. [151] used direct determination of Bi in urine and whole blood samples by using ETAAS. On-line preconcentration coupled to ETAAS was used for the determination of Bi in urine samples and 13.0 ng/mL detection limit was obtained for this technique [152]. Shemirani et al. determined Bi by using cloud point extraction ETAAS in biological and water samples [153].

Hydride generation coupled to atomic spectrometric methods has been used currently for the determination of Bi in different matrices. Trace amounts of Bi in metallurgical materials was determined with hydride generation AAS and detection limit of 16 ng Bi was achieved [154]. Zhang et al. developed a simple and robust method for determination of Bi with flow injection hydride generation atomic absorption spectrometry [155]. Diverse matrix effects on the determination of bismuth in nickel-based alloys and pure copper by flow-injection hydride generation AAS were investigated. Sodium tetrahydroborate was used as the reductant [156].

Moreover, atomic fluorescence and plasma sources were used together with hydride generation for determination of Bi. The preconcentration of bismuth on a nylon fiber-packed microcolumn was carried out based on the retention of bismuth complex and on-line separation and preconcentration system coupled to hydride generation AFS was used for the determination of Bi in water and urine samples [157]. Feng et al. [158] applied hydride generation system with ICP-AES to determine Bi in a marine sediment material and the limit of detection for the developed method was 1.2 ng/mL. Chang and Jiang [159] introduced vapor generation ETV ICP-MS system for the determination of Bi in several water reference samples. Bi was converted to its vapor form and

collected on platinum treated graphite surface and by desorption of collected Bi species the detection was done with ICP-MS.

1.7. Purpose of the Study

In this study, W-coil Atom Trap ETA and W-coil Atom Trap ETV systems were used to evaluate the performance of ETA and ETV systems with W-coil. For this purpose bismuth (Bi) was selected as the analyte. For the improvement of sensitivity, atom trapping was used and W-coil was used for this purpose. W-coil was coated with rhodium (Rh) for surface modification and to make the life-time of W-coil longer. Both systems were compared with respect to their analytical performance, practical use and resistance to interference elements. As the interference elements, the other most common hydride forming elements As, Sb, Se, Te and Sn were selected.

CHAPTER 2

EXPERIMENTAL

2.1. Instrumentation

Varian AA140 (Victoria, Australia) atomic absorption spectrometer equipped with a deuterium arc background correction system was used for absorbance measurements. Instrument was computer controlled and data were processed by the help of SpectrAA software (version 5.1). Varian High Intensity UltrAA Coded hollow cathode lamp operating at 10.0 mA was used for Bi at the analytical line of 223.1 nm with 0.2 nm spectral bandwidth.

Table 2.1 Operating conditions of Varian AA140

Parameter	Value
Measurement wavelength, nm	223.1
Spectral bandpass, nm	0.2
Lamp current, mA	10.0
Read time, s	10.0
Measurement mode	Peak height

Operating conditions presented in Table 2.1 was used for bismuth, in continuous flow hydride generation, W-coil atom trap ETA, W-coil atom trap ETV and interference studies.

2.2. Chemicals and reagents

All reagents used throughout the studies were of analytical grade or higher purity. 1000 mg/L stock solution of Bi was prepared from bismuth(III)nitrate (Fisher Scientific) in 1.0 mol/L HCl. The working solutions were prepared with necessary dilutions from 10.0 mg/L and 1.0 mg/L that were in 1.0 mol/L HCl. For acidification of working solutions, proanalysis grade HCl was used (Merck, Darmstadt, Germany).

For the interference study, 1000 mg/L stock solution for As(III), Sb(III) and Se(IV), were prepared by dissolving required mass of sodium arsenite (Fisher Scientific, New Jersey, USA), potassium antimony(III) tartrate ($C_4H_4KO_7Sb$) (Sigma-Aldrich), sodium selenite (Ventron, Karlsruhe, Germany) respectively, in deionised water. 1000 mg/L Te(IV) stock solution was prepared by dissolving suitable mass of TeO_2 (Fisher Laboratory Chemical, U.S.A.) in 10% (v/v) HCl (Merck, Darmstadt, Germany) solution by means of Elma S40 H ultrasonic water bath (Germany). 1000 mg/L stock solution of Sn(IV) (Merck, Darmstadt, Germany) was used. In the interference study, transition metals including Fe (High Purity Standards, SC, USA), Co(II) ($CoCl_2$, Merck, Darmstadt, Germany), Cu(II) ($Cu(NO_3)_2$, Merck, Darmstadt, Germany), Ni (from Ni metal, High Purity Standards, SC, USA) and Mn(II) ($Mn(NO_3)_2$, Merck, Darmstadt, Germany) were used. Moreover, Al^{3+} ($Al(NO_3)_3$, Merck, Darmstadt, Germany), Na^+ (Na_2CO_3 , High Purity Standards, SC, USA) and Ca^{2+} ($Ca(NO_3)_2$, Merck, Darmstadt, Germany) were used for the interference studies.

Powdered proanalysis grade $NaBH_4$ (Merck, Darmstadt, Germany) was used to prepare 0.5% (w/v) of reductant solution in 0.2% (w/v) NaOH (Merck). The reductant solution was prepared daily.

High purity Ar (99.999) and high purity H₂ (99.999 %) gases were used (Linde Gaz, Ankara, Turkey) in this study.

Solutions were diluted by using 18 M Ω -cm deionized water obtained from TKA (Thermo Scientific, Stockland, Germany) Pacific PW reverse osmosis water purification system.

Prepared solutions are transported and stored in polypropylene bottles. All glassware and plastic bottles used in the study were immersed in 10% (v/v) HNO₃ solution at least 24 hours and rinsed with deionized water before use.

2.3. Hydride Generation System

The experiments were carried out in continuous flow using Gilson Minipuls 3 (Villers Le Bell, France) 4-channel peristaltic pumps to transport analyte and reductant solutions. Two-stop red-red color coded 1.14 mm ID Tygon® peristaltic pump tubings were employed for pumping analyte and reductant solutions through the peristaltic pump. In order to remove waste solution from gas liquid separator, Gilson Minipuls 3 4-channel peristaltic pump was utilized. The schematic representation of the continuous flow hydride generation system is shown in Figure 2.1.

Solutions were transported by the tubings that were made of polytetrafluoroethylene (PTFE) with 0.56 mm i.d and supplied from Cole Parmer (USA). The reaction and stripping coils were also made from the same PTFE tubing in different lengths. For the junction points of tubing and carrier gas, 3 way T-shaped PTFE connectors (Cole Palmer, Illinois, USA) were used.

High purity Ar gas was required for stripping of solutions and transportation of volatile species to the atomization unit. For experimental studies performed with W-coil, H₂ gas was also introduced to the system. The flow rates of Ar and H₂ were controlled by two separate rotameters (Cole Parmer). The rotameters were calibrated regularly by a soap bubble flow meter.

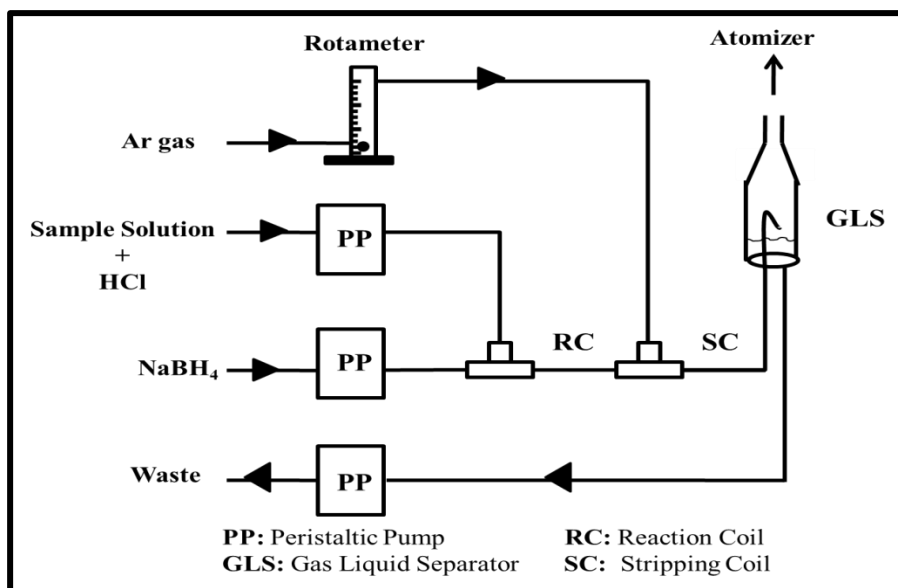


Figure 2.1 The experimental set up for continuous flow hydride generation system for Bi.

Gas liquid separator (GLS) that is made of borosilicate glass was used for the separation of gaseous analyte species from the liquid phase. The design of cylindrical type of GLS used in this study is given in Figure 2.2.

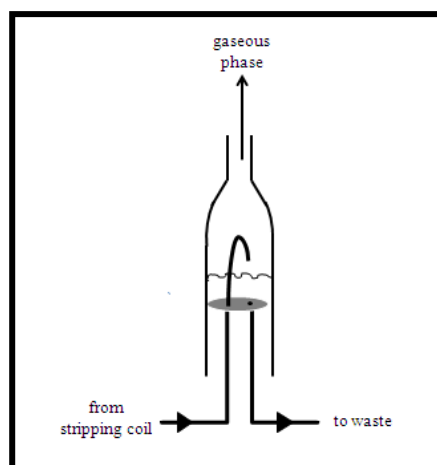


Figure 2.2 Schematic representation of cylindrical type GLS.

2.4. Atomization Units and Atom Cell

2.4.1. Continuous Flow Hydride Generation System

An Externally Heated Quartz T-tube Atomizer (EHQTA) is most widely used atomizer in hydride generation methods. EHQTA, supplied by Çalışkan Cam, Ankara, served as an atomizer for continuous flow hydride generation and W-coil Atom Trap ETV systems. It was inserted into a lab-made ceramic electrical heater. When EHQTA was used for the first time, its surface was saturated by using 100 mL of 1.0 mg/L analyte solution. The dimensions of the QTA and schematic representation are shown in Figure 2.3.

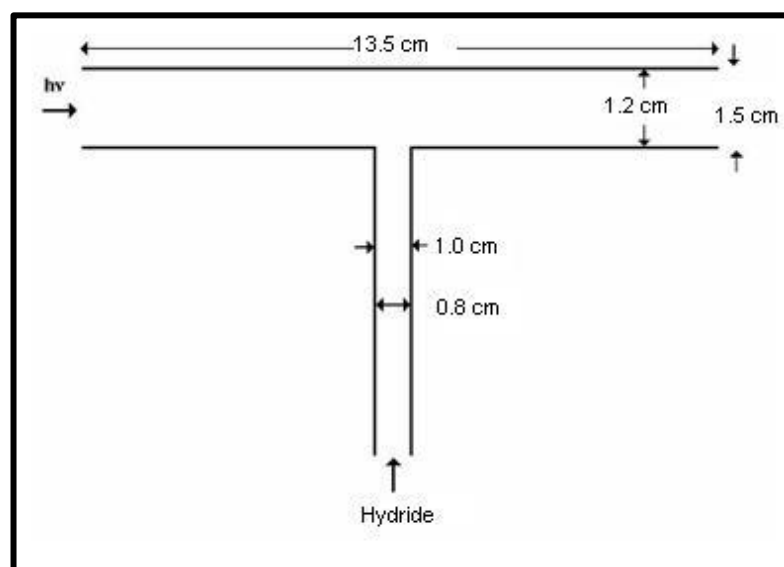


Figure 2.3 The schematic representation of the EHQTA.

QTA can be heated externally on a stoichiometric air acetylene flame or in an electrical heater. In this study, QTA was heated in a lab-made ceramic electrical heater (Figure 2.4). This unit was placed to the position of burner head and its position was aligned with the beam pathway of the spectrometer. A lab-made resistively heated cylindrical ceramic furnace was designed for the dimensions of

QTA with 1.8 cm outer diameter and 14 cm length. There were two semi-cylindrical ceramics inside the heater that can cover the top and the bottom parts of the horizontal arm of quartz T-tube atomizer. Ceramic part was covered and insulated with quartz wool and placed inside an aluminum box. In order to control the temperature of the heater, a GEMO DT109 temperature controller (Gürbüzöğlü Elektronik, Ankara, Turkey) was coupled with the heater. A thermocouple was inserted into the semi-cylindrical part of the ceramic in order to monitor the temperature. The temperature was measured with thermocouple and the temperature controller was set to desired atomization temperature (950 °C). The temperature of QTA was kept constant with this lab-made ceramic electrical heater system.



Figure 2.4 Lab-made ceramic electrical heater used to heat QTA to atomization temperature [160] .

EHQTA together with lab-made ceramic electrical heater was as the atomizer used in continuous flow hydride generation and W-coil Atom Trap ETV systems.

2.4.2. W-coil Atom Trap ETA

As the name implies, W-coil served as both atomizer and atom trap in W-coil Atom Trap ETA system.

There are two different atomization units used for W-coil Atom Trap ETA system. The schematic representation of the first atomization unit is given in Figure 2.5.

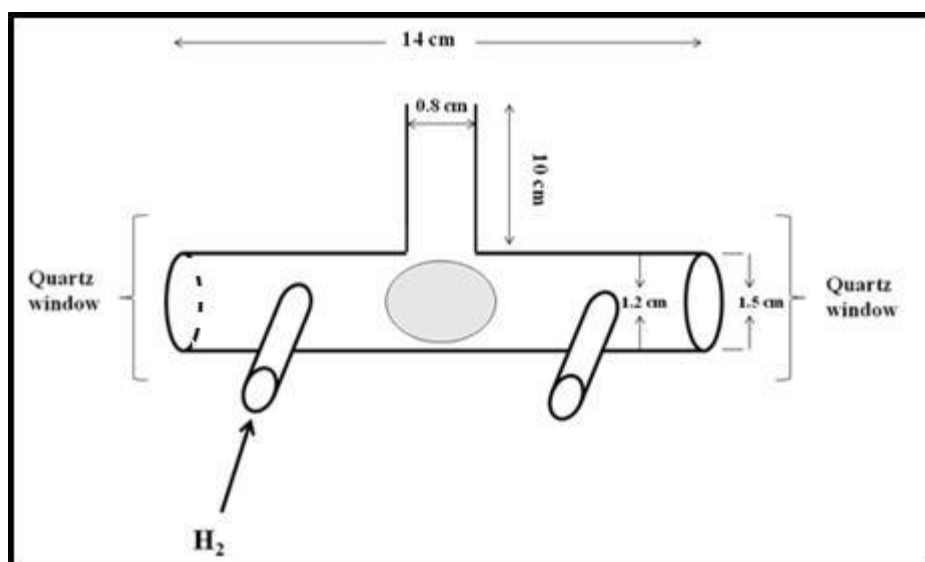


Figure 2.5 The atomization unit for W-coil Atom Trap ETA system.

The atomization unit was made of glass (Glass Shop, Department of Chemistry, METU) and placed on the burner head. W-coil was inserted in the middle of the atomization unit from an opening hole and fixed with a glass joint that was filled with silicone. Generated hydride species from the GLS was introduced through a

glass tube (0.8 cm o.d.) that was extended as near as possible to the surface of W-coil (Figure 2.6).

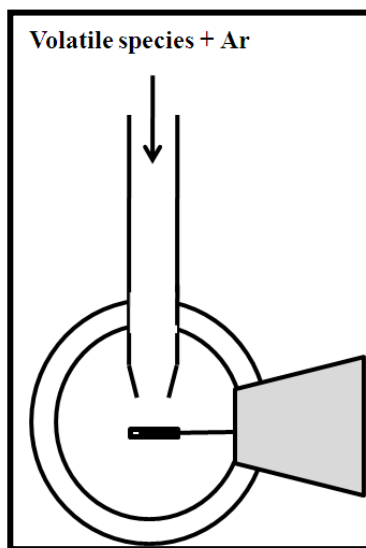


Figure 2.6 The side view of W-coil Atom Trap ETA atomization unit.

The second atomization unit that was made of glass (Glass Shop, Department of Chemistry, METU) and utilized for W-coil atom trap ETA system was different from the first atomization unit regarding its hydride introduction to the surface of W-coil. Design of the glass cell used for the atomization is similar to that of first atomization unit (Figure 2.7). The atomization unit was placed on the 10 cm burner head.

A quartz capillary (Glass Shop, Department of Chemistry, METU) was inserted in a syringe. The syringe with quartz capillary was placed on top of the atomization unit. The hydride species transported from GLS was introduced through this quartz capillary that was brought as close as possible to the W-coil surface. This configuration was useful when W-coil was used as a trap. The side view of the syringe attached W-coil Atom Trap ETA atomization unit is given in Figure 2.8.

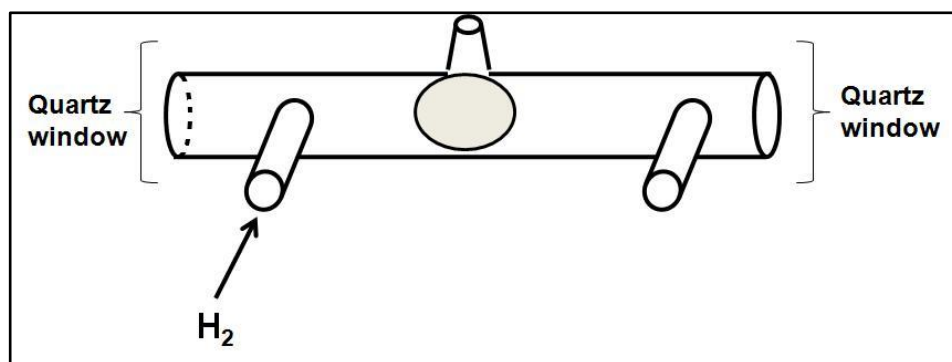


Figure 2.7 The atomization unit used for syringe attached W-coil Atom Trap ETA system.

The resistive heating of W-coil was achieved by applying an ac voltage by using a 750 W transformer and a variable potential power supply (Variac) that is connected to main electricity through a power switch. The input voltage of variable potential power supply was 220 V.

In order to protect W-coil against oxidation, H_2 gas was introduced to provide a reducing environment. H_2 gas introduction was achieved from the tube opening in front of the glass cell. For both of the designs for atomization unit, H_2 was introduced.

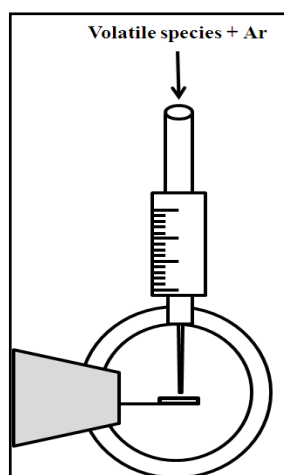


Figure 2.8 The side view of the syringe attached W-coil Atom Trap ETA atomization unit.

2.4.3. W-coil Atom Trap ETV

The atomization unit used for W-coil Atom Trap ETV system was the same with that of continuous flow hydride generation system. EHQTA was used as the atomizer for W-coil atom trap ETV. The dimensions of QTA are given in Figure 2.3. EHQTA was heated with the lab-made ceramic electrical heater and the atomization temperature (Figure 2.4) was 950 °C. When quartz T-tube was used firstly, its surface was saturated using the gaseous analyte formed by using 100 mL of 1.0 mg/L analyte solution.

2.5. W-coil as a Vaporization Unit

In W-coil Atom Trap ETV system, W-coil was used as both the trap and the vaporization unit. In other studies regarding W-coil ETV systems, W-coil has been placed in inlet arm of EHQTA [56,118,119]. In our study, a separate vaporization unit made of glass was constructed (Glass Shop, Department of Chemistry, METU). Two different configurations were utilized for W-coil Atom Trap ETV vaporization unit. The second one is to be used with syringe attached.

The first vaporization unit is shown in Figure 2.9. The heating of W-coil was achieved by the same process which was used for W-coil Atom Trap ETA system. W-coil was inserted in a glass joint that was filled with silicone to fix the W-coil. The position of W-coil was adjusted to provide largest area for maximum trapping efficiency.

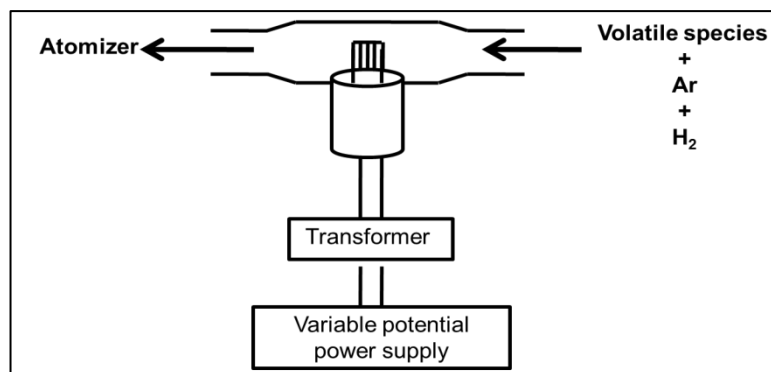


Figure 2.9 Vaporization unit for W-coil Atom Trap ETV system.

The second vaporization unit used for W-coil Atom trap ETV system was the syringe attached system. A quartz capillary was inserted inside the syringe. The syringe was attached to the glass cell (Glass Shop, Department of Chemistry, METU) constructed for vaporization unit. The hydride species were transferred through the quartz capillary to the surface of W-coil. The schematic representation of syringe attached vaporization unit for W-coil Atom Trap ETV is given in Figure 2.10.

For both of the configurations, H_2 gas was introduced. Different from the first configuration, in the syringe attached vaporization unit carrier Ar gas was added to the system. It was used to transfer the re-volatilized species to the atomizer. The atomizer used for both of the system was EHQTA.

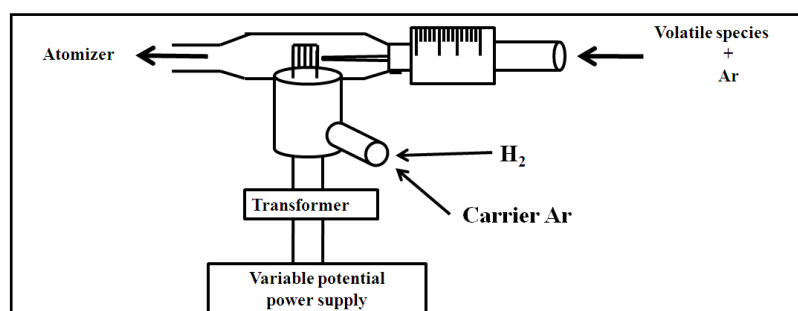


Figure 2.10 The syringe attached vaporization unit for W-coil Atom Trap ETV system.

2.6. Trap System

W-coil was the trapping medium for both W-coil Atom Trap ETA and W-coil Atom Trap ETV systems. W-coil was extracted from a 150 W, 15 V projector bulb (Philips Focusline, Germany). It is inexpensive and easily handled. It provides a large surface area for trapping. The dimensions of W-coil are given in Figure 2.11.

In W-coil Atom Trap ETA systems, W-coil is both the trapping and the atomizer, therefore trapping and atomization take place on the same surface (Figure 2.6, Figure 2.8). For W-coil Atom Trap ETV systems, W-coil was functioning in modes of trapping and vaporization unit. After the species are released from the trap atomization takes place in EHQTA. The detailed procedure will be given in the following sections (2.8.2 and 2.8.3).

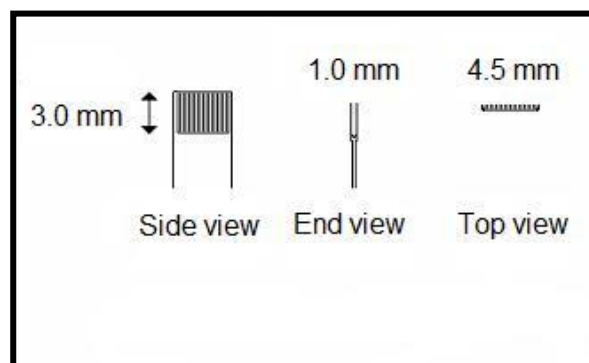


Figure 2.11 Dimensions of W-coil extracted from a projector bulb.

2.7. Interference study

The interference study was performed with CF-HG, W-coil Atom Trap ETA and W-coil Atom Trap ETV systems. The chemicals and reagents used in the interference study were given in Section 2.2.

2.7.1. Instrumentation

The same operating conditions of given in Table 2.1 were used during interference studies performed with CF-HG, W-coil Atom Trap ETA and W-coil Atom Trap ETV systems.

As, Sb, Se, Te and Sn were selected among the interference elements whose effect on analytical signal of Bi were observed to investigate the trapping, atomization and revolatilization profiles with W-coil Atom Trap ETA and W-coil Atom Trap ETV systems. For As and Sn, a Photron coded hollow cathode lamps were used and the wavelengths of interest were 193.7 nm and 235.5 nm, respectively. Varian High Intensity UltrAA Coded hollow cathode lamp was employed for Sb and Se at 217.6 nm and 196.0 nm, respectively. Varian high intensity hollow cathode lamp for Te operating at 214.3 nm was used.

The operating conditions of the instrument were varied according to the element of interest. The operating parameters for interference elements are listed in Table 2.2.

Table 2.2 Operating conditions of Varian AA140 for interference elements.

Parameter	As	Sb	Se	Te	Sn
Measurement wavelength, nm	193.7	217.6	196.0	214.3	235.5
Spectral bandpass, nm	0.5	0.2	1.0	0.2	0.5
Lamp current, mA	12.0	10.0	15	15	8.0
Read time, s	5	5	5	5	5
Measurement mode	Peak height	Peak height	Peak height	Peak height	Peak height

2.7.2. Interference study with W-coil Atom Trap ETA and W-coil Atom Trap ETV

The preliminary studies regarding interferences were performed with hydride generation system shown in Figure 2.1. This experimental set up was applied to W-coil Atom Trap ETA and W-coil Atom Trap ETV systems. The interfering elements were selected from the hydride forming elements (As, Sb, Se, Te, Sn), transition metals (Fe, Co, Ni, Cu, Mn) and alkali-earth metals (Na, Ca, Al, Si). The analyte concentration was selected as 0.3 ng/mL Bi and the interference elements were added to analyte solution using 1, 10, 50 and 500 mass ratio of interferent/analyte.

Detailed studies regarding interference study were continued with a different configuration of CF-HG system. Two configurations were used in this part of the study. They were different in terms of analyte/interference solution transport to the atomization or vaporization unit.

The first experimental set up for interference study is given in Figure 2.12. The system was consisting of two separate GLS, therefore the system was called twin-channel hydride generation system.

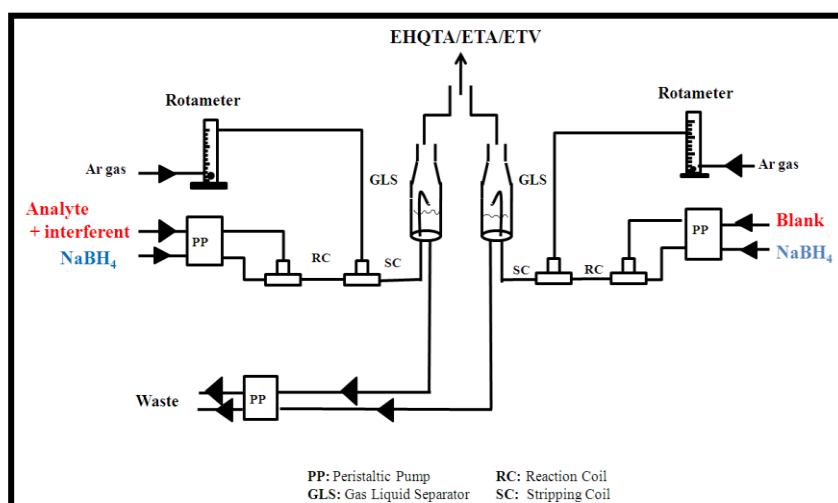


Figure 2.12 Experimental set-up for twin-channel hydride generation system in which analyte and interference elements were transferred together using the same GLS.

For this experimental set up for twin-channel hydride generation system, interference elements were spiked to analyte solutions. Analyte and interference elements were present in the same solution and pumped through the same channel. From the other channel blank solution was transferred. Hydrides from analyte/interferent solution and blank combined down-stream of gas liquid separators and sent to vaporization and/or atomization units.

Schematic representation of second experimental set up for twin-channel hydride generation system is given in Figure 2.13.

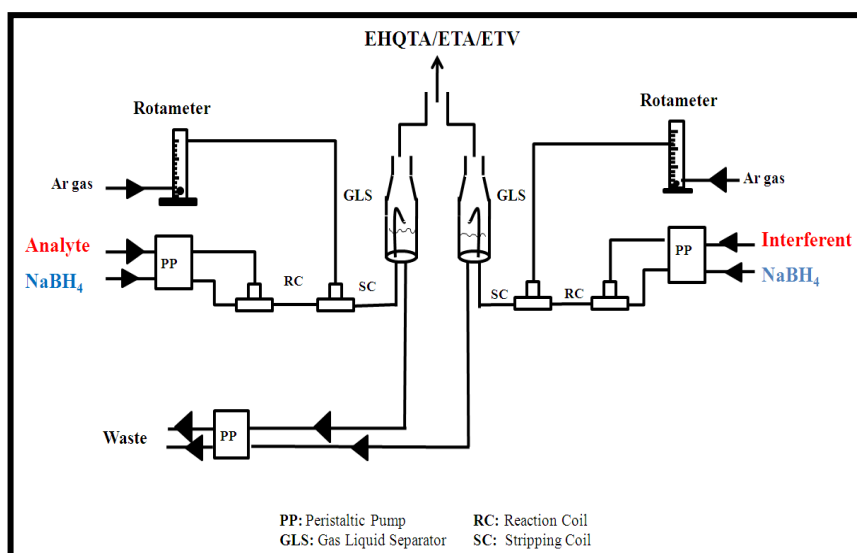


Figure 2.13 Experimental set-up for twin-channel hydride generation system in which analyte and interference element were transferred separately.

For this experimental set up (Figure 2.13), analyte and interference element solutions were prepared separately. They were passing through separate GLS. Hydrides of analyte and interference elements are combined down-stream of gas liquid separators and were sent to vaporization and/or atomization units.

These two experimental set-ups were used in the interference study of CF-HG, W-coil atom trap ETA and W-coil atom trap ETV studies.

2.8. Procedures

2.8.1. Continuous Flow Hydride Generation System

In continuous flow hydride generation system, acidified analyte solution and reductant solutions were pumped through peristaltic pumps at a constant flow rate of 3.0 mL/min for the both. The analyte solution was prepared in 1.0 mol/L HCl solution. The reductant solution was containing 0.5% (w/v) of NaBH₄ and stabilized in 0.2% (w/v) NaOH. Ar gas was introduced to CF-HG system to strip the volatile species. The optimized value for stripping Ar gas was 220 mL/min. The length of reaction and stripping coils were 15.0 cm and 2.0 cm, respectively. The duration for one signal at continuous mode was 10 seconds. Each result was the mean of at least two replicate measurements.

All the optimized values in CF-HG were used for W-coil Atom Trap ETA and W-coil Atom Trap ETV systems except the flow rate of Ar gas. Ar gas flow rate was optimized according to the system used.

2.8.2. W-coil Atom Trap ETA

In W-coil Atom Trap ETA studies, the same values for the optimized hydride generation conditions were used except for Ar gas flow rate. Additionally, H₂ gas was introduced to the system. Ar and H₂ flow rate values were optimized in this system. The sample and reductant solutions were pumped at a constant flow rate by the peristaltic pump in CF mode. The generated volatile species were transported to the W-coil surface that was heated previously to the trapping temperature. After trapping period was completed, the peristaltic pumps were switched off and all the

species collected on W-coil surface were revolatilized and atomized at once by increasing the temperature of W-coil to atomization temperature. The revolatilization and atomization take place almost simultaneously at the location. During trapping and atomization stages, Ar and H₂ flow rates were kept constant. In these experiments, syringe attachment was not used.

In the second part of this study, syringe attached configuration was used (Figure 2.8). The pumps were activated to transport solutions of sample and reductant in CF mode. The generated hydride species passed through gas liquid separator were introduced to the W-coil surface via a quartz capillary. The quartz capillary was pushed to 1.0 mm above the W-coil and kept on the W-coil surface during the trapping period. When trapping period was completed, the peristaltic pumps were deactivated and W-coil was switched off. Additionally, quartz capillary was pulled back. The temperature was raised to atomization temperature for release and atomization of the collected species on W-coil surface and revolatilization and atomization took place almost simultaneously at the same location. During trapping and release stages Ar and H₂ gas flow rates were kept constant.

For both of the studies, the integration time was kept as 5 seconds. The results obtained throughout the optimization of the system were the mean of at least two replicate measurements.

Because the trap signals were transient and very sharp, the integrated absorbance values were affected by the lamp noise and the very slight drifts in the base line caused large errors in peak area values. The peak height values are the basis of the measurements. The optimization of experimental parameters was performed by changing one variable at a time. While optimizing one parameter, the others were kept at their optimum value.

2.8.3. W-coil Atom Trap ETV

W-coil Atom Trap ETV studies were carried out with CF mode. Hydride generation parameters optimized for CF-HG system were used for W-coil Atom Trap ETV system except for Ar gas flow rate. The flow rate of Ar was optimized for W-coil atom trap ETV. H₂ gas introduction was performed to prevent oxidation of W-coil.

According to the system with schematic representation in Figure 2.9, sample and reductant solution were pumped by peristaltic pump in CF mode. Hydrides from the generator were directed to the surface of W-coil already heated to trapping temperature. When trapping period was completed, peristaltic pumps were closed, and the Ar flow rate was increased for releasing stage. Then the temperature of W-coil was raised to revolatilization temperature and collected species were revolatilized and carried to EHQTA for the atomization.

The other study regarding W-coil Atom Trap ETV system was performed with the attachment of syringe to the vaporization unit as shown in Figure 2.10. In this system, in addition to stripping Ar gas, extra carrier Ar gas was introduced. The solutions of sample and reductant were pumped by peristaltic pumps in CF mode. Hydrides from the generator were passed through a quartz capillary inserted in a syringe. By the help of the piston of syringe, quartz capillary was directed to almost 1.00 mm away from the W-coil surface. W-coil was heated to the optimized temperature at which analyte was collected on W-coil. Carrier Ar gas was turned off in the trapping period. It is required for revolatilization stage for the transportation of revolatilized species to the atomizer. When trapping period was over, pumps were deactivated. The quartz capillary was withdrawn. The carrier Ar gas flow rate was increased and temperature of W-coil was raised to the revolatilization temperature and revolatilization took place. Revolatilized species were transported to the atomizer by the help of carrier Ar gas. Atomization of these species was held on EHQTA at 950 °C.

For both of the studies, the integration time was kept as 5 seconds. The results obtained throughout the optimization of system were the mean of at least two replicate measurements. The peak height measurement was performed for the signal evaluation.

2.8.4. Interference Study

The preliminary interference studies were performed by using W-coil Atom Trap ETA and W-coil Atom Trap ETV systems. The details of the procedure applied are given in Sections 2.8.2 and 2.8.3. This study was limited to the elements selected mainly from hydride forming elements that were As, Sb, Se, Te and Sn.

2.8.4.1. Continuous Flow Hydride Generation System

Twin channel hydride generation system was used for detailed interference study. The first application was done with CF-HG system. In the first experimental set up (Figure 2.12), analyte/interference and reductant solution were transferred from peristaltic pumps. From the second hydride generator blank and reductant solutions were transported by peristaltic pumps. From both of the sides solutions were pumped in CF mode. Volatile species pass through the gas liquid separators and were combined after gas liquid separators and sent to the atomizer that was EHQTA.

For the second experimental set up (Figure 2.13) in which analyte solution and interferent solution were transferred separately, the study was performed in CF mode. Analyte and reductant solutions were pumped from first channel with peristaltic pump; interferent and reductant solution were transferred from the second channel with other peristaltic pump. They combined after the gas liquid separators, then sent to atomizer that was EHQTA.

2.8.4.2. W-coil Atom Trap ETA

Twin channel hydride generation system was used in CF mode in W-coil Atom Trap ETA system. For both of the experimental set-ups for twin channel hydride generation systems, the procedure applied for W-coil Atom Trap ETA system was the same. Hydrides generated from both sides of the twin channel hydride generation met after GLSs and introduced to the surface W-coil that was heated to trapping temperature. When collection of hydride species was completed, the pumps at the both sides of twin channel hydride generation systems were deactivated. The temperature of the W-coil was increased to release and atomize of the trapped species. The analyte concentration was 2.0 ng/mL and acidified in 1.0 mol/L HCl. The collection on W-coil was held on for 60 second. Signals were obtained for 5 seconds integration time. After each trapping and atomization cycle one cleaning step was applied. The signals were transient height and peak height measurement was taken into account.

The trapping and atomization profiles of the interference elements were studied with W-coil atom trap hydride generation system. Single channel including single gas liquid separator hydride generation system was used for this part of the interference study. The interference elements were acidified with 1.0 mol/L HCl and 0.5 % (w/v) NaBH₄ stabilized in 0.2 % (w/v) NaOH reductant solution was used. The optimum conditions for bismuth for this study except for trapping and atomization temperature were applied in this part. In Table 2.3 the hydride generation, trapping and release (atomization) conditions for interference elements are listed.

Table 2.3 Hydride generation, trapping and release (atomization) conditions for As, Sb, Se, Te and Sn with Rh coated W-coil Atom Trap ETA.

PARAMETERS	As	Sb	Se	Te	Sn
Concentration of element, ng/mL	5.0	5.0	10.0	5.0	100.0
Concentration of HCl, mol/L	1.0	1.0	1.0	1.0	1.0
Concentration of NaBH ₄ , % (w/v), stabilized in 0.2 % (w/v) NaOH	0.5	0.5	0.5	0.5	0.5
Flow rate of sample, mL/min	3.0	3.0	3.0	3.0	3.0
Flow rate of NaBH ₄ , mL/min	3.0	3.0	3.0	3.0	3.0
Trapping Ar flow rate, mL/min	125	125	125	125	125
Release Ar flow rate, mL/min	125	125	125	125	125
Trapping H ₂ flow rate, mL/min	150	150	150	150	150
Release H ₂ flow rate, mL/min	150	150	150	150	150
Trapping temperature, °C	1018	544	277	620	620
Release (atomization) temperature, °C	1742	2177	2177	2177	2177

Signals were obtained for 5 seconds integration time. After each trapping and atomization cycle one cleaning step was applied. The signals were transient and peak height measurements were used.

2.8.4.3. W-coil Atom Trap ETV

The interference study performed with W-coil Atom Trap ETV system was carried out with twin channel hydride generation system. The analyte and interferent solutions were pumped together in the same solution or separately from different channels. All the solutions were transferred from peristaltic pumps were in CF mode. The generated hydride species from both sides of the channels came together after gas liquid separators. Then they were sent to the W-coil placed as the trapping and vaporization unit (Figure 2.9). The volatile species coming from generators were collected on the heated W-coil. When collection period was over, all peristaltic pumps were switched off. Carrier Ar gas flow rate was increased and temperature of W-coil was brought to revolatilization temperature. Then release of trapped species was realized. Released species were carried to EHQTA for atomization.

By using single GLS hydride generation system, the trapping and revolatilization profiles of the interference elements were obtained. The procedure used for this part of the study was the same for previous one (2.8.3) used for W-coil Atom Trap ETV studies. The solutions containing interference elements were acidified with 1.0 mol/L HCl and the reductant solution was 0.5 % (w/v) NaBH₄ in 0.2 % (w/v) NaOH. Hydride generation, trapping and release (revolatilization) conditions for As, Sb, Se, Te and Sn with W-coil Atom Trap ETV system were summarized in Table 2.4.

The analyte concentration was 2.0 ng/mL and acidified in 1.0 mol/L HCl. The collection on W-coil was continued for 60 s. The measurement of the signal was adjusted as 5 s reading time. After each trapping and revolatilization cycle one cleaning step for W-coil was applied. The signals were transient and peak height measurement was taken into account.

Table 2.4 Hydride generation, trapping and release (revolatilization) conditions for As, Sb, Se, Te and Sn with W-coil atom trap ETV.

PARAMETERS	As	Sb	Se	Te	Sn
Concentration of element, ng/mL	10.0	10.0	10.0	10.0	1000.0
Concentration of HCl, mol/L	1.0	1.0	1.0	1.0	1.0
Concentration of NaBH ₄ , % (w/v), stabilized in 0.2 % (w/v) NaOH	0.5	0.5	0.5	0.5	0.5
Flow rate of sample, mL/min	3.0	3.0	3.0	3.0	3.0
Flow rate of NaBH ₄ , mL/min	3.0	3.0	3.0	3.0	3.0
Trapping Ar flow rate, mL/min	125	125	125	125	125
Release Ar flow rate, mL/min	125	125	125	125	125
Carrier Ar flow rate (revolatilization), L/min	1.5	1.5	1.5	1.5	1.5
Trapping H ₂ flow rate, mL/min	150	150	150	150	150
Release H ₂ flow rate, mL/min	150	150	150	150	150
Trapping temperature, °C	620	262	277	262	462
Release (revolatilization) temperature, °C	1696	1696	1742	1742	1742
Atomization temperature, °C	950	950	950	950	950

The last part of interference study performed with W-coil atom trap ETV was following the signal of interference element in CF-HG, CF-HG during collection on W-coil and revolatilization. This part of the study was limited to the interference elements As, Sb and Se.

2.8.5. Coating of W-coil Surface

W-coil surface was modified with Rh as a permanent modifier. 1000 mg/L Rh stock solution was used for coating of W-coil surface. 20 μ L of Rh solution was injected manually to the surface of W-coil. A temperature programming given in Table 2.5 was applied. The same procedure was repeated 10 times to increase the coated mass of rhodium. During the coating procedure Ar and H₂ flow rates were 125 and 150 mL/min, respectively.

Table 2.5 Temperature program used for W-coil surface with Rh.

	Time, s	Temperature, °C
1. step	60	462
2. step	30	620
3. step	10	1300
4. step	3	1742

2.8.6. Temperature Measurement of W-coil

The temperature control of W-coil was done manually with variable power supply (Variac, Şimşek Labor teknik, Ankara) that was connected to main electricity. 750 W transformer was inserted between the variac and W-coil.

Temperature measurement was performed with thermocouple and infrared thermometer (Mirage, IRCON, Santa Cruz, USA). Up to 700 °C, the temperature was measured with thermocouple. The temperature sensing tip of thermocouple was covered with alumina-glass water mixture to keep this part from deformation with high temperature. Thermocouple was positioned to W-coil surface as near as possible to determine W-coil temperature correctly. W-coil temperature above 1000 °C was

measured with pyrometer. Graphite furnace of the atomic absorption spectrometer (VARIAN GTA120, Walnut Creek, CA) was used for the calibration of pyrometer.

2.9. Accuracy Check

In order to verify the accuracy of W-coil Atom Trap ETA and W-coil Atom Trap ETV, NIST 1643e “Trace Elements in Water” standard was used. The contents of the SRM are listed in

Table 2.6. The direct calibration method was used for W-coil Atom Trap ETA system. Standard addition method was employed for W-coil Atom Trap ETV system. For the analysis of SRM, the appropriate dilutions for the analysis of SRM were performed.

Table 2.6 Certified values for Trace Elements in SRM 1643e.

Element	Mass Fraction ($\mu\text{g}/\text{kg}$)			Mass Concentration ($\mu\text{g}/\text{L}$)		
Aluminum	138.33	\pm	8.4	141.8	\pm	8.6
Antimony	56.88	\pm	0.60	58.30	\pm	0.61
Arsenic	58.98	\pm	0.70	60.45	\pm	0.72
Barium	531.0	\pm	5.6	544.2	\pm	5.8
Beryllium	13.64	\pm	0.16	13.98	\pm	0.17
Bismuth	13.75	\pm	0.15	14.09	\pm	0.15
Boron	154.0	\pm	3.8	157.9	\pm	3.9
Cadmium	6.408	\pm	0.071	6.568	\pm	0.073
Calcium	31 500	\pm	1 100	32 300	\pm	1 100
Chromium	19.90	\pm	0.23	20.40	\pm	0.24
Cobalt	26.40	\pm	0.32	27.06	\pm	0.32
Copper	22.20	\pm	0.31	22.76	\pm	0.31
Iron	95.7	\pm	1.4	98.1	\pm	1.4
Lead	19.15	\pm	0.20	19.63	\pm	0.21
Lithium	17.0	\pm	1.7	17.4	\pm	1.7
Magnesium	7 841	\pm	96	8 037	\pm	98
Manganese	38.02	\pm	0.44	38.97	\pm	0.45
Molybdenum	118.5	\pm	1.3	121.4	\pm	1.3
Nickel	60.89	\pm	0.67	62.41	\pm	0.69
Potassium	1 984	\pm	29	2 034	\pm	29
Rubidium	13.80	\pm	0.17	14.14	\pm	0.18
Selenium	11.68	\pm	0.13	11.97	\pm	0.14
Silver	1.036	\pm	0.073	1.062	\pm	0.075
Sodium	20 230	\pm	250	20 740	\pm	260
Strontium	315.2	\pm	3.5	323.1	\pm	3.6
Tellurium	1.07	\pm	0.11	1.09	\pm	0.11
Thallium	7.263	\pm	0.094	7.445	\pm	0.096
Vanadium	36.93	\pm	0.57	37.86	\pm	0.59
Zinc	76.5	\pm	2.1	78.5	\pm	2.2

CHAPTER 3

RESULTS AND DISCUSSION

This study deals with the use of tungsten coil as electrothermal atomization and electrothermal vaporization in atomic absorption spectrometry. In order to investigate their use, in this scope Bi was selected as the analyte.

In the first part of the study, continuous flow hydride generation conditions for Bi were investigated and optimum conditions for this system were established. Flow rates of NaBH₄, sample solutions and carrier Ar gas and concentrations of NaBH₄ and HCl were optimized. The linear range and calibration plot were obtained and analytical figures of merit were calculated for this system.

The second part of the study includes the optimization of W-coil Atom Trap ETA and W-coil Atom Trap ETV for Bi. The surface of W-coil was modified with Rh since the signals obtained with bare W-coil were not reproducible. Trapping, atomization/revolatilization temperatures, Ar and H₂ gas flow rates for trapping and atomization/revolatilization stages and trapping period were optimized for both of the systems. Calibration studies were performed and analytical figures of merit for both of the systems were obtained.

In the third part of the system, quartz capillary attached W-coil Atom Trap ETA and also W-coil Atom Trap ETV systems were studied. Quartz capillary was inserted into a syringe. By the help of the syringe the movement of capillary was easily handled; in addition, in this set-up, even when the capillary was drawn, airtight conditions were kept. The surface of W-coil was coated with rhodium as in the previous part.

Trapping, atomization/revolatilization temperatures, Ar and H₂ gas flow rates for trapping and atomization/revolatilization stages and trapping period were optimized for both of the systems. Linear range and calibration plots for both of the systems were obtained and analytical figures of merit were evaluated. The accuracy checks regarding both systems were performed.

The interference study was performed in the fourth part of the study. The interference study covered continuous flow HGAAS, W-coil Atom Trap ETA and W-coil Atom Trap ETV systems. Some interference elements had an enhancement effect on the Bi signal. Therefore detailed studies regarding these elements were performed. Twin channel CF-HG system was employed for all the systems. Moreover, the trapping and atomization/revolatilization profiles for interference elements were carried out. The behavior of the interference elements in CF-HG, trapping and revolatilization stages were investigated with W-coil Atom Trap ETV system. The effect of increasing revolatilization temperature on interference elements were additionally studied in this part.

3.1. Continuous Flow Hydride Generation System

This part involves the optimization conditions for continuous flow hydride generation system. The detection was done by AAS using an EHQTA. Optimization studies are described in the following parts.

3.1.1. Optimization of HCl and NaBH₄ Concentrations

The reductant and acid concentrations are crucial parameters in hydride generation systems. Bi in acidified solution reacts with tetrahydroborate to generate bismuthine, BiH₃. The reaction coil and stripping coil lengths were 15.0 cm and 2.0 cm, respectively. To determine the optimum HCl and NaBH₄ concentrations, Bi concentration was adjusted to 20 ng/mL. During optimization of HCl and NaBH₄ concentrations, the stripping Ar flow rate was 220 mL/min. The flow rates of sample

and reductant were 3.0 mL/min. All NaBH₄ solutions were prepared in 0.2 % (w/v) NaOH in order to prevent hydrolysis and for better stability. The NaBH₄ solutions were prepared in the concentration range of 0.3-1.5 % (w/v). In order to find the optimum HCl concentration, HCl concentration in the analyte solution was varied between 0.5 and 2.0 mol/L. The optimization of HCl and NaBH₄ concentrations were carried out together. The absorbance value obtained for Bi signal was recorded for every acid concentration and its corresponding NaBH₄ concentrations. The results obtained for varied HCl and NaBH₄ concentrations are given in Figure 3.1.

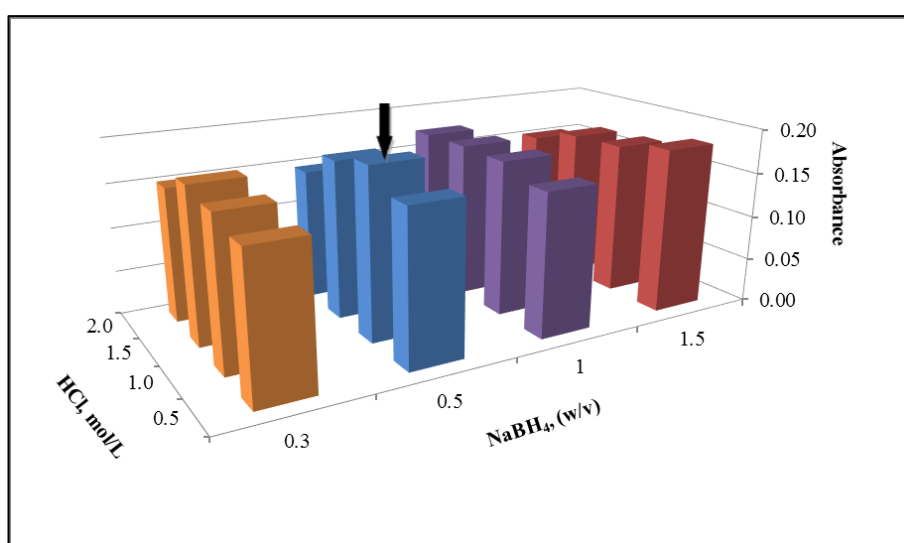


Figure 3.1 Variation of CF HGAAS signal with NaBH₄ and HCl concentration for 20 ng/mL Bi sample solution. Sample and reductant flow rates were adjusted to 3.0 mL/min.

The optimum concentration of NaBH₄ was found to be 0.5% (w/v). The HCl concentration in sample solution was selected as 1.0 mol/L.

3.1.2. Optimization of Sample and Reductant Flow Rate

The sample and reductant solutions were pumped separately by peristaltic pumps. In this section, the effect of sample and reductant flow rates was investigated. For this optimization Bi concentration was kept at 20 ng/mL and stripping Ar flow rate was 220 mL/min. The sample flow rate was varied between 1.0 to 4.0 mL/min. The optimum flow rate for sample solution was selected as 3.0 mL/min at which the highest absorbance value for Bi observed (Figure 3.2).

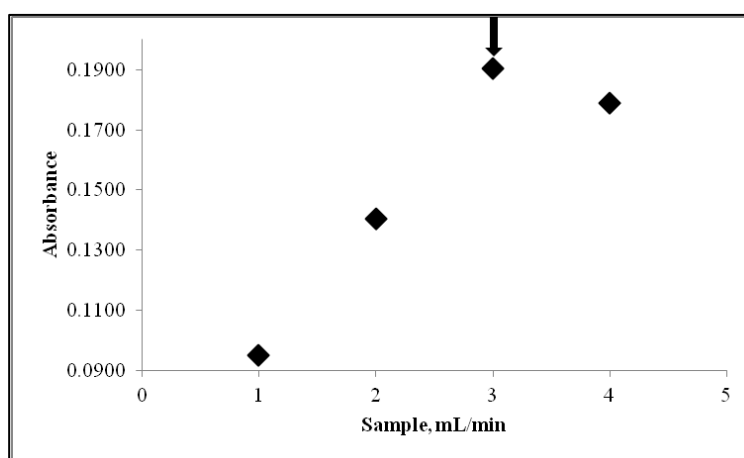


Figure 3.2 Effect of sample flow rate on the analytical signal of 20 ng/mL Bi solution. Sample solution was prepared in 1.0 mol/L HCl and 0.5 % (w/v) NaBH₄ was used.

The variations of Bi signal for NaBH₄ flow rate was measured within the range of 1.0 to 4.0 mL/min. The optimum flow rate was selected as 3.0 mL/min for NaBH₄. Higher the flow rates of NaBH₄ lower the analytical signal of Bi (Figure 3.3).

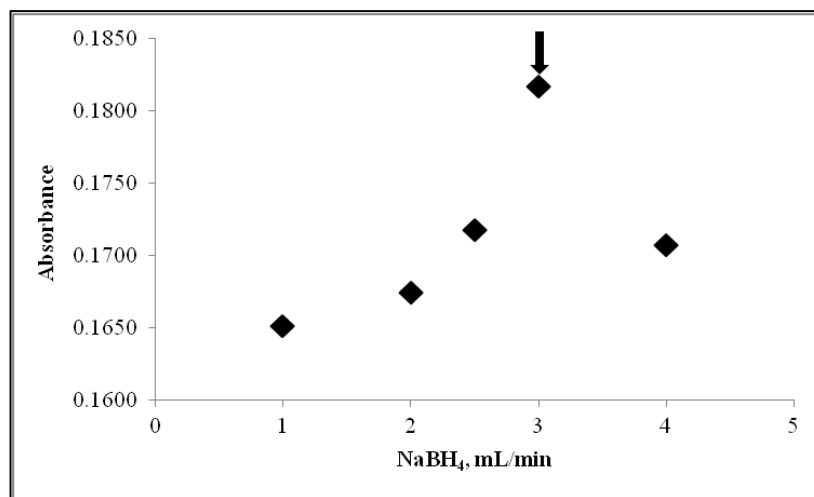


Figure 3.3 Effect of reductant flow rate on 20 ng/mL Bi signal. The sample flow rate was 3.0 mL/min and prepared in 1.0 mol/L HCl. The concentration of NaBH₄ was 0.5% (w/v).

3.1.3. Optimization of Stripping Argon Flow Rate

Stripping argon is introduced between the reaction and stripping coils and is used to separate the volatile species from the liquid phase and transport these species from GLS to the atomizer. The optimization of flow rate of Ar is critical since it affects the analyte signal significantly. The effect of Ar flow rate on 20 ng/mL Bi is given in Figure 3.4. The optimum value for Ar flow rate was adjusted to 220 mL/min. Although the lower flow rate of Ar has highest signal but the signals obtained for this value were not stable during measurement time. The higher value for Ar flow rate resulted in a decrease in signal due to the dilution of the volatile species during atomization in EHQA.

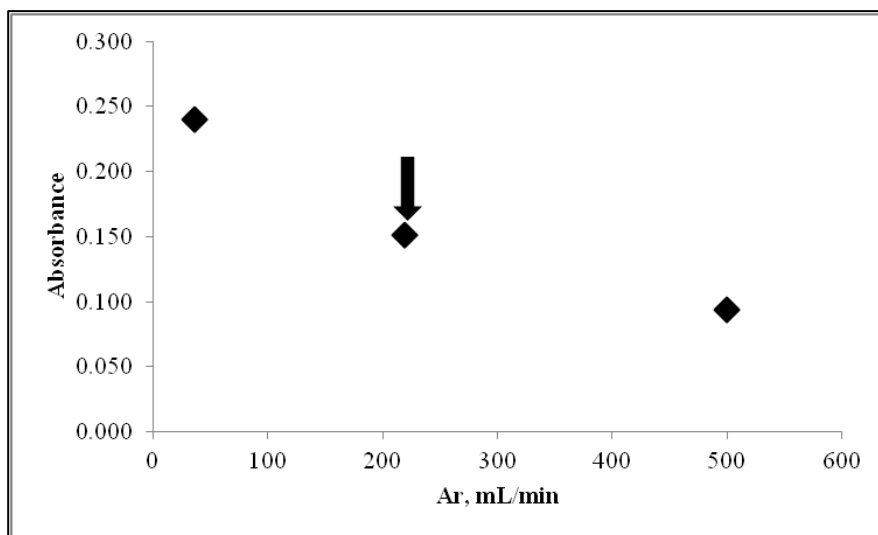


Figure 3.4 Effect of stripping Ar flow rate on analytical signal of 20 ng/mL Bi. Sample solution was prepared in 1.0 mol/L HCl solution and pumped at 3.0 mL/min flow rate. 0.5% (w/v) NaBH₄ was used at a flow rate of 3.0 mL/min.

Finally, optimized parameters for CF-HGAAS system are listed in Table 3.1. These parameters were used for CF-HG system coupled to W-coil atom trap ETA and W-coil atom trap ETV systems. Stripping Ar gas optimized in each study.

Table 3.1 Optimized parameters for CF-HGAAS system.

PARAMETERS	RESULTS
Concentration of HCl, mol/L	1.0
Concentration of NaBH ₄ , % (w/v), stabilized in 0.2 % (w/v) NaOH	0.5
Flow rate of sample, mL/min	3.0
Flow rate of NaBH ₄ , mL/min	3.0
Length of reaction coil, cm	15
Length of stripping coil, cm	2.0
Stripping gas (Ar), mL/min	220
Atomization temperature, °C	950

3.1.4. Calibration Plot and Linear Range for CF-HGAAS system

The calibration plot for Bi was obtained for the solutions ranging from 5.0 ng/mL to 150 ng/mL (Figure 3.5). It was observed that the calibration plot was linear between 5.0 ng/mL to 70 ng/mL (Figure 3.6). After this point deviation from linearity was observed. The best line equation obtained for the calibration plot and correlation coefficient were $y = 0.0052x + 0.0006$ and 0.9992, respectively; x is analyte concentration in ng/mL and y is the absorbance value.

LOD and LOQ values for the system were 1.1 and 3.6 ng/mL, respectively. LOD and LOQ values were calculated from 5 replicate measurements of smallest concentration of 5.0 ng/mL Bi. Characteristic concentration was found as 0.80

ng/mL and calculated from the absorbance value of 20 ng/mL Bi. Analytical figures of merit of CF-HGAAS are given Table 3.2.

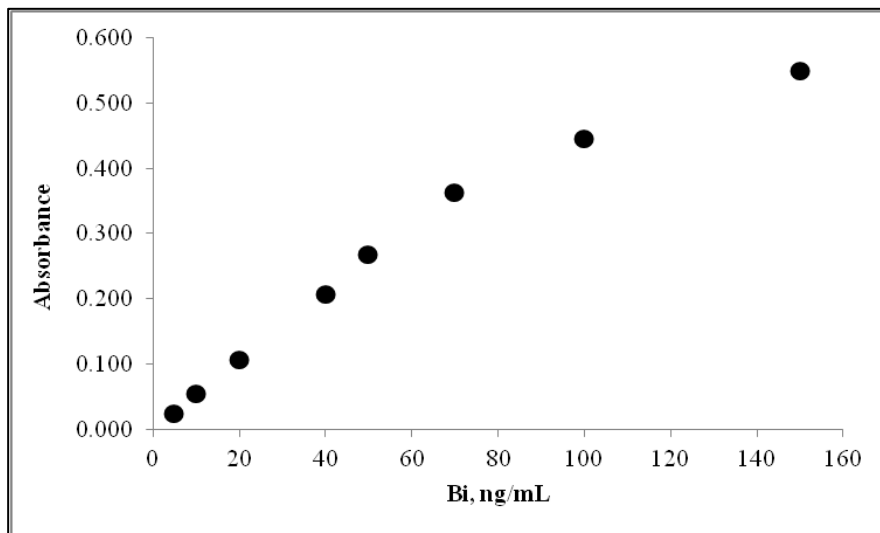


Figure 3.5 Calibration plot for CF-HGAAS system for Bi solutions. Sample solution was prepared in 1.0 mol/L HCl solution and pumped at 3.0 mL/min flow rate. 0.5 % (w/v) NaBH₄ was used at a flow rate of 3.0 mL/min.

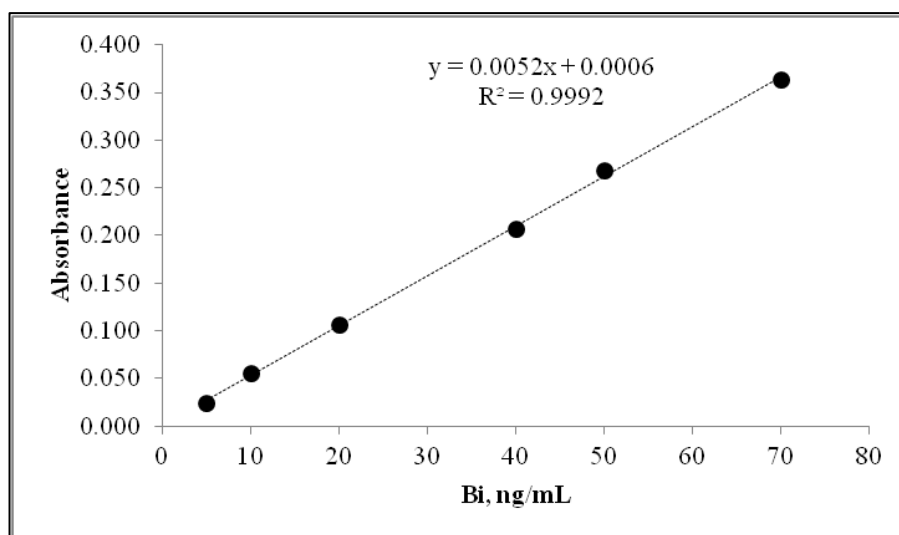


Figure 3.6 Linear portion calibration plot of the calibration plot obtained for CF-HGAAS system.

Table 3.2 Analytical figures of merit for CF-HGAAS system.

Limit of Detection, LOD, $3\sigma/m$ (N=5) ng/mL	1.10
Limit of Quantification, LOQ, $10\sigma/m$ (N=5) ng/mL	3.60
Characteristic Concentration, C_0 ng/mL	0.80
Linear Range, ng/mL	5-70
Precision, % RSD (N=5) for 5.0 ng/mL Bi	3.36

3.2. Rh coated W-coil Atom Trap Electrothermal Atomization System

In this part of the study, W-coil was functioning as both the atom trap and the atomizer. This operation is called as electrothermal atomization (ETA). In this system the gaseous bismuthine (BiH_3) was transported to the surface of W-coil,

preheated to collection temperature, and the species were collected on the W-coil surface for a certain period of time. When collection period was completed, temperature of W-coil was raised rapidly to the atomization temperature and a transient signal was obtained. The detection was done with AAS instrument.

The surface of W-coil was modified with Rh. Studies based on uncoated W-coil and Rh coated W-coil were carried out. It was observed that data obtained with bare W-coil were not sufficiently reproducible. Surface modification of W-coil with Rh improved the sensitivity and results were reasonable. The coating procedure was represented in section 2.8.5.

For the Rh coated W-coil Atom Trap ETA system, optimizations were made for Ar and H₂ gas flow rates, temperatures at trapping and atomization stages and the collection period.

3.2.1. Optimization of Argon Flow Rate at Trapping and Atomization Stages

The optimum Ar flow rates at trapping and atomization stages were determined and optimization graphs were given in Figure 3.7 and Figure 3.8, respectively. During these stages only Ar flow rate was varied for the determination of optimum gas flow rate for collection and atomization stages while H₂ flow rate was kept constant at 150 mL/min for both collection and atomization stages.

Ar was introduced to the system in order to strip the volatile species from solution flow and transport them to trapping and atomization mediums. For the trapping and atomization stages stripping Ar flow rate is important for both transportation efficiency and residence time of analyte atoms in the atomizer. As the Ar flow rate increases transport of analyte is achieved more sufficiently, but dilution of analyte atoms during atomization takes place at high flow rates. As the flow rate decreases residence time increases, hence the trapping efficiency is enhanced as analyte atoms stay for a long time in the atomization zone. As a result, stripping Ar flow rate has to be high enough to transport volatile species to atomizer and be as low as possible to

increase the residence time. Moreover, cooling effect of H₂ causes changes in W-coil temperature during collection period at low Ar flow rates. Therefore Ar flow rate should be high enough also for keeping the temperature of W-coil constant during the collection stage.

As the flow rate of Ar was raised for trapping and atomization stages, the signals were dropped drastically because of the reasons stated above. Therefore, for convenient application, 125 mL/min was selected as an appropriate flow rate of Ar gas for both trapping and atomization steps.

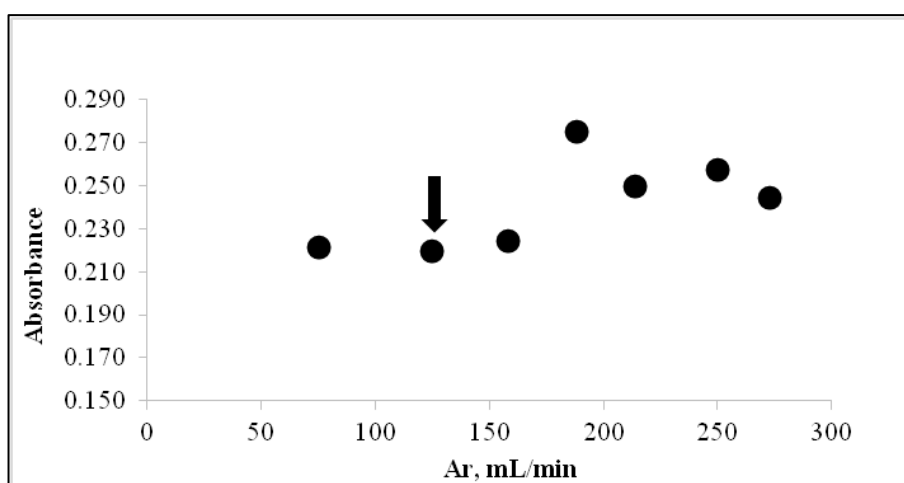


Figure 3.7 Effect of Ar flow rate at trapping stage on signal of 5.0 ng/mL Bi solution trapped over 60 s time period with Rh coated W-coil Atom Trap ETA system. Sample solution was pumped at 3.0 mL/min. Trapping temperature and atomization temperatures were adjusted to 1064 °C and 1960 °C, respectively.

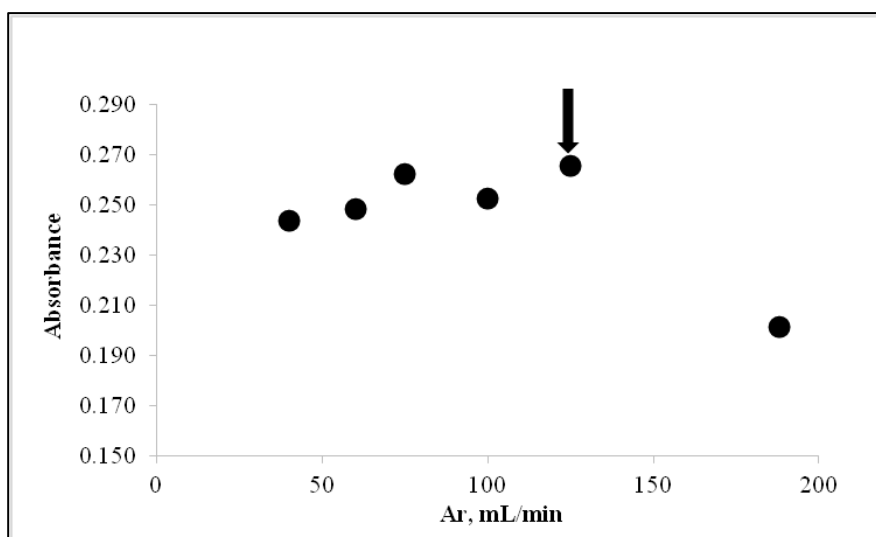


Figure 3.8 Effect of Ar flow rate at atomization stage on signal of 5.0 ng/mL Bi solution trapped over 60 s time period with Rh coated W-coil Atom Trap ETA system. Sample solution was pumped at 3.0 mL/min. Trapping temperature and atomization temperatures were adjusted to 1064 °C and 1960 °C, respectively.

3.2.2. Optimization of Hydrogen Flow Rate at Trapping and Atomization Stages

In studies related with W-coil, the introduction of H₂ gas is crucial, since to prevent oxidation of W-coil, reducing environment is required and H₂ gas provides a reducing environment and prevents W-coil from oxidation. In this study, CF-HG system was coupled with W-coil Atom Trap ETA system. Although production of H₂ takes place during HG process, this production was not enough to prevent the oxidation of W-coil. Therefore additional H₂ gas was introduced. While varying the H₂ flow rate, Ar flow rate was 125 mL/min at both trapping and atomization stages.

The effect of H₂ flow rate on analytical signal for trapping stage and atomization is shown in Figure 3.9. For the trapping period, flow rates higher than 150 mL/min resulted in lower signals. The first reason for this decrease may be the cooling effect of H₂ on the temperature of W-coil. This cooling effect was due to the higher thermal conductivity of H₂, 446×10^{-6} (cal/s.cm)(°C/m), which is approximately 10 times

higher than that of Ar, 43×10^{-6} (cal/s.cm)(°C/m) [161]. At higher temperatures of W-coil cooling effect of H₂ was diminished. The second reason of low signals at high flow rates may be the dilution of volatile species during trapping period.

At the atomization stage, analytical signal was dropped as the flow rate of H₂ was increased. The high flow rate of gas decreases the residence time of the atoms during atomization; in addition, the cooling effect as discussed above should be also effective. The flow rate of H₂ was adjusted to 150 mL/min for both trapping and atomization stages. The same flow rate was used for trapping and atomization stages since it was not practical to adjust gas flow rates at each cycle. Lower flow rates of H₂ resulted in oxidation of W-coil, therefore were not preferred. The plot for the variation of analytical signal versus H₂ flow rate is given in Figure 3.10.

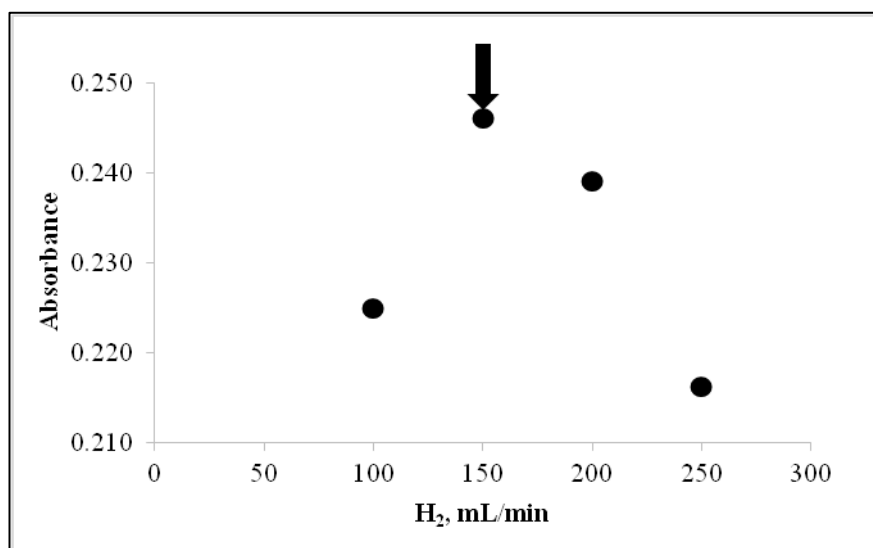


Figure 3.9 Effect of H₂ flow rate at trapping stage on signal of 5.0 ng/mL Bi solution trapped over 60 s time period with Rh coated W-coil Atom Trap ETA system. Sample solution was pumped at 3.0 mL/min. Trapping temperature and atomization temperatures were adjusted to 1064 °C and 1960 °C, respectively.

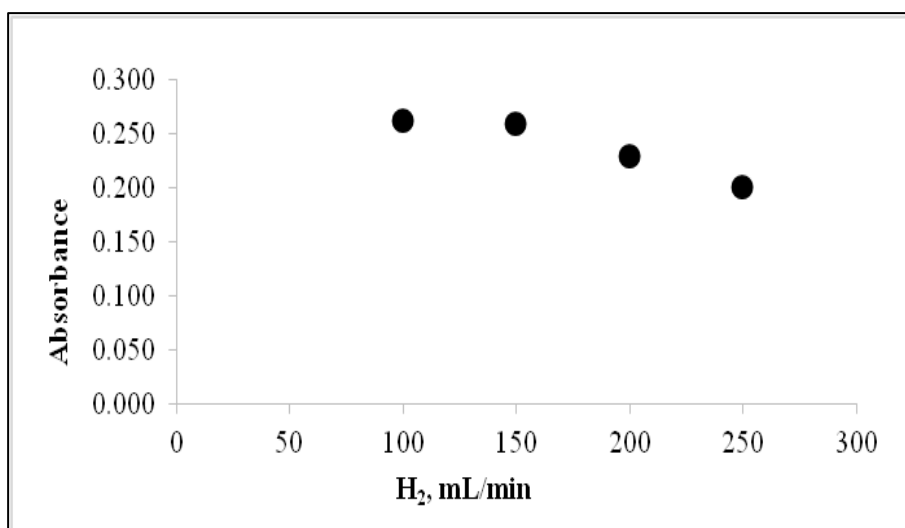


Figure 3.10 Effect of H₂ flow rate at atomization stage on signal of 5.0 ng/mL Bi solution trapped over 60 s time period with Rh coated W-coil Atom Trap ETA system. Sample solution was pumped at 3.0 mL/min. Trapping temperature and atomization temperatures were adjusted to 1064 °C and 1960 °C, respectively.

3.2.3. Optimization of Trapping and Atomization Temperatures

The relationship between analytical signal and trapping and atomization temperatures are indicated in Figure 3.11. For the selection of optimum trapping temperature the signal was evaluated after each atomization cycle. The optimum trapping temperature range was narrow and sharp decrease was observed for temperatures higher than 1000 °C. This sharp decrease can be attributed to the release of trapped species during trapping period. The optimum trapping temperature was selected as 462 °C (1.60 V).

Atomization stage temperature was selected at the point where complete atomization was achieved. The peak height of signal obtained at low temperatures was low due to the slow rate of analyte release and thus broadening of the analytical signal was observed. As the temperature was getting higher, increase in analytical signal was observed and optimum value was chosen as 2177 °C (10.65 V). There was no significant change in the analytical signal for higher temperature (2300 °C). At this

temperature (2177 °C) analyte species could be released completely from W-coil surface and therefore memory effect was not observed after atomization cycle. The results obtained for the optimization of temperature are also given in Figure 3.11.

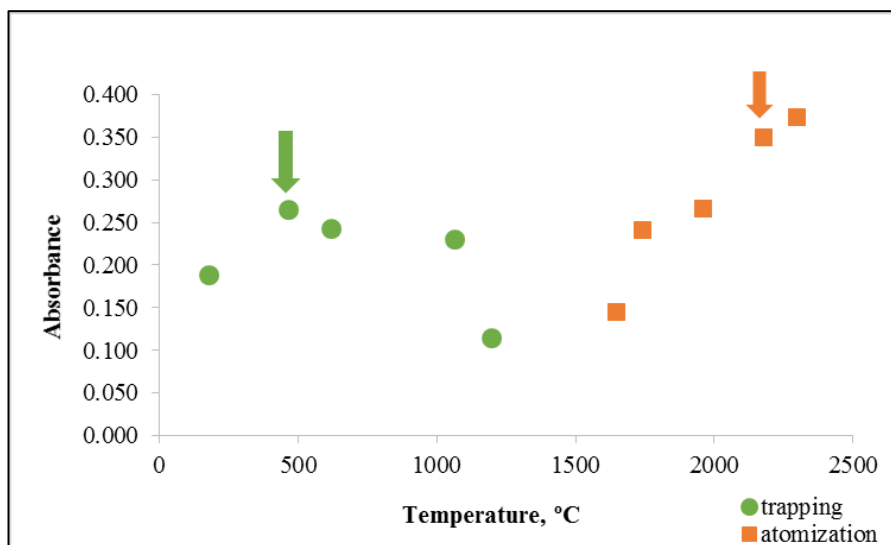


Figure 3.11 The effect of temperature at trapping and atomization stages on 5.0 ng/mL Bi trapped over 60 s.

3.2.4. Optimization of Collection Period

The correlation between trapping time and analytical signal was observed by varying the trapping period between 30-150 seconds and the results are given in Figure 3.12. The analytical signal increased linearly between 30 seconds and 120 seconds. As the collection period was increased, the signal did not further increase. 120 seconds was selected as the proper collection period and calibration plot was obtained by using this value.

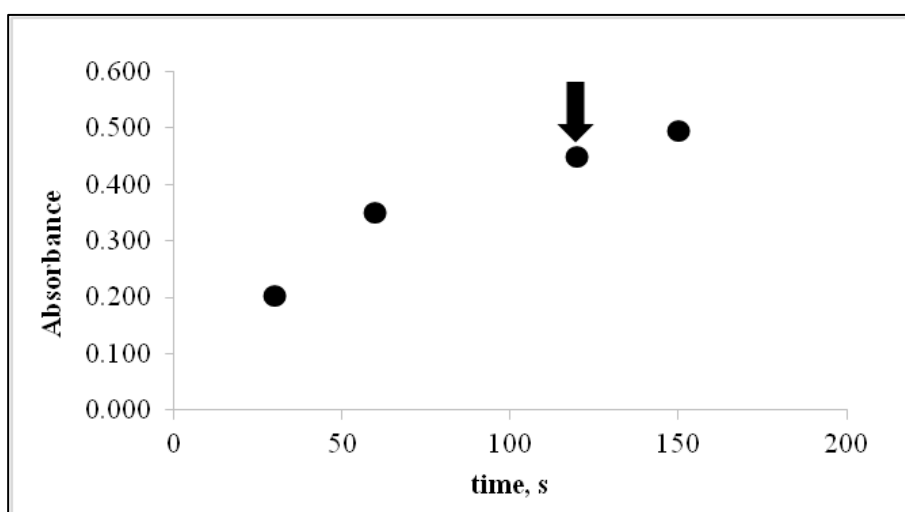


Figure 3.12 Effect of trapping period on 5.0 ng/mL Bi signal. Sample was pumped at 3.0 mL/min. Trapping and atomization temperature were adjusted to 462 °C and 2177 °C, respectively.

The optimum conditions for Rh coated W-coil atop trap ETA system are given in Table 3.3.

Table 3.3 Optimum conditions used for Rh coated W-coil atom trap ETA system.

PARAMETERS	RESULTS
Concentration of HCl, mol/L	1.0
Concentration of NaBH ₄ , % (w/v), stabilized in 0.2 % (w/v) NaOH	0.5
Flow rate of sample, mL/min	3.0
Flow rate of NaBH ₄ , mL/min	3.0
Length of reaction coil, cm	15
Length of stripping coil, cm	2.0
Trapping Ar flow rate, mL/min	125
Release Ar flow rate, mL/min	125
Trapping H ₂ flow rate, mL/min	150
Release H ₂ flow rate, mL/min	150
Trapping temperature, °C	462
Release (atomization) temperature, °C	2177

3.2.5. Calibration Plot and Linear Range for Rh coated W-coil Atom Trap ETA System

The calibration plot was obtained for Bi standard solutions ranging from 0.2 ng/mL to 20 ng/mL. The plot of concentration versus signal is given in Figure 3.13. The measurements were based on peak height of the analytical signal. It was found that the plot was linear between the concentrations of 0.2 ng/mL and 2.0 ng/mL Bi with a collection period of 120 seconds. Above this value, deviation from linearity was observed. The best line equation and determination coefficient were, $y = 0.1453x + 0.0333$ and 0.9991, respectively (Figure 3.14); x is analyte concentration in ng/mL and y is the absorbance value.

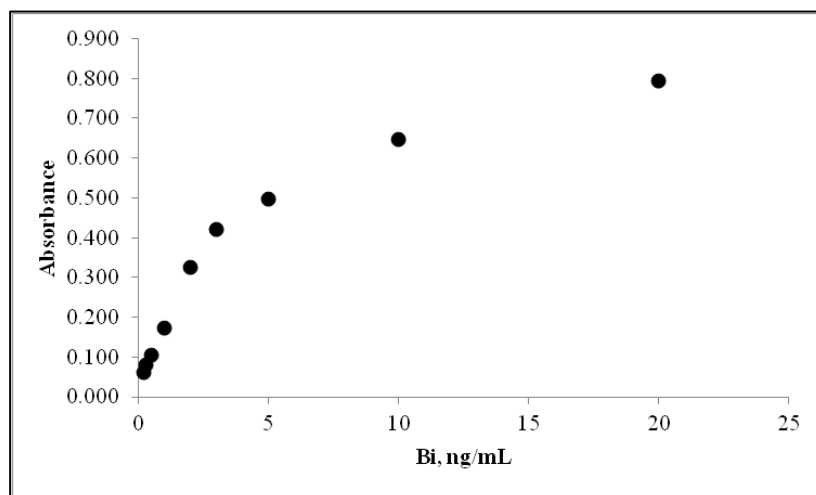


Figure 3.13 Calibration plot obtained for Bi collected over 120 s. The sample flow rate was 3.0 mL/min; trapping and atomization temperatures were 462 °C and 2177 °C, respectively.

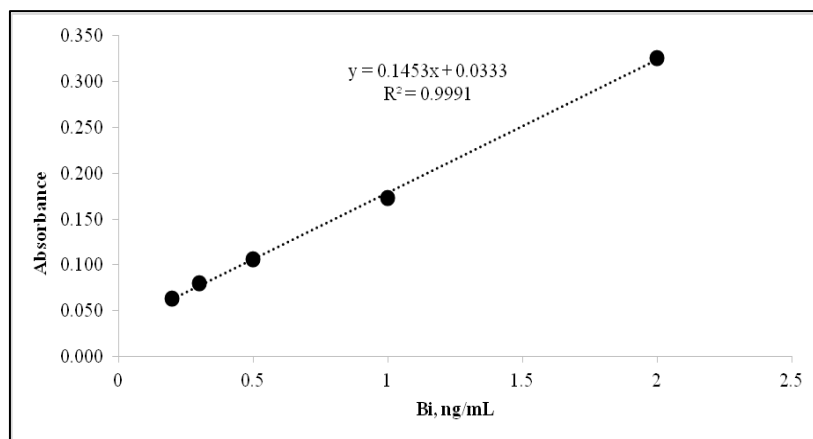


Figure 3.14 Linear portion of the calibration plot obtained for Bi trapped over 120 s. Sample flow rate was 3.0 mL/min; trapping and atomization temperatures were 462 °C and 2177 °C, respectively.

Peak profile of the analytical signal from a trap measurement is shown in Figure 3.15; it can be noticed that the half width of the transient signal was less than 0.5 s.

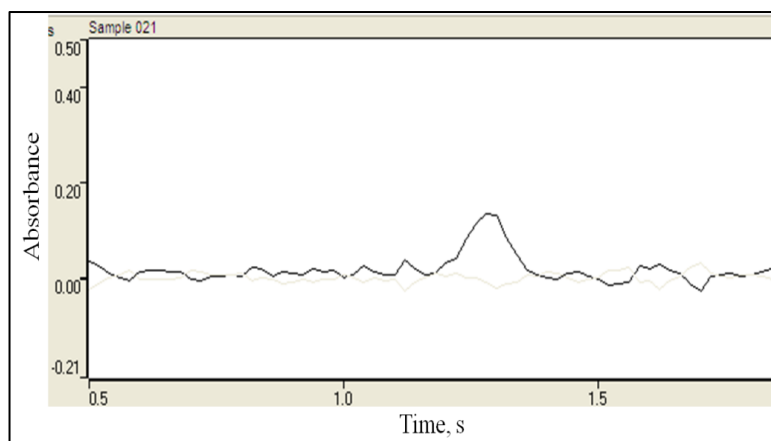


Figure 3.15 The analytical signal obtained by Rh coated W-coil atom trap ETA method for Bi; 6.0 mL of sample solution of 0.5 ng/mL Bi were collected for 120 s.

3.2.6. Analytical Figures of Merit

LOD, LOQ, characteristic concentration, C_0 , and characteristic mass, m_0 , relative standard deviation (RSD) values for peak height were calculated as given in Table 3.4. Collection period was 120 s and 3.0 mL/min was used for sample flow rate.

Table 3.4 Analytical figures of merit for Rh coated W-coil Atom Trap ETA. Volatile Bi species were trapped for 120 s at a flow rate of 3.0 mL/min.

Limit of Detection, LOD, $3\sigma/m$ (N=8) ng/mL	0.046
Limit of Quantification, LOQ, $10\sigma/m$ (N=8) ng/mL	0.152
Linear Range, ng/mL	0.2-2.0
Characteristic Concentration, C_0 ng/mL	0.025
Characteristic mass, m_0 pg	150
Precision, % RSD (N=8) for 0.20 ng/mL Bi	3.48

3.3. Syringe Attached Rh Coated W-coil Atom Trap Electrothermal Atomization System

In this part W-coil was used as the trapping medium and atomizer. The atomization unit, made of glass, used in this part was same as the one used in the previous part (Section 3.2) in its shape and size. In this configuration volatile species were introduced on W-coil surface via a quartz capillary inserted in a syringe. The aim of using syringe was to handle the movement of quartz capillary. Quartz capillary was kept on the surface of W-coil during trapping period. When the trapping period was over, capillary was pulled back by the help of the piston of syringe.

The parameters that were optimized in CF-HGAAS (Table 3.1) were used directly except that the flow rate of stripping Ar. Additionally, H₂ gas was introduced and optimization of flow rate at trapping and atomization stages were performed. Trapping and atomization temperatures were established and linear calibration plot was obtained.

3.3.1. Optimization of Argon Flow Rate at Trapping and Atomization Stages

The Ar flow rate was established for trapping and atomization stages. During optimization of Ar flow rate, H₂ gas was introduced to the system at 100 mL/min at both trapping and atomization stages. The trapping and atomization temperatures were adjusted to 462 °C and 2177 °C, respectively.

For the trapping stage, stripping Ar flow rate is important for the reasons that were stated in the section 3.2.1. In Figure 3.16, the effect of Ar flow rate at trapping period on analytical signal is shown. The flow rates lower than 75 mL/min was probably not sufficient to transport the volatile species to the trapping medium causing an inefficient hydride separation from the liquid phase. The signals remained nearly constant for the flow rates between 75 and 160 mL/min. The signal dropped significantly after 160 mL/min Ar. The reasons could be the dilution of volatile species during collection and/or insufficient time for volatile species to interact and be captured by W-coil. Therefore, 75 mL/min was selected as an optimum Ar flow rate at the trapping period.

For the atomization stage, optimum Ar flow rate was selected as 75 mL/min and the relevant optimization graph is indicated in Figure 3.17. The signals obtained for lower or higher flow rates for Ar than 75 mL/min were lower. Lower flow rates could not be enough to transport volatile species to the atomizer. At high flow rates, the analytical signal became smaller due to the reduced residence time and dilution of analyte species in the atomizer. Moreover, there was no need to change Ar flow rate for trapping and atomization stages. This provides convenience during measurements.

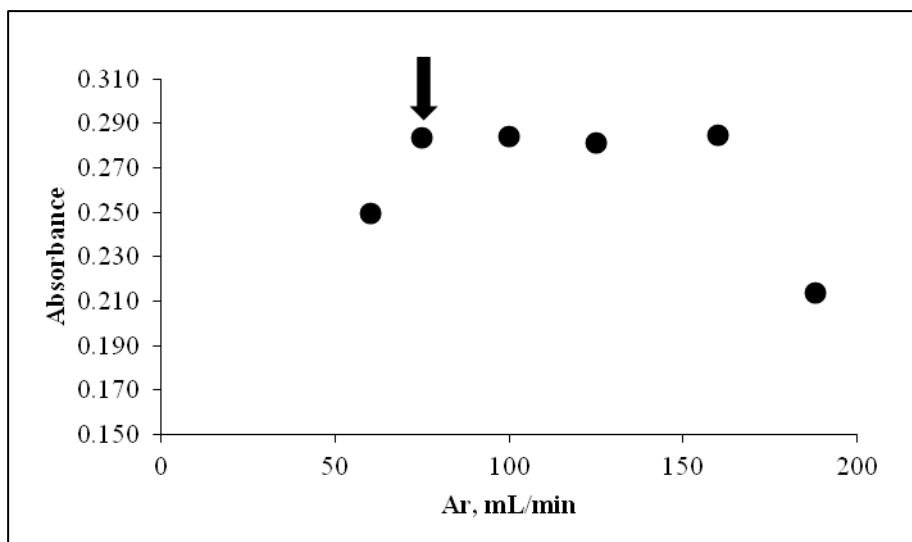


Figure 3.16 Effect of Ar flow rate on the signal for 2.0 ng/mL Bi at trapping stage. The sample flow rate was 3.0 mL/min and Bi was collected for 60 s. Trapping and atomization temperatures were 462 °C and 2177 °C, respectively.

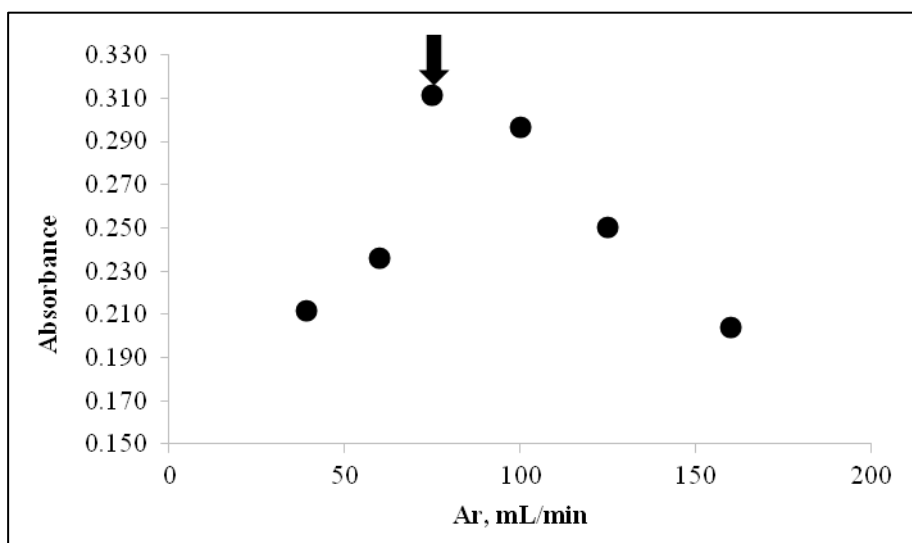


Figure 3.17 Effect of Ar flow rate on the signal for 2.0 ng/mL Bi at atomization stage. The sample flow rate was 3.0 mL/min and collected for 60 s. Trapping and atomization temperatures were 462 °C and 2177 °C, respectively.

3.3.2. Optimization of Hydrogen Flow Rate at Trapping and Atomization Stages

In this section, the flow rate of H₂ gas was optimized for trapping and atomization stages. The introduction of H₂ was independent from hydride generation system; it was introduced from the open hole of glass atomization unit. For the optimization purposes, H₂ gas flow rate was varied and Ar flow rate was kept at 75 mL/min at trapping and atomization stages. At trapping stage, according to the peak height measurements, the lowest peak height was 16% less than the highest value and the highest measurement was obtained for 75 mL/min H₂. The variation of the signal with H₂ is given Figure 3.18. The slight decrease in the analytical signal at higher flow rates was considered to be the consequence of cooling effect of hydrogen since the temperature was also affected by the hydrogen flow rate. In order to find the optimum flow rate of H₂ at atomization stage, H₂ flow rate was varied between 75 mL/min to 200 mL/min. 150 mL/min was selected as optimum value. The plot of analytical signal versus H₂ flow rate is given Figure 3.19. Although, the highest signal was obtained for 75 mL/min at trapping stage; 150 mL/min was selected optimum for both stages for convenience. Since there was not much difference between the signals obtained for 75 and 150 mL/min H₂, it was not necessary to change the flow rates at trapping and atomization for each measurement.

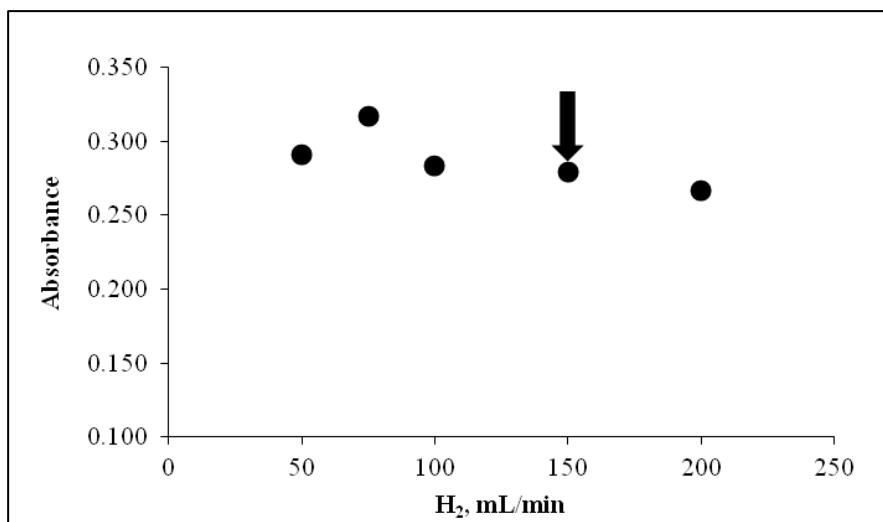


Figure 3.18 Effect of H₂ flow rate on the signal for 2.0 ng/mL Bi at trapping stage. The sample flow rate was 3.0 mL/min and collected for 60 s. Trapping and atomization temperatures were 462 °C and 2177 °C, respectively.

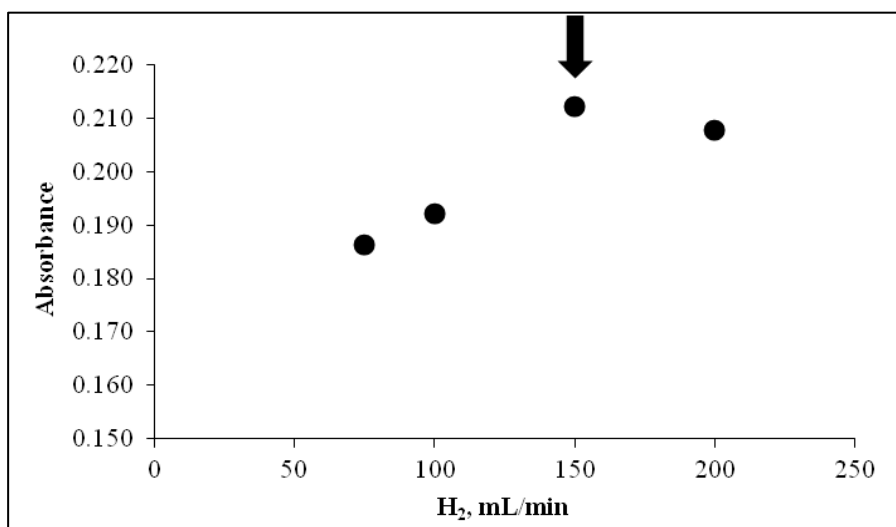


Figure 3.19 Effect of H₂ flow rate on the signal for 2.0 ng/mL Bi at atomization stage. The sample flow rate was 3.0 mL/min and collected for 60 seconds. Trapping and atomization temperatures were 462 °C and 2177 °C, respectively.

3.3.3. Optimization of Trapping and Atomization Temperatures

The trapping and atomization temperatures were optimized after establishing optimum gas flow rates, since they could affect the temperature of W-coil, especially in trapping period. During optimization of trapping and atomization temperatures, Flow rates of Ar and H₂ were kept constant at 75 and 150 mL/min, respectively.

The dependence of analytical signal on temperature for both trapping and atomization stages were evaluated and are shown in Figure 3.20. The optimum trapping temperature for bismuthine reaches to maximum at 462 °C; for higher temperature values, a sharp decrease was observed in the trapping efficiency due to loss of analyte during collection stage. The peak height of analytical signal obtained by atomization temperature of 1742 °C was low, since the rate of atomization could be slower and thus the broadening of the analytical signal was observed. As the atomization temperature was raised the enhancement of the peak height of the analytical signal. Since there was not much enhancement was obtained for temperature higher than 2177 °C, this value was selected as an optimum atomization temperature.

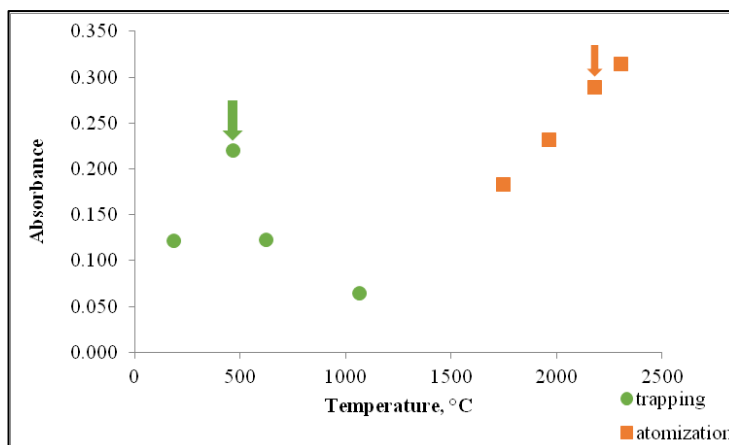


Figure 3.20 The effect of temperature at trapping and atomization stages on 2.0 ng/mL Bi trapped over 60 s. During the variations of trapping and atomization temperatures, a constant release temperature of 2177 °C and a constant trapping temperature of 462 °C, respectively, were employed.

3.3.4. Optimization of Collection Period

The trapping period was extended from 30 seconds to 150 seconds. While extending the time period, peak height of analytical signal was increased since the amount of trapped species were increased. The results obtained for collection period are indicated in Figure 3.21. 120 s trapping was selected for the collection period and calibration plot was obtained trapping bismuthine for 120 s.

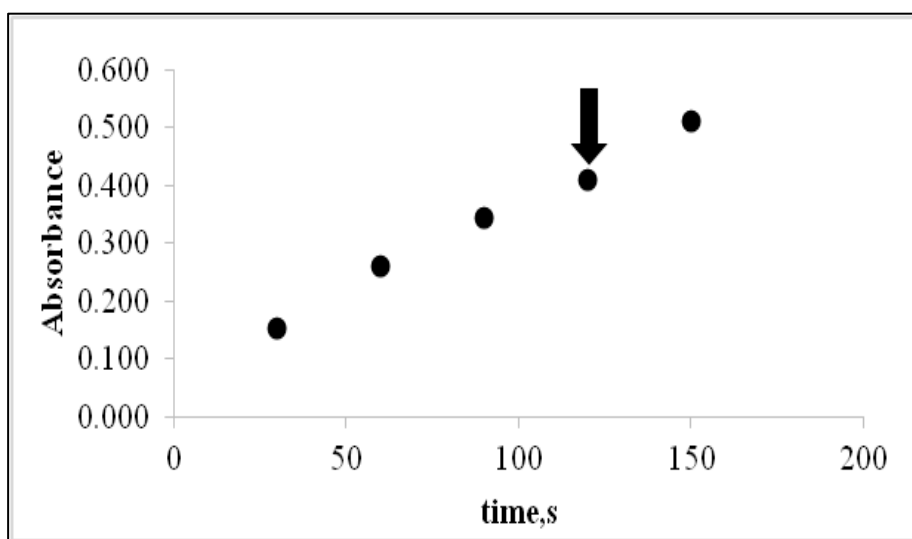


Figure 3.21 Effect of collection period on analytical signal of 2.0 ng/mL Bi pumped at 3.0 mL/min.

The parameters optimized for syringe attached Rh coated W-coil atom trap system are summarized in Table 3.5.

Table 3.5 Optimum conditions used for syringe attached Rh coated W-coil atom trap ETA system.

PARAMETERS	RESULTS
Concentration of HCl, mol/L	1.0
Concentration of NaBH ₄ , % (w/v), stabilized in 0.2 % (w/v) NaOH	0.5
Flow rate of sample, mL/min	3.0
Flow rate of NaBH ₄ , mL/min	3.0
Length of reaction coil, cm	15
Length of stripping coil, cm	2.0
Trapping Ar flow rate, mL/min	75
Release Ar flow rate, mL/min	75
Trapping H ₂ flow rate, mL/min	150
Release H ₂ flow rate, mL/min	150
Trapping temperature, °C	462
Release (atomization) temperature, °C	2177

3.3.5. Calibration Plot and Linear Range for Syringe Attached Rh coated W-coil Atom Trap ETA System

Calibration plot was obtained for Bi with syringe attached Rh coated W-coil atom trap ETA system and it is indicated in Figure 3.22. The calibration plot ($R^2 = 0.9979$) was linear from 0.1 to 0.5 ng/mL Bi shown in Figure 3.23. The calibration plot was drawn by using peak height values; the best line equation was $y = 0.3542x + 0.0237$; x is the analyte concentration in ng/mL and y is the absorbance value.

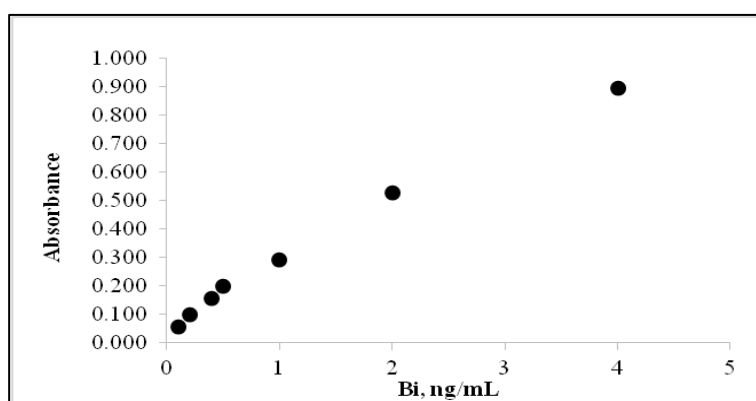


Figure 3.22 Calibration plot obtained for Bi collected over 120 s. The sample flow rate was 3.0 mL/min, trapping and atomization temperatures were 462 °C and 2177°C, respectively.

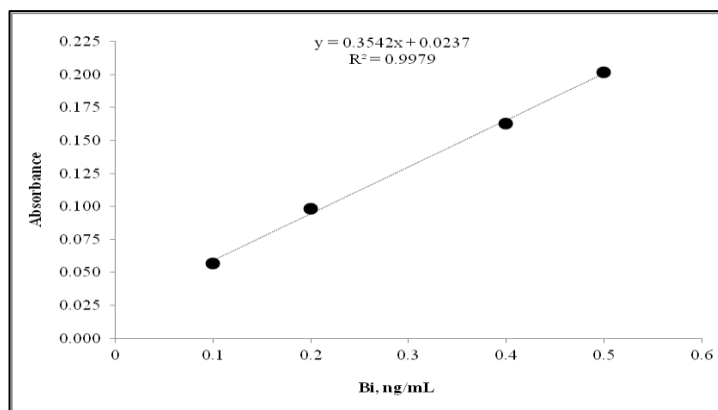


Figure 3.23 Linear range of the calibration plot obtained for Bi collected over 120 s. The sample flow rate was 3.0 mL/min, trapping and atomization temperatures were 462 °C and 2177°C, respectively.

The analytical signal obtained for 0.4 ng/mL Bi collected for 120 s with 3.0 mL/min flow rate is shown in Figure 3.24.

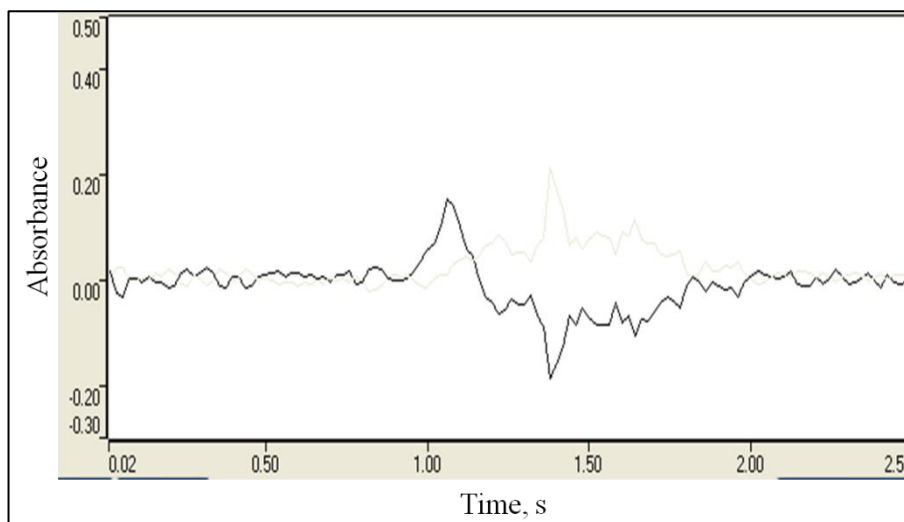


Figure 3.24 The analytical signal obtained by syringe attached Rh coated W-coil atom trap ETA method for Bi; 6.0 mL of sample solution of 0.4 ng/mL Bi were collected in 120 s.

3.3.6. Analytical Figures of Merit

The analytical figures of merit for syringe attached Rh coated W-coil atom trap ETA system are given in Table 3.6. The analytical figures of merit were calculated by using peak height values of analytical signal. The limit of detection was found to be 0.018 ng/mL for 8 consecutive measurements of 0.1 ng/mL Bi solution. Characteristic concentration obtained for this system for 6.0 mL of sample was 0.011 ng/mL.

Table 3.6 Analytical figures of merit for syringe attached Rh coated W-coil atom trap ETA system. Volatile Bi species were for 120 s at a flow rate of 3.0 mL/min.

Limit of Detection, LOD, $3\sigma/m$ (N=8) ng/mL	0.018
Limit of Quantification, LOQ, $10\sigma/m$ (N=8) ng/mL	0.058
Liner Range, ng/mL	0.1-0.5
Characteristic Concentration, C_0 ng/mL	0.011
Characteristic mass, m_0 pg	66
Precision, % RSD (N=8) for 0.10 ng/mL Bi	3.36

The analytical figures of merit for syringe attached Rh coated W-coil atom trap ETA, Rh coated W-coil atom trap ETA and CF-HGAAS systems are summarized in

Table 3.7 in order to compare the suggested techniques developed for determination of Bi. The enhancement factor in limit of detection ($3\sigma/m$) which was calculated for 0.1 ng/mL was found to be 61 when syringe attached W-coil atom trap ETA system was compared with CF-HGAAS. The characteristic concentration was calculated as 0.011 ng/mL and this value was 72 times lower as compared with CF-HGAAS system. The attachment of quartz capillary to the system provides enhancement factor of about 3.0 when compared to W-coil atom trap ETA system with respect to

limit of detection. The comparison regarding characteristic concentration yielded 2.3 times lower values as compared to W-coil atom trap ETA system.

Table 3.7 Analytical figures of merit for syringe attached Rh coated W-coil atom trap ETA, Rh coated W-coil atom trap ETA and CF-HGAAS systems.

	Syringe Attached W-coil atom trap ETA	W-coil atom trap ETA	CF- HGAAS
LOD, ng/mL	0.018	0.046	1.10
C₀, ng/mL	0.011	0.025	0.80

3.3.7. Accuracy of the Method

The accuracy of the method was evaluated by CRM, Natural Water (1643e). Determination of Bi in CRM was carried out by diluting 1.0 mL of CRM to 50.0 mL and the solution was acidified with 1.0 mol/L HCl. The resultant concentration of Bi in the solution was approximately 0.30 ng/mL. Direct calibration method was used for the analysis of CRM. The results are given in Table 3.8.

Table 3.8 Result of the analysis of CRM and the certified values for Bi using syringe attached Rh coated W-coil Atom Trap ETA system (n=3).

Concentration found, ng/mL	14.1 ± 0.5
Certified value, ng/mL	14.09 ± 0.15

3.4. Rh coated W-coil Atom Trap Electrothermal Vaporization System

In this section, W-coil was used as the vaporization unit. The atomization took place in electrically heated QTA. The vaporization unit was made of glass and inserted between the GLS and atomizer. Generated volatile species coming from GLS were collected on W-coil inserted in the vaporization unit. When collection was over, temperature was raised to revolatilization temperature. Revolatilized species were transported to the EHQTA for atomization.

The parameters that were optimized in CF-HGAAS were used directly except that the flow rate of stripping Ar. Additionally, H₂ gas was introduced and optimization of its flow rate at trapping and revolatilization stages were performed. Trapping and revolatilization temperatures were established and linear calibration plot was obtained.

3.4.1. Optimization of Stripping Argon Flow Rate at Trapping and Revolatilization Stages

During optimization of stripping Ar flow rate, the flow rate of H₂ was kept constant. Only the stripping argon flow was varied during the optimization of stripping gas flow rate. The variations of the signal as a function of stripping argon flow rate for trapping stage are given Figure 3.25. The peak heights of the signals were taken into account. The effect of flow rate of stripping argon on the analytical signal was observed between 10 mL/min and 80 mL/min. At lower flow rates, the peak height dropped probably due to the insufficient hydride separation from liquid phase and transportation to the trapping medium. The optimum flow rate for stripping argon was selected as 45 mL/min. Above this value, the signal decreased due to the limited time for the interaction with W-coil.

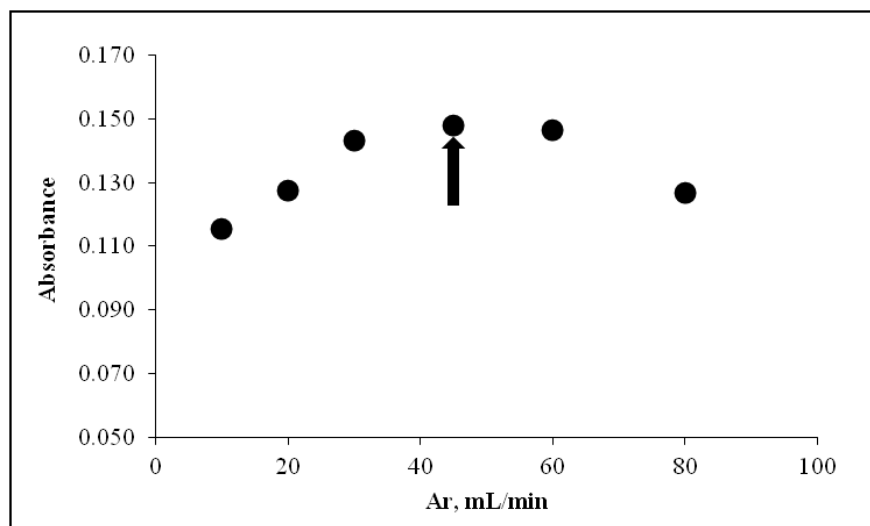


Figure 3.25 The effect of stripping argon flow rate at trapping stage on the signal of 2.0 ng/mL Bi that was collected for 60 s. The flow rate for H₂ was 150 mL/min. Trapping and revolatilization temperatures were 262 °C and 1960 °C, respectively. Temperature of EHQTA was 950 °C.

Optimization of argon flow rate revolatilization stage was performed by keeping argon flow rate at 45 mL/min at the trapping period. The H₂ flow rate was 150 mL/min for trapping and revolatilization stages. At revolatilization stage, when the temperature is increased to revolatilization temperature, argon flow rate has to be high enough to transport volatilized species to the atomizer efficiently. In this case, at low flow rates of Ar, the transportation of revolatilized species could be slow and peaks were broad. As the Ar flow rate was raised signal increased consequently. The dependency of analytical signal of Bi with respect to argon flow rate at revolatilization stage is indicated in Figure 3.26. The highest peak height was obtained for 120 mL/min argon.

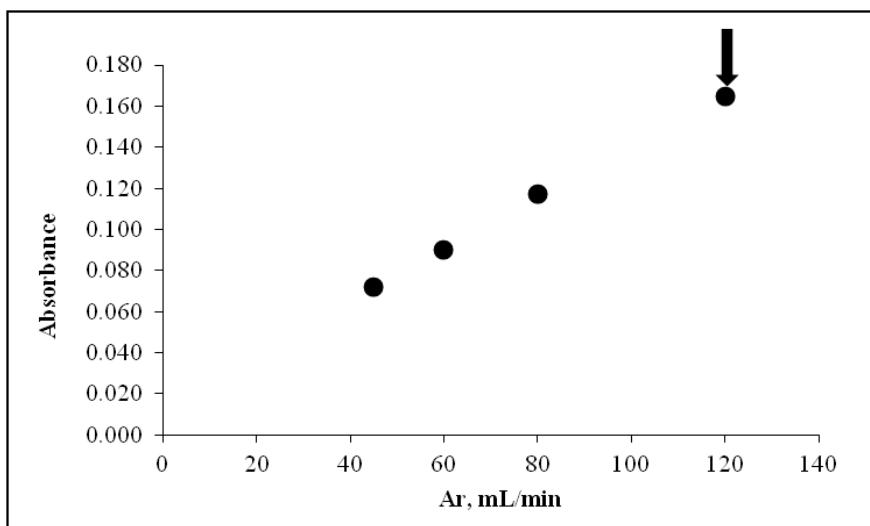


Figure 3.26 The effect of stripping argon flow rate at revolatilization stage on the signal of 2.0 ng/mL Bi that was collected for 60 s. The flow rate for H₂ was 150 mL/min. Trapping and revolatilization temperatures were 262 °C and 1960 °C, respectively. Temperature of EHQTA was 950 °C.

3.4.2. Optimization of Stripping Hydrogen Flow Rate at Trapping and Revolatilization Stages

The effect of hydrogen flow rate on the analytical signal of Bi was also investigated at trapping and revolatilization stages by varying only the hydrogen flow rate. H₂ was inserted to the system between GLS and vaporization unit and it was not involved in stripping the analyte from solution. The argon flow rate at trapping and revolatilization stages were 45 mL/min and 120 mL/min, respectively. At trapping period the flow rate of H₂ was varied between 50 mL/min and 250 mL/min. The variation of the signal with H₂ flow rate at trapping period is given in Figure 3.27. The maximum peak height measurement was obtained for 150 mL/min H₂ flow rate and it was selected as the optimum value for trapping stage.

The effect of H₂ flow rate at revolatilization stage was also investigated and results are given in Figure 3.28. No significant effect of H₂ at flow rates higher than 150

mL/min was observed. Therefore, H₂ flow rate was chosen as 150 mL/min for both stages regarding the ease of application.

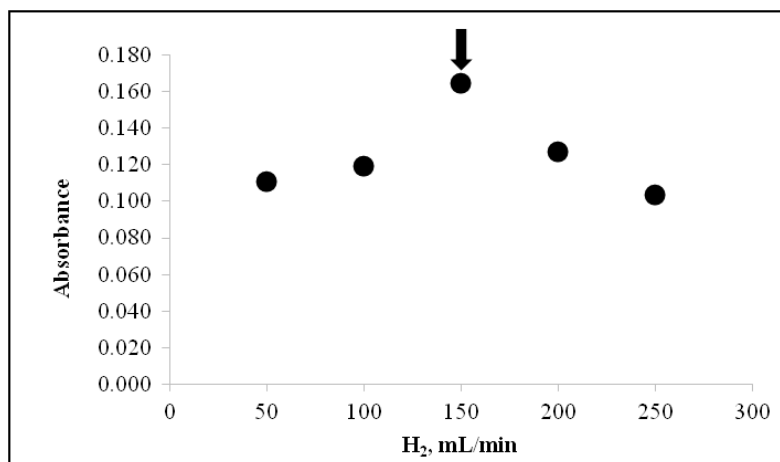


Figure 3.27 The effect of H₂ flow rate at trapping stage on the signal of 2.0 ng/mL Bi that was collected for 60 s. Trapping and revolatilization temperatures were 262 °C and 1960 °C, respectively. Temperature of EHQTA was 950 °C.

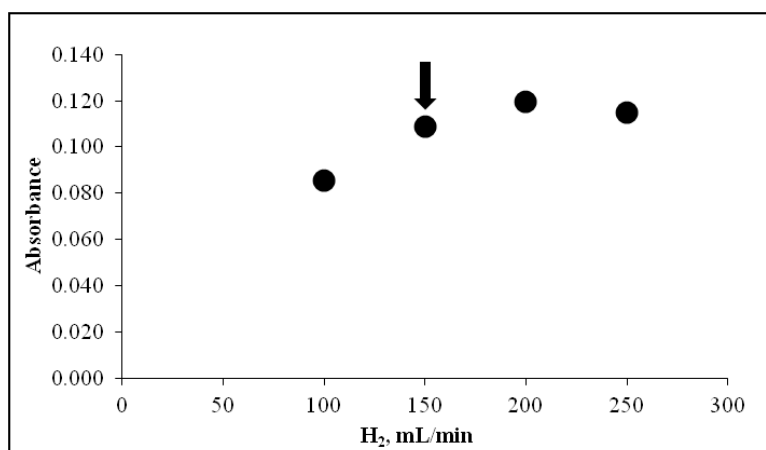


Figure 3.28 The effect of H₂ flow rate at trapping stage on the signal of 2.0 ng/mL Bi that was collected for 60 s. Trapping and revolatilization temperatures were 262 °C and 1960 °C, respectively. Temperature of EHQTA was 950 °C.

3.4.3. Optimization of Trapping and Revolatilization Temperatures

Temperatures at trapping and revolatilization stages were established after the optimization of argon and H₂ flow rates because of their effect on temperature of W-coil. The variations in the analytical signal of Bi as a function of trapping and releasing temperature are given in Figure 3.29. The trapping temperature profile for Bi with ETV system was narrow. Temperatures higher than 180 °C resulted in decrease in analytical signal due to partial release of trapped species. The trapped species release from the surface at 1960 °C. The rate of revolatilization was slow at the temperatures lower than 1960 °C and the signals obtained for that temperatures were less reproducible. The signals obtained for temperatures above 1960 °C were only 3% higher. Therefore, at this temperature rapid and sufficient release of trapped species could be achieved.

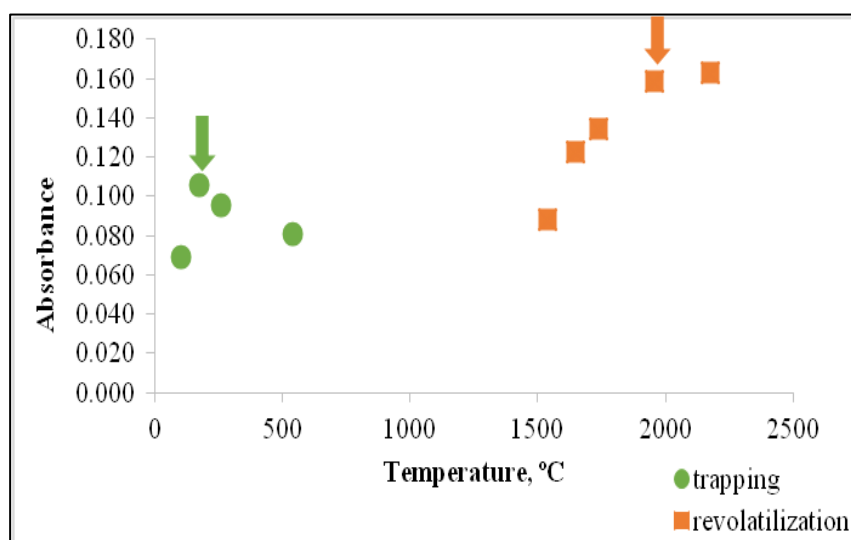


Figure 3.29 The effect of trapping and revolatilization temperatures on analytical signal for Bi trapped for 60 s. During the variations of collection and release temperatures, a constant release temperature of 1960 °C and a constant collection temperature of 180 °C, respectively, were employed. The signals were obtained by collecting 2.0 ng/mL Bi in 1.0 mol/L HCl.

The optimized parameters for this part of the study were summarized in Table 3.9.

Table 3.9 Optimum conditions used for Rh coated W-coil atom trap ETV system.

PARAMETERS	RESULTS
Concentration of HCl, mol/L	1.0
Concentration of NaBH ₄ , % (w/v), stabilized in 0.2 % (w/v) NaOH	0.5
Flow rate of sample, mL/min	3.0
Flow rate of NaBH ₄ , mL/min	3.0
Length of reaction coil, cm	15
Length of stripping coil, cm	2.0
Trapping Ar flow rate, mL/min	45
Release Ar flow rate, mL/min	120
Trapping H ₂ flow rate, mL/min	150
Release H ₂ flow rate, mL/min	150
Trapping temperature, °C	180
Release (atomization) temperature, °C	1960

3.4.4. Calibration Plot and Linear Range for Rh coated W-coil Atom Trap ETV System

The calibration plot obtained for Rh coated W-coil Atom Trap ETV system was given in Figure 3.30. The calibration plot was obtained for the concentrations ranging from 0.5 ng/mL to 5.0 ng/mL. Volatile species of Bi were trapped over 120 s time period and the sample was pumped with the flow rate of 3.0 mL/min. The measurements were based on peak height values. It can be seen from the Figure 3.30 that the deviation from linearity was observed for the concentrations of Bi above 2.0 ng/mL. The linear portion of the calibration plot is given in Figure 3.31. The best line

equation and determination coefficient were, $y = 0.1168x + 0.0095$ and 0.9997, respectively, x is analyte concentration in ng/mL and y is the absorbance value.

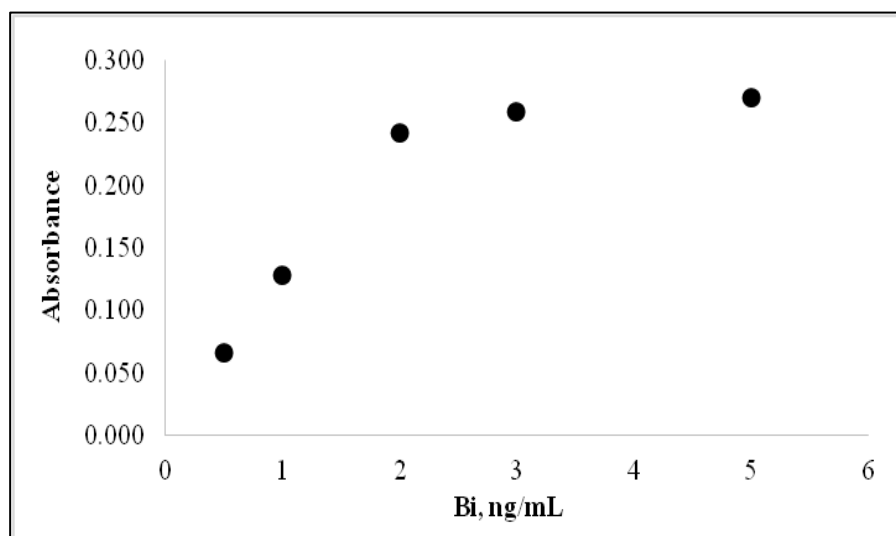


Figure 3.30 Calibration plot obtained for Bi collected over 120 s. The sample flow rate was 3.0 mL/min; trapping and revolatilization temperatures were 180 °C and 1960°C, respectively. Temperature of EHQTA was 950 °C.

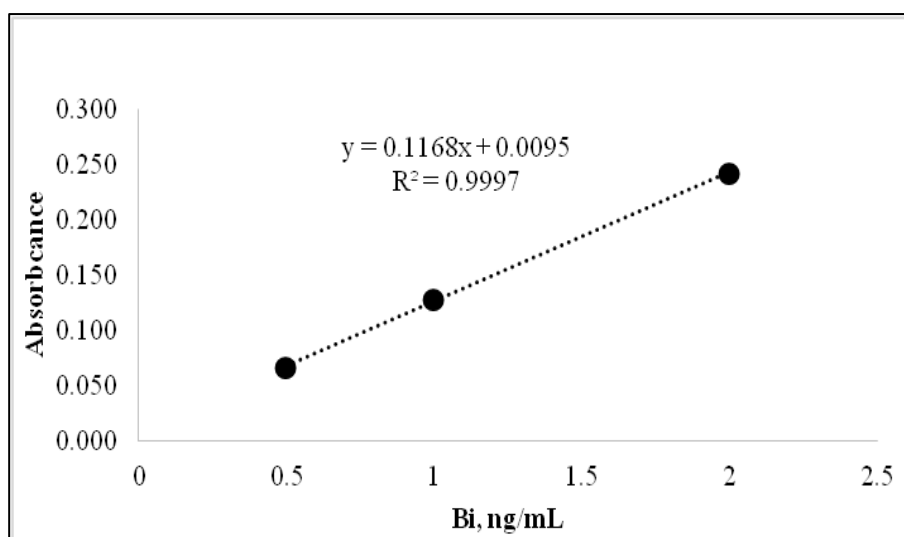


Figure 3.31 Linear range of the calibration plot obtained for Bi collected over 120 s. The sample flow rate was 3.0 mL/min; trapping and revolatilization temperatures were 180 °C and 1960 °C, respectively. Temperature of EHQTA was 950 °C.

3.4.5. Analytical Figures of Merit

The analytical figures of merit of the method for Bi with Rh coated W-coil Atom Trap ETV system are given in Table 3.10; peak height was used in the calculations. The trapping period was 120 s. The LOD was obtained for 6 consecutive measurements of the lowest concentration that was 0.5 ng/mL and it was found as 0.047 ng/mL. The characteristic concentration was calculated as 0.036 ng/mL.

Table 3.10 The analytical figures of merit for Rh coated W-coil Atom Trap ETV system. The volatile Bi species was trapped for 120 s at a flow rate of 3.0 mL/min.

Limit of Detection, LOD, $3\sigma/m$ (N=6) ng/mL	0.047
Limit of Quantification, LOQ, $10\sigma/m$ (N=6) ng/mL	0.157
Linear Range, ng/mL	0.5-2
Characteristic Concentration, C_0 ng/mL	0.036
Characteristic Mass, m_0 pg	216
Precision, % RSD (N=6) for 0.50 ng/mL Bi	1.98

3.5. Syringe Attached Rh Coated W-coil Atom Trap Electrothermal Vaporization System

In this part W-coil was operating as a trapping medium and vaporizer. The atomization unit was EHQTA. The vaporization unit that was made of glass was inserted between GLS and EHQTA. In this configuration volatile species were introduced on W-coil surface via a quartz capillary inserted in a syringe and this syringe was attached to the vaporization unit. The aim of using the syringe was to

handle the movement of quartz capillary. Quartz capillary was kept on the surface of W-coil during trapping period. When the trapping period was over, capillary was pulled back by the help of the piston of syringe; airtight conditions were kept.

The parameters that were optimized in CF-HGAAS were used directly except that the flow rate of stripping Ar. Additionally, carrier Ar gas was added to the system to carry the revolatilized to the atomizer. Moreover, H₂ gas was introduced to the system. The optimization of flow rates of gases at trapping and atomization stages were performed. Trapping and atomization temperatures were optimized and linear calibration plot was obtained.

3.5.1. Optimization of Stripping Argon Flow Rate at Trapping and Revolatilization stages

The optimum stripping Ar flow rate were established for trapping and revolatilization stages while keeping H₂ flow rate constant at 100 mL/min. Carrier Ar gas was introduced and the flow was switched off during trapping period and it was brought to 1.50 L/min at revolatilization stage.

The optimization graphs for stripping Ar flow rate at trapping and revolatilization stages are given in Figure 3.32 and Figure 3.33, respectively. At trapping period the signal obtained for 60 mL/min was the highest. However, the signal increased as the Ar flow rate was increased to 120 mL/min for revolatilization stage. Since additional carrier Ar gas was used at revolatilization stage, there was no need to observe the variation of the signal at higher flow rates than 120 mL/min for the release of trapped species. For the trapping stage the signals obtained for 60 mL/min and 120 mL/min were not different from each other. Therefore, 120 mL/min stripping Ar flow rate was selected as optimum for both trapping and revolatilization stages.

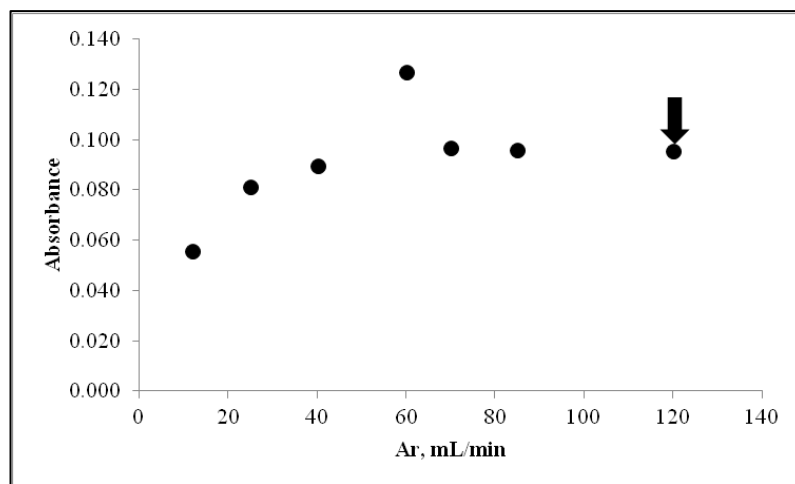


Figure 3.32 Effect of stripping Ar flow rate on the analytical signal at the trapping period; H₂ flow rate was 100 mL/min, release Ar flow rate was 120 mL/min; 1.0 ng/mL Bi was used and pumped at 3.0 mL/min.

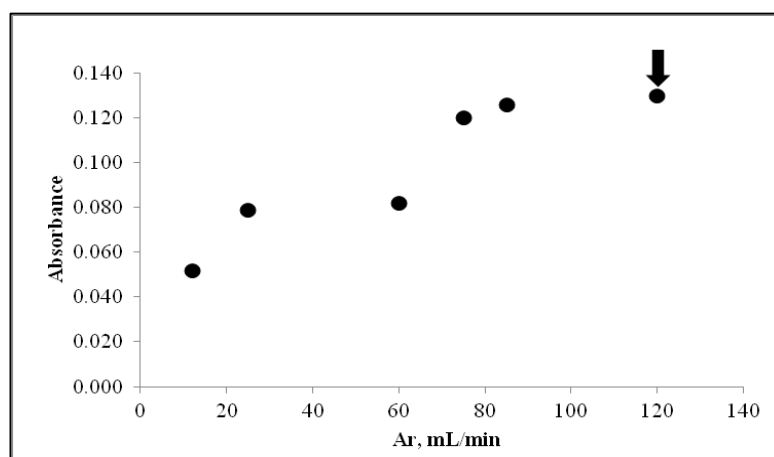


Figure 3.33 Effect of stripping Ar flow rate on the analytical signal at the revolatilization stage; H₂ flow rate was 100 mL/min, trapping Ar flow rate was 120 mL/min; 1.0 ng/mL Bi was used and pumped at 3.0 mL/min.

3.5.2. Optimization of Carrier Argon Flow Rate at Trapping and Revolatilization Stages

Stripping Argon was not enough to carry the revolatilized species to the atomizer. The introduction of carrier Ar to the system is given in Figure 2.10. As the flow rate of Ar was increased at revolatilization stage signal was also enhanced. During trapping period the high flow rates of Ar cause the signal to be dropped. The Ar flow rate had to be kept at minimum flow rate, but at revolatilization stage high flow rate was required. Therefore the high flow rate of Ar was achieved by introducing additional flow meter for carrier Ar gas. The optimization of carrier Ar gas was performed for both trapping and revolatilization stages while keeping stripping Ar flow rate and H₂ flow rate constant, 120 mL/min and 100 mL/min, respectively.

The graphs obtained for optimization of carrier Ar gas flow rate at trapping and revolatilization stages are given in Figure 3.34 and Figure 3.35, respectively. The effect of carrier Ar flow rate on analytical signal was different for trapping and revolatilization stages. During trapping, the signal decreased when carrier Ar flow rate was increased. Therefore, the stripping Ar flow rate was sufficient for trapping volatile species. Carrier Ar was kept closed at the trapping stage. The carrier Ar gas was crucial at revolatilization stage. The flow rate had to be high enough to transport released analyte species to the atomizer. The signal was enhanced significantly up to 1.5 L/min and this value was selected as optimum value.

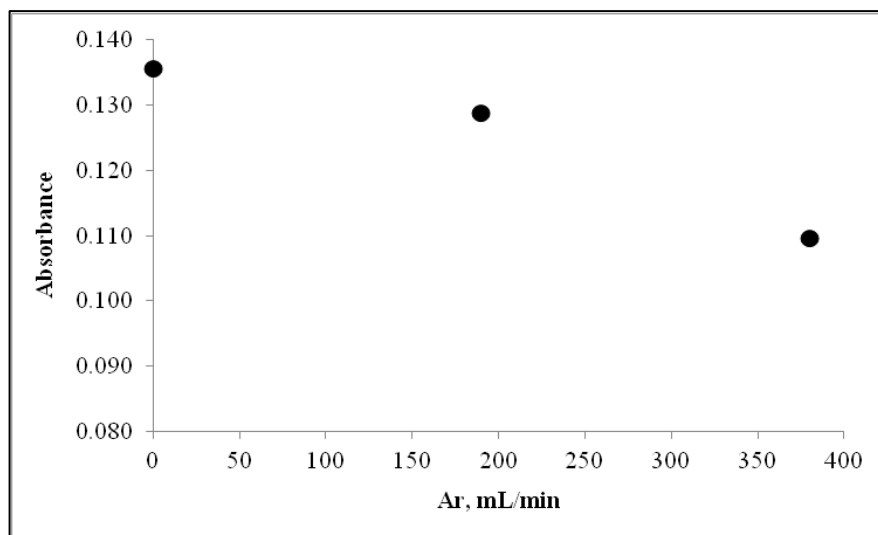


Figure 3.34 Effect of carrier Ar flow rate on the analytical signal at the trapping period; H₂ flow rate was 100 mL/min, stripping Ar flow rate was 120 mL/min; 1.0 ng/mL Bi was used and pumped at 3.0 mL/min.

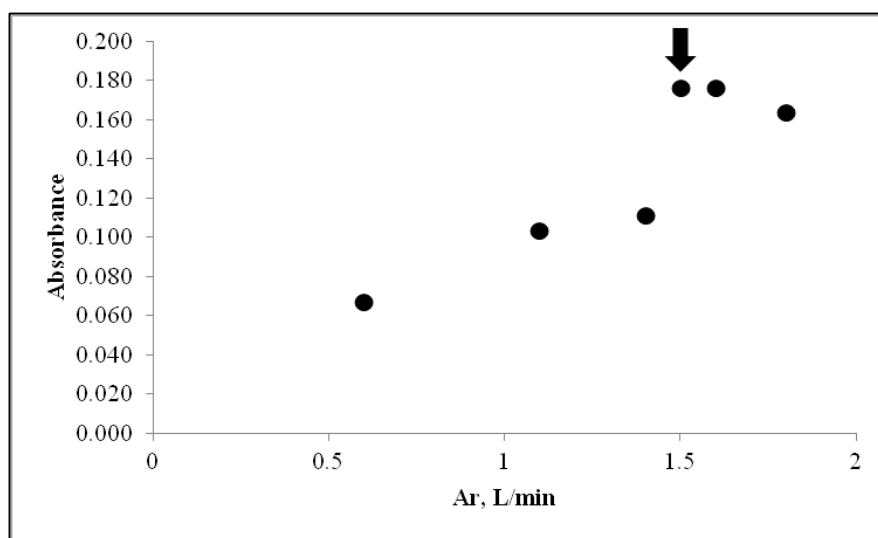


Figure 3.35 Effect of carrier Ar flow rate on the analytical signal at the revolatilization period; H₂ flow rate was 100 mL/min, stripping Ar flow rate was 120 mL/min; 1.0 ng/mL Bi was used and pumped at 3.0 mL/min.

3.5.3. Optimization of Hydrogen Flow Rate at Trapping and Revolatilization Stages

The effect H₂ flow rate on the trapping and revolatilization stages were investigated by changing only H₂ flow rate. It was introduced behind the vaporization unit (Figure 2.10). The measurements were done according to the peak heights. The variation of the signal for trapping and revolatilization stages is given in Figure 3.36 and Figure 3.37, respectively. The signal was significantly decreased for the flow rates higher than 150 mL/min where below this value signal was not affected significantly. As a result, 150 mL/min was chosen as an optimum value. The same trend was also observed for revolatilization stage. Higher flow rates caused a decrease in the signal and 150 mL/min was the optimum H₂ flow rate for revolatilization stage.

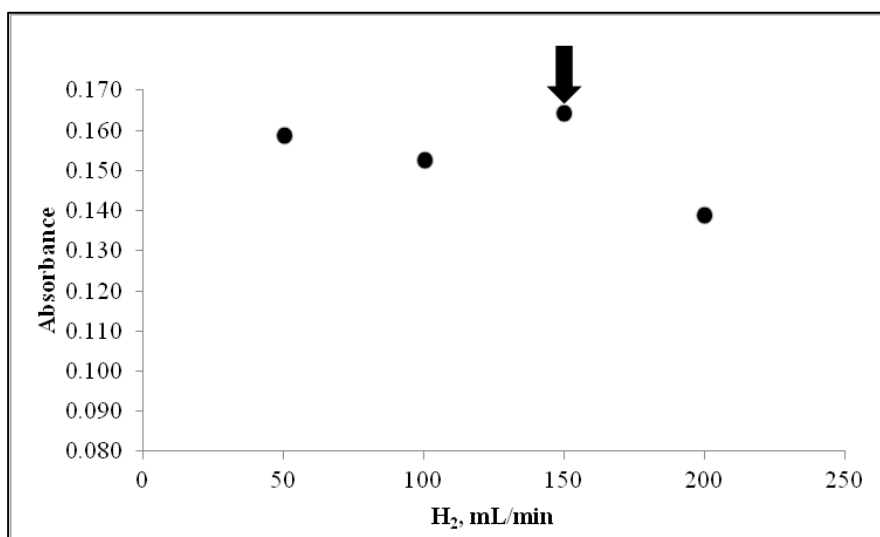


Figure 3.36 Effect of H₂ flow rate on the analytical signal at the trapping period; Ar flow rate was 120 mL/min; 1.0 ng/mL Bi was used and pumped at 3.0 mL/min.

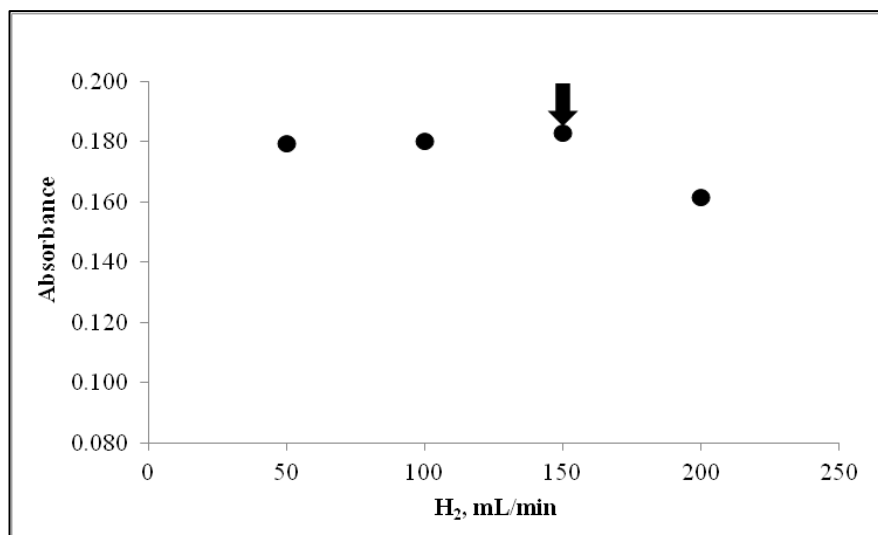


Figure 3.37 Effect of H₂ flow rate on the analytical signal at the revolatilization period; Ar flow rate was 120 mL/min; 1.0 ng/mL Bi was used and pumped at 3.0 mL/min.

3.5.4. Optimization of Trapping and Revolatilization Temperatures

The temperature optimization was done after establishing the optimum conditions of gas flow rates, since they had an effect on the W-coil temperature. The variation of the analytical signal as a function of trapping a revolatilization temperature is indicated in Figure 3.38. The volatile species of Bi could be trapped at 227 and 300 °C. The temperatures higher than 300 °C caused a decrease in the signal probably due to the release of collected species on the W-coil surface. The trapping temperature was selected as 300 °C. The collected species could be released at 1390 °C, but the peaks that were obtained for this temperature was broad. As the temperature was increased peak shape became narrower and rapid release rate was achieved. The trapped species revolatilized sufficiently at 1542 °C. In order to preserve the surface coating and prolong the lifetime of W-coil the use of higher release temperature was avoided.

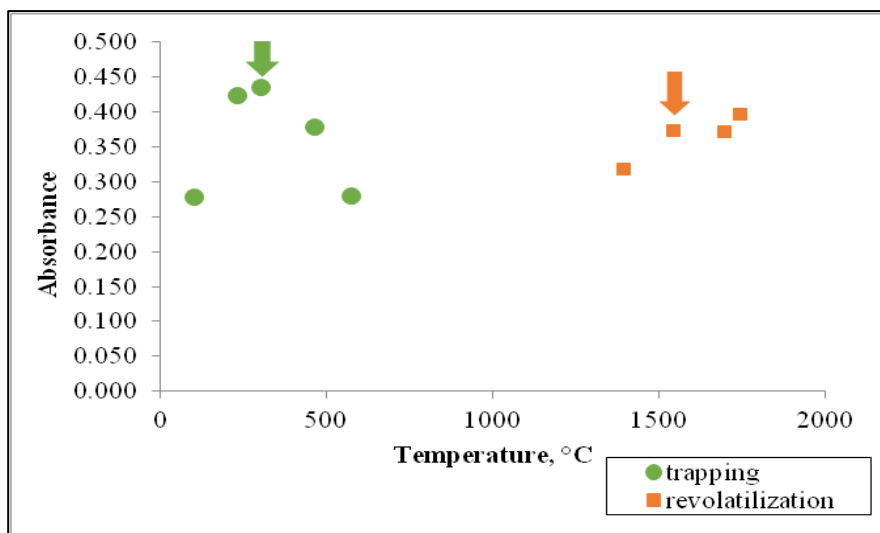


Figure 3.38 The effect of trapping and revolatilization temperatures on analytical signal for Bi. During the variations of collection and release temperatures, a constant release temperature of 1960 °C and a constant collection temperature of 300 °C, respectively, were employed. The signals were obtained by collecting 1.0 ng/mL Bi for 60 s trapping. The temperature of EHQTA was 950 °C.

The parameters that were used for syringe attached Rh coated W-coil atom trap ETV system are summarized in Table 3.11.

Table 3.11 The optimum conditions used for syringe attached Rh coated W-coil atom trap ETV system.

PARAMETERS	RESULTS
Concentration of HCl, mol/L	1.0
Concentration of NaBH ₄ , % (w/v), stabilized in 0.2 % (w/v) NaOH	0.5
Flow rate of sample, mL/min	3.0
Flow rate of NaBH ₄ , mL/min	3.0
Length of reaction coil, cm	15
Length of stripping coil, cm	2.0
Trapping Ar flow rate, mL/min	120
Release Ar flow rate, mL/min	120
Trapping H ₂ flow rate, mL/min	150
Release H ₂ flow rate, mL/min	150
Carrier Ar flow rate mL/min (trapping)	-
Carrier Ar flow rate L/min (revolatilization)	1.5
Trapping temperature, °C	300
Release (revolatilization) temperature, °C	1542
Atomization temperature, °C	950

3.5.5. Calibration Plot and Linear Range for Syringe Attached Rh coated W-coil Atom Trap ETV System

The calibration plot and linear portion of the calibration plot were obtained with syringe attached Rh coated W-coil Atom Trap ETV system. The measurements were done on the basis of peak height. The calibration plot obtained for 120 s collection with 3.0 mL/min sample flow rate is given in Figure 3.39. The calibration plot started at 0.1 ng/mL Bi and deviation from linearity was observed beginning from 0.5 ng/mL. The calibration plot was linear between 0.1 ng/mL to 0.3 ng/mL and the linear portion and best line equation are indicated in Figure 3.40. The best line equation was $y = 0.6283x + 0.0415$ with the determination coefficient of 0.9995; x is analyte concentration and y is the absorbance value.

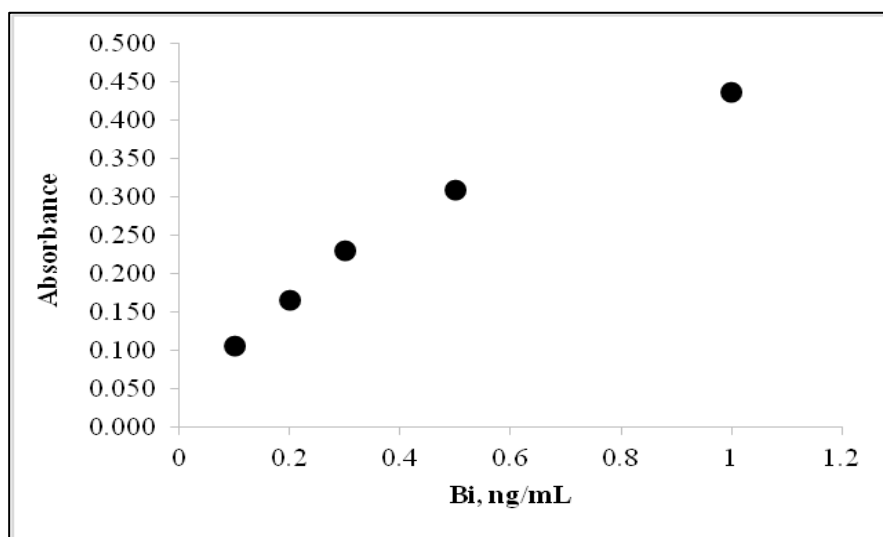


Figure 3.39 The calibration plot with syringe attached Rh coated W-coil Atom Trap ETV system for Bi collected for 120 s. The collection period was 120 s and sample flow rate was 3.0 mL/min.

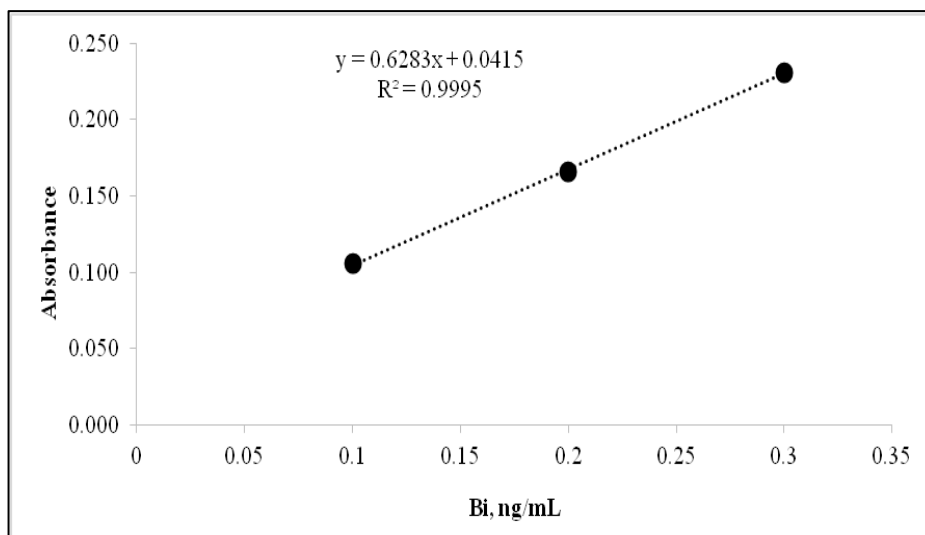


Figure 3.40 Linear portion of the calibration plot for Bi collected for 120 s and best line equation.

The analytical signal obtained for 0.2 ng/mL Bi collected for 120 s at a flow rate of 3.0 mL/min is indicated in Figure 3.41.

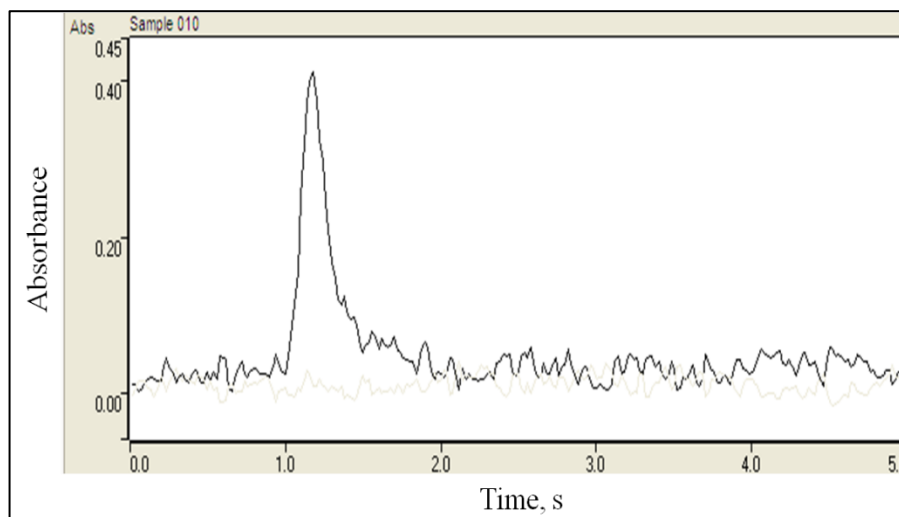


Figure 3.41 The analytical signal obtained with syringe attached Rh coated W-coil Atom Trap ETV system for 0.2 ng/mL. The collection period was 120 s and sample flow rate was 3.0 mL/min.

The calibration plot for 60 s collection was also obtained by using the same system. The calibration plot and linear portion of the calibration plot are given in Figure 3.42 and Figure 3.43, respectively. The calibration plot was linear between 0.1 ng/mL to 2.0 ng/mL with 1.0 minute collection. Therefore, linear range was wider with 60 s collection than 120 s collection.

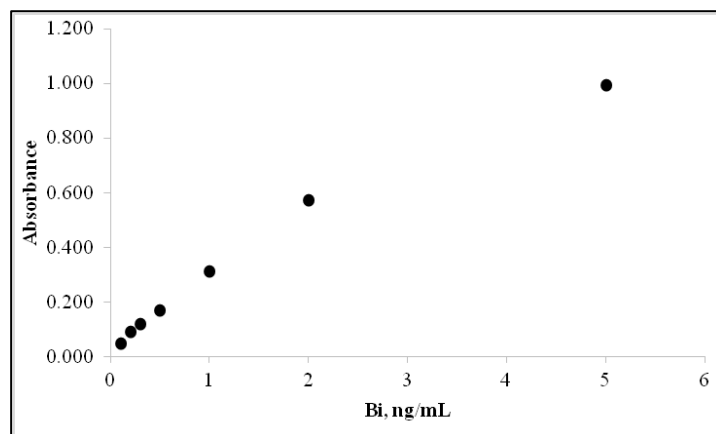


Figure 3.42 The calibration plot for Bi with syringe attached Rh coated W-coil Atom Trap ETV system. The collection period was 60 s and sample flow rate was 3.0 mL/min.

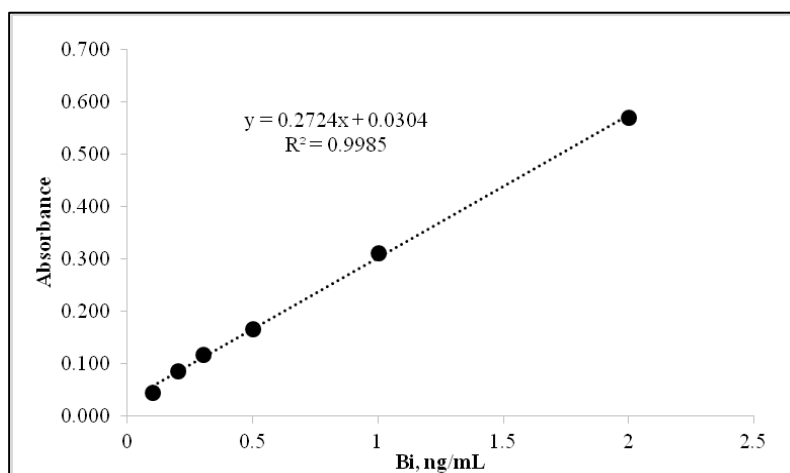


Figure 3.43 Linear portion of the calibration plot and best line equation for 60 s collection.

3.5.6. Analytical Figures of Merit

The analytical figures of merit of the method, which were calculated by using the peak height values of analytical signal, are given in Table 3.12. The analytical figures of merit were calculated for 60 s and 120 s collection period. The sample flow rate was 3.0 mL/min. The limit of detections for 60 s and 120 s collection period s were 0.022 and 0.026 ng/mL, respectively. The characteristic concentration for 60 s collection was found as 0.0062 ng/mL and 0.0029 ng/mL was calculated for 120 s collection.

Table 3.12 Analytical figures of merit for Bi obtained for 60 s and 120 s collection period.

	60 s collection	120 s collection
Limit of Detection, LOD, $3\sigma/m$ (N=5) ng/mL	0.022	0.026
Limit of Quantification, LOQ, $10\sigma/m$ (N=5) ng/mL	0.066	0.086
Characteristic Concentration, C_0 ng/mL	0.0062	0.0029
Characteristic mass, m_0 pg	18.6	17.4
Precision, % RSD (N=5) for 0.10 ng/mL Bi	1.3	1.7

The improvements of syringe attached Rh coated W-coil atom trap ETV system regarding limit of detection and characteristic concentration with respect to the Rh coated W-coil atom trap ETV and CF-HGAAS systems are summarized in Table 3.13. The limit of detection and characteristic concentration values were calculated for 120 s collection.

Table 3.13 Analytical figures of merit for syringe attached Rh coated W-coil atom trap ETV, Rh coated W-coil atom trap ETV and CF-HGAAS systems.

	Syringe Attached W-coil atom trap ETV (120 s collection)	W-coil atom trap ETV (120 s collection)	CF-HGAAS
LOD, ng/mL	0.026	0.047	1.10
C₀, ng/mL	0.0029	0.036	0.80

The enhancement factor in limit of detection ($3\sigma/m$) which was calculated for 0.1 ng/mL was found to be 42 when syringe attached Rh coated W-coil atom trap ETV system was compared with CF-HGAAS. The characteristic concentration was calculated as 0.0029 ng/mL and this value was 276 times lower than CF-HGAAS system. The attachment of quartz capillary to the system provides enhancement factor of 2.0 when compared to W-coil atom trap ETV system with respect to the limit of detection. The comparison regarding characteristic concentration yielded 12 times lower value as compared to W-coil atom trap ETV system.

3.5.7. Accuracy of the Method

The accuracy of syringe attached Rh coated W-coil atom trap ETV system was performed with using CRM, Natural Water (1643e). The direct calibration method did not work with this system; therefore standard addition method was applied for the accuracy check. The solutions were acidified with HCl and the resultant HCl concentration was 1.0 mol/L. 1.0 mL of CRM solutions were spiked to Bi containing standard solutions. The results are given in Table 3.14.

Table 3.14 Result of the analysis of CRM and the certified values (n=3).

Concentration found, ng/mL	13.64 ± 0.47
Certified value, ng/mL	14.09 ± 0.15

3.6. The Comparison of the Developed Methods

The limits of detection of the developed methods were compared with the values given in the literature and the comparison is given in Table 3.15. The limit of detection obtained for developed methods were comparable with the other methods or better. The absolute LOD values obtained by ICP-MS systems including *in-situ* atom trap were much better than developed methods in this study. However, these methods are not cost effective and they are not available for most of the laboratories. In addition, it should be remembered that trap systems improve concentration LOD values only. The use of W-coil systems functioning as either ETA or ETV can be applied inexpensively in all laboratories having simple AA spectrometer.

Table 3.15 Comparison of the limit of detection and the sample volume of the method with those of others in literature.

Method	Concentration LOD, ng/mL	Absolute LOD, pg	Volume, mL	Literature
W-trap ETA*	0.018	108	6	This study
W-trap ETV**	0.026	156	6	This study
Preconcentration ETAAS	0.013	2.80	0.213	[152]
Atom trap SQT- FAAS	1.60	57600	36	[162]
Preconcentration HG-ICP-AES	0.020	2000	100	[163]
W-trap HGAAS	0.0027	49	18	[56]
<i>In-situ</i> trapping QTA-AAS	0.039	780	20	[164]
<i>In-situ</i> trapping ETV-ICP-MS	0.003	6	2	[159]
HS-SDME HG- ETV-ICP-MS	0.01	0.030	0.003	[165]

* Syringe attached Rh coated W-coil atom trap ETA system

** Syringe attached Rh coated W-coil atom trap ETV system

3.7. Interference Study

Interference study employing Rh coated W-coil Atom Trap ETA and Rh coated W-coil atom trap ETV systems were performed. The quartz capillary was eliminated from these systems for easy application of analysis of numerous amounts of interferent solutions. The conditions optimized for syringe attached W-coil atom trap ETA and ETV conditions were taken into account (Table 3.5 and Table 3.11). The interference elements were selected from hydride forming elements (As, Sb, Se, Te and Sn), transition metals (Fe, Co, Ni, Cu and Mn) and alkali-earth metals (Na, Ca, Al, Si). Bi concentration was selected as 0.3 ng/mL in 1.0 mol/L HCl. The oxidation states of the hydride forming elements were As(III), Sb(III), Se(IV), Te(IV) and Sn(IV). The effects of interference were measured by varying interferent/analyte ratio. Interference/analyte (mass/mass) ratios were kept at 1, 10, 50 and 500. The signal obtained for 0.3 ng/mL Bi solution was normalized to 100. The signal obtained for interferent containing Bi solutions was compared with the normalized signal. Two replicates of measurements were performed for interference studies with W-coil Atom Trap ETA and ETV systems.

3.7.1. Interference Study with Rh coated W-coil Atom Trap ETA System

It has been extensively reported that hydride generation based on tetrahydroborate reduction is susceptible to suffer from interference from other hydride forming elements and transition metals. Gas phase interference was generally encountered with hydride forming elements and liquid phase interference could be resulted from transition metals [120].

The interference effects of hydride forming elements on the analytical signal of Bi are represented in Figure 3.44. Tolerance towards the potential interference effects of hydride forming elements was observed for the elements As, Se and Sn. Te and Sb caused a depression on the signal 500-fold concentration ratio. Liu et al. stated that the depression on the signal of Bi in the presence of Te was observed at the mass ratio above 500 [120].

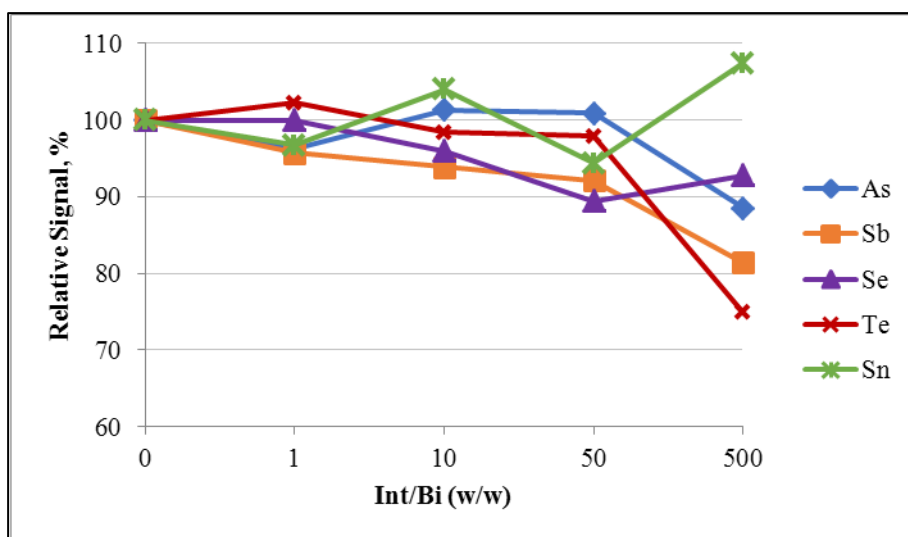


Figure 3.44 Interference effects of hydride forming elements on analytical signal of 0.3 ng/mL Bi collected for 60 s using Rh coated W-coil Atom Trap ETA. The trapping and atomization temperatures were 462 °C and 2177 °C, respectively.

In hydride generation studies interference effects of transition metals are observed frequently. They can react with THB to produce their hydrides or metallic forms and form insoluble precipitates. The metallic particulates can accumulate inside of GLS, reaction and stripping coil, transfer tubings between GLS and atomizer and make these dark gray. These metallic particulates coprecipitate analyte or adsorb the analyte hydride [132]. Therefore, the transition metals interfere with analyte negatively. The interference effects of transition metals (Fe, Co, Ni, Cu, and Mn) are indicated in Figure 3.45. Ni and Cu are well known interferents in HGAAS for the determination of hydride forming elements including Bi [166,167]. However, the interference effects of these elements were not observed with W-coil atom trap ETA system. Among the transition metals Co and Mn caused a decreased in the signal at the average of 15% at the 500-fold interferent/analyte ratio.

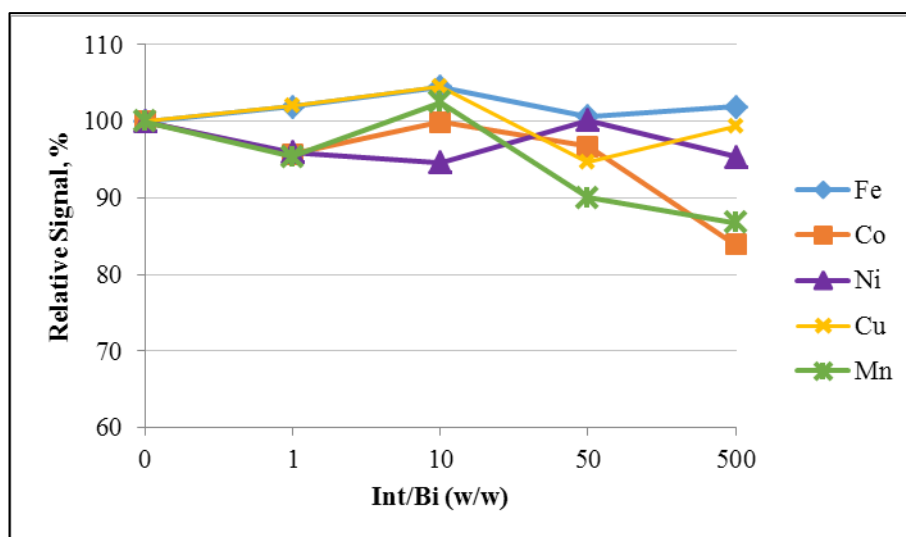


Figure 3.45 Interference effects of transition metals on analytical signal of 0.3 ng/mL Bi collected for 60 s using Rh coated W-coil Atom Trap ETA. The trapping and atomization temperatures were 462 °C and 2177 °C, respectively.

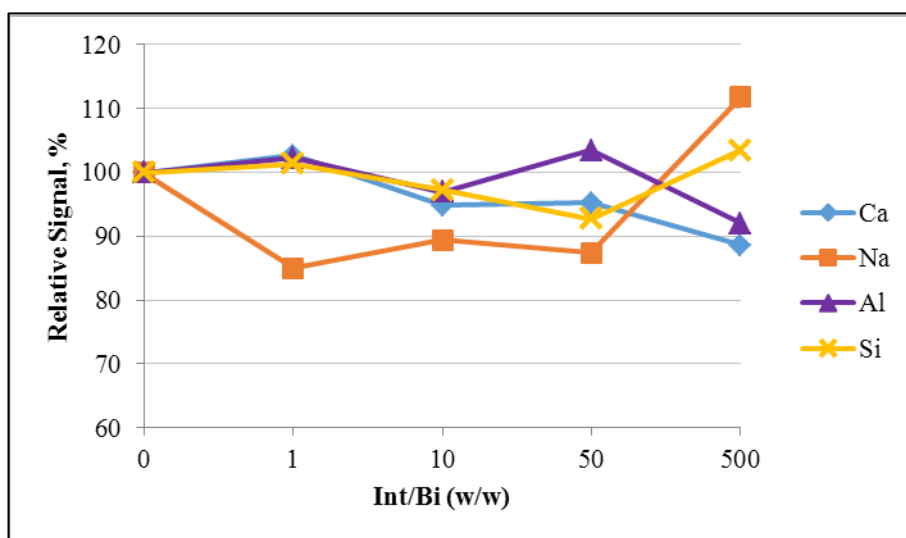


Figure 3.46 Interference effects of earth-based elements on analytical signal of 0.3 ng/mL Bi collected for 60 s using Rh coated W-coil Atom Trap ETA. The trapping and atomization temperatures were 462 °C and 2177 °C, respectively.

The last series of interferents were selected from earth-based elements (Ca, Na, Al and Si) and their effects on the analytical of Bi are shown in Figure 3.46. Presence of

Na in the solution had caused approximately 15% decrease in the Bi signal. However, the decrease disappeared at 500-fold interferent/analyte.

3.7.2. Interference Study with Rh coated W-coil Atom Trap ETV System

The interference study was also carried out for Rh coated W-coil Atom Trap ETV system and the effects of hydride forming elements, transition metals and earth-based elements were investigated.

The hydride forming elements had a different effect on W-coil ETV system compared to W-coil ETA system. The effects of these elements on the analytical signal of Bi are given in Figure 3.47. The tolerance level of W-coil ETA system was higher for the elements As, Se and Sn. The use of W-coil as a vaporizer improved the tolerance level for Sb and Te. The analytical signal of Bi with ETV system was affected in the presence of As, Se and Sn. Among the interferents, As and Se caused the enhancement of the signal at 500-fold mass ratio (Figure 3.47). The atomization with W-coil ETV system was performed with QTA that has lower atomization temperature than ETA. Graphite atomizers provides better tolerance to interferences than QTA [92], since the atomization takes place at temperatures above 2000 °C. Therefore, W-coil functioning as atomizer is expected to have better tolerance towards the interferents than QTA. The lower tolerance level of W-coil ETV system regarding As, Se and Sn could be partly due to the lower atomization temperature in QTA.

The interference effects of transition metals on the analytical signal of Bi for W-coil ETV system are given in Figure 3.48. The most severe interferents for hydride forming elements among the transition metals are Co, Ni and Cu. W-coil ETV system was tolerable the interference effects of Fe, Co, Ni, Cu and Mn. The analytical signal of Bi was not affected significantly for these elements.

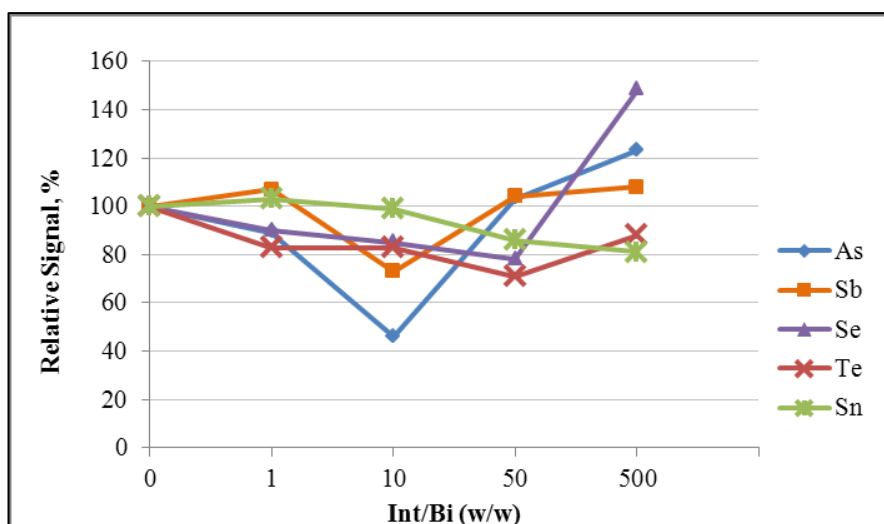


Figure 3.47 Interference effects of hydride forming elements on analytical signal of 0.3 ng/mL Bi collected for 60 s using Rh coated W-coil Atom Trap ETV. The trapping and revolatilization temperature were 300 °C and 1542 °C, respectively. The temperature of EHQTA was 950 °C.

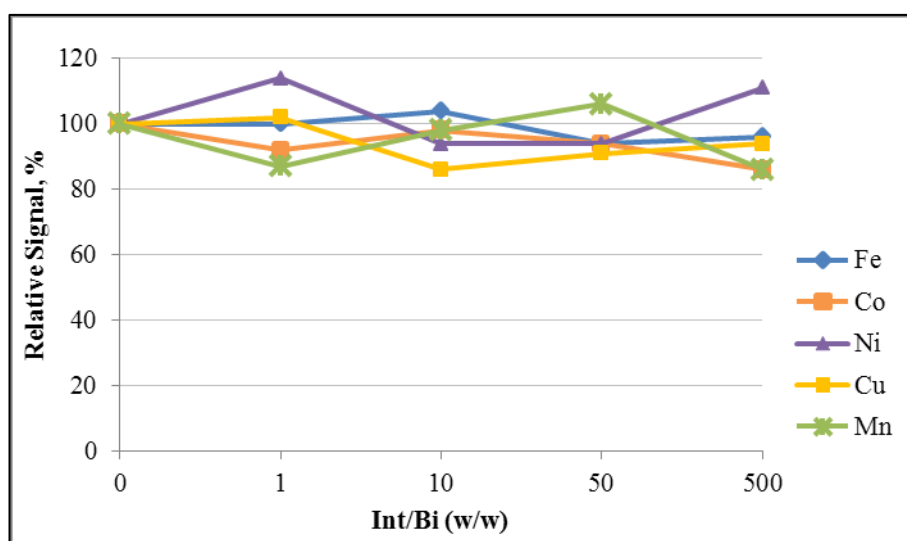


Figure 3.48 Interference effects of transition metals on analytical signal of 0.3 ng/mL Bi collected for 60 s using Rh coated W-coil Atom Trap ETV system. The trapping and revolatilization temperature were 300 °C and 1562 °C, respectively. The temperature of EHQTA was 950 °C.

The interference effects of earth-based elements were also investigated with W-coil ETV system and the results are represented in Figure 3.49. As seen from the results that those elements had no significant effects on the signal of Bi with W-coil ETV system. In particular the behavior with Na is to be noted as compared to ETA results.

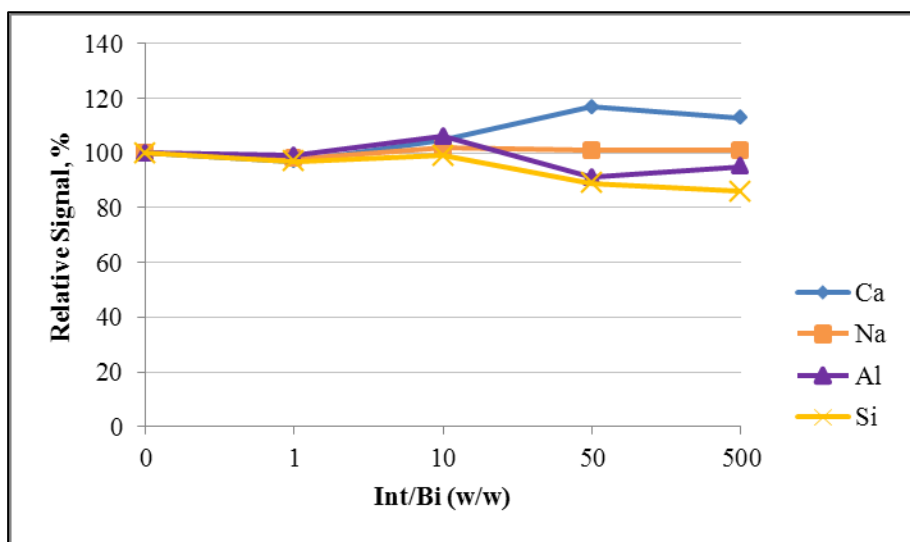


Figure 3.49 Interference effects of earth based element on analytical signal of 0.3 ng/mL Bi collected for 60 s Rh coated W-coil Atom Trap ETV system. The trapping and revolatilization temperature were 300 °C and 1542 °C, respectively. The temperature of EHQTA was 950 °C.

The interference study performed with ETA and ETV system were preliminary studies. The results regarding both of the systems are summarized in Table 3.16. The results obtained with hydride forming, transition element and earth based elements are listed in the table.

Table 3.16 Interference studies performed with Rh coated W-coil Atom Trap ETA and Rh coated W-coil Atom Trap ETV. Bi concentration was 0.3 ng/mL.

		Mass ratio (Int/Bi)				
		0	1	10	50	500
		Relative signal				
As	W-coil ETA	100	96±3	97±6	101±4	89±2
	W-coil ETV	100	89±15	46±11	103±19	123±12
Sb	W-coil ETA	100	96±15	94±16	92±6	81±3
	W-coil ETV	100	107±6	73±6	104±11	108±6
Se	W-coil ETA	100	100±3	96±4	89±5	93±3
	W-coil ETV	100	90±2	85±6	78±6	148±4
Te	W-coil ETA	100	102±6	98±3	98±3	75±4
	W-coil ETV	100	83±6	83±5	71±16	88±11
Sn	W-coil ETA	100	97±6	104±9	94±3	108±6
	W-coil ETV	100	103±6	99±8	86±4	81±6
Fe	W-coil ETA	100	102±4	104±6	101±4	102±9
	W-coil ETV	100	100±11	104±21	94±11	96±12
Co	W-coil ETA	100	96±8	100±6	97±9	84±5
	W-coil ETV	100	92±10	98±10	94±10	86±12

Table 3.16 continued.

Ni	W-coil ETA	100	97±3	95±4	100±3	95±1
	W-coil ETV	100	114±12	94±15	94±6	111±17
Cu	W-coil ETA	100	102±6	104±3	95±1	99±3
	W-coil ETV	100	102±10	86±23	91±14	94±11
Mn	W-coil ETA	100	95±8	102±7	90±7	86±1
	W-coil ETV	100	87±1	98±4	106±10	86±1
Ca	W-coil ETA	100	103±4	95±3	95±3	87±12
	W-coil ETV	100	97±5	105±4	117±16	113±11
Na	W-coil ETA	100	85±14	89±11	87±19	112±9
	W-coil ETV	100	98±5	102±5	101±5	101±6
Al	W-coil ETA	100	102±8	97±5	103±7	92±2
	W-coil ETV	100	99±9	106±14	91±6	95±1
Si	W-coil ETA	100	101±4	97±14	93±10	103±3
	W-coil ETV	100	97±4	99±4	89±8	86±8

3.7.3. Interference Study with Twin-channel Hydride Generation System

The preliminary interference studies carried out using W-coil Atom Trap ETA and ETV systems were performed with a hydride generation system containing single gas-liquid separator. The source of interference regarding liquid and/or gas phase interferences could not be determined easily. The interference studies placed in this part were performed with twin-channel hydride generation system. Twin-channel hydride generator consisted of two gas-liquid separators.

In the interference study performed by D'ulivo et al. [129]; the researchers carried out experiments by using twin-channel continuous flow hydride generator in which analyte and interferent were pumped from separate channels. It was stated that the liquid phase interference was eliminated with this system. The twin-channel hydride generator was also used to investigate the interference effects of As, Sb and Bi hydrides on Se(IV) [130]. By using this system, the separate and independent hydride generation and introduction of analyte and interferent hydrides were achieved.

In this study twin-channel hydride generator system was used in two different modes. In the first mode, analyte and interferent were mixed in the same solution and pumped from one channel, from the second channel blank solution (1.0 mol/L HCl solution) was transferred (Figure 2.12). The introduction of blank solution was required to keep the hydrogen yielded from hydride generation reaction constant. In the second mode, the analyte and interference were transported from the separate channels of twin-channel hydride generators. The generated analyte and interferent hydrides were combined after gas liquid separators and sent to vaporization and/or atomization unit together (Figure 2.13).

Interference studies employing CF-HGAAS, Rh coated W-coil Atom Trap ETA and Rh coated W-coil Atom Trap ETV systems were performed. The interference elements were selected from hydride forming elements (As, Sb, Se, Te and Sn). The oxidation states of the elements were As(III), Sb(III), Se(IV), Te(IV), Sn(IV). Bi concentration was selected as 20 ng/mL Bi for twin channel CF-HGAAS system and

2.0 ng/mL in 1.0 mol/L HCl for twin channel CF-HG W-coil Atom Trap ETA and ETV systems. The effects of interference were measured by varying interferent/analyte ratio. Interference/analyte (mass/mass) ratio was kept at 1, 10, 50 and 500. The signal obtained for 2.0 ng/mL Bi solution was normalized to 100 and considered as reference signal. The signal obtained for interferent containing Bi solutions was compared according to normalized signal. Two replicates of measurements were performed for interference studies with W-coil Atom Trap ETA and ETV systems.

3.7.3.1. Interference Study with CF-HGAAS System

Hydride generation provides the separation of hydride forming elements from the matrix elements present in the same solution. However, HGAAS is prone to interferences both in condensed phase and in gas phase. The interference effects could occur during hydride generation step and in the atomizer. The interferences in the reaction step usually suppress the formation of hydrides from analyte and thus the analytical signal is also decreased. Atomization interference is caused by other hydride forming elements and results in the suppression of the analytical signal. The interferent can form stable, mixed diatomic molecules such as AsSb [168] decreasing the free analyte atom formation. In addition, interfering hydride elements consume the radicals resulting the lower efficiencies of free analyte atom formation in the atomizer [131].

The interference study was started with the investigation of interference effects of hydride forming elements (As, Sb, Se, Te and Sn) with CF-HGAAS. Twin-channel hydride generation system was applied. The effects of interferences on Bi signal when Bi and interferent were together in the same solution are given in Figure 3.50. The effect of Se and Te were observed at 500 fold mass ratio as a decrease in the signal. When the analyte and interferent were pumped separately the effect of Te almost disappeared and the signal Bi was 16% decreased in the presence of Se in the gas phase. The results for all interferences elements pumped separately from analyte are

given in Figure 3.51. Flores et al. [169] stated that Se has an effect on the Bi signal with QTA. When atomizer was MMQTA, the effect of Se on Bi signal was not changed. Therefore, they suggested interferences occur either in liquid phase or in the inlet arm of the atomizer. For this study, the trend of interferences was similar with the results stated by Flores et al. As a result, it could be concluded that the interference effects of Se and Te were most probably originated from liquid phase with CF-HGAAS, since the Bi signal was mostly affected in the presence of interferent in the same solution.

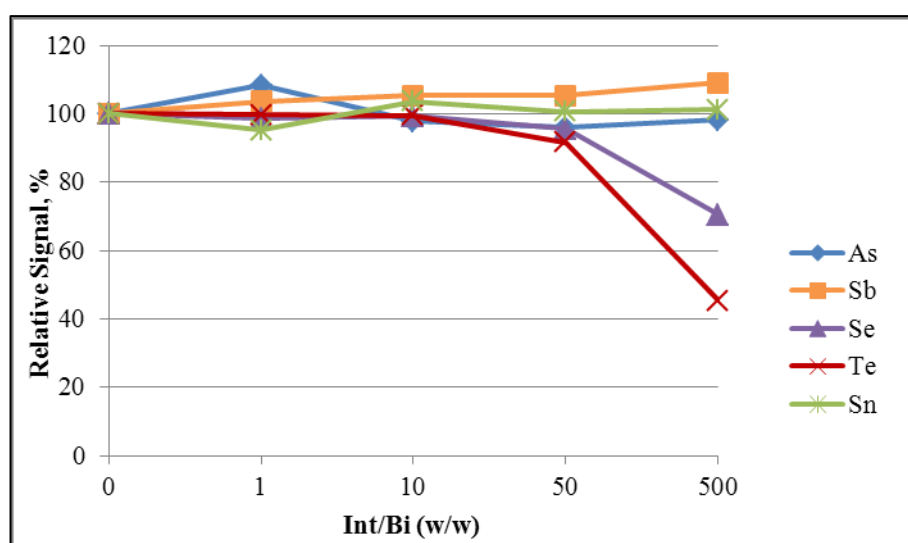


Figure 3.50 Interference effects of hydride forming elements on analytical signal of 20 ng/mL Bi using twin-channel CF-HGAAS system. Analyte and interferent were placed in the same solution and pumped from one channel, from the second channel blank solution was transferred. The temperature of EHQTA was 950 °C.

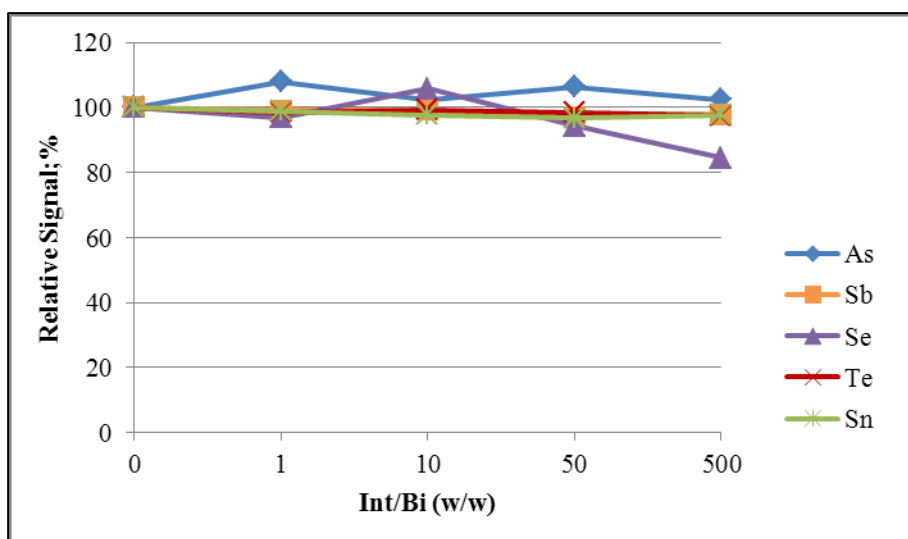


Figure 3.51 Interference effects of hydride forming elements on analytical signal of 20 ng/mL Bi using twin-channel CF-HGAAS system. The analyte and interferent were transported from the separate channels of twin-channel hydride generators. Temperature of EHQTA was 950 °C.

3.7.3.2. Interference Study with Rh-coated W-coil Atom Trap ETA System

The interference effects of As, Sb, Se, Te and Sn were investigated with twin channel CF-HG system coupled to Rh coated W-coil Atom Trap ETA system. The results for twin channel HG system in which analyte and interferent were in same solution are given in Figure 3.52. The Bi signal was diminished almost 50% when interferents were Sb and Te. Moreover, Se had a suppression effect on the analyte signal about 20% at 500 fold interferent/analyte ratio.

Interference effects on Bi signal when analyte and interferents were transferred separately are represented in Figure 3.53. In this mode, the interference effect of Sb and Te was more effective in this mode than indicated in Figure 3.52. In this mode 40% and 30% decrease in the signal at 500 fold interferent/analyte ratio was resulted from the presence of Se and As, respectively.

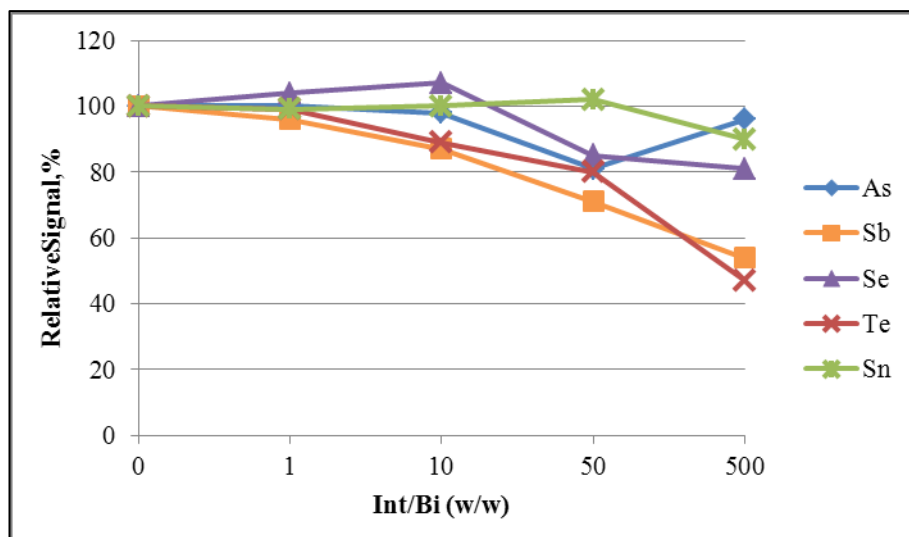


Figure 3.52 Interference effects of hydride forming elements on analytical signal of 2.0 ng/mL Bi collected for 60 s using twin-channel CF-HG system of Rh coated W-coil Atom Trap ETA system. Analyte and interferent were placed in the same solution and pumped from one channel, from the second channel blank solution was transferred. The trapping and atomization temperatures were 462 °C and 2177 °C, respectively.

The interferents affected the Bi signal significantly when they were pumped separately with the analyte. The source of interference was most probably in gas phase. It could take place during transport of hydrides to trapping medium, during trapping period and/or atomization.

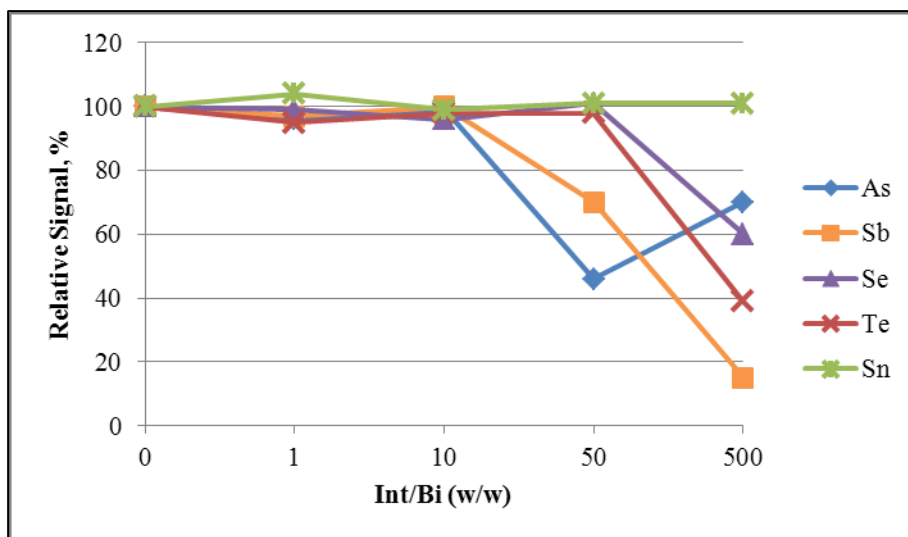


Figure 3.53 Interference effects of hydride forming elements on analytical signal of 2.0 ng/mL Bi collected for 60 s using twin-channel CF-HG system of Rh coated W-coil Atom Trap ETA system. The analyte and interference were transported from the separate channels of twin-channel hydride generators. The trapping and atomization temperatures were 462 °C and 2177 °C, respectively.

3.7.3.2.1 Trapping and Atomization Temperature Ranges for Interference Elements

It may be suggested that the effect of interferences on the Bi signal with W-coil Atom Trap ETA system take place in gas phase. The signal could be affected during the trapping period and/or atomization. Bi signal could be affected due to the fact that generated interferent hydride species could be trapped and preconcentrated on W-coil and became more populated during atomization stage. Therefore, the different behaviors of interferences regarding the two different modes of twin-channel hydride generation system with W-coil Atom Trap ETA system directed to investigate the trapping and atomization temperature profiles of interference elements.

In this part of the study, single channel CF-HG system was used. The hydride generation conditions for Bi were applied to the interference elements. The working standard solutions of individual interference elements were prepared in 1.0 mol/L

HCl and the concentration of reductant (NaBH_4) was 0.5 % (w/v). The optimum concentration for each interference element to obtain an analytical signal under the optimum conditions of Bi was different. The W-coil surface was modified with Rh. Volatile species generated from interference elements were collected for 60 s on Rh coated W-coil surface.

Figure 3.54 illustrates the trapping and atomization range for As(III). The concentration of As was selected as 5.0 ng/mL. The trapping range for As was investigated in the temperatures between 179 and 1150 °C. Hydrides of As could be trapped at a wide range and the highest signal was obtained at 1018 °C. The signal decreased above this temperature. The optimum trapping temperature for bismuthine was found to be 462 °C and it could be seen from Figure 3.54 arsine could also be trapped at this temperature. As was one of the interferent that caused a decrease in the signal of Bi with W-coil Atom Trap ETA system.

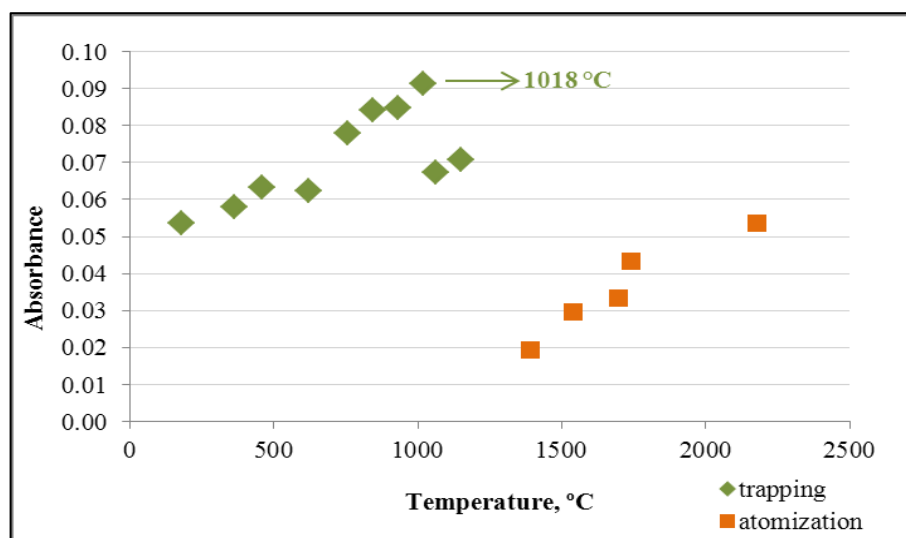


Figure 3.54 The trapping and atomization behavior for 5.0 ng/mL As in 1.0 mol/L HCl using Rh coated W-coil Atom Trap ETA. The hydrides of As was collected for 60 s at a flow rate of 3.0 mL/min. During the investigation of trapping range the atomization temperature was 1742 °C and for atomization range, trapping temperature was kept at 1018 °C.

The interference effect of Sb(III) was towards the decreasing the Bi signal for twin-channel CF-HG system operating at two different modes. When Sb was separated from analyte solution and transported individually, Sb affected the analytical signal of Bi more significantly. Trapping profile of Sb indicated that stibine could be preconcentrated partially at the optimum trapping temperature of bismuthine (462 °C). The signal obtained from stibine collection at 462 °C was 18% lower than highest signal of stibine trapped at 544 °C (Figure 3.55). The decrease in Bi signal in the presence of Sb in liquid or gas phase was probably due to the similar trapping conditions for both of the elements. Bismuthine and stibine were collected on quartz surface of the inlet arm of the multiple microflame [170]. According to the result of this interference study, Sb was found to be the strongest interferent to Bi in collection mode. Sb and Bi co-trapped and also volatilized together due to their very similar preconcentration conditions. Therefore, atomization interference may also arise.

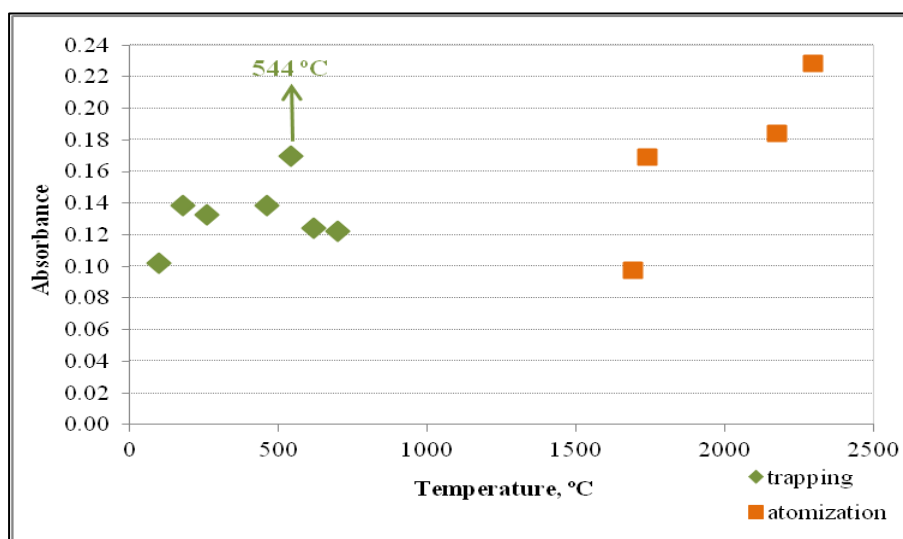


Figure 3.55 The trapping and atomization behavior for 5.0 ng/mL Sb in 1.0 mol/L HCl using Rh coated W-coil Atom Trap ETA. The hydrides of Sb were collected for 60 s at a flow rate of 3.0 mL/min. During the investigation of trapping range the atomization temperature was 2177 °C and for atomization range, trapping temperature was kept at 544 °C.

The trapping and atomization profile for Se(IV) is given in Figure 3.56. The optimum trapping temperature was found to be 227 °C for selenium hydrides. After this, a sharp decrease was observed. Selenium hydrides could be trapped at a cooler surface as compared to bismuthine. The partial collection of selenium hydrides at 462 °C could be achieved; however it was not as efficiently trapped as stibine at this temperature. Se also caused a decrease in Bi signal. The reason behind the decrease could be attributed to the fact that both elements are collected on W-coil and atomize at the same condition.

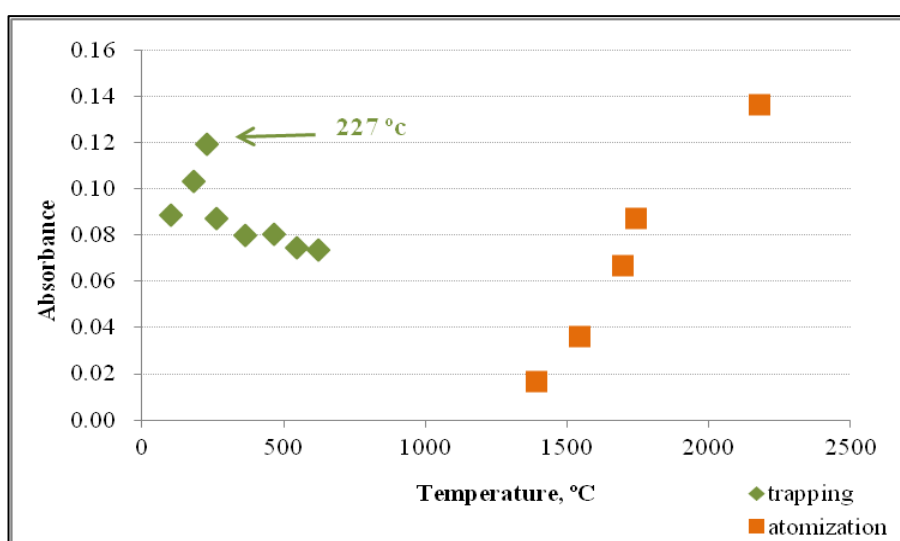


Figure 3.56 The trapping and atomization behavior for 10.0 ng/mL Se in 1.0 mol/L HCl using Rh coated W-coil Atom Trap ETA. The hydrides of Se were collected for 60 s at a flow rate of 3.0 mL/min. During the investigation of trapping range the atomization temperature was 2177 °C and for atomization range, trapping temperature was kept at 227 °C.

Te(IV) led to significant reduction of Bi signal at 500 fold mass ratio (Figure 3.53). The trapping temperature range for this interferent was investigated and the results are given in Figure 3.57. Te hydrides could be collected in a wide temperature range. The maximum signal was reached when the temperature was 620 °C.

However, the difference between the maximum signal obtained at 620 °C and the signal obtained at 462 °C (optimum trapping temperature for bismuthine) was 9.0%. It could be stated that hydrides of Te could be collected at the optimum trapping temperature for bismuthine. Therefore, the reason for decrease of Bi signal by Te could be attributed to the similar trapping range.

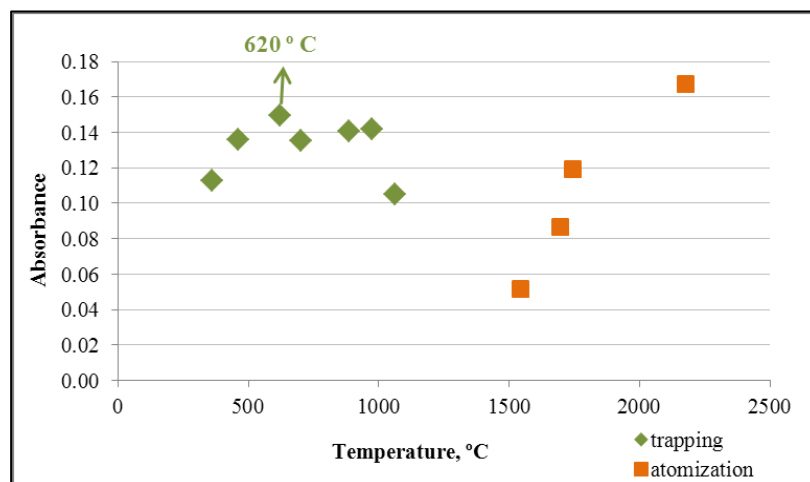


Figure 3.57 The trapping and atomization behavior for 5.0 ng/mL Te in 1.0 mol/L HCl using Rh coated W-coil Atom Trap ETA. The hydrides of Te were collected for 60 seconds at a flow rate of 3.0 mL/min. During the investigation of trapping range the atomization temperature was 2177 °C and for atomization range, trapping temperature was kept at 620 °C.

The results obtained for trapping and atomization profile of Sn(IV) are indicated in Figure 3.58. The interference of Sn for all interferent/analyte ratios could be tolerated for both twin-channel CF-HG modes.

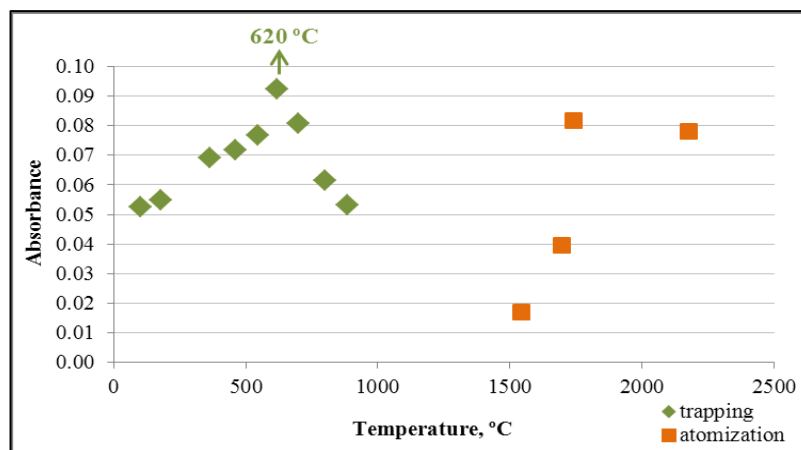


Figure 3.58 The trapping and atomization behavior for 100 ng/mL Sn in 1.0 mol/L HCl using Rh coated W-coil Atom Trap ETA. The hydrides of Sn were collected for 60 s at a flow rate of 3.0 mL/min. During the investigation of trapping range the atomization temperature was 2177 °C and for atomization range, trapping temperature was kept at 620 °C.

One of the reasons of the suppression of the analyte signal with W-coil Atom Trap ETA could be the similar trapping and releasing behaviors of interferent species and analyte on W-coil; this can be seen in Figure 3.54, Figure 3.55, Figure 3.56, Figure 3.57 and Figure 3.58. Therefore it is likely that as the analyte is trapped and released this will be accompanied by the similar behavior and thus the presence of interferent. Formation of non-atomic species may be lowering the analyte free atom population resulting in a decrease in signal.

Another reason could result from non-uniform temperature around W-coil atomizer. The rapid atomization takes place sufficiently with W-coil due to the high atomization temperature, ca. 2200 °C; however, as the distance from W-coil surface increases, temperature is decreasing sharply; there is a sharp temperature gradient. Thus, the medium becomes available for the formation of non-atomic species, resulting in the decrease of analytical signal [123].

For the behaviors of Sb and Se, as shown in Figure 3.73 and Figure 3.77, respectively, there are increasing signal trends at the stages of CF-HG and untrapped CF-HG in the presence of interferent. This indicates that the trapped analyte will lower. The decrease in ETA signal in presence of these intereferents may be explained also by this behavior.

3.7.3.3. The Interference Study with Rh-coated W-coil Atom Trap ETV System

In this part, the interference effects of As, Sb, Se, Te and Sn were investigated with twin-channel CF-HG system coupled to Rh-coated W-coil Atom Trap ETV system. Twin-channel CF-HG system was used and it was applied in two different modes. The results obtained with twin-channel CF-HG system in which analyte and interferent were in the same solution are given in Figure 3.59. In this system, the interference effects of Te and Sn were minimal; the analytical signal of Bi was not affected in the presence of these interferents. However; As, Sb and Se led to the enhancement of signal. The enhancement effect of these elements was effective starting from 50 fold mass ratio of interferent/analyte.

The same effect was observed with twin-channel CF-HG system in which the analyte and interferent were transported separately. The results for this mode are given in Figure 3.60. The interference effect of Te and Sn on the signal of Bi was not significant. The signal of Bi was significantly affected by As, Sb and Se and they caused increase in the signal. The enhancement of the signal was observed at 50 and 500 interferent/analyte ratios. The case most frequently encountered in interference study is the suppression of the analyte signal by the interferent elements. However, in some cases, the positive effects of interferent on the analyte signal could be observed due to the formation of volatile or non-volatile compound in a gas/condensed phase reaction between analyte and matrix [33]. The interference effects of As, Sb and Se were observed in twin-channel CF-HG system operating at two modes. The enhancement effect was the result for both of the twin-channel CF-HG modes. The

interference effect could be effective during hydride generation step, trapping, revolatilization and atomization. The presence of interferent might increase the amount of volatile hydrides that were transferred to the gas phase, thus; the amount of analyte hydrides preconcentrated on W-coil could be enhanced. The interferent in the gas phase could form diatomic compound with the analyte (Bi-As, Bi-Sb, Bi-Se) that could increase the release efficiency and transfer to QTA of trapped analyte species from W-coil surface. Therefore, the amount of analyte species arrived to atomization zone could increase.

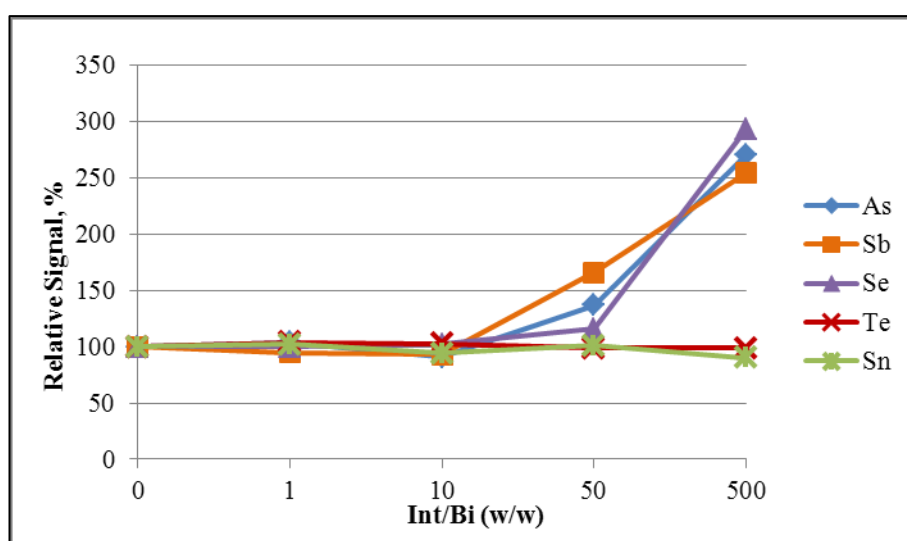


Figure 3.59 Interference effects of hydride forming elements on analytical signal of 2.0 ng/mL Bi collected for 60 s with twin-channel CF-HG system of Rh coated W-coil Atom Trap ETV. Analyte and interferent were placed in the same solution and pumped from one channel, from the second channel blank solution was transferred. The trapping and revolatilization temperatures were 300 °C and 1542 °C, respectively. Temperature of EHQTA was 950 °C.

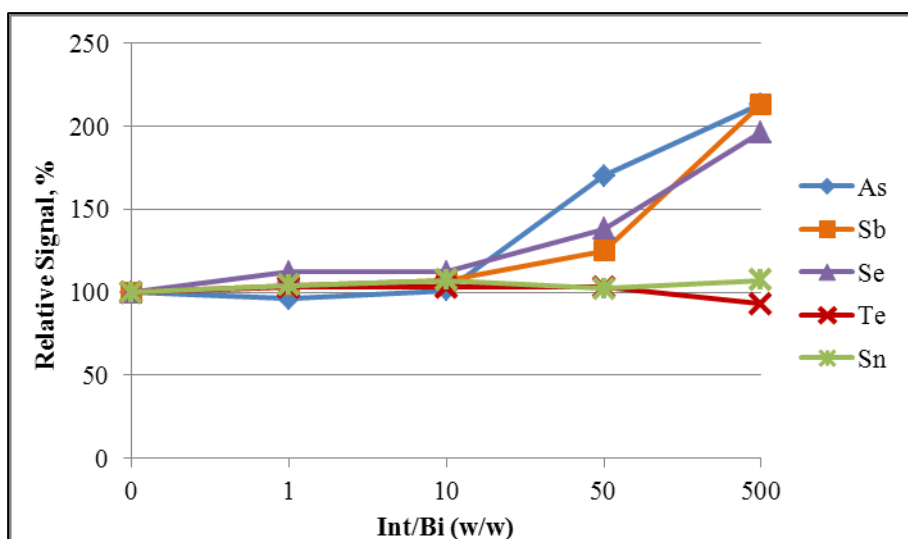


Figure 3.60 Interference effects of hydride forming elements on analytical signal of 2.0 ng/mL Bi collected for 60 s using twin-channel CF-HG system of Rh coated W-coil Atom Trap ETV. The analyte and interferent were transported from the separate channels of twin-channel hydride generators. The trapping and revolatilization temperatures were 300 °C and 1542 °C, respectively. Temperature in EHQTA was 950 °C.

3.7.3.3.1 Trapping and Revolatilization Temperature Ranges for Interference Elements

In this part of the study, the trapping and revolatilization temperature range for individual interference elements were investigated. The enhancement of the analytical signal of Bi by As, Sb and Se led to investigation of the trapping and revolatilization temperature profile for interferents.

Single channel CF-HG system was used. The hydride generation conditions for Bi were applied to the interference elements. The working standard solutions of individual interference elements were prepared in 1.0 mol/L HCl and the concentration of reductant (NaBH_4) was 0.5 % (w/v). For each interferent the optimum concentration to obtain an analytical signal under the optimum conditions of Bi was investigated and the signal for which analytical signal was obtained was

taken into account. The W-coil surface was modified with Rh. Volatile species generated from interference elements were collected for 60 s on Rh coated W-coil surface. The atomization temperature in EHQTA was kept at 950 °C.

The results regarding the trapping and revolatilization temperature range optimization for As(III) are shown in Figure 3.61. The concentration selected for As was 10.0 ng/mL. Arsine species were collected efficiently at 620 °C and they were released at 1696 °C. The optimum collection and release temperature for bismuthine with ETV system was 300 °C and 1542 °C, respectively. Arsine could be collected when trapping temperature was kept at the optimum trapping temperature of bismuthine.

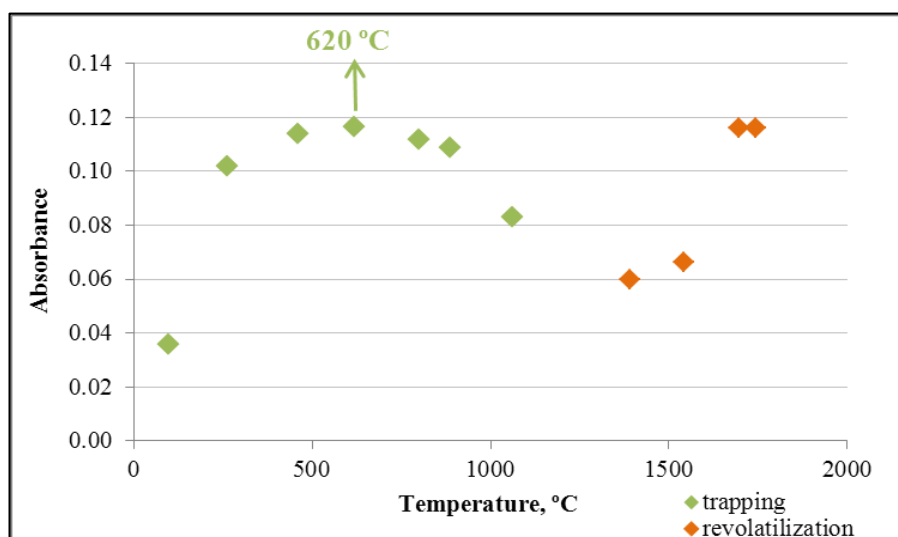


Figure 3.61 The trapping and revolatilization temperature behavior for 10.0 ng/mL As in 1.0 mol/L HCl using Rh coated W-coil Atom Trap ETV. The hydrides of As were collected for 60 s at a flow rate of 3.0 mL/min. During the investigation of trapping range, the revolatilization temperature was 1696 °C and for revolatilization range, trapping temperature was kept at 620 °C. Temperature of EHQTA was 950 °C.

Optimization of the trapping and revolatilization temperature of Sb(III) under the conditions of Bi was performed and the results are given in Figure 3.62. The maximum signal for optimization of trapping temperature was obtained for 262 °C and trapped Sb species were released at 1696 °C. Above 262 °C, the partial release of trapped Sb species occurred and signal decreased. The trapping and revolatilization temperature range of Sb was similar to that of Bi.

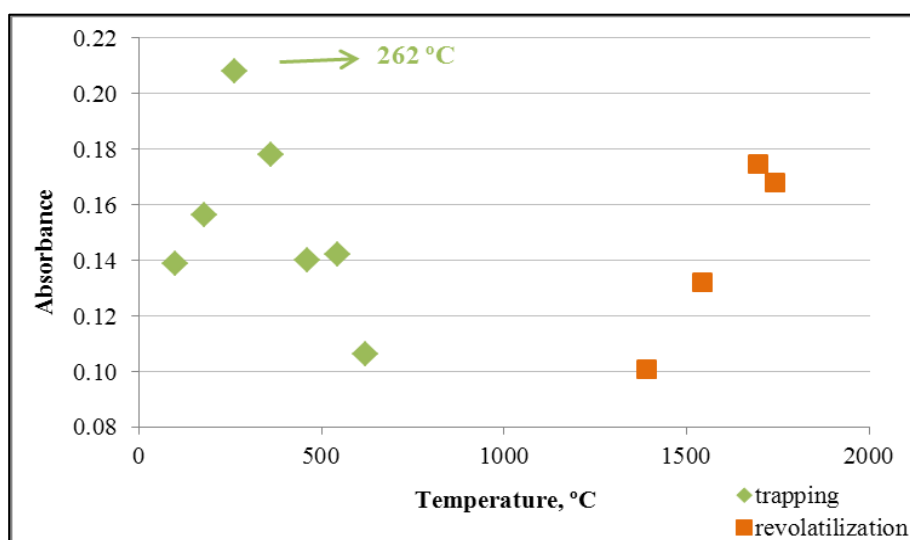


Figure 3.62 The trapping and revolatilization temperature behavior for 10.0 ng/mL Sb in 1.0 mol/L HCl using Rh coated W-coil Atom Trap ETV. The hydrides of Sb were collected for 60 seconds at a flow rate of 3.0 mL/min. During the investigation of trapping range, the revolatilization temperature was 1696 °C and for revolatilization range, trapping temperature was kept at 262 °C. Temperature of EHQTA was 950 °C.

The results for trapping and revolatilization temperature range of Se are shown in Figure 3.63. The signals were obtained for 10 ng/mL Se(IV) collected for 60 seconds. While optimizing the trapping temperature revolatilization temperature was 1696 °C. The optimum temperatures for trapping and revolatilization were found to be 227 °C and 1742 °C, respectively. The decrease of the signal was observed above

the optimum trapping temperature for Se. The release of trapped Se species was observed at the optimum trapping temperature for bismuthine.

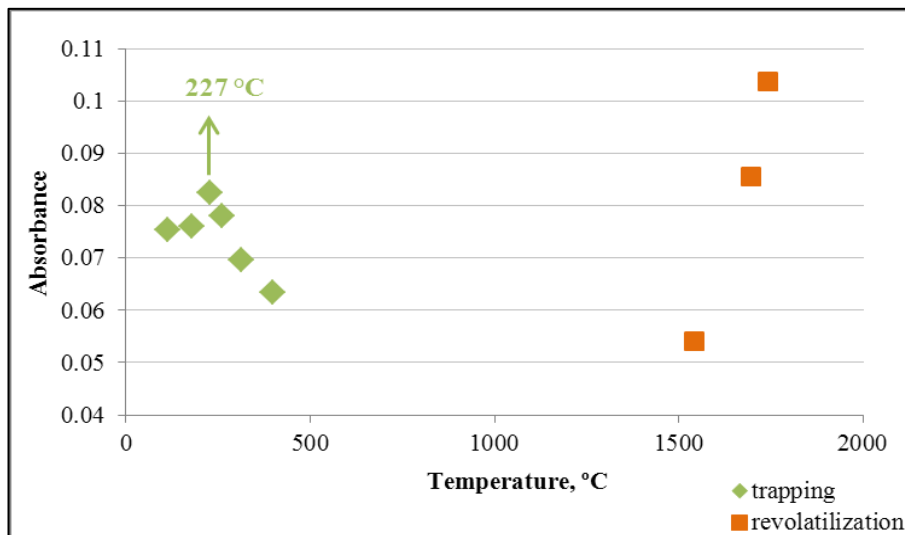


Figure 3.63 The trapping and revolatilization temperature behavior for 10.0 ng/mL Se 1.0 mol/L HCl using Rh coated W-oil Atom Trap ETV. The hydrides of Se were collected for 60 s at a flow rate of 3.0 mL/min. During the investigation of trapping range, the revolatilization temperature was 1696 °C and for revolatilization range, trapping temperature was kept at 277 °C. Temperature of EHQTA was 950 °C.

The temperature optimization for trapping and revolatilization stages were performed for Te(IV) and Sn(IV), and the results for Te and Sn are given in Figure 3.64 and Figure 3.65, respectively. 262 °C was found as optimum collection temperature for Te under optimum HG conditions for Bi. The release of trapped Te species could be achieved sufficiently at 1742 °C. The trapping profile of Te was similar to that was found for Bi. However, the analytical signal of Bi was not affected significantly in the presence of Te. To obtain an analytical signal for Sn under the optimum HG conditions for Bi was difficult. During the temperature optimization for trapping and revolatilization 1.0 mg/L Sn working solution was used. The optimum trapping and release temperatures were to be 462 and 1742 °C, respectively. According to the

interference study with ETV, it was found that Bi signal was not affected significantly by Sn. The signal obtained from Sn was low despite of high concentration of Sn solution. One of the reasons for the lack of interference should be the relative absence of Sn on W-coil trap.

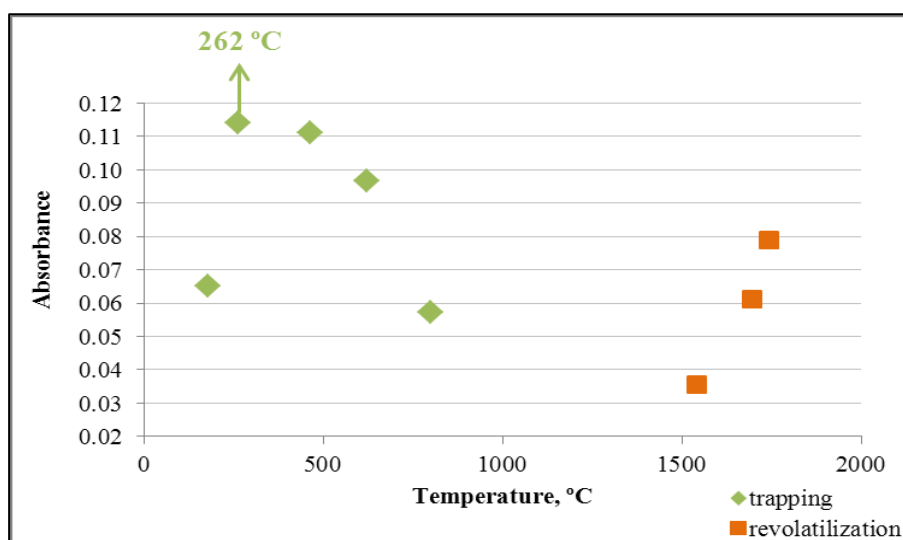


Figure 3.64 The trapping and revolatilization temperature behavior for 10.0 ng/mL Te in 1.0 mol/L HCl using Rh coated W-coil Atom Trap ETV. The hydrides of Te were collected for 60 s at a flow rate of 3.0 mL/min. During the investigation of trapping range, the revolatilization temperature was 1696 °C and for revolatilization range, trapping temperature was kept at 262 °C. Temperature of EHQTA was 950 °C.

The comparison of revolatilization temperatures of interferent and analyte did not give sufficient information regarding the behavior of interferent during revolatilization stage. As the release temperature was increased the signal was also increasing. Therefore, the results obtained for revolatilization temperature were not distinctive.

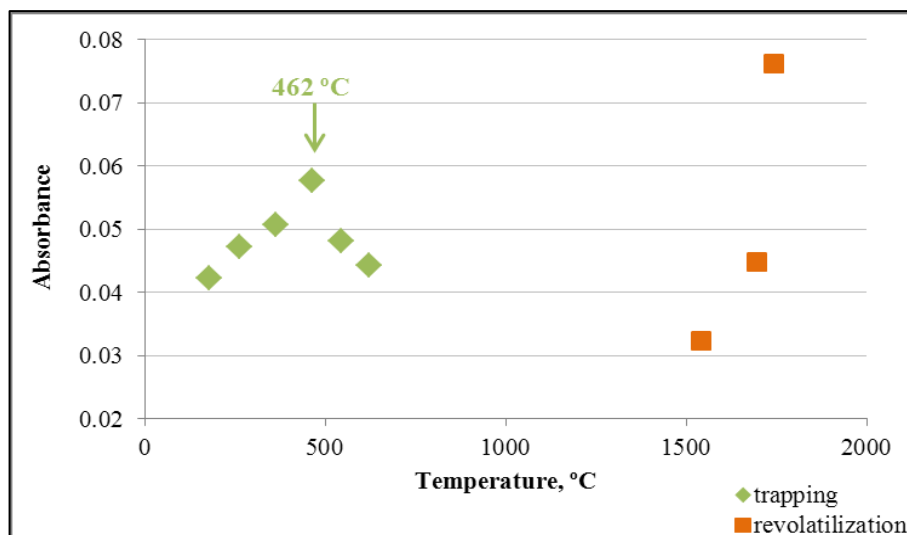


Figure 3.65 The trapping and revolatilization temperature behavior for 1.0 mg/L Sn in 1.0 mol/L HCl using Rh coated W-coil Atom Trap ETV. The hydrides of Sn were collected for 60 s at a flow rate of 3.0 mL/min. During the investigation of trapping range, the revolatilization temperature was 1696 °C and for revolatilization range, trapping temperature was kept at 462 °C. Temperature of EHQTA was 950 °C.

3.7.3.3.2 Effect of Interferent during Continuous Flow Hydride Generation, Trapping and Revolatilization Stages in ETV

The effect of interference element including As(III), Sb(III) and Se(IV) was towards the enhancement of analytical signal with Rh coated W-coil Atom Trap ETV system and EHQTA. The enhancement effect could be observed at any stage of the system. Therefore, the individual stages of the system regarding i) continuous flow HG system, ii) trapping period and iii) revolatilization stages were investigated in terms of behavior of interferent. Moreover, an effort was made to identify in which stage the effect of interference elements were more severe and how the behavior of Bi signal was affected by interference element at each stage. The whole signal was divided into three parts, namely, i) CF-HG, ii) untrapped CF-HG and iii) revolatilization. The schematic representation is illustrated in Figure 3.66. Firstly, the signal of CF-HG was recorded. While recording the CF signal, W-coil was not

heated; thus, there was not any trapping of analyte species. Secondly, W-coil was heated to trapping temperature and during this period the continuous flow signal was recorded. The continuous flow signal was the signal produced from the hydrides of untrapped species. Lastly, when trapping period was completed, temperature of W-coil was brought to revolatilization temperature and the signal obtained from the atomization of released species from W-coil.

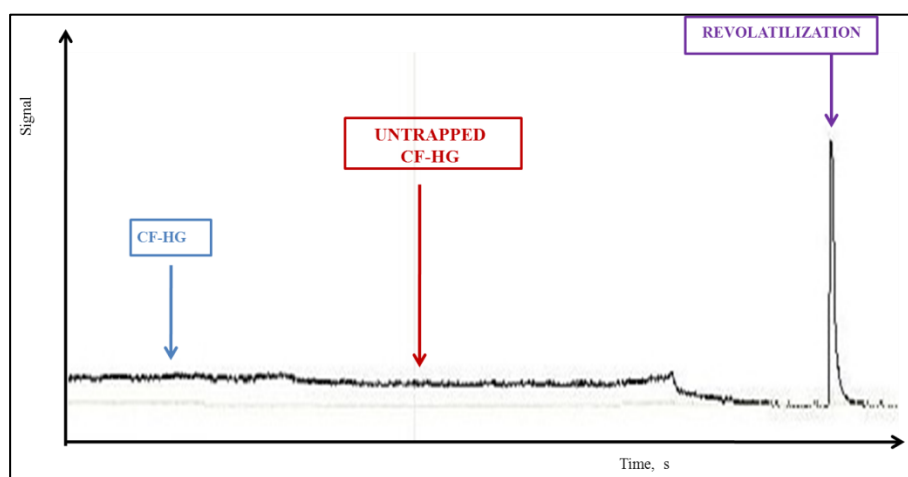


Figure 3.66 The schematic representation of the signal obtained from CF-HG, untrapped CF-HG and revolatilization.

In order to see the effect of interference elements on each stage, the selection of analyte concentration was important. The analyte concentration was selected as 10.0 ng/mL for Bi, therefore this concentration was suitable to detect CF-HG signal sufficiently. The trapping period was shortened to 20 s to minimize the trapping signal with high concentration of Bi. The interference effects of As, Sb and Se were investigated due to their enhancement effect on the Bi signal. The interferent/analyte ratios were 1, 10, 50 and 500 fold. The signals were reported as relative signal which was converted to 100. The Bi signal was taken as 100 and the signals obtained in the presence of interferences were normalized according to relative signal of Bi. The signals were normalized in accordance with the related stage. For example, the CF-

HG signal of Bi was considered as 100 and the CF-HG signal obtained with the interferent was normalized regarding this signal. The same calculation was done for normalization of the signal for untrapped CF-HG and revolatilization stages.

In this study, twin-channel CF-HG system operating at two modes was used. In the first mode, analyte and interference element were transferred together from the same solution and transferred from same channel. The second channel was used to transport blank solution. In the second one, analyte and interference element were present in different solutions and were sent through different channels.

As(III) as an interferent yielded the results are indicated in Figure 3.67. The analyte and As were spiked into the same solution and pumped together. Blue and orange lines indicated the signal obtained from CF-HG and CF-HG of untrapped species, respectively. The trend of signals of both stages was similar and As did not affect the signal significantly. However, the revolatilization signal (purple line) obtained in the presence of As was increased at the interferent/analyte ratios of 10, 50 and 500.

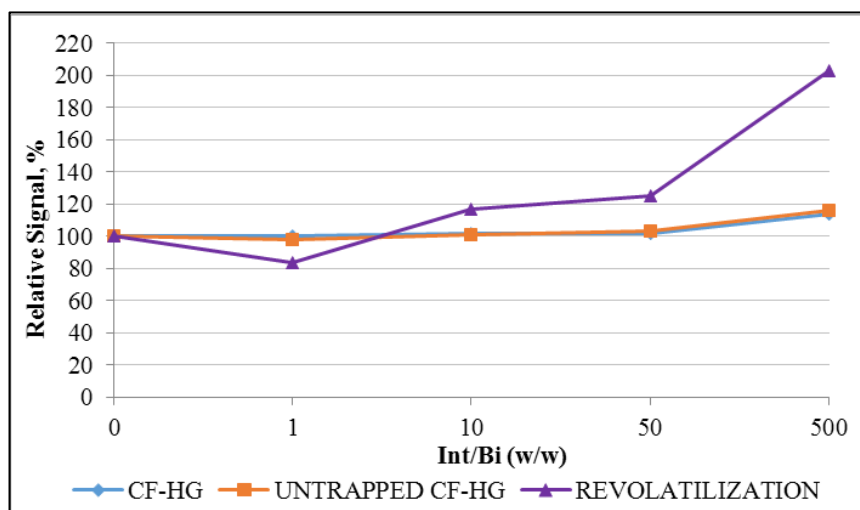


Figure 3.67 The effect of As on Bi signal regarding CF-HG, CF-HG of untrapped species and revolatilization stages. The Bi concentration was 10.0 ng/mL in 1.0 mol/L HCl and Bi was trapped for 20 s. As and Bi were in the same solution and pumped together from the same channel, the blank solution was transferred from the

second channel. The trapping and revolatilization temperatures were 300 °C and 1542 °C, respectively. Temperature in EHQTA was 950 °C.

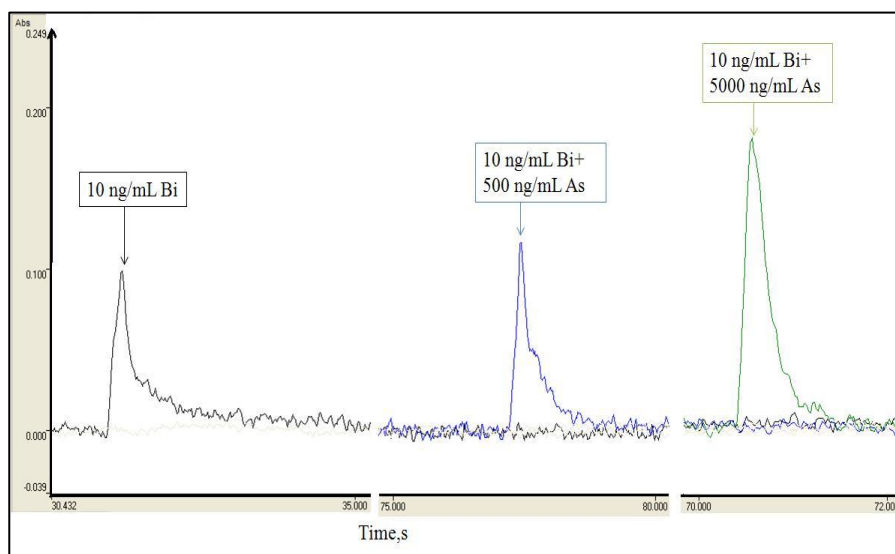


Figure 3.68 The signals that were obtained for 10.0 ng/mL Bi, 500 ng/mL As + 10.0 ng/mL Bi and 5000 ng/mL As + 10.0 ng/mL Bi. The signals were taken during the revolatilization stage. As and Bi were in the same solution and transferred together from the same channel.

The interference effect of As when analyte and As were transferred separately is shown in Figure 3.69. The effect of As on the CF-HG signal obtained without trap and with trap was similar. The same trend was followed for both of the stages. The enhancement effect was observed for revolatilization signal at 50 and 500 fold interferent/analyte ratios. At 500 fold mass ratio, the analytical signal of Bi was twice more than the signal of Bi without As.

The shape of the signals indicated in Figure 3.70 were similar to those shown in Figure 3.69. The tail observed in 10.0 ng/mL Bi signal disappeared with the increase in As concentration and thus signal become higher and sharper. The bandwidth 10.0 ng/mL Bi signal was 2.8 s. The bandwidth of the signals obtained for Bi and As pumped from separate channels was 1.1 s.

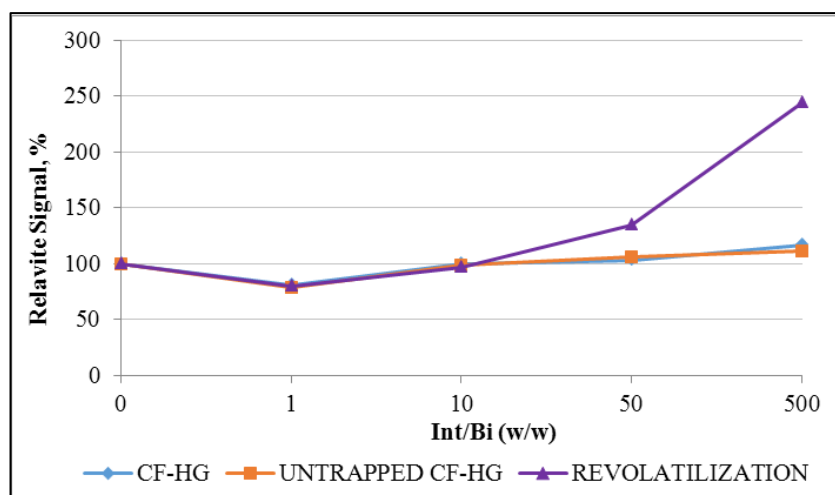


Figure 3.69 The effect of As on Bi signal regarding CF-HG, CF-HG of untrapped species and revolatilization stages. The Bi concentration was 10.0 ng/mL in 1.0 mol/L HCl and Bi was trapped for 20 s. As and Bi solutions were transferred separately. The trapping and revolatilization temperatures were 300 °C and 1542 °C, respectively. Temperature of EHQTA was 950 °C.

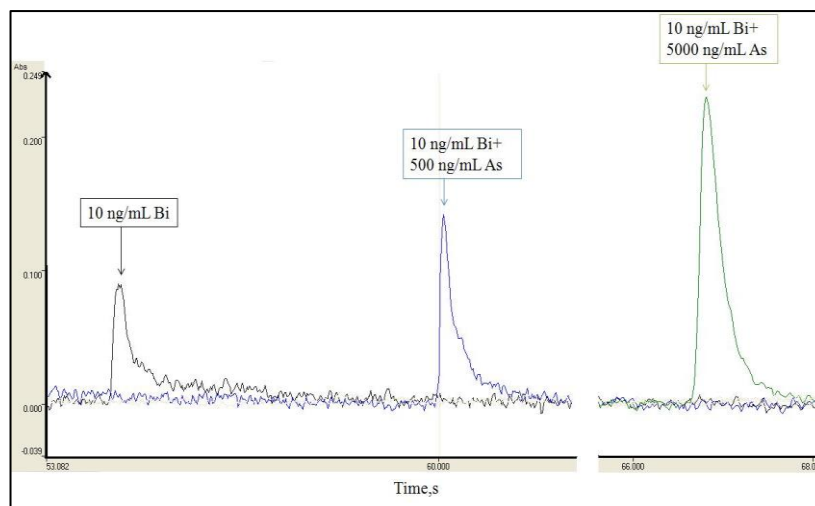


Figure 3.70 The signals that were obtained for 10.0 ng/mL Bi, 500 ng/mL As + 10.0 ng/mL Bi and 5000 ng/mL As + 10.0 ng/mL Bi. The signals were taken during the revolatilization stage. As and Bi were in separate solutions and transferred from different channels.

The presence of Bi and Sb in the same solution yielded the results indicated in Figure 3.71. The interference effect of Sb was observed in all stages. The signals belonged to CF-HG and untrapped CF-HG was increased in the presence of Sb. The enhancement of the signal at revolatilization stage was more significant than the other stages.

The shapes of the signals were also indicated in Figure 3.72. The signals were obtained for 10.0 ng/mL Bi and 100 ng/mL Sb + 10.0 ng/mL Bi, 500 ng/mL Sb + 10.0 ng/mL Bi and 5000 ng/mL Sb + 10.0 ng/mL Bi solutions. The bandwidth of 10.0 ng/mL Bi signal was 1.5 s. The bandwidths of signals for Sb containing Bi solutions become narrower and signals were higher.

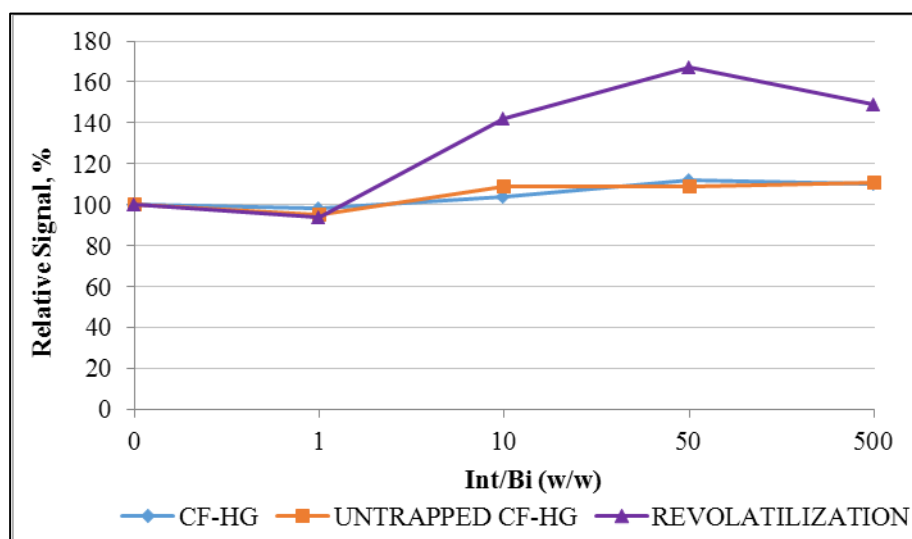


Figure 3.71 The effect of Sb on Bi signal regarding CF-HG, CF-HG of untrapped species and revolatilization stages. The Bi concentration was 10.0 ng/mL in 1.0 mol/L HCl and Bi was trapped for 20 s. Sb and Bi were in the same solution and pumped together from the same channel; the blank solution was transferred from the second channel. The trapping and revolatilization temperatures were 300 °C and 1542 °C, respectively. Temperature of EHQTA was 950 °C.

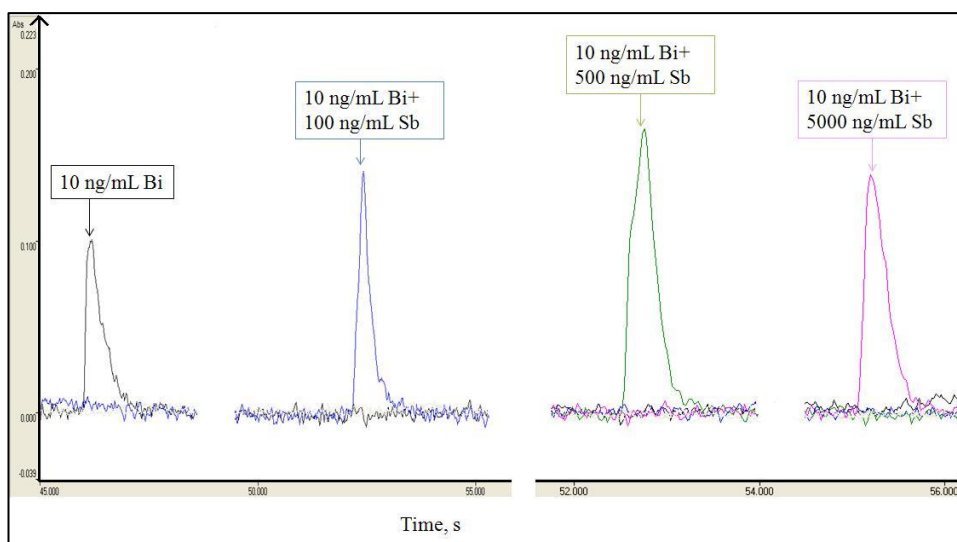


Figure 3.72 The signals that were obtained for 10.0 ng/mL Bi and 100 ng/mL Sb + 10.0 ng/mL Bi, 500 ng/mL Sb + 10.0 ng/mL Bi and 5000 ng/mL Sb+ 10.0 ng/mL Bi. The signals were taken during the revolatilization stage. Sb and Bi were in the same solution and transferred together from the same channel.

The similar enhancement effect was investigated with Sb as an interferent when analyte and Sb were transferred separately. The results obtained for three stages are shown in Figure 3.73. When Sb was transported from separately from Bi, the increase in Bi signal started with interferent/analyte ratio of 1 and the representative signals are given in Figure 3.74. The bandwidth of Bi was 1.5 s. The signal obtained for 10 ng/mL Sb + 10 ng/mL Bi case had the bandwidth of 1.0 s. As the concentration of Sb was increased the signals became narrower and bandwidth was 0.7 s.

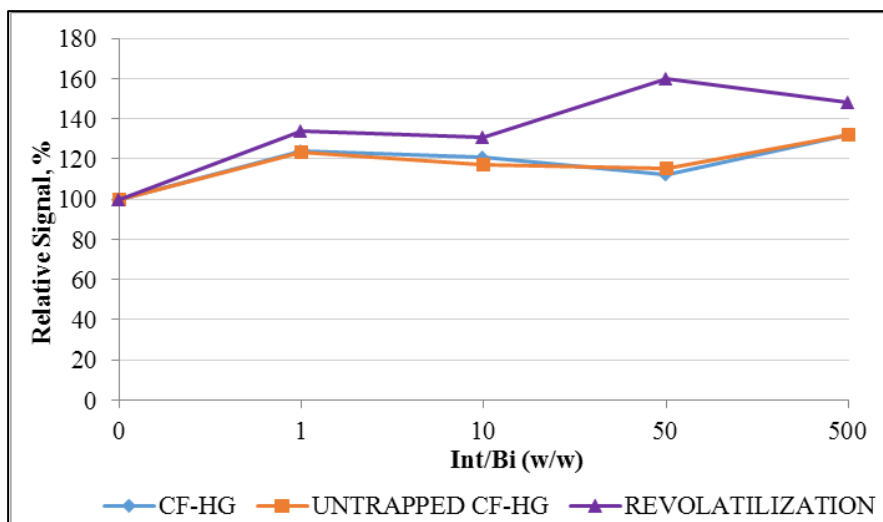


Figure 3.73 The effect of Sb on Bi signal regarding CF-HG, CF-HG of untrapped species and revolatilization stages. The Bi concentration was 10.0 ng/mL in 1.0 mol/L HCl and Bi was trapped for 20 s. Sb and Bi solutions were transferred separately. The trapping and revolatilization temperatures were 300 °C and 1542 °C, respectively. Temperature in EHQTA was 950 °C.

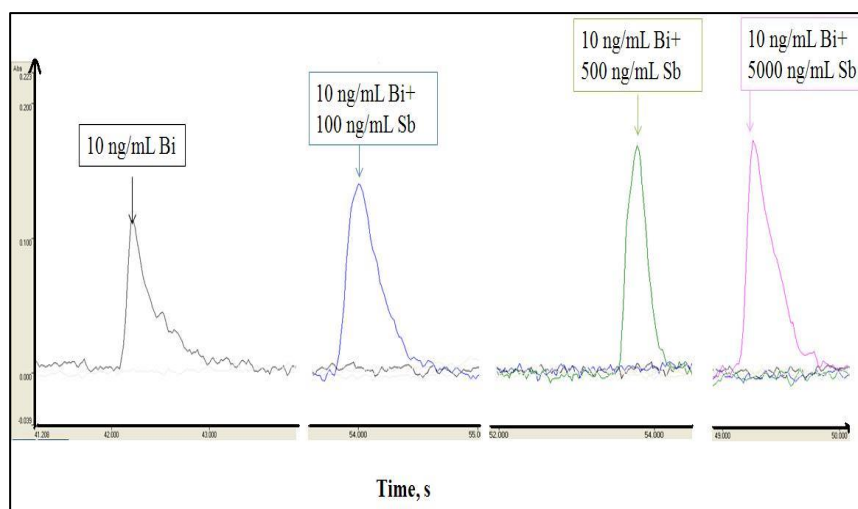


Figure 3.74 The signals that were obtained for 10.0 ng/mL Bi, 100 ng/mL Sb + 10.0 ng/mL Bi, 500 ng/mL Sb + 10.0 ng/mL Bi and 5000 ng/mL Sb + 10.0 ng/mL Bi solutions. The signals were taken during the revolatilization stage. Sb and Bi were in separate solutions and transferred from different channels.

The presence of Se in the analyte solution yielded the results indicated in Figure 3.75. The Bi signals of CF-HG (blue line) and CF-HG of untrapped species (orange line) was not significantly affected by Se present in the same solution with Bi. During these stages, the system could tolerate the effect of Se. The signals obtained for revolatilization stage were decreased for the interferent/analyte ratios of 1, 10 and 50. The enhancement of the Bi signal occurred at 500 fold interferent/analyte ratio.

The signals obtained for 10.0 ng/mL Bi and 5.0 mg/L Se containing 10.0 ng/mL Bi solutions are given in Figure 3.76. The bandwidth of 10.0 ng/mL Bi signal was 2.3 s. When Se was added to analyte solution, the bandwidth of the signal become narrower that was 0.7 s.

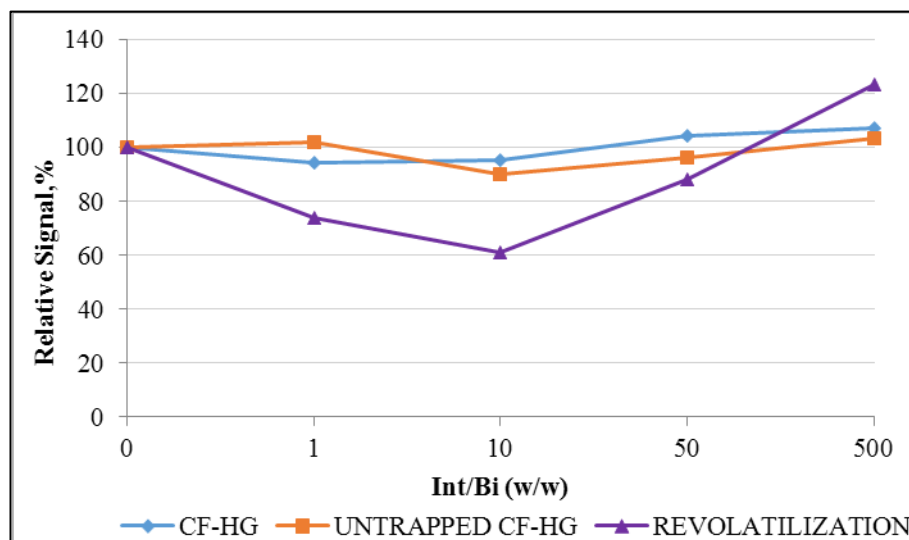


Figure 3.75 The effect of Se on Bi signal regarding CF-HG, CF-HG of untrapped species and revolatilization stages. The Bi concentration was 10.0 ng/mL in 1.0 mol/L HCl and Bi was trapped for 20 s. Se and Bi were in the same solution and pumped together from the same channel, the blank solution was transferred from the second channel. The trapping and revolatilization temperatures were 300 °C and 1542 °C, respectively. Temperature of EHQTA was 950 °C.

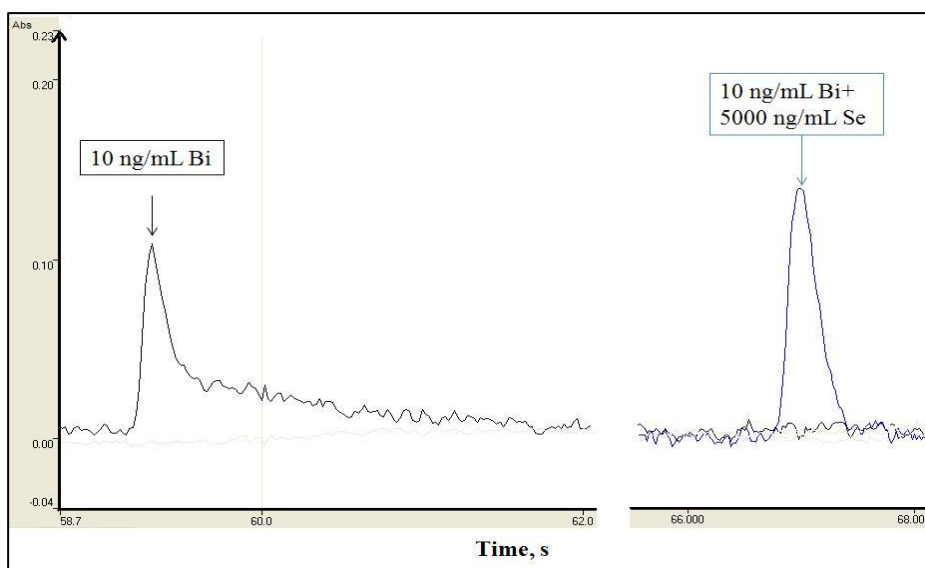


Figure 3.76 The signals that were obtained for 10.0 ng/mL Bi and 5000 ng/L Se + 10.0 ng/mL Bi solutions. The signals were taken during the revolatilization stage. Se and Bi were in the same solution and transferred together from the same channel.

The interference effect of Se when it was transferred separately from the analyte increased significantly at CF-HG and untrapped CF-HG stages. The enhancement of the signals took place and corresponding results are given in Figure 3.77. The signals belonged to revolatilization stage were decreasing when interferent/analyte ratios were 1, 10 and 50. The signal at 500 fold interferent/analyte ratio was enhanced. Figure 3.78 represents the signals for 10.0 ng/mL Bi and 10.0 ng/mL Bi solution + 5000 ng/mL Se. The difference between those signals was the bandwidths. Signal of Bi has the bandwidth of 2.3 s and Se containing Bi solution yielded the signal of 0.7 s bandwidth. Therefore, there was not significant enhancement effect observed with Se, but the bandwidth become narrower with the presence of Se.

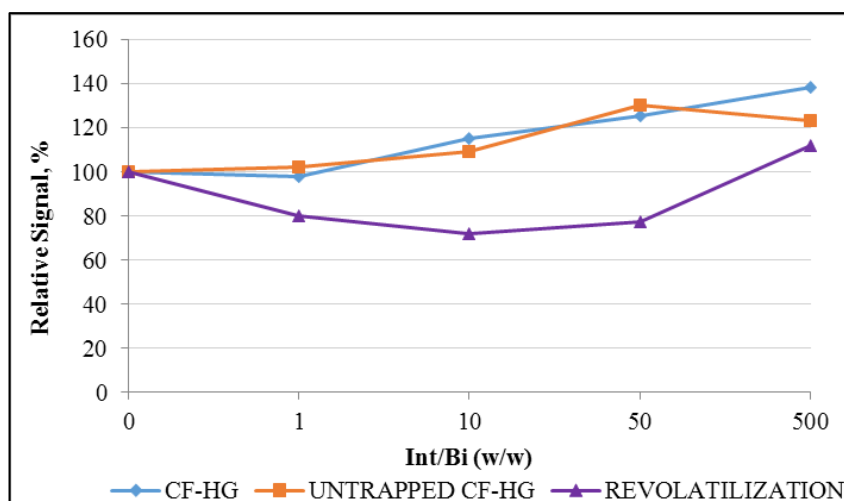


Figure 3.77 The effect of Se on Bi signal regarding CF-HG, CF-HG of untrapped species and revolatilization stages. The Bi concentration was 10.0 ng/mL in 1.0 mol/L HCl and Bi was trapped for 20s. Se and Bi solutions were transferred separately. The trapping and revolatilization temperatures were 300 °C and 1542 °C, respectively. Temperature of EHQTA was 950 °C.

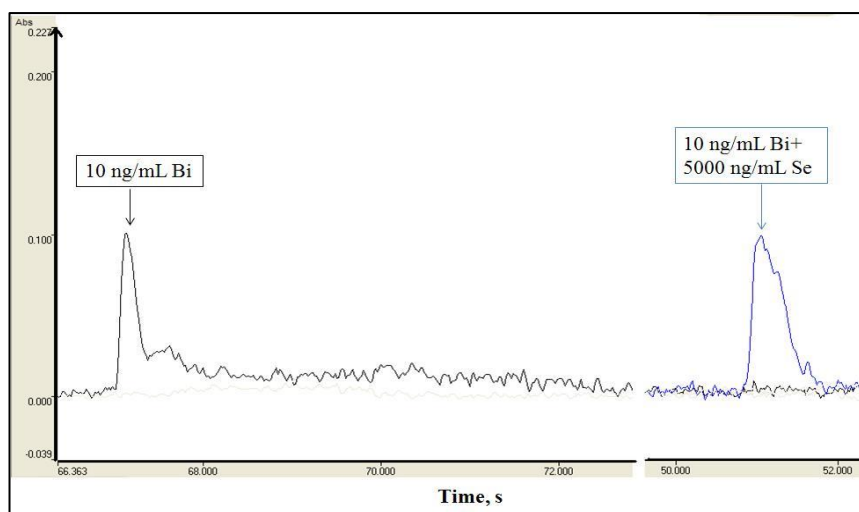


Figure 3.78 The signals that were obtained for 10.0 ng/mL Bi, 5.0 mg/L Se + 10.0 ng/mL Bi. The signals were taken during the revolatilization stage. Se and Bi were in separate solutions and transferred from different channels.

The results obtained with this part of the study are summarized in Table 3.17.

Table 3.17 The results of interference study regarding the effects of interferent on the signal of Bi in the stages namely; CF-HG (1), untrapped CF-HG (2) and revolatilization (3) with twin-channel CF-HG system in which Bi and interferent in same solution (a) and separate solutions (b).

Mass ratio (Int/Bi)		As			Sb			Se		
		1	2	3	1	2	3	1	2	3
0		100	100	100	100	100	100	100	100	100
1	a	100	98	84	98	95	94	94	102	74
	b	81	79	80	124	123	134	98	102	80
10	a	102	101	117	104	109	142	95	90	61
	b	100	99	96	121	117	131	115	109	72
50	a	102	103	125	112	109	167	104	96	88
	b	103	106	134	112	115	160	125	130	77
500	a	114	116	203	110	111	149	107	103	123
	b	116	111	244	132	132	148	138	123	112

The enhancement of CF-HG signal regardless of analyte and interferent were in the same solution or not was investigated especially for Sb and Se. While heating QTA by electrical furnace in the inlet arm of the QTA was also heated and these regions became a trapping medium. When bismuth was alone there was a possibility for volatile bismuth species to be trapped on the hot regions in the inlet arm of the QTA,

thus; the atomization signal produced from CF-HG could be low due to this reason. In the presence of interferents, bismuth could form dimers with interferents during the transportation to the atomizer. The formation of these compounds could prevent bismuth species to be trapped on the inlet arm of the QTA. Therefore, CF-HG signal could be enhanced due to the higher amount of bismuth species transported to atomization zone. Another possibility is that interferent species could also be trapped in the inlet arm of EHQTA and the sites available for analyte would be lowered. This could also lead to an increase in signal.

In this part of the study, the CF-HG signal was followed in the stage called untrapped CF-HG. The CF-HG signal of untrapped bismuth species were recorded during that stage. The signals belonging to CF-HG and CF-HG of untrapped species were not affected significantly in the presence of As. Therefore, the interference effect could not be related with the trapping stage. If there were any enhancement related with trapping, CF-HG signal obtained during trapping period could have been reduced indicating that bismuth was trapped more efficiently on W-coil surface. However; the signal on that period was not changed significantly. Therefore, the variations on the Bi signal with As was not related with the co-trapping of As with Bi. The reason of enhancement of signal in the presence of As could be resulted from the revolatilization stage. Moreover, CF-HG signal recorded during collection period was increasing in the presence of Sb and Se. This situation could be attributed to the reduction of collection of analyte on W-coil in the presence of interference. Krejčí et al. stated that Bi collected on molybdenum surface was affected in the presence of As, Sb and Se [125]. The suppression effect was investigated for these interferents. The interference effect of Se could be attributed to the formation of diatomic species of Bi-Se(g) at trapping temperature range of Bi. Consequently, formation of this compound could reduce the trapping efficiency. It was found that gaseous molecules formed on vaporization of liquid solutions of Bi-Sb, Bi-As in the temperature range of 300-750 °C [171,172]. It was investigated that the tetratomic and diatomic species including Bi₃As, Bi₂Sb₂, Bi₂As₂, BiSb₃, BiAs₃, BiSb and BiAs. The vaporization of Bi₂Se₃ yielded the formation of gaseous species of BiSe(g) and Bi(g) with continuous heating at 1050 K [173]. During collection of analyte on W-coil, the hot

surface of coil could behave as a reactor to support the formation of analyte-interferent compounds (Bi-As, Bi-Se and Bi-Sb). The formation of analyte-interferent compounds could reduce the trapping efficiency of analyte and this led to a small enhancement of bismuth signal obtained from CF-HG during trapping stage and its species that reach to the atomizer. The relatively low increase in the CF-HG signal during trapping stage could be observed due to this situation.

The enhancement effect was observed dominantly at revolatilization stage with As, Sb and Se. The common behavior of the interferents was making the Bi signal sharper. Broad analyte signal become sharper, thus bandwidth of the signals was narrower. The reason of this situation could be attributed to the high temperature used for the release of collected analyte species on W-coil surface. High temperature (1500 °C) applied to release the trapped species could enable the formation free analyte atoms. There was a temperature gradient between QTA and ETV unit. During the transportation of analyte to the QTA, the formation of analyte-interferent diatomic or polyatomic molecules could be possible under that temperature conditions. The analyte in the form of analyte-interferent species was transported to the atomizer heated at 950 °C and the number of analyte species reaching to the atomizer could be raised. As a result the enhancement on the Bi signal could be observed. The other reason of increase in the signal could be the support of intereferents during the release of analyte from W-coil. Interferents may promote trapped analyte species to be released more easily and rapidly from the W-coil. Therefore, the amount of analyte species that reach to the atomizer could be raised to yield an enhanced signal.

3.7.3.3.3 Effect of Increasing Temperature on the Behavior of Interferents at Revolatilization Stage

The enhancement on the Bi signal was thought to take place at revolatilization stage with Rh coated W-coil Atom Trap ETV system. As, Sb and Se were the interferents

caused enhancement. Therefore, the experiments carried out in this part were performed with As, Sb and Se. Te and Sn were not included in this part of the study.

The temperature at which complete release of trapped Bi species achieved was 1542 °C. A cleaning step after releasing step was applied and no signal was observed. However, interferences affected the Bi signal at this temperature. In this part, the effect of release temperature on interferences was investigated. The trapping temperature was kept constant at 300 °C while varying the revolatilization temperature.

Twin-channel CF-HG system was used for this part of the study. It was operating in two modes in which analyte and interferent were together in the same solution and transported separately. The analyte concentration was 10.0 ng/mL prepared in 1.0 mol/L HCl. The enhancement effect was significant at 500 fold interferent/analyte ratio. Therefore, solutions containing interferences were prepared at 500 fold interferent/analyte ratio.

Reference Bi signal was measured at each temperature. The analyte signal measured in the presence of interferences was compared to that of obtained in the absence of the interferent (reference signal). The comparison between analyte signal and reference signal was performed for each temperature. The reference signal was considered as 100 for each temperature value and correlation was done accordingly.

The results for twin-channel CF-HG system in which analyte and interferent together in the same solution are listed in Table 3.18. It can be seen from the results that increasing the revolatilization temperature suppressed the enhancement of the analyte signal.

Effect of temperature on the interferent behavior with twin-channel CF-HG system where analyte and interferent were transferred separately was performed and the related results are given Table 3.19. The trend was similar to the results indicated in Table 3.18. As the temperature was raised, the enhancement on the analyte signal was dropped. Therefore, increase in release temperature enhanced the Bi signal and

the signal obtained in the absence and presence of interferent came closer to each other.

Table 3.18 Effect of revolatilization temperature on the behavior of As, Se and Sb in Rh coated W-coil atom Trap ETV experiments. The analyte concentration was 10.0 ng/mL and was trapped for 20 s. The concentration of As, Se and Sb was 500 fold interferent/Bi ratio. Analyte and interferent were in the same solution and pumped from same channel. Blank was transferred from the second channel. The trapping temperature was kept at 300 °C. Temperature of EHQTA was 950 °C.

Relative signal (%)				
T (°C)	Bi (10.0 ng/mL)	As (5000 ng/mL)	Se (5000 ng/mL)	Sb (5000 ng/mL)
1542	100	122±7	129±10	120±6
1678	100	123±10	106±8	116±6
1780	100	116±10	117±19	104±11

Table 3.19 Effect of revolatilization temperature on the behavior of As, Se and Sb. The analyte concentration was 10.0 ng/mL. The concentration of As, Se and Sb was 500 fold interferent/Bi ratio. Analyte and interferent were in the separate solution and pumped from different channel. The trapping period was 20 seconds and the trapping temperature was kept at 300 °C.

Relative signal (%)				
T (°C)	Bi (10.0 ng/mL)	As (5000 ng/mL)	Se (5000 ng/mL)	Sb (5000 ng/mL)
1542	100	140±7	149±10	139±5
1678	100	128±5	121±10	111±2
1780	100	118±4	114±3	117±5

The signals measured at each revolatilization temperature value are indicated in Figure 3.79 and Figure 3.80. Absorbance values for Bi (without interferent) obtained for corresponding revolatilization temperature was shown in blue color. This line can be compared with the others that indicated the absorbance values for analyte with interferent. The difference between Bi alone and with interferent was significant at 1542 °C. It was decreased with increase in temperature. The signals of Bi without interferent and with interferent were increased as the revolatilization temperature was raised. However, the degree of enhancement of Bi signal in the absence of interferent was more than that of Bi signal in the presence of interferent. Therefore, the enhancement effect caused by interferents was suppressed with increasing revolatilization temperature.

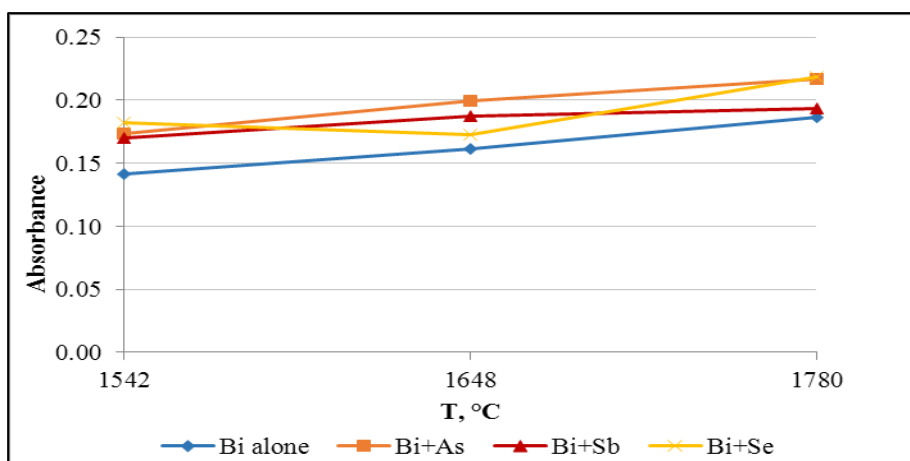


Figure 3.79 The absorbance values of the signals obtained for 10.0 ng/mL Bi, 10.0 ng/mL+ 5.0 mg/L As, 10.0 ng/mL+ 5.0 mg/L Sb, and 10.0 ng/mL+ 5.0 mg/L Se. The signals were measured at 1542 °C, 1678 °C and 1780 °C. The trapping temperature was kept at 300 °C. Temperature in EHQTA was 950 °C. The analyte and interferent were in the same solution and transferred from the same channel.

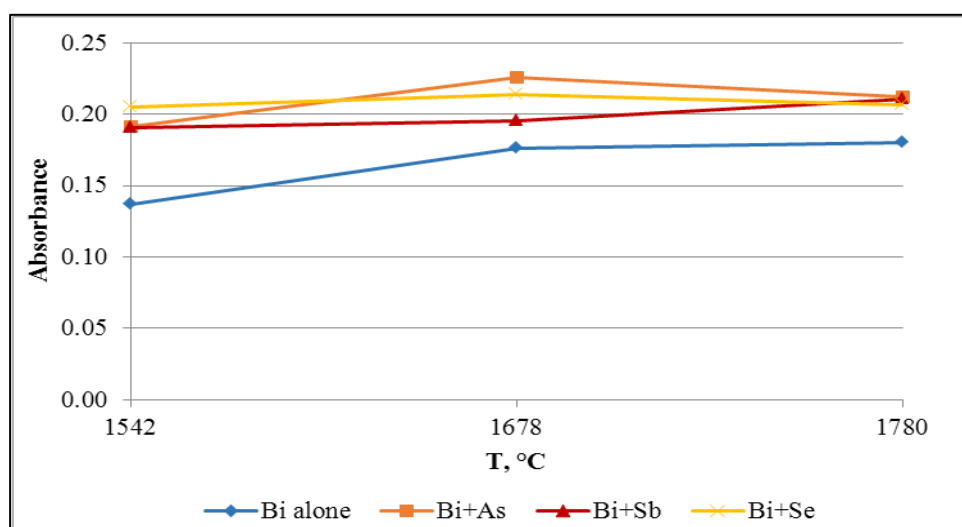


Figure 3.80 The absorbance values of the signals obtained for 10.0 ng/mL Bi, 10.0 ng/mL+ 5.0 mg/L As, 10.0 ng/mL+ 5.0 mg/L Sb, and 10.0 ng/mL+ 5.0 mg/L Se. The signals were measured at 1542 °C, 1678 °C and 1780 °C. The trapping temperature was kept at 300 °C. Temperature in EHQTA was 950 °C. The analyte and interferent were transported separately from different channels.

The schematic representation of the signals obtained at each revolatilization temperature is given in Figure 3.81. Those signals were measured without interferent. Figure 3.81 shows how Bi signal was affected with increasing releasing temperature. The signal measured at 1780 °C was 32 % more than that obtained at 1542 °C. Tailing observed in the signal was reduced with increased temperature. However, an increase on the background absorption was observed for the signal measured at 1780 °C.

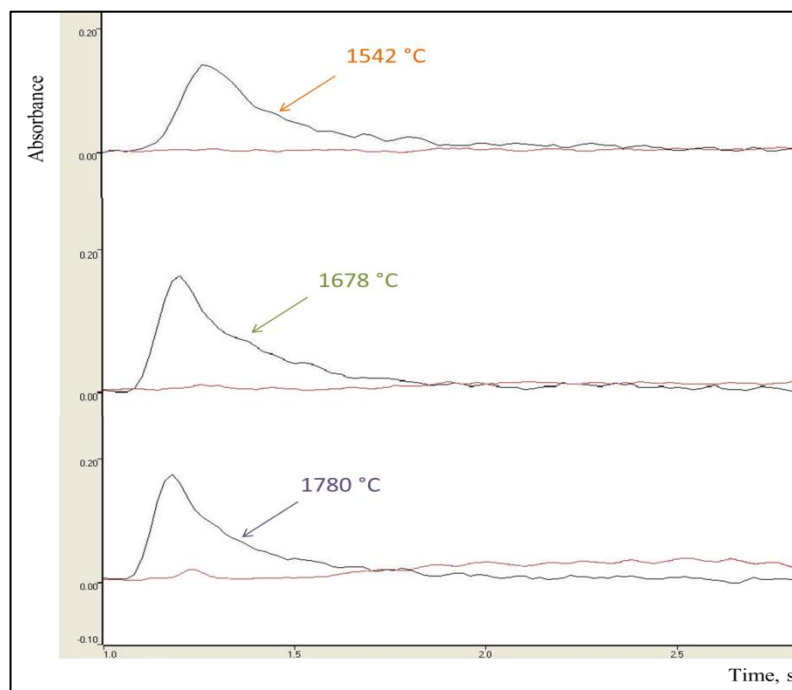


Figure 3.81 The signals of 10.0 ng/mL Bi obtained at 1542 °C, 1678 °C and 1780 °C. Bi was trapped for 20 seconds at 300 °C. Temperature of EHQTA was 950 °C. (Red colored line indicates the background signal.)

3.7.3.3.4 Bismuth as an Interference Element

In this section behavior of Bi as an interference element was studied. Rh coated W-coil Atom Trap ETV system was used for this part of the study; syringe system was not used. Sb was selected as the analyte, since it has severe enhancement effect on Bi

signal. This study was carried out to investigate whether Bi has the same effect on Sb or not.

The system used for this section was single-channel CF-HG system with Rh coated W-coil Atom Trap ETV system. The optimum conditions for hydride generation were selected for Sb(III). The working solutions of Sb were prepared in 0.1 mol/L HCl solution and 1.2% (w/v) NaBH₄ was used for reductant solution. Stibine was trapped on Rh coated W-coil at 262 °C for 60 seconds. Revolatilization and atomization temperature were 1742 °C and 950°C, respectively. Bi was added to Sb solutions at 50 and 500 fold interferent/analyte (w/w) ratios and Sb concentration was kept at 10.0 ng/mL. The Sb signal without Bi was normalized to 100 (reference signal). The results obtained for interference effect of Bi on Sb were listed in Table 3.20.

Table 3.20 The interference effect of Bi on Sb using Rh coated W-coil Atom Trap ETV system and optimized conditions for Sb(III). The concentration of Sb was 10.0 ng/mL in 0.1 mol/L HCl.

Mass ratio (Bi/Sb)	Relative signal for Sb
0	100
50	111 ± 13
500	67 ± 9

The enhancement of the signal for 50 fold interferent/analyte ratio was approximately 10 %, this result could be accepted in the tolerance limit. On the other hand, Bi suppressed Sb signal significantly (33 %) at 500 fold interferent-analyte ratio. It was stated that Bi was the most pronounced interferent for Sb [113,169]. It could be preconcentrated on quartz trap with the efficiency of 55 % under the optimum conditions of Sb [113]. Therefore, the suppression of the signal could be result from the co-trapping of Bi and Sb on W-coil.

In another experiment, working solutions of Sb were prepared according to the optimum conditions used for Bi. Sb solutions were prepared in 1.0 mol/L HCl solution and concentration of NaBH₄ was 0.5% (w/v). Bi was spiked to Sb solutions at 500 mass ratio of Bi to Sb and the concentration of Sb was 10.0 ng/mL. Stibine was trapped on Rh coated W-coil at 300 °C for 60 s. Revolatilization and atomization temperature were 1542 °C and 950 °C, respectively. The results obtained for the interference effect of Bi on Sb signal are indicated in Table 3.21.

Table 3.21 The interference effect of Bi on Sb using Rh coated W-coil Atom Trap ETV system and optimized conditions for Bi. The concentration of Sb was 10.0 ng/mL in 1.0 mol/L HCl.

Mass ratio (Bi/Sb)	Relative signal for Sb
0	100
500	97 ± 4

The result from the Table 3.21 indicated that there was no significant effect of Bi on the analytical signal Sb, under the optimum conditions of Bi. Bismuth did not cause any significant enhancement effect on Sb signal as Sb led to the enhancement on Bi signal.

3.8. The Comparison of ETA and ETV Systems

W-coil atom trap ETA and ETV system were used throughout this study. ETA and ETV system were compared in terms their analytical performance and behavior on interferences. Two systems had significantly different behaviors towards analytical performance and especially interferences.

One of the main differences was observed regarding their operation. W-coil in ETA system was used as both the trapping medium and the atomizer. Both functions were included in the same unit. On the other hand, W-coil in ETV system served as both the trapping medium and the revolatilization unit and released species upon revolatilization were transported to atomizer that was the EHQTA. Therefore, the process of revolatilization and atomization took place in separate units and location.

Hydrogen gas was used for the protection of W-coil from oxidation. On the other hand, hydrogen may also be effective during atomization near W-coil free H atoms are likely to be present; however, further research is needed to support this hypothesis. Ar gas was introduced to the system for the transportation of hydride species to the trapping and/or atomization unit. The purpose of introduction of Ar and H₂ gas was the same for both of the system. ETV system was different from ETA system in terms of additional introduction of Ar carrier gas. Additional carrier Ar gas was used to transport the released species to the atomizer at revolatilization stage; otherwise, the stripping Ar gas flow was not sufficient to achieve the efficient transportation of released species.

W-coil ETA and ETV systems could be correlated regarding their analytical performance. The sample flow rate was 3.0 mL/min for all conditions and the calculations were done according to the 120 s trapping period. LOD and characteristic concentrations (C_0) are demonstrated in Table 3.22. As seen on table, limits of detection for both systems were comparable. Syringe attached system for ETA and ETV yielded LOD values very close to each other.

One difference was to be noted regarding SRM analyses. Direct calibration method was sufficient for the method validation of ETA system. However, standard additions method was required with ETV system; this is a negative aspect for the use of ETV in complex matrices.

Table 3.22 Comparison of the analytical performance of the W-coil atom trap ETA and ETV systems.

	W-coil atom trap ETA	Syringe Attached W- coil atom trap ETA	W-coil atom trap ETV	Syringe Attached W- coil atom trap ETV
LOD, ng/mL	0.046	0.018	0.047	0.026
C₀, ng/mL	0.025	0.011	0.036	0.0029

The interference behavior of the W-coil ETA and ETV systems was investigated in this study. Detailed studies were carried out to examine how Bi signal was affected in the presence of interferents regarding the both systems. The interfering effects of As, Sb, Se, Te and Sn were observed. The results obtained for interference study performed with CF-HGAAS, W-coil Atom Trap ETA and ETV systems are given in Table 3.23. The results belong to the signals obtained with 500 fold mass ratio (w/w) of interferent to analyte, since the most significant effect of interferents were observed at this ratio.

Using ETA, the presence of these interferents caused significant suppression of the analyte signal. The most severe interference effect was generated by Sb and Te. The reason of the suppression of the analyte signal could be attributed to the co-trapping of analyte and interferent.

Table 3.23 Effects of interference on the analytical signal of Bi with CF-HGAAS, Rh coated W-coil Atom Trap ETA and Rh coated W-coil Atom Trap ETV. The mass ratio (w/w) of interferent to analyte was 500 fold. Analyte concentration for CF-HGAAS was 10.0 ng/mL and 2.0 ng/mL for ETA and ETV systems.

		As	Sb	Se	Te	Sn
CF-HGAAS	Bi+I*	98	109	70	45	101
	Bi and I**	102	98	84	97	98
ETA	Bi+I*	96	54	81	47	90
	Bi and I**	70	15	60	39	101
ETV	Bi+I*	270	254	293	99	90
	Bi and I**	213	213	196	103	93

*Bi and interferent were in same solution.

**Bi and interferent were transferred separately.

The results related to the interference study followed by W-coil ETV system showed different behavior from ETA. Twin channel CF-HG system was used for interference study with ETA and ETV systems. In this system, Sn and Te did not influence the analyte signal significantly. The common interferents for both of the system were As, Sb and Se. These interferents reduced the analyte signal with ETA system; on the other hand the enhancement effect from these interferents was observed with ETV system. The interference effects could be due to the formation of interferent-analyte compounds such as BiAs, BiSb and BiSe that may help the release of analyte from W-coil.

The correlation of ETA and ETV systems regarding the behavior of As, Sb and Se is demonstrated in Figure 3.82, Figure 3.83 and Figure 3.84, respectively. Suppression

of the signal with ETA system and enhancement of signal with ETV system can be seen from the graphs.

For the behaviors of Sb and Se, as shown in Figure 3.73 and Figure 3.77, respectively, there are increasing signal trends at the stages of CF-HG and untrapped CF-HG in the presence of interferent. This indicates that the trapped analyte will lower. The decrease in ETA signal in presence of these intereferents may be explained also by this behavior.

The paragraph above partly explains the decrease in ETA because of the analyte population on W-trap. This is also valid for ETV experiments, where an increase in analyte signal was observed in presence of intereferents. It is possible that the differences in release kinetics with and without intereferent, may be compensating the analyte loss on W-coil consequently resulting in higher analyte signal.

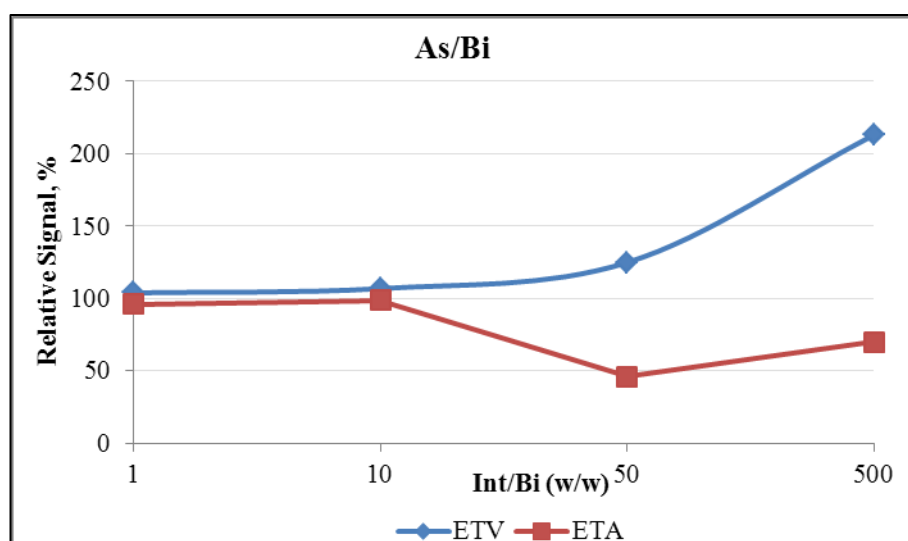


Figure 3.82 Comparison of Bi signal obtained in the presence As with ETA and ETV systems. Analyte concentration was 2.0 ng/mL and trapping period was 60 s for both of the systems.

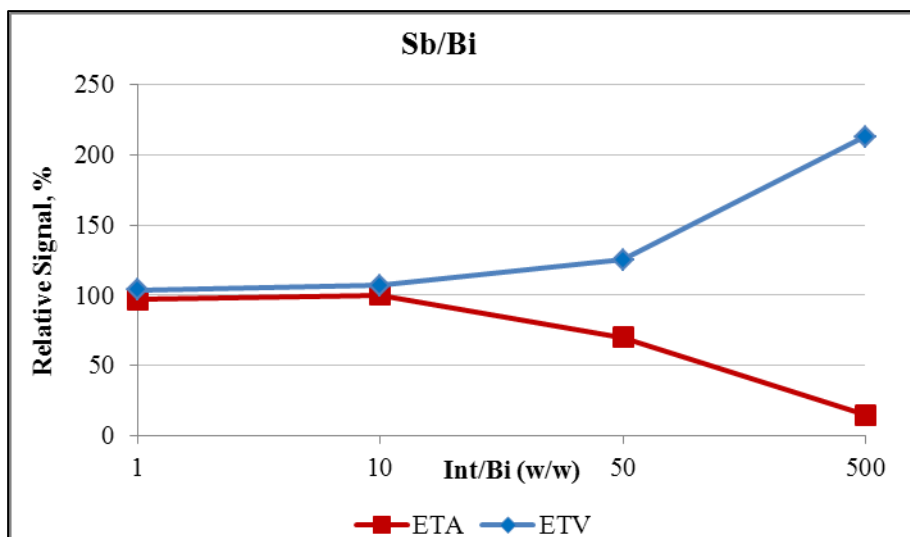


Figure 3.83 Comparison of Bi signal obtained in the presence Sb with ETA and ETV systems. Analyte concentration was 2.0 ng/mL and trapping period was 60 s for both of the systems.

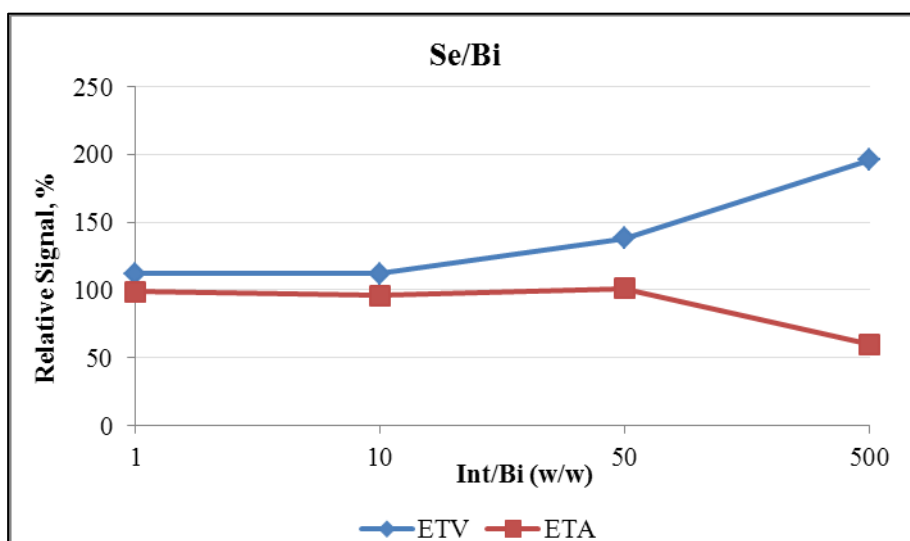


Figure 3.84 Comparison of Bi signal obtained in the presence Se with ETA and ETV systems. Analyte concentration was 2.0 ng/mL and trapping period was 60 s for both of the systems.

CHAPTER 4

CONCLUSIONS

In this study, the method development regarding W-coil Atom Trap ETA and ETV systems were performed and their analytical performance and behavior towards the interferences were compared. Bismuth was selected as the analyte throughout the study. W-coil surface was modified with Rh since bare W-coil yielded results that were not reproducible. Surface coating was preferred to obtain reproducible data, protect coil surface and prolong the life-time of W-coil.

In the first part of the study Rh coated W-coil Atom Trap ETA system and syringe attached Rh coated W-coil Atom Trap ETA systems were developed. CF-HG system was coupled to W-coil Atom Trap system. Generated hydride species were collected on heated W-coil surface and temperature of coil was raised to atomization temperature and trapped species were volatilized and atomization took place. In this configuration W-coil was operating as both the trapping and the atomization unit. In addition, quartz capillary was used for the introduction of hydride species near to the W-coil surface; this system was named as syringe attached Rh coated W-coil Atom Trap ETA. The parameters were optimized for both of the systems and analytical figures of merit were calculated. Limit of detection and characteristic concentration of Rh coated W-coil Atom Trap ETA system were 0.046 and 0.025 ng/mL, respectively. In syringe attached Rh coated W-coil Atom Trap ETA system, LOD and characteristic concentration values were found as 0.018 and 0.011 ng/mL, respectively.

Secondly, Rh coated W-coil Atom Trap ETV system and syringe attached Rh coated W-coil Atom Trap ETV systems were developed. CF-HG system was coupled to W-coil Atom Trap system. Hydride species were collected on the pre-heated W-coil surface and collected species were released by raising temperature to the volatilization temperature. Revolatilized species were transported to the atomization unit, EHQTA, heated to 950 °C. W-coil in ETV system was functioning as a trapping and volatilization unit. Atomization process took place in another location, QTA. Two systems were developed; without quartz capillary and with quartz capillary. The parameters were optimized for both of the systems and analytical figures of merit were calculated. LOD and characteristic concentration values obtained for Rh-coated W-coil Atom Trap ETV system were 0.047 and 0.036 ng/mL, respectively. For syringe attached system, LOD and characteristic concentration values were calculated as 0.026 and 0.0029 ng/mL, respectively.

In literature, interferences of ETA [124,174] and ETV [119] systems have been investigated separately; however, any studies regarding the comparison of interferences for both approaches has not been performed. In this study the interferences were studied by comparing the trends exhibited by both approaches. In order to understand the nature of the interference, a twin-channel CF-HG system containing two gas liquid separators was used.

For Rh coated W-coil atom trap ETA system, among the selected interference elements, Te and Sb significantly suppressed the signal. In order to understand the behavior of the interferences trapping and atomization temperature profiles were investigated under the optimum conditions of Bi except the stage temperatures. The optimum trapping temperature for Sb and Te were found to be 544 °C and 620 °C, respectively. It was found that these elements can be trapped in broad range of temperature and the trapping conditions for these interferences were similar with Bi. Therefore, these interferences and Bi can be co-trapped and also volatilized together due to their very similar preconcentration conditions. As a result, suppression on the Bi signal was observed.

Rh coated W-coil atom trap ETV system for Bi had a completely different behavior pattern compared to Rh coated W-coil atom trap ETA system. By using the twin-channel system, a detailed interference study with Rh coated W-coil atom trap ETV system was carried out. It was found that As, Se and Sb significantly enhanced the analytical signal of Bi. The effect was minimal for Te and Sn. The temperature and revolatilization profile for interferents were conducted under the optimum conditions for Bi. It was observed that As and Sb had similar preconcentration conditions with Bi.

The effects of interferents during continuous flow hydride generation, trapping and revolatilization stages were examined in ETV studies. The whole signal was divided into three parts, namely, CF-HG, untrapped CF-HG and revolatilization. The interference effect was studied for each part separately. The enhancement of CF-HG signal was investigated especially for Sb and Se. In the presence of interferents, bismuth could form interferent-analyte compounds that could prevent Bi from trapping on hot regions of inlet arm of QTA. Therefore, CF-HG signal could be enhanced due to the higher amount of bismuth species transported to the atomization zone. Another reason may be the competition for sites on inner surface of inlet arm of upstream EHQTA. The signals originated from CF-HG were not affected significantly in the presence of As. Secondly; CF-HG signal was followed during trapping stage called untrapped CF-HG. The CF-HG signal of untrapped bismuth species were recorded during trapping stage. CF-HG signal recorded during collection period was increasing in the presence of Sb and Se. Heated W-coil could behave as a reactor to promote the formation of diatomic compounds of interferent and analyte. This caused the reduction of trapping efficiency of analyte. Therefore, the amount of bismuth species that reach to the atomizer without being trapped could be increased. The increase in the CF-HG signal during trapping stage could be observed due to this situation. The effect of As on the signal obtained for untrapped CF-HG was not significant. The last and the third part is the revolatilization stage. The enhancement effect was observed dominantly at revolatilization stage with As, Sb and Se. The common behavior of the interferents was to make the Bi signal sharper. The enhancement of the signal can be resulted from formation of analyte-

interferent diatomic or polyatomic molecules during transportation of volatilized species to the atomizer, since there was temperature gradient between vaporizer and QTA that could provide the formation of analyte-interferent species. The amount of analyte, in the form of analyte-interferent species, reaching to the atomizer (QTA) could be raised. As a result the enhancement on the Bi signal could be observed. The other reason of increase due to the fact that interferents may promote trapped analyte species to be released more easily from the W-coil. Therefore, the amount of analyte species that reach to the atomizer could be increased to yield an enhanced signal.

Series of experiments related with the effect of increasing temperature at volatilization stage on the behavior of interferents were carried out. The signals of Bi without interferent and with interferent increased as the volatilization temperature was raised. However, the degree of enhancement of Bi signal in the absence of interferent was more than that of Bi signal in the presence of interferent. Therefore, the enhancement effect caused by interferents was suppressed with increasing volatilization temperature.

Lastly, Rh coated W-coil atom trap ETV system was used to see whether Bi had an interference effect on the interferents or not. Sb was selected as an analyte, since it has severe enhancement effect on Bi signal. The results showed that Bi suppressed the signal of Sb when the optimum conditions were adjusted according to Sb. However, Bi did not affect the Sb signal under the optimum conditions used for Bi.

In conclusion, methods of Rh coated W-coil Atom Trap ETA and Rh coated W-coil Atom Trap ETV were developed. The systems were compared in terms of their analytical performance and interference behavior. In order to have a reasonable comparison most of the parameters were kept same and constant for ETA and ETV modes. The similarities and differences of two systems were discussed. Limits of detection were comparable to each other. Syringe attached system for ETA and ETV yielded LOD values close to each other. Introduction of volatile species with the quartz capillary near to the trapping surface did not provide significant improvement regarding the sensitivity. In order to extend the applicability of these methods use of quartz capillary can be eliminated, since the movement of capillary was required in

each step resulting in a longer time spent for analyses. According to the literature, LOD values obtained by ICP-MS systems including *in-situ* atom trap in graphite tube [159] were much better than methods developed in this study. However, these methods are not cost effective and they are not available for most of the laboratories. The use of W-coil systems functioning as either ETA or ETV can be applied inexpensively in all laboratories having simple AA spectrometers.

The comparison of W-coil ETA and ETV systems can be done regarding their practicability. Two systems were different from each other regarding the carrier gas introduction to the system. The flow rates of Ar and H₂ gases were kept constant for W-coil ETA system. However; ETV system requires additional carrier Ar gas for analyte transport to atomizer; this flow was switched off during the collection stage. The optimum flow rate was adjusted at each cycle of analysis. This application makes the time required for analysis longer. The adjustment of Ar gas flow rate in each cycle could be one of the drawbacks of the W-coil atom trap ETV system. Moreover, the positive side of using ETA system is the operation of W-coil as both trapping and atomization unit. The trapping and atomization take place in the same medium; therefore they can be gathered in a same unit. For ETV system, since atomization takes place in QTA, the units for trapping and atomization are different. There is a requirement of extra heating system for EHQTA. On the other hand, extra heating system is not necessary for ETA. This could be another advantage of ETA over ETV.

The results related to interference study conducted with W-coil ETV and ETA systems showed that interferences behave differently with these systems. In W-coil Atom Trap ETV system, Sn and Te did not influence the analyte signal significantly. The common interferences for both of the system were As, Sb and Se. These interferences reduced the analyte signal with ETA system; on the other hand the enhancement effect was observed with ETV system. The optimized volatilization temperature in ETV (1542 °C) system was lower than the atomization temperature in ETA (2177 °C) system. This could be an advantage of ETV over ETA since using low temperature makes the lifetime of W-coil and its coating longer. However, the

results obtained with interference study indicated that increasing revolatilization temperature decrease the enhancement effect of interference elements. Therefore, the temperature advantage of W-coil ETV system has become unimportant.

REFERENCES

- [1] J. Sardans, F. Montes, J. Penuelas, Determination of As, Cd, Cu, Hg and Pb in biological samples by modern electrothermal atomic absorption spectrometry, *Spectrochim. Acta - Part B At. Spectrosc.* 65 (2010) 97–112. doi:10.1016/j.sab.2009.11.009.
- [2] M. Resano, F. Vanhaecke, M.T.C. de Loos-Vollebregt, Electrothermal vaporization for sample introduction in atomic absorption, atomic emission and plasma mass spectrometry—a critical review with focus on solid sampling and slurry analysis, *J. Anal. At. Spectrom.* 23 (2008) 1450–1475. doi:10.1039/b807756h.
- [3] D.J. Butcher, Advances in Electrothermal Atomization Atomic Absorption Spectrometry: Instrumentation, Methods, and Applications *Advances in Electrothermal Atomization Atomic Absorption Spectrometry: Instrumentation, Methods, and Applications*, *Appl. Spectrosc. Rev.* 41 (2007) 15–34. doi:10.1080/05704920500385460.
- [4] B. Welz, M. Sperling, *Atomic Absorption Spectrometry*, 3rd ed., Wiley-VCH Verlag GmbH, Germany, 1999.
- [5] M.G.R. Vale, N. Oleszczuk, W.N.L. dos Santos, Current Status of Direct Solid Sampling for Electrothermal Atomic Absorption Spectrometry—A Critical Review of the Development between 1995 and 2005, *Appl. Spectrosc. Rev.* 41 (2006) 377–400. doi:10.1080/05704920600726167.
- [6] J.A.C. Broekaert, *Analytical Atomic Spectrometry with Flames and Plasmas*, 2. Edition, Wiley-VCH Verlag GmbH & Co. KGaA, 2005.
- [7] M. Tüzen, Determination of heavy metals in soil, mushroom and plant

- samples by atomic absorption spectrometry, *Microchem. J.* 74 (2003) 289–297. doi:10.1016/S0026-265X(03)00035-3.
- [8] K. Bakkali, N.R. Martos, B. Souhail, E. Ballesteros, Characterization of trace metals in vegetables by graphite furnace atomic absorption spectrometry after closed vessel microwave digestion, *Food Chem.* 116 (2009) 590–594. doi:10.1016/j.foodchem.2009.03.010.
- [9] M. Tüzen, Determination of heavy metals in fish samples of the middle Black Sea (Turkey) by graphite furnace atomic absorption spectrometry, *Food Chem.* 80 (2003) 119–123. doi:10.1016/S0308-8146(02)00264-9.
- [10] M.J. Cal-Prieto, M. Felipe-Sotelo, A. Carlosena, J.M. Andrade, P. López-Mahía, S. Muniategui, D. Prada, Slurry sampling for direct analysis of solid materials by electrothermal atomic absorption spectrometry (ETAAS). A literature review from 1990 to 2000, *Talanta.* 56 (2002) 1–51. doi:10.1016/S0039-9140(01)00543-4.
- [11] I. López-garcía, M. Sánchez-merlos, M. Hernández-crdocha, Arsenic and antimony determination in soils and sediments by graphite furnace atomic absorption spectrometry with slurry sampling, 52 (1997) 437–443.
- [12] D. Baralkiewicz, H. Gramowska, M. Kózka, A. Kanecka, Determination of mercury in sewage sludge by direct slurry sampling graphite furnace atomic absorption spectrometry, *Spectrochim. Acta Part B At. Spectrosc.* 60 (2005) 409–413. doi:10.1016/j.sab.2005.01.010.
- [13] S.J. Huang, S.J. Jiang, Determination of lead in fish samples by slurry sampling electrothermal atomic absorption spectrometry, *Analyst.* 125 (2000) 1491–1494. doi:10.1039/B003484N.
- [14] A. V Zmozinski, T. Llorente-Mirandes, I.C.F. Damin, J.F. López-Sánchez, M. Goreti, R. Vale, B. Welz, M.M. Silva, Direct solid sample analysis with graphite furnace atomic absorption spectrometry—A fast and reliable screening procedure for the determination of inorganic arsenic in fish and seafood, *Talanta.* 134 (2014) 224–231. doi:10.1016/j.talanta.2014.11.009.

- [15] A. de Jesus, M.B. Dessuy, C.S. Huber, A. V. Zmozinski, A.T. Duarte, M.G.R. Vale, J.B. Andrade, Determination of antimony in pet containers by direct analysis of solid samples using graphite furnace atomic absorption spectrometry and leaching studies, *Microchem. J.* 124 (2016) 222–227. doi:10.1016/j.microc.2015.08.016.
- [16] D. Lide, *CRC Handbook of Chemistry and Physics*, 75th ed., CRS Press, Boca Raton, 1994.
- [17] X. Hou, B.T. Jones, Tungsten devices in analytical atomic spectrometry, *Spectrochim. Acta - Part B At. Spectrosc.* 57 (2002) 659–688. doi:10.1016/S0584-8547(02)00014-9.
- [18] M.F. Giné, F.J. Krug, V.A. Sass, B.F. Reis, J.A. Nóbrega, H. Berndt, Determination of cadmium in biological materials by tungsten coil atomic absorption spectrometry, *J. Anal. At. Spectrom.* 8 (1993) 243–245. doi:10.1039/JA9930800243.
- [19] M. Williams, Piepmeir E.H., Commercial Tungsten Filament Atomizer For Analytical Atomic Spectrometry, *Anal. Chem.* 44 (1972) 1342–1344. doi:10.1021/ac60315a038.
- [20] H. Berndt, G. Schaldach, Simple Low Cost Tungsten Coil Atomizer For Electrothermal Atomic Absorption Spectrometry, *J. At. Spectrom.* 3 (1988) 709–712. doi:10.1039/JA9880300709.
- [21] K. Ohta, S. Itoh, T. Mizuno, Electrothermal atomic-emission spectrometric determination of lithium with a metal-tube atomizer and a matrix modifier, *Talanta.* 38 (1991) 325–328. doi:10.1016/0039-9140(91)80055-5.
- [22] P. Ljung, E. Nyström, O. Axner, W. Frech, Detection of titanium in electrothermal atomizers by laser-induced fluorescence. Part 2. Investigation of various types of atomizers, *Spectrochim. Acta Part B At. Spectrosc.* 52 (1997) 703–716. doi:10.1016/S0584-8547(96)01676-X.
- [23] K. Dittrich, H. Berndt, J.A.C. Broekaert, G. Schaldach, G. Tölg, Comparative study of injection into a pneumatic nebuliser and tungsten coil electrothermal

- vaporisation for the determination of rare earth elements by inductively coupled plasma optical emission spectrometry, *J. Anal. At. Spectrom.* 3 (1988) 1105–1110. doi:10.1039/JA9880301105.
- [24] R. Tsukahara, M. Kubota, Some characteristics of inductively coupled plasma-mass spectrometry with sample introduction by tungsten furnace electrothermal vaporization, *Spectrochim. Acta Part B At. Spectrosc.* 45 (1990) 779–787. doi:10.1016/0584-8547(90)80057-P.
- [25] M.M. Silva, R.B. Silva, F.J. Krug, J.A. Nobrega, H. Berndt, Determination of barium in waters by tungsten coil electrothermal atomic absorption spectrometry, *J. Anal. At. Spectrom.* 9 (1994) 861–865. doi:10.1039/JA9940900861.
- [26] C.G. Bruhn, V.N. Huerta, J.Y. Neira, Chemical modifiers in arsenic determination in biological materials by tungsten coil electrothermal atomic absorption spectrometry, *Anal. Bioanal. Chem.* 378 (2004) 447–455. doi:10.1007/s00216-003-2285-3.
- [27] X. Wen, Q. Deng, J. Wang, S. Yang, X. Zhao, A new coupling of ionic liquid based-single drop microextraction with tungsten coil electrothermal atomic absorption spectrometry, *Spectrochim. Acta Part A Mol. Biomol. Spectrosc.* 105 (2013) 320–325. doi:10.1016/j.saa.2012.12.040.
- [28] A. Salido, C.L. Sanford, B.T. Jones, Determination of lead in blood by chelation with ammonium pyrrolidine dithio-carbamate followed by tungsten-coil atomic absorption spectrometry, *Spectrochim. Acta Part B At. Spectrosc.* 54 (1999) 1167–1176. doi:10.1016/S0584-8547(99)00054-3.
- [29] K. Ohta, T. Mizuno, Atom formation processes in the presence of ammonium thiocyanate in a thin-wall tungsten tube atomizer for atomic absorption spectrometry, *Spectrochim. Acta Part B At. Spectrosc.* 44 (1989) 95–100.
- [30] K. Ohta, M. Yokoyama, S. Itoh, S. Kaneco, T. Mizuno, Determination of aluminium in biological materials by electrothermal atomic absorption spectrometry with a tungsten tube atomizer, *Anal. Chim. Acta.* 291 (1994) 115–120.

- [31] T. Černohorský, S. Kotrlý, Determination of beryllium in drinking and waste water by tungsten furnace atomic absorption spectrometry, *J. Anal. At. Spectrom.* 10 (1995) 155–160. doi:10.1039/JA9951000155.
- [32] S. Xiao-quan, B. Radziuk, B. Welz, O. Vyskočilová, Determination of manganese in river and sea-water samples by electrothermal atomic absorption spectrometry with a tungsten atomizer, *J. Anal. At. Spectrom.* 8 (1993) 409–413. doi:10.1039/JA9930800409.
- [33] N. Tokman, S. Akman, Investigation of interference mechanism of cobalt chloride on the determination of bismuth by electrothermal atomic absorption spectrometry, *Spectrochim. Acta Part B At. Spectrosc.* 60 (2005) 291–298. doi:10.1016/j.sab.2004.11.001.
- [34] A.B. Volynsky, Mechanisms of action of platinum group modifiers in electrothermal atomic absorption spectrometry, *Spectrochim. Acta Part B At. Spectrosc.* 55 (2000) 103–150. doi:10.1016/S0584-8547(99)00175-5.
- [35] B. Welz, G. Schlemmer, J.R. Mudakavi, Palladium nitrate–magnesium nitrate modifier for electrothermal atomic absorption spectrometry. Part 5. Performance for the determination of 21 elements, *J. Anal. At. Spectrom.* 7 (1992) 1257–1271. doi:10.1039/JA9920701257.
- [36] P.V. de Oliveira, F.J. Krug, M.M. Silva, J.A. Nóbrega, Z.F. Queiroz, F.R.P. Rocha, Influence of Na, K, Ca and Mg on lead atomization by tungsten coil atomic absorption spectrometry, *J. Braz. Chem. Soc.* 11 (2000) 136–142. doi:10.1590/S0103-50532000000200006.
- [37] Z.F. Queiroz, F.J. Krug, P. V Oliveira, M.M. Silva, J.A. Nóbrega, Electrothermal behavior of sodium, potassium, calcium and magnesium in a tungsten coil atomizer and review of interfering effects, *Spectrochim. Acta Part B At. Spectrosc.* 57 (2002) 49–61. doi:10.1016/S0584-8547(01)00350-0.
- [38] X. Hou, Z. Yang, B.T. Jones, Determination of selenium by tungsten coil atomic absorption spectrometry using iridium as a permanent chemical modifier, *Spectrochim. Acta - Part B At. Spectrosc.* 56 (2001) 203–214. doi:10.1016/S0584-8547(00)00305-0.

- [39] B. Hu, S. Li, G. Xiang, M. He, Z. Jiang, Recent Progress in Electrothermal Vaporization–Inductively Coupled Plasma Atomic Emission Spectrometry and Inductively Coupled Plasma Mass Spectrometry, *Appl. Spectrosc. Rev.* 42 (2007) 203–234. doi:10.1080/05704920601184317.
- [40] O.Y. Ataman, Vapor generation and atom traps: Atomic absorption spectrometry at the ng/L level, *Spectrochim. Acta - Part B At. Spectrosc.* 63 (2008) 825–834. doi:10.1016/j.sab.2008.03.013.
- [41] T. Kántor, Electrothermal vaporization and laser ablation sample introduction for flame and plasma spectrometric analysis of solid and solution samples, *Spectrochim. Acta Part B At. Spectrosc.* 56 (2001) 1523–1563. doi:10.1016/S0584-8547(01)00266-X.
- [42] A.M. Gunn, D.L. Millard, G.F. Kirkbright, Optical emission spectrometry with an inductively coupled radio-frequency argon plasma source and sample introduction with a graphite rod electrothermal vaporization device. Part I. Instrumentation assembly and performance characteristics, *Analyst.* 130 (1978) 1231. doi:10.1039/an9780301066.
- [43] M. Aramendía, M. Resano, F. Vanhaecke, Electrothermal vaporization-inductively coupled plasma-mass spectrometry: A versatile tool for tackling challenging samples - A critical review., *Anal. Chim. Acta.* 648 (2009) 23–44. doi:10.1016/j.aca.2009.06.027.
- [44] D.C. Grégoire, R.E. Sturgeon, Analyte transport efficiency with electrothermal vaporization inductively coupled plasma mass spectrometry, *Spectrochim. Acta Part B At. Spectrosc.* 54 (1999) 773–786. doi:10.1016/S0584-8547(99)00008-7.
- [45] M.-L. Lin, S.-J. Jiang, Determination of As, Cd, Hg and Pb in herbs using slurry sampling electrothermal vaporisation inductively coupled plasma mass spectrometry., *Food Chem.* 141 (2013) 2158–2162. doi:10.1016/j.foodchem.2013.04.105.
- [46] W.-H. Hsu, S.-J. Jiang, A.C. Sahayam, Determination of Cu, As, Hg and Pb in vegetable oils by electrothermal vaporization inductively coupled plasma mass

- spectrometry with palladium nanoparticles as modifier., *Talanta*. 117 (2013) 268–272. doi:10.1016/j.talanta.2013.09.013.
- [47] D. Pozebon, V.L. Dressler, A.J. Curtius, Determination of copper, cadmium, lead, bismuth and selenium(iv) in sea-water by electrothermal vaporization inductively coupled plasma mass spectrometry after on-line separation, *J. Anal. At. Spectrom.* 13 (1998) 363–369. doi:10.1039/a707849h.
- [48] E.S. Chaves, F.G. Lepri, J.S.A. Silva, D.P.C. de Quadros, T.D. Saint’Pierre, A.J. Curtius, Determination of Co, Cu, Fe, Mn, Ni and V in diesel and biodiesel samples by ETV-ICP-MS, *J. Environ. Monit.* 10 (2008) 1211–1216. doi:10.1039/b809501a.
- [49] S.N. Hanna, B.T. Jones, A Review of Tungsten Coil Electrothermal Vaporization as a Sample Introduction Technique in Atomic Spectrometry, *Appl. Spectrosc. Rev.* 46 (2011) 624–635. doi:10.1080/05704928.2011.582659.
- [50] P. Wu, X. Wen, L. He, Y. He, M. Chen, X. Hou, Evaluation of tungsten coil electrothermal vaporization-Ar/H₂ flame atomic fluorescence spectrometry for determination of eight traditional hydride-forming elements and cadmium without chemical vapor generation, *Talanta*. 74 (2008) 505–511. doi:10.1016/j.talanta.2007.06.013.
- [51] K. Levine, K.A. Wagner, B.T. Jones, Low-Cost, Modular Electrothermal Vaporization System for Inductively Coupled Plasma Atomic Emission Spectrometry, *Appl. Spectrosc.* 52 (1998) 1165–1171.
- [52] X. Hou, K.E. Levine, A. Salido, B.T. Jones, M. Ezer, S. Elwood, J.B. Simeonsson, Tungsten Coil Devices in Atomic Spectrometry: Absorption, Fluorescence, and Emission, *Anal. Chem.* 73 (2001) 175–180. doi:10.1021/anal99175a011.
- [53] A.C. Davis, C.P. Calloway, B.T. Jones, Direct determination of cadmium in urine by tungsten-coil inductively coupled plasma atomic emission spectrometry using palladium as a permanent modifier, *Talanta*. 71 (2007) 1144–1149. doi:10.1016/j.talanta.2006.06.005.

- [54] C.G. Young, B.T. Jones, Determination of the total carbon in soft drinks by tungsten coil electrothermal vaporization inductively coupled plasma spectrometry, *Microchem. J.* 98 (2011) 323–327. doi:10.1016/j.microc.2011.03.001.
- [55] G.L. Donati, R.S. Amais, J. a Nobrega, Tungsten coil electrothermal matrix decomposition and sample vaporization to determine P and Si in biodiesel by inductively coupled plasma mass spectrometry, *J. Anal. At. Spectrom.* 28 (2013) 280–287. doi:10.1039/C2JA30306J.
- [56] O. Cankur, N. Ertas, O.Y. Ataman, Determination of bismuth using on-line preconcentration by trapping on resistively heated W coil and hydride generation atomic absorption spectrometry, *J. Anal. At. Spectrom.* 17 (2002) 603–609. doi:10.1039/b201365g.
- [57] C. Zheng, R.E. Sturgeon, X. Hou, UV photochemical vapor generation and in situ preconcentration for determination of ultra-trace nickel by flow injection graphite furnace atomic absorption spectrometry, *J. Anal. At. Spectrom.* 24 (2009) 1452–1458. doi:10.1039/b909962j.
- [58] S. Cerutti, S. Moyano, J. Marrero, P. Smichowski, L.D. Martinez, On-line preconcentration of nickel on activated carbon prior to its determination by vapor generation associated to inductively coupled plasma optical emission spectrometry, *J. Anal. At. Spectrom.* 20 (2005) 559–561. doi:10.1039/b500467p.
- [59] C.I.S. Narcise, L. dlC. Coo, F.R. del Mundo, On-line preconcentration and speciation of arsenic by flow injection hydride generation atomic absorption spectrophotometry, *Talanta.* 68 (2005) 298–304. doi:10.1016/j.talanta.2005.08.055.
- [60] Y. Gao, W. Yang, C. Zheng, X. Hou, L. Wu, On-line preconcentration and in situ photochemical vapor generation in coiled reactor for speciation analysis of mercury and methylmercury by atomic fluorescence spectrometry, *J. Anal. At. Spectrom.* 26 (2011) 126–132. doi:10.1039/C0JA00137F.
- [61] H. Wu, Y. Jin, W. Han, Q. Miao, S. Bi, Non-chromatographic speciation

- analysis of mercury by flow injection on-line preconcentration in combination with chemical vapor generation atomic fluorescence spectrometry, *Spectrochim. Acta Part B At. Spectrosc.* 61 (2006) 831–840. doi:10.1016/j.sab.2006.04.008.
- [62] R.E. Sturgeon, Z. Mester, Analytical Applications of Volatile Metal Derivatives, *Appl. Spectrosc.* 56 (2002) 202A–213A.
- [63] P. Wu, L. He, C. Zheng, X. Hou, R.E. Sturgeon, Applications of chemical vapor generation in non-tetrahydroborate media to analytical atomic spectrometry, *J. Anal. At. Spectrom.* 25 (2010) 1217–1246. doi:10.1039/c003483e.
- [64] J.A. Nóbrega, R.E. Sturgeon, P. Grinberg, G.J. Gardner, C.S. Brophy, E.E. Garcia, UV photochemical generation of volatile cadmium species, *J. Anal. At. Spectrom.* 26 (2011) 2519–2523. doi:10.1039/c1ja10252d.
- [65] F. Laborda, E. Bolea, J.R. Castillo, Electrochemical hydride generation as a sample-introduction technique in atomic spectrometry: fundamentals, interferences, and applications, *Anal. Bioanal. Chem.* 388 (2007) 743–751. doi:10.1007/s00216-006-1037-6.
- [66] P. Pohl, Hydride generation – recent advances in atomic emission spectrometry, *TrAC Trends Anal. Chem.* 23 (2004) 87–101. doi:10.1016/S0165-9936(04)00306-1.
- [67] C. Moor, J.W.H. Lam, R.E. Sturgeon, A novel introduction system for hydride generation-inductively coupled plasma mass spectrometry: determination of selenium in biological materials, *J. Anal. At. Spectrom.* 15 (2000) 143–149. doi:10.1039/a909296j.
- [68] W. Holak, Gas-sampling technique for arsenic determination by atomic absorption spectrophotometry, *Anal. Chem.* 41 (1969) 1712–1713. doi:10.1021/ac60281a025.
- [69] J. Dedina, Generation of Volatile Compounds for Analytical Atomic Spectroscopy, *Encycl. Anal. Chem.* (2010) 1–39.

doi:10.1002/9780470027318.a9127.

- [70] Y.-L. Feng, R.E. Sturgeon, J.W. Lam, Chemical vapor generation characteristics of transition and noble metals reacting with tetrahydroborate(III), *J. Anal. At. Spectrom.* 18 (2003) 1435–1442. doi:10.1039/b307675j.
- [71] W.B. Robbins, J.A. Caruso, Development of hydride generation methods for atomic spectroscopic analysis, *Anal. Chem.* 51 (1979) 889A–898A. doi:10.1021/ac50044a002.
- [72] A. D’Ulivo, Chemical vapor generation by tetrahydroborate(III) and other borane complexes in aqueous media: A critical discussion of fundamental processes and mechanisms involved in reagent decomposition and hydride formation, *Spectrochim. Acta Part B At. Spectrosc.* 59 (2004) 793–825. doi:10.1016/j.sab.2004.04.001.
- [73] M.E. Sigrist, H. Beldoménico, Determination of inorganic arsenic species by flow injection hydride generation atomic absorption spectrometry with variable sodium tetrahydroborate concentrations, *Spectrochim. Acta Part B At. Spectrosc.* 59 (2004) 1041–1045. doi:10.1016/j.sab.2004.04.003.
- [74] L. Elçi, Z. Arslan, J.F. Tyson, Determination of lead in wine and rum samples by flow injection-hydride generation-atomic absorption spectrometry, *J. Hazard. Mater.* 162 (2009) 880–885. doi:10.1016/j.jhazmat.2008.05.113.
- [75] E. Ródenas-Torralba, Á. Morales-Rubio, M. de la Guardia, Multicommutation hydride generation atomic fluorescence determination of inorganic tellurium species in milk, *Food Chem.* 91 (2005) 181–189. doi:10.1016/j.foodchem.2004.08.016.
- [76] N. Zhang, N. Fu, Z. Fang, Y. Feng, L. Ke, Simultaneous multi-channel hydride generation atomic fluorescence spectrometry determination of arsenic, bismuth, tellurium and selenium in tea leaves, *Food Chem.* 124 (2011) 1185–1188. doi:10.1016/j.foodchem.2010.07.033.
- [77] X. Jiang, W. Gan, S. Han, Y. He, Determination of Te in soldering tin using

- continuous flowing electrochemical hydride generation atomic fluorescence spectrometry, *Spectrochim. Acta Part B At.* 63 (2008) 710–713. doi:10.1016/j.sab.2008.03.017.
- [78] P. Cava-Montesinos, M.L. Cervera, A. Pastor, M. de la Guardia, Determination of As, Sb, Se, Te and Bi in milk by slurry sampling hydride generation atomic fluorescence spectrometry, *Talanta.* 62 (2004) 173–182. doi:10.1016/S0039-9140(03)00411-9.
- [79] P. Smrkolj, V. Stibilj, Determination of selenium in vegetables by hydride generation atomic fluorescence spectrometry, *Anal. Chim. Acta.* 512 (2004) 11–17. doi:10.1016/j.aca.2004.02.033.
- [80] M. Grotti, C. Lagomarsino, R. Frache, Multivariate study in chemical vapor generation for simultaneous determination of arsenic, antimony, bismuth, germanium, tin, selenium, tellurium and mercury by inductively coupled plasma optical emission spectrometry, *J. Anal. At. Spectrom.* 20 (2005) 1365–1373. doi:10.1039/b510803a.
- [81] E.J. dos Santos, A.B. Herrmann, V.L.A. Frescura, A.J. Curtius, Evaluation of slurry preparation procedures for the simultaneous determination of Hg and Se in biological samples by axial view ICP OES using on-line chemical vapor generation, *Anal. Chim. Acta.* 548 (2005) 166–173. doi:10.1016/j.aca.2005.06.002.
- [82] P. Pohl, R.E. Sturgeon, Simultaneous determination of hydride- and non-hydride-forming elements by inductively coupled plasma optical emission spectrometry, *TrAC Trends Anal. Chem.* 29 (2010) 1376–1389. doi:10.1016/j.trac.2010.07.015.
- [83] L. Abrankó, Z. Stefánka, P. Fodor, Possibilities and limits of the simultaneous determination of As, Bi, Ge, Sb, Se, and Sn by flow injection–hydride generation–inductively coupled plasma–time-of-flight, *Anal. Chim. Acta.* 493 (2003) 13–21. doi:10.1016/S0003-2670(03)00803-1.
- [84] G. Centineo, M. Bayón, A. Sanz-Medel, Flow injection analysis with inductively coupled plasma time-of-flight mass spectrometry for the

- simultaneous determination of elements forming hydrides and its, *J. Anal. At.* 15 (2000) 1357–1362. doi:10.1039/B004032K.
- [85] A.S. Luna, R.E. Sturgeon, R.C. de Campos, Chemical Vapor Generation: Atomic Absorption by Ag, Au, Cu, and Zn Following Reduction of Aquo Ions with Sodium Tetrahydroborate(III), *Anal. Chem.* 72 (2000) 3523–3531. doi:10.1021/ac000221n.
- [86] T. Matoušek, R.E. Sturgeon, Surfactant assisted chemical vapour generation of silver for AAS and ICP-OES: a mechanistic study, *J. Anal. At. Spectrom.* 18 (2003) 487–494. doi:10.1039/b211540a.
- [87] M.H. Arbab-Zavar, M. Chamsaz, A. Youssefi, M. Aliakbari, Flow injection electrochemical hydride generation atomic absorption spectrometry for the determination of cadmium in water samples, *Microchem. J.* 108 (2013) 188–192. doi:10.1016/j.microc.2012.10.017.
- [88] K.C. Thompson, D.R. Thomerson, Atomic-absorption studies on the determination of antimony, arsenic, bismuth, germanium, lead, selenium, tellurium and tin by utilising the generation of covalent hydrides, *Analyst.* 99 (1974) 595–601. doi:10.1039/an9749900595.
- [89] R.C. Chu, G.P. Barron, P.A.W. Baumgarner, Arsenic determination at submicrogram levels by arsine evolution and flameless atomic absorption spectrophotometric technique, *Anal. Chem.* 44 (1972) 1476–1479. doi:10.1021/ac60316a042.
- [90] J. Dědina, A. D’Ulivo, L. Lampugnani, T. Matoušek, R. Zamboni, Selenium hydride atomization, fate of free atoms and spectroscopic temperature in miniature diffusion flame atomizer studied by atomic absorption spectrometry, *Spectrochim. Acta Part B At. Spectrosc.* 53 (1998) 1777–1790. doi:10.1016/S0584-8547(98)00223-7.
- [91] A. D’Ulivo, J. Dědina, L. Lampugnani, A. Selecká, Mechanism of atomization interference by oxygen at trace level in miniature flame hydride atomizers, *Spectrochim. Acta - Part B At. Spectrosc.* 60 (2005) 1270–1279. doi:10.1016/j.sab.2005.06.004.

- [92] J. Dědina, Atomization of volatile compounds for atomic absorption and atomic fluorescence spectrometry: On the way towards the ideal atomizer, *Spectrochim. Acta - Part B At. Spectrosc.* 62 (2007) 846–872. doi:10.1016/j.sab.2007.05.002.
- [93] T. Matoušek, J. Dědina, A. Selecká, Multiple microflame quartz tube atomizer - Further development towards the ideal hydride atomizer for atomic absorption spectrometry, *Spectrochim. Acta - Part B At. Spectrosc.* 57 (2002) 451–462. doi:10.1016/S0584-8547(01)00400-1.
- [94] J. Dedina, D.L. Tsalev, *Hydride Generation Atomic Absorption Spectrometry*, Wiley & Sons Inc., Chichester, 1995.
- [95] A.S. Ribeiro, M.A.Z. Arruda, S. Cadore, A quartz tube atomizer with tungsten coil: a new system for vapor atomization in atomic absorption spectrometry, *J. Anal. At. Spectrom.* 17 (2002) 1516–1522. doi:10.1039/b207605c.
- [96] A.S. Ribeiro, M.A.Z. Arruda, S. Cadore, Determination of bismuth in metallurgical materials using a quartz tube atomizer with tungsten coil and flow injection-hydride-generation atomic absorption spectrometry, *Spectrochim. Acta - Part B At. Spectrosc.* 57 (2002) 2113–2120. doi:10.1016/S0584-8547(02)00173-8.
- [97] A. Gáspár, H. Berndt, Thermospray flame furnace atomic absorption spectrometry (TS-FF-AAS) — a simple method for trace element determination with microsamples in the $\mu\text{g/l}$ concentration range, *Spectrochim. Acta Part B At. Spectrosc.* 55 (2000) 587–597. doi:10.1016/S0584-8547(00)00183-X.
- [98] E.C. Figueiredo, J. Dedina, M.A.Z. Arruda, Metal furnace heated by flame as a hydride atomizer for atomic absorption spectrometry: Sb determination in environmental and pharmaceutical samples, *Talanta.* 73 (2007) 621–628. doi:10.1016/j.talanta.2007.04.021.
- [99] G. Drasch, L.V. Meyer, G. Kauert, Application of the furnace atomic-absorption method for the detection of arsenic in biological samples by means of the hydride technique, *Fresenius Zeitschrift Fur Anal. Chemie.* 304 (1980)

141–142.

- [100] E. Yildirim, TELLURIUM SPECIATION USING HYDRIDE GENERATION ATOMIC ABSORPTION SPECTROMETRY AND in-situ GRAPHITE CUVETTE TRAPPING, Middle East Technical University, 2009.
- [101] E. Yildirim, P. Akay, Y. Arslan, S. Bakirdere, O.Y. Ataman, Tellurium speciation analysis using hydride generation in situ trapping electrothermal atomic absorption spectrometry and ruthenium or palladium modified graphite tubes, *Talanta*. 102 (2012) 59–67. doi:10.1016/j.talanta.2012.06.002.
- [102] E. Nováková, P. Rychlovský, T. Resslerová, J. Hraníček, V. Červený, Electrochemical generation of volatile form of cadmium and its in situ trapping in a graphite furnace, *Spectrochim. Acta Part B At. Spectrosc.* 117 (2016) 42–48. doi:10.1016/j.sab.2016.01.003.
- [103] M. Masrourniaa, R. Shadmehri, M. Masrournia, Electrochemical hydride generation of tin(II) and its determination by electrothermal atomic absorption spectrometry with in situ trapping in the graphite tube atomizer, *Toxicol. Environ. Chem.* 93 (2011) 1332–1340. doi:10.1080/02772248.2011.590492.
- [104] H.T. Uggerud, W. Lund, Use of Palladium and Iridium as Modifiers in the Determination of Arsenic and Antimony by Electrothermal Vaporization Inductively Coupled Plasma Mass Spectrometry, Following In Situ Trapping of the Hydrides, *J. Anal. At. Spectrom.* 12 (1997) 1169–1174. doi:10.1039/a701805c.
- [105] S. Garboś, M. Wałcerz, E. Bulska, A. Hulanicki, Simultaneous determination of Se and As by hydride generation atomic absorption spectrometry with analyte concentration in a graphite furnace coated with zirconium, *Spectrochim. Acta Part B At. Spectrosc.* 50 (1995) 1669–1677. doi:10.1016/0584-8547(96)83514-2.
- [106] P. Bermejo-Barrera, J. Moreda-Piñeiro, A. Moreda-Piñeiro, A. Bermejo-Barrera, Direct trace determination of lead in estuarine water using in situ preconcentration of lead hydride on Ir, Zr and W-coated graphite tubes, *Anal.*

Chim. Acta. 368 (1998) 281–289. doi:10.1016/S0003-2670(98)00214-1.

- [107] H.O. Haug, Study on stable coatings for determination of lead by flow-injection hydride generation and in situ concentration in graphite furnace atomic absorption spectrometry, *Spectrochim. Acta Part B At. Spectrosc.* 51 (1996) 1425–1433. doi:10.1016/0584-8547(96)01464-4.
- [108] R.E. Sturgeon, S.N. Willie, G.I. Sproule, P.T. Robinson, S.S. Berman, Sequestration of volatile element hydrides by platinum group elements for graphite furnace atomic absorption, *Spectrochim. Acta Part B At. Spectrosc.* 44 (1989) 667–682. doi:10.1016/0584-8547(89)80065-5.
- [109] L.-L. Yang, D.-Q. Zhang, In situ preconcentration and determination of trace arsenic in botanical samples by hydride generation-graphite furnace atomic absorption spectrometry with Pd–Zr as chemical modifier, *Anal. Chim. Acta.* 491 (2003) 91–97. doi:10.1016/S0003-2670(03)00798-0.
- [110] D. Karadeniz Korkmaz, N. Ertaş, O.Y. Ataman, A novel silica trap for lead determination by hydride generation atomic absorption spectrometry, *Spectrochim. Acta - Part B At. Spectrosc.* 57 (2002) 571–580. doi:10.1016/S0584-8547(01)00379-2.
- [111] D. Korkmaz, C. Demir, F. Aydın, O.Y. Ataman, Cold vapour generation and on-line trapping of cadmium species on quartz surface prior to detection by atomic absorption spectrometry, *J. Anal. At. Spectrom.* 20 (2005) 46–52. doi:10.1039/b410584b.
- [112] I. Menemenlioğlu, D. Korkmaz, O.Y. Ataman, Determination of antimony by using a quartz atom trap and electrochemical hydride generation atomic absorption spectrometry, *Spectrochim. Acta - Part B At. Spectrosc.* 62 (2007) 40–47. doi:10.1016/j.sab.2006.11.007.
- [113] J. Kratzer, J. Dědina, In situ trapping of stibine in externally heated quartz tube atomizers for atomic absorption spectrometry, *Spectrochim. Acta - Part B At. Spectrosc.* 60 (2005) 859–864. doi:10.1016/j.sab.2005.04.004.
- [114] J. Kratzer, J. Dědina, Stibine and bismuthine trapping in quartz tube atomizers

- for atomic absorption spectrometry — Method optimization and analytical applications, *Spectrochim. Acta Part B At. Spectrosc.* 63 (2008) 843–849. doi:10.1016/j.sab.2008.03.011.
- [115] J. Kratzer, J. Dědina, Arsine and selenium hydride trapping in a novel quartz device for atomic-absorption spectrometry, *Anal. Bioanal. Chem.* 388 (2007) 793–800. doi:10.1007/s00216-006-1048-3.
- [116] F. Barbosa, S.S. de Souza, F.J. Krug, In situ trapping of selenium hydride in rhodium-coated tungsten coil electrothermal atomic absorption spectrometry, *J. Anal. At. Spectrom.* 17 (2002) 382–388. doi:10.1039/b111129a.
- [117] O. Cankur, O.Y. Ataman, Chemical vapor generation of Cd and on-line preconcentration on a resistively heated W-coil prior to determination by atomic absorption spectrometry using an unheated quartz absorption cell, *J. Anal. At. Spectrom.* 22 (2007) 791–799. doi:10.1039/b603489f.
- [118] S. Titretir, E. Kendüzler, Y. Arslan, I. Kula, S. Bakirdere, O.Y. Ataman, Determination of antimony by using tungsten trap atomic absorption spectrometry, *Spectrochim. Acta - Part B At. Spectrosc.* 63 (2008) 875–879. doi:10.1016/j.sab.2008.03.021.
- [119] İ. Kula, Y. Arslan, S. Bakirdere, O.Y. Ataman, A novel analytical system involving hydride generation and gold-coated W-coil trapping atomic absorption spectrometry for selenium determination at ng l⁻¹ level, *Spectrochim. Acta Part B At. Spectrosc.* 63 (2008) 856–860. doi:10.1016/j.sab.2008.03.020.
- [120] R. Liu, P. Wu, K. Xu, Y. Lv, X. Hou, Highly sensitive and interference-free determination of bismuth in environmental samples by electrothermal vaporization atomic fluorescence spectrometry after hydride trapping on iridium-coated tungsten coil, *Spectrochim. Acta - Part B At. Spectrosc.* 63 (2008) 704–709. doi:10.1016/j.sab.2008.03.010.
- [121] R. Liu, P. Wu, M. Xi, K. Xu, Y. Lv, Inorganic arsenic speciation analysis of water samples by trapping arsine on tungsten coil for atomic fluorescence spectrometric determination, *Talanta.* 78 (2009) 885–890.

doi:10.1016/j.talanta.2008.12.067.

- [122] S.S. de Souza, D. Santos, F.J. Krug, F. Barbosa, Exploiting in situ hydride trapping in tungsten coil atomizer for Se and As determination in biological and water samples, *Talanta*. 73 (2007) 451–457. doi:10.1016/j.talanta.2007.04.031.
- [123] O. Alp, N. Ertaş, In situ trapping of antimony hydride on iridium-coated tungsten coil and interference studies, *J. Anal. At. Spectrom.* 23 (2008) 976–980. doi:10.1039/b801451e.
- [124] O. Alp, N. Ertaş, Determination of tin by in situ trapping of stannane on a resistively heated iridium treated tungsten coil surface and interference studies, *Talanta*. 81 (2010) 516–520. doi:10.1016/j.talanta.2009.12.035.
- [125] P. Krejčí, B. Dočekal, Z. Hrušovská, Trapping of hydride forming elements within miniature electrothermal devices. Part 3. Investigation of collection of antimony and bismuth on a molybdenum foil strip following hydride generation, *Spectrochim. Acta - Part B At. Spectrosc.* 61 (2006) 444–449. doi:10.1016/j.sab.2006.03.006.
- [126] İ. Osama, Determination of Cadmium by Cold Vapour Generation Atom Trapping Atomic Absorption Spectrometry, Middle East Technical University, 2000.
- [127] X. Guo, X. Guo, Determination of ultra-trace amounts of selenium by continuous flow hydride generation AFS and AAS with collection on gold wire, *J. Anal. At. Spectrom.* 16 (2001) 1414–1418. doi:10.1039/b105737p.
- [128] E. Henden, Y. İşlek, M. Kavas, N. Aksuner, O. Yayayürük, T.D. Çiftçi, R. İlktaç, A study of mechanism of nickel interferences in hydride generation atomic absorption spectrometric determination of arsenic and antimony, *Spectrochim. Acta Part B At. Spectrosc.* 66 (2011) 793–798. doi:10.1016/j.sab.2011.10.001.
- [129] A. D'Ulivo, J. Dědina, Interferences in hydride atomization studied by atomic absorption and atomic fluorescence spectrometry, *Spectrochim. Acta - Part B*

- At. Spectrosc. 51 (1996) 481–498. doi:10.1016/0584-8547(95)01447-0.
- [130] Z. Furdíková, B. Dočekal, Trapping interference effects of arsenic, antimony and bismuth hydrides in collection of selenium hydride within iridium-modified transversally-heated graphite tube atomizer, *Spectrochim. Acta - Part B At. Spectrosc.* 64 (2009) 323–328. doi:10.1016/j.sab.2009.03.001.
- [131] B. Welz, M. Melcher, Mutual interactions of elements in the hydride technique in atomic absorption spectrometry: Part 1. Influence of selenium on arsenic determination, *Anal. Chim. Acta.* 131 (1981) 17–25. doi:10.1016/S0003-2670(01)93529-9.
- [132] A.R. Kumar, P. Riyazuddin, Chemical interferences in hydride-generation atomic spectrometry, *TrAC - Trends Anal. Chem.* 29 (2010) 166–176. doi:10.1016/j.trac.2009.12.002.
- [133] J. Dedina, Interference of volatile hydride-forming elements in selenium determination by atomic absorption spectrometry with hydride generation, *Anal. Chem.* 54 (1982) 2097–2102. doi:10.1021/ac00249a043.
- [134] N. Yang, H. Sun, Bismuth: Environmental Pollution and Health Effects, in: *Encycl. Environ. Heal.*, 2011: pp. 414–420. doi:10.1016/B978-0-444-52272-6.00374-3.
- [135] E. Merian, M. Anke, M. Ihnat, M. Stoeppler, *Elements and Their Compounds in the Environment: Occurrence, Analysis and Biological Relevance*, 2nd ed., Wiley-VCH Verlag GmbH & Co. KGaA, 2004.
- [136] A. Kabata-Pendias, H. Pendias, *Trace elements in soils and plants*, 3rd ed., Boca Raton, Fla.; London: CRC Press, London, 2000.
- [137] M. Filella, How reliable are environmental data on “orphan” elements? The case of bismuth concentrations in surface waters, *J. Environ. Monit.* 12 (2010) 90–109. doi:10.1039/B914307F.
- [138] J. Feldmann, E.M. Krupp, D. Glindemann, A. V Hirner, W.R. Cullen, Methylated bismuth in the environment, *Appl. Organomet. Chem.* 13 (1999) 739–748. doi:10.1002/(SICI)1099-0739(199910)13:10<739::AID-

AOC925>3.0.CO;2-Z.

- [139] G. Nordberg, B.A. Fowler, M. Nordberg, Handbook on the toxicology of metals, 4th ed., Elsevier B.V., 2015.
- [140] S. Hočevár, B. Ogorevc, J. Wang, B. Pihlar, A study on operational parameters for advanced use of bismuth film electrode in anodic stripping voltammetry, *Electroanalysis*. 14 (2002) 1707–1712. doi:10.1002/elan.200290014.
- [141] Y. Cho, D. Park, D. Park, Selective oxidation of hydrogen sulfide to ammonium thiosulfate and sulfur over vanadium-bismuth oxide catalysts, *Res. Chem. Intermed.* 28 (2002) 419–431. doi:10.1163/156856702760346833.
- [142] S. Ng, J. Xue, J. Wang, Bismuth titanate from mechanical activation of a chemically coprecipitated precursor, *J. Am. Ceram.* 85 (2002) 2660–2665. doi:10.1111/j.1151-2916.2002.tb00512.x.
- [143] L. Brunton, J. Lazo, K. Parker, Goodman & Gilman's The Pharmacological Basis of Therapeutics, 11th ed., Mc Graw Hill, 2006.
- [144] H. DuPont, C. Ericsson, M. Farthing, Expert review of the evidence base for self-therapy of travelers' diarrhea, *J. Travel.* 16 (2009) 161–171. doi:10.1111/j.1708-8305.2009.00300.x.
- [145] C. Reilly, Metal contamination of food: its significance for food quality and human health, 3rd ed., Blackwell Science, 2002.
- [146] Y. Sano, H. Satoh, M. Chiba, M. Okamoto, Oral toxicity of bismuth in rat: single and 28-day repeated administration studies, *J. Occup. Health.* 47 (2005) 293–298. doi:10.1539/joh.47.293.
- [147] W. Serfontein, R. Mekel, Bismuth toxicity in man II. Review of bismuth blood and urine levels in patients after administration of therapeutic bismuth formulations in relation to the problem of therapeutic bismuth formulations in relation to the problem of bismuth toxicity in man, *Res. Commun. Chem. Pathol. Pharmacol.* 26 (1979) 391–411.
- [148] P. Schramel, I. Wendler, J. Angerer, The determination of metals (antimony,

- bismuth, lead, cadmium, mercury, palladium, platinum, tellurium, thallium, tin and tungsten) in urine samples by inductively coupled plasma-mass spectrometry, *Int. Arch. Occup. Environ. Health.* 69 (1997) 219–223. doi:10.1007/s004200050140.
- [149] N. Velitchkova, E.N. Pentcheva, N. Daskalova, Determination of arsenic, mercury, selenium, thallium, tin and bismuth in environmental materials by inductively coupled plasma emission spectrometry, *Spectrochim. Acta - Part B At. Spectrosc.* 59 (2004) 871–882. doi:10.1016/j.sab.2004.03.004.
- [150] F. Barbosa Jr, E.C. Lima, R.A. Zanão, F.J. Krug, The use of a W-Rh permanent modifier for direct determination of bismuth in urine and whole blood by electrothermal atomic absorption spectrometry, *J. Anal. At. Spectrom.* 16 (2001) 842–846. doi:10.1039/B103161A.
- [151] C.G. Magalhães, B.R. Nunes, M.B. Oss Giacomelli, J.B.B. da Silva, Direct determination of bismuth in urine samples by electrothermal atomic absorption spectrometry: study of chemical modifiers, *J. Anal. At. Spectrom.* 18 (2003) 787–789. doi:10.1039/B302633G.
- [152] Y.-H. Sung, S.-D. Huang, On-line preconcentration system coupled to electrothermal atomic absorption spectrometry for the simultaneous determination of bismuth, cadmium, and lead in urine, *Anal. Chim. Acta.* 495 (2003) 165–176. doi:10.1016/j.aca.2003.07.009.
- [153] F. Shemirani, M. Baghdadi, M. Ramezani, M.R. Jamali, Determination of ultra trace amounts of bismuth in biological and water samples by electrothermal atomic absorption spectrometry (ET-AAS) after cloud point extraction, *Anal. Chim. Acta.* 534 (2005) 163–169. doi:10.1016/j.aca.2004.06.036.
- [154] S. CADORE, N. BACCAN, Continuous Hydride Generation System for the Determination of Trace Amounts of Bismuth in Metallurgical Materials by Atomic Absorption Spectrometry Using an On-line Stripping-type Generator/Gas–Liquid Separator, *J. Anal. At. Spectrom.* 12 (1997) 637–642. doi:10.1039/A606553H.

- [155] Y. Zhang, S.B. Adeloju, Flow injection–hydride generation atomic absorption spectrometric determination of selenium, arsenic and bismuth, *Talanta*. 76 (2008) 724–730. doi:10.1016/j.talanta.2008.03.056.
- [156] H.-M. Liu, S.-Y. Chen, P.-H. Chang, S.-J.J. Tsai, Determination of bismuth, selenium and tellurium in nickel-based alloys and pure copper by flow-injection hydride generation atomic absorption spectrometry—with ascorbic acid prereduction and cupferron chelation–extraction, *Anal. Chim. Acta*. 459 (2002) 161–168. doi:10.1016/S0003-2670(02)00105-8.
- [157] H. Wu, B. Du, C. Fang, Flow Injection On-line Preconcentration Coupled with Hydride Generation Atomic Fluorescence Spectrometry for Ultra-Trace Amounts of Bismuth Determination in Biological and Environmental Water Samples, *Anal. Lett.* 40 (2007) 2772–2782. doi:10.1080/00032710701588119.
- [158] Y.L. Feng, H.W. Chen, H.Y. Chen, L.C. Tian, Sequential determination of tin, arsenic, bismuth and antimony in marine sediment material by inductively coupled plasma atomic emission spectrometry using a small concentric hydride generator and L-cysteine as prereductant, *Fresenius J. Anal. Chem.* 361 (1998) 155–157. doi:10.1007/s002160050853.
- [159] C.C. Chang, S.J. Jiang, Determination of Hg and Bi by electrothermal vaporization inductively coupled plasma mass spectrometry using vapor generation with in situ preconcentration in a platinum-coated graphite furnace, *Anal. Chim. Acta*. 353 (1997) 173–180. doi:10.1016/S0003-2670(97)87775-6.
- [160] E. Özdemir, DETERMINATION OF INDIUM BY VAPOUR GENERATION ATOMIC, Middle East Technical University, 2014.
- [161] R.C. Weast, *Handbook of Chemistry and Physics*, 53rd ed., Chemical Rubber Pub., 1972.
- [162] E. Kılınc, S. Bakırdere, F. Aydın, O.Y. Ataman, In situ atom trapping of Bi on W-coated slotted quartz tube flame atomic absorption spectrometry and interference studies, *Spectrochim. Acta Part B At. Spectrosc.* 89 (2013) 14–19. doi:10.1016/j.sab.2013.08.008.

- [163] S. Moyano, R.G. Wuilloud, R.A. Olsina, J.A. Gásquez, L.D. Martinez, On-line preconcentration system for bismuth determination in urine by flow injection hydride generation inductively coupled plasma atomic emission spectrometry, *Talanta*. 54 (2001) 211–219. doi:10.1016/S0039-9140(01)00310-1.
- [164] J. Kratzer, J. Dědina, In situ trapping of bismuthine in externally heated quartz tube atomizers for atomic absorption spectrometry, *Spectrochim. Acta - Part B At. Spectrosc.* 63 (2008) 843–849. doi:10.1016/j.sab.2008.03.011.
- [165] S. Gil, M.T.C. de Loos-Vollebregt, C. Bendicho, Optimization of a single-drop microextraction method for multielemental determination by electrothermal vaporization inductively coupled plasma mass spectrometry following in situ vapor generation, *Spectrochim. Acta Part B At. Spectrosc.* 64 (2009) 208–214. doi:10.1016/j.sab.2008.12.002.
- [166] P. Schramel, L.-Q. Xu, Determination of arsenic, antimony, bismuth, selenium and tin in biological and environmental samples by continuous flow hydride generation ICP-AES without gas-liquid separator, *Fresenius' J. Fresenius J Anal Chem.* 340 (1991) 41–47.
- [167] P. Pohl, W. Zyrnicki, Study of chemical and spectral interferences in the simultaneous determination of As, Bi, Sb, Se and Sn by hydride generation inductively coupled plasma atomic emission spectrometry, *Anal. Chim. Acta.* 468 (2002) 71–79. doi:10.1016/S0003-2670(02)00602-5.
- [168] K. Dittrich, R. Mandry, Investigations into the Improvement of the Analytical Application of the Hydride Technique in Atomic Absorption Spectrometry by Matrix Modification and Graphite Furnace Atomisation Part 1. Analytical Results, *Analyst.* (1986).
- [169] É.M. de Moraes Flores, A. Medeiros Nunes, V. Luiz Dressler, J. Dědina, Multiple microflame quartz tube atomizer: Study and minimization of interferences in quartz tube atomizers in hydride generation atomic absorption spectrometry, *Spectrochim. Acta - Part B At. Spectrosc.* 64 (2009) 173–178. doi:10.1016/j.sab.2008.11.007.

- [170] J. Kratzer, J. Dědina, Stibine and bismuthine trapping in quartz tube atomizers for atomic absorption spectrometry - Method optimization and analytical applications, *Spectrochim. Acta - Part B At. Spectrosc.* 63 (2008) 843–849. doi:10.1016/j.sab.2008.03.011.
- [171] F.J. Kohl, J.E. Prusaczyk, K.D. Carlson, New gaseous molecules of the pnictides, *J. Am. Chem. Soc.* 89 (1967) 5501–5502. doi:10.1021/ja00997a063.
- [172] F.J. Kohl, K.D. Carlson, Dissociation energies of bismuth-antimony molecules, *J. Am. Chem. Soc.* 90 (1968) 4814–4817. doi:10.1021/ja01020a012.
- [173] M.L. Cafaro, G. Bardi, V. Piacente, Vaporization study of solid bismuth selenide (Bi_2Se_3), *J. Chem. Eng. Data.* 29 (1984) 78–80. doi:10.1021/je00035a026.
- [174] O. Alp, N. Ertaş, In-situ trapping arsenic hydride on tungsten coil and comparing interference effect of some hydride forming elements using different types of atomizers, *Microchem. J.* 128 (2016) 108–112. doi:10.1016/j.microc.2016.03.021.

CURRICULUM VITAE

Name : MERCAN Pınar
Place of birth : Ankara
Date of birth : 07.02.1984
Sex : Female
Marital Status : Married

Education

Undergraduate : June 2007, METU Chemistry Department
Ms : January 2010, METU Chemistry Department
Ph D. : to be completed in February 2017, METU Chemistry Department

Scientific Experience

Research Ass. : 11.2007 – 03.2016, METU, Chemistry Department

Scientific Interests

- Analytical method development and validation
- the speciation of trace elements with chromatographic and non-chromatographic techniques
- Atomic Absorption Spectrometry (AAS)
- Hydride generation and preconcentration methods
- Atom traps
- Inductively Coupled Optical Emission Spectrometry (ICP-OES)
- Chromatographic techniques

Publications

Yıldırım, E., **Akay, P.**, Arslan, Y., Bakirdere, S., Ataman, O. Y., Tellurium speciation analysis using hydride generation *in situ* trapping electrothermal atomic absorption spectrometry and ruthenium or palladium modified graphite tubes, **Talanta**, 102 (2012) 59-67.

International Conferences Attended

1. **Mercan P.**, Ataman, O.Y., Use Of Tungsten Coil System As Electrothermal Vaporizer And Electrothermal Atomizer In Atomic Spectrometry, 9th Aegean Analytical Chemistry Days, 29 Sept- 03 October 2014, Khios, Greece.
2. **Mercan, P.**, Atıcı, S., Ataman, O.Y., Inorganic Tellurium Speciation Using Tungsten-coil Atom Trap and Hydride Generation Atomic Absorption Spectrometry, 6th Black Sea Basin Conference on Analytical Chemistry, 10-14 September 2013, Trabzon, Turkey.
3. Dügencili, B., Yıldırım, E., **Akay, P.**, Ataman, O.Y., Interactive Effects of Arsenic and Selenium in Green Onion (*Alliumcepa* L.), 8th Aegean Analytical Chemistry Days, 16-20 September 2012, İzmir, Turkey.
4. Yıldırım, E., **Akay, P.**, Arslan, Y., Bakırdere, S., Ataman, O.Y., Tellurium speciation using hydride generation atomic absorption Spectrometry and in-situ graphite cuvette trapping, 7th Aegean Analytical Chemistry Days, 29 September-3 October 2010, Lesvos, Greece.
5. **Akay, P.**, Arslan, Y., Bakirdere, S., Yıldırım, E., Ataman, O.Y., Inorganic antimony speciation using tungsten coil atom trap and hydride generation atomic absorption spectrometry, 6th International Conference Instrumental Methods of Analysis Modern Trends and Applications, 4-8 October 2009, Athens, Greece.
6. Yıldırım, E., Arslan, Y., Bakirdere, S., **Akay, P.**, Ataman, O.Y., Determination of Zinc by vapor generation atomic absorption spectrometry,

6th International Conference Instrumental Methods of Analysis Modern Trends and Applications, 4-8 October 2009, Athens, Greece.

7. Yıldırım, E., **Akay, P.**, Bakirdere, S., Ataman, O.Y., Determination of lead by in-situ graphite cuvette trapping hydride generation atomic absorption spectrometry, 5th Black Sea Basin Conference on Analytical Chemistry, 23-26 September 2009, Fatsa-Ordu, Turkey.

National Conferences Attended

1. **Mercan P.**, Bora S., Ataman, O.Y., Rodyum Kaplı Tungsten Sarmal Atom Tuzaklı ve Hidrür Oluşturmalı Atomik Absorpsiyon Spektrometrisi ile Bizmut Tayini, 7. Ulusal Analitik Kimya Kongresi, 1-5 Eylül 2014, Kahramanmaraş, Türkiye.
2. **Akay, P.**, Yıldırım, E., Arslan, Y., Bakirdere, S., Ataman, O.Y., Inorganic Antimony Speciation Using Tungsten Coil Atom Trap and Hydride Generation Atomic Absorption Spectrometry, Uluslararası Katılımlı XII. Ulusal Spektroskopi Kongresi, 18-22 Mayıs 2011, Side-Antalya, Türkiye.
3. Ataman, S., Karaman, G., Bora S., **Akay, P.**, Arslan Y., Bakirdere, S., Korkmaz, M., Ataman O.Y., İdrar Örneklerinde ICP-OES ile Bor Tayini, XI. Ulusal Spektroskopi Kongresi, 23-26 Haziran 2009, Ankara, Türkiye.

REFERENCES

1. Prof. Dr. O. Yavuz Ataman
Department of Chemistry, METU, ataman@metu.edu.tr
2. Assoc. Prof. Dr. Gülay Ertaş
Department of Chemistry, METU, gertas@metu.edu.tr